GASEOUS HALOALKANES REACTED ON CLEAN METAL SURFACES

REACTIONS OF GASEOUS HALOALKANES ON CLEAN TRANSITION METAL SURFACES

by

Robert W. Egan

B.Sc., Brown University, 1965

A thesis submitted to the Faculty of Graduate Studies and Research in partial fulfillment of the requirements for the degree of Doctor of Philosophy

Department of Chemistry
McGill University
Montreal, Canada

June, 1972

To the memory of the late

Henry J. Revere

whose continual confidence and encouragement

helped make this possible.

ACKNOWLEDGMENTS

The guidance and assistance provided by Dr. J.F. Harrod, under whose direction this research was conducted, is gratefully acknowledged.

For their patience, understanding, encouragement and general cheerfulness, I express my appreciation to my family, Susanne, Robert and Séan. I especially extend my sincere gratitude to Susanne, my wife, for typing this manuscript and for exhibiting the fortitude which helped make our years at McGill a truely rewarding and enjoyable experience.

In addition, I would like to recognize the confidence and support demonstrated throughout the years by both Susanne's and my parents.

To Dr. L.E. St. Pierre for introducing me to McGill and encouraging me throughout my studies and to Dr. W.R. Summers for helpful discussion concerning this research, I express my gratitude.

Finally, I acknowledge the fellowship support provided by the Xerox Corporation (1968-69) and the National Research Council of Canada (1969 72).

Ph.D. CHEMISTRY

R. W. Egan

REACTIONS OF GASEOUS HALOALKANES ON CLEAN TRANSITION METAL SURFACES

A B S T R A C T

The properties and mechanisms of the dehydrohalogenation of haloalkanes on atomically clean surfaces of the first row transition metals have been investigated.

To compare the properties of these metals, haloalkanes were selected from the catalytic (HX and olefin generated) and non-catalytic (all chlorine retained by surface) classes previously detected on titanium. The former reactions were similar on halided surfaces of all the metals. Kinetics and activation parameters were determined. Although all the chloride was retained during each reaction in the latter catagory, surface deactivation occurred rapidly for all the metals except titanium and manganese. Where possible, reaction order and activation parameters were determined.

Initial reactions on unreacted or lightly reacted surfaces were also studied and three types of behavior detected: dehydrohalogenation, retentive adsorption and hydrogenation.

Reaction mechanisms on halided surfaces were studied by time and concentration order determinations, halo-exchange experiments, examining the effect of reaction products and studying the specificity of halided surfaces for certain reactions.

TABLE OF CONTENTS (i)

page

page

III. REACTIONS OF HALOALKANES WITH THE FIRST ROW TRANSITION METALS

page

page

page

VIII. SUGGESTIONS FOR FURTHER WORK

IX. APPENDICES

X. REFERENCES

Figure page

I. INTRODUCTION

II. EXPERIMENTAL PROCEDURES

III. REACTIONS OF HALOALKANES WITH THE FIRST ROW TRANSITION METALS

LIST OF TABLES

I) INTRODUCTION

I-A) Origin of the Problem

Following a report (Matlack and Breslow, 1965) that ethylene polymerization could be catalyzed by titanium, ballmilled in the presence of haloalkane, Harrod and Summers undertook a study of the same reaction on atomically clean titanium surfaces. Although under these conditions no polymerization ensued, a novel series of haloalkane dehydrohalogenation reactions was discovered and investigated (Harrod and Summers, 1971; Summers and Harrod, 1972).

Several extensions of this work seemed worthwhile and two have been pursued in the present investigations.

1) The ability of the first row transition metals to effect haloalkane dehydrohalogenation has been investigated. Haloalkanes were selected to typify both the catalytic and non-catalytic modes of reaction observed previously with titanium.

2) A detailed experimental investigation of possible reaction mechanisms has been undertaken.

Germane to these studies are the physical properties of transition metals and their complexes, homogeneous and heterogeneous haloalkane decompositions and the general properties of heterogeneous catalysts. Each will

be introduced in the following discussion.

I-B) Surface Reactivity

In addition to chemical composition, the two factors most critical to reactivity of a surface are its cleanliness and area. For metals, the former is altered by the extent to which the surface is exposed to contaminant gases prior to investigation. The latter, on the other hand, is determined by the geometric area of the surface, the rate of film deposition, film thickness and surface temperature.

To maintain maximum cleanliness, the surface is deposited at as low a residual gas pressure as possible. Customarily, this is achieved by a combination of mechanical, diffusion and cryoscopic pumping. The clean lifetime of a surface can be calculated from Equation I-1 (Roberts and Vanderslice, 1963).

$$t_c = \alpha n_m / \beta \nu \qquad \text{I-1}$$

Where t_c is the clean lifetime of the surface, α the tolerable contamination level expressed as a fraction of a monolayer, n_m the number of surface sites per monolayer and ν the number of molecules striking a unit area of surface per second.

The time required to form a monolayer of surface contaminant ($\beta = 1$) is a few hours at 10^{-9} Torr, but only a few seconds at 10^{-6} Torr. Hence, the present studies have been conducted with films deposited at

around 10^{-9} Torr.

Pressures of 10^{-9} Torr, or less, have probably been obtained for several decades; however, only since the invention of the inverted ion gauge (Bayard and Alpert, 1950) has it been possible to measure pressures below about 10^{-8} Torr. With the ability to monitor such low pressures, it is now possible to conduct experiments with surfaces of known purity.

For metal films, the actual surface area is frequently significantly greater than the geometric surface area. This is described by the roughness factor, R, which is the ratio of the actual area to the geometric area. For porous surfaces, the actual surface area increases with film thickness making R/w a more accurate measure of a film roughness (w is the specific film weight). Typical values of this parameter for the transition metals at 0°C are: tungsten, 270-360; molybdenum, 550-680; chromium, 480-650; tantalum, 270; niobium, 350; iron, 200-300; cobalt, 97; nickel, 86-130; rhodium, 200-330; platinum, 140; palladium, 40-150 and titanium, 200-240 (Anderson and Baker, 1971a).

Surface area decreases with increasing film deposition temperature. For example, relative R/w values taking the value at 0°C as unity are: tungsten; 1.0, 0°C; 1.0, 250°C; 0.77, 350°C; 0.32, 400°C: nickel; 5.3, -183°C; 3.53, -78°C, 1.0, 0°C; 0.64, 100°C; 0.17, 200°C: titanium; 1.0, 0°C; 0.10, 200°C, (Anderson and Baker, 1971a). Thus the

thermal effect on titanium and nickel are not drastically different and the sintering at about 200°C should be similar for all the first row transition metals.

I-C) Physical Properties of Transition Metal Compounds

Several properties of transition metals and their compounds are relevant to understanding the products and kinetics of the reactions to be discussed herein. Some, such as hydrogen solubility, thermodynamic stability and lattice structures, are discussed in detail in the appendices and will not be pursued further in the introduction.

Based on the principles of molecular orbital or crystal field theory, trends in most thermodynamic properties vary predictably across the first row of transition metals. The relationship between divalent halide lattice energy and metal cation is double humped with a minimum at manganese(II), a d^5 structure (Figure I-1). The same type of relationship holds for heats of hydration and ionic radii of divalent cations. For trivalent cations, on the other hand, the turning point occurs at iron, also a d^5 structure (Orgel, 1960).

In each of these high spin species the cation is octahedrally coordinated, splitting the 3d orbitals into two sets (t_{2g} and e_g) of non-degenerate states. In terms of molecular orbital theory, t_{2g} is non-bonding and e_g antibonding in this environment. Introducing electrons into

t_{2g} orbitals would not affect the metal-ligand bond strength whereas introducing them into e_g orbitals would weaken it.

FIGURE I-1 (Dunn, 1965)

Lattice Energies of the Transition Metal Dihalides

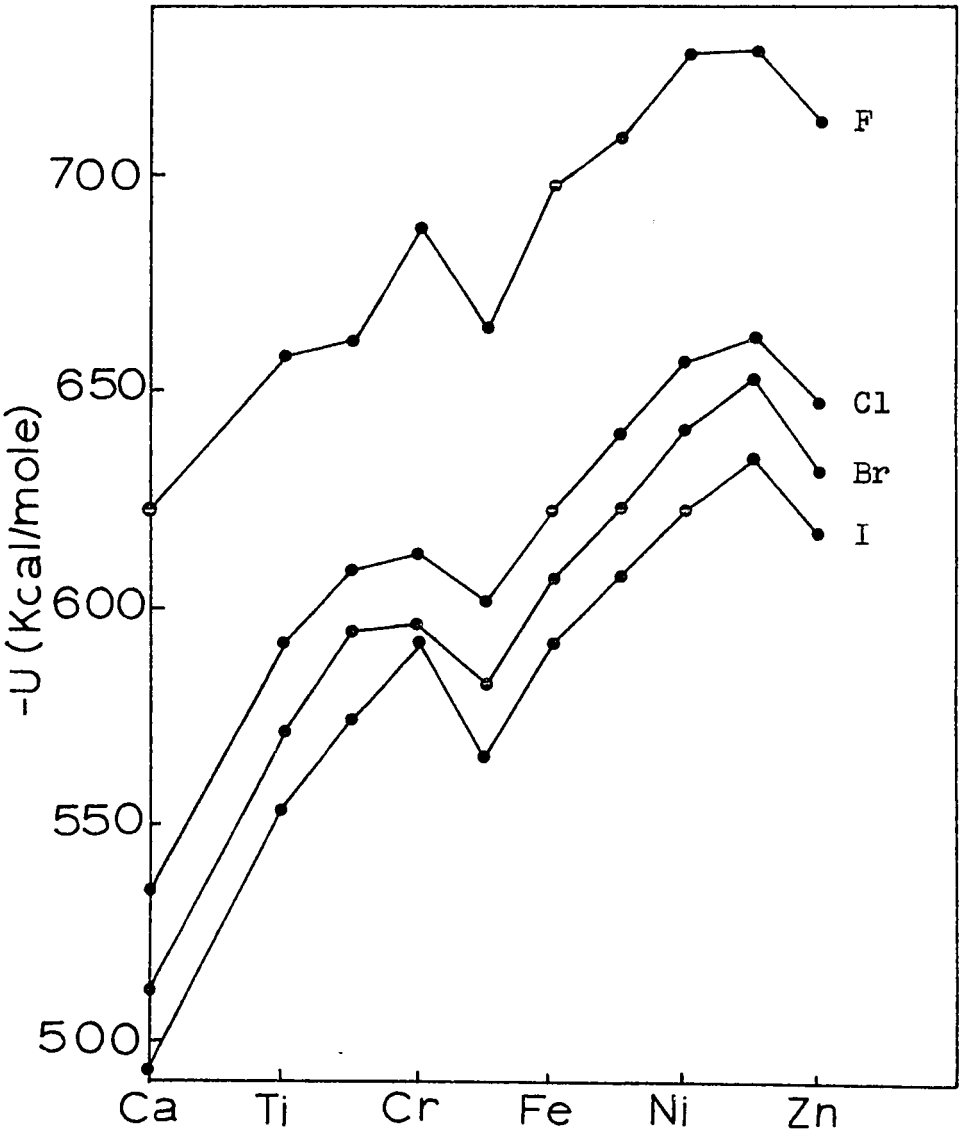

In terms of crystal field theory, t_{2g} orbitals interact less than e_g orbitals with the ligands. Thus, electrons in t_{2g} orbitals would cause less electron-electron repulsion and lead to stronger bonding than those in e_g orbitals. Therefore, high spin d^0, d^5 and d^{10} complexes appear as in the absence of orbital splitting and the others deviate from this ideal behavior. Hence, properties such as lattice energy and heats of hydration should and do vary in similar fashion to ionic radius and bond strength.

I-D) Homogeneous Olefin Forming Reactions

Homogeneous olefin forming reactions have been investigated in both solution and the gas phase. In solution, a variety of reaction mechanisms have been observed such as E-1, E-2, E-1cb and radical processes. These are distinguishable by their kinetics, products, solvent and substituent effects or isotopic labelling. Although elimination reactions frequently occur in competition with substitution reactions, each catagory is clearly defined and distinguishable.

While in solution, solvent molecules can participate in the activation process, this is not possible in the gas phase. Hence, pyrolytic reactions proceed with greater difficulty and are generally conducted at several hundred degrees.

Hydrogen halide elimination from

haloalkanes is one of four important types of pyrolytic olefin forming reactions. The others are decompositions of carboxylic esters, xanthates (the Chugaev reaction), and amine oxides (the Cope reaction). The Chugaev and Cope reactions are favored as preparative techniques because they can be conducted at lower temperatures with no isomerization of resulting olefins. However, from a mechanistic viewpoint, the dehydrohalogenation of haloalkanes has been studied most extensively.

Most studies of pyrolytic dehydrohalogenations have been conducted by Maccoll and his coworkers and have recently been reviewed (Maccoll, 1964). Haloalkane decompositions were generally conducted between 400-500°C in vessels previously coated with a carbon film to avoid surface catalysis. Reactions of chlorides, bromides and iodides were first order in haloalkane with pre-exponential factors very close to 10^{13} sec^{-1}, the value predicted by collision theory. They were so closely clustered and so randomly distributed around 10^{13} that changes in reaction rate were attributed solely to variations in activation energy. These were generally between 40 and 60 Kcal/mole in the order chlorides > bromides > iodides.

Some reactions proceeded contrary to the general simple molecular mechanisms. For example, primary bromides, halomethanes and dichlorides dehydrohalogenated by chain mechanisms (Barton and Howlett, 1949) and

iodoalkanes decomposed to iodine, olefin and paraffin (Benson, 1962). In addition, with no β-hydrogen 1-chloro-2,2-dimethylpropane generated a mixture of butenes possibly representing the first gas phase Wagner-Meerwein rearrangement (Thomas, 1961). After dehydrohalogenation, the products could rearrange since hydrogen halides are known to catalyze cis-trans isomerization and double bond migration. Thus, the products always represent the thermodynamically most stable mixture of olefins.

The mechanism of formation of olefin and hydrogen halide from haloalkane by a molecular mechanism has been studied in detail. Possible contributions from radical processes have been eliminated using free radical inhibitors such as propene and cyclohexene (Maccoll, 1957). Based on changes in activation energy with structural variations, Maccoll has proposed a mechanism for haloalkane pyrolyses which differs from the Ei cis elimination normally accepted for ester, xanthate and amine oxide decompositions. The effects of α and β methylation, α and β phenylation, β vinylation, and α methoxy substitution very closely parallel those found for E1 and SN1 reactions in solution (Maccoll and Thomas, 1955). In addition, for the methyl series, changes in heterolytic bond dissociation energy more closely parallel changes in activation energies than do homolytic bond dissociation energies.

This led Maccoll and Thomas (1955) to propose a 'quasi-heterolytic transition state involving

considerable charge separation in the carbon-halogen bond. Dissociated ions could not result since that would require between 150 and 200 Kcal/mole; however, ion pairs were suggested.

I-E) Self Hydrogenation and Retentive Adsorption of Mono-olefins Induced by Transition Metals

Hydrogenation of several olefins and other unsaturated hydrocarbons, both in the presence and absence of hydrogen, has been reviewed in detail by Bond (1962). Generation of paraffin from olefin in the absence of an independent supply of hydrogen has been termed self hydrogenation. The self hydrogenation of ethylene has been investigated on nickel (Beeck, 1950; Jenkins and Rideal, 1955), tungsten (Trapnell, 1952), palladium (Stephens, 1959) and iridium (Roberts, 1963). Only Roberts utilized ultrahigh vacuum, so whether the other catalysts truly represented the metal surface is unknown.

The similar behavior of each of the metals is described by the following sequence of reactions. Two processes occurred, retentive adsorption where hydrocarbon residues remained on the surface and hydrogenation where paraffin was released into the gas phase. On nickel, tungsten and palladium, approximately the first quarter of a monolayer equivalent of ethylene was retentively adsorbed. Admission of another aliquot resulted in the instantaneous generation of traces of ethane along with extensive retentive

adsorption. Subsequent doses were progressively less retentively adsorbed and less hydrogenated until the film eventually became inactive in both respects.

With iridium, the first dose of 1.5×10^{18} ethylene molecules was only 70% retentively adsorbed and ethane was the predominant product. However, traces of methane and hydrogen were also detected. Reaction with a larger initial dose (2.4×10^{18} molecules) was incomplete. Roberts did not specify surface areas so this may have been quantitatively as well as qualitatively the same as for the other three metals.

Rideal and Stephens explained the reactions of ethylene on nickel and palladium, in terms of surface induced dissociation of ethylene into chemisorbed acetylenic residues and hydrogen atoms respectively. Surface hydrogen could then have been used to generate paraffin either by reaction with non-chemisorbed ethylene (nickel) or acetylinic residues (palladium). The decrease in reaction rate was attributed to hydrocarbon residues. Studies of the heats of adsorption of ethylene with several transition metals (Beeck, 1950) suggests as the order of reactivity toward olefin adsorption: $Ta \approx W \approx Cr > Fe \approx Ni \approx Rh > Cu \approx Au$.

Although studied in greater detail and more fully understood, hydrogenation in the presence of hydrogen will not be discussed since it is not directly relevant to the reactions studied herein -see Bond (1964) for review.

I-F) Heterogeneous Dehydrohalogenation of Haloalkanes on Non-transition Metal Surfaces

Haloalkanes have been heterogeneously dehydrohalogenated to olefin and hydrogen halide on surfaces of the alkali metal halides (Noller, 1956). These reactions were conducted on heated beds of the desired catalyst with the product vapors collected in expandable sacs and measured manometrically (Schwab, 1946).

Noller determined activation parameters for the dehydrohalogenations of chloroethane, 1-chloropropane, 2-chloropropane, 1-chlorobutane, 2-chlorobutane, and 2-chloro-2-methylpropane. Activation energies varied from 8 Kcal/mole for 2-chloro-2-methylpropane on RbCl at about 100°C to 53 Kcal/mole for 1-chloropropane on KCl at about 400°C. In general, there was a compensation effect between frequency factor and activation energy.

Based on this data, Noller proposed that activation energy was related to metal halide lattice spacing and suggested that the surface facilitated heterolytic cleavage of both the C-Cl and C-H bonds. Similar to Balandin's multiplet theory, this required that the haloalkane fit properly into the surface site to induce the maximal effect. The required spacing would vary among the chloroalkanes causing variations in activation energy. This mechanism is similar to that proposed by Maccoll and Thomas (1955) for homogeneous

reactions.

Schwab and Noller (1954) also examined the dehydrohalogenation of chloroethane on SiO_2, Al_2O_3 and $CaCl_2$ surfaces finding activation energies of 24.5, 13.2 and 11.4 Kcal/mole respectively. On alkali metal chloride surfaces, Swinbourne (Maccoll, 1964) studied the dehydrochlorination of chlorocyclohexane finding activation energies of 11, 13, 17 and 25 Kcal/mole for LiCl, NaCl, KCl and RbCl respectively.

More recently, Anderson and McConkey (1967) investigated the reactions of chloromethane and dichloromethane on sodium surfaces deposited under high vacuum. These generated gas phase methane, ethane and ethylene with all the chlorine and some of the carbon retained by the surface. In the case of chloromethane, the reaction was photosensitive and seemed to occur between surface methyl and chloromethyl anions.

I-G) Heterogeneous Dehydrohalogenation of Haloalkanes on Transition Metal Surfaces

I-G-1) General

Haloalkane dehydrohalogenation reactions have been more thoroughly studied on transition metals than on the main group metals. The products, the kinetics and the possibility of reversible carbon-halogen dissociation have been examined and will be discussed in that order.

Noller and Ostemeier (1959) studied the reactions of chloroalkanes on transition metal oxides, nitrides, and carbides. The same set of chloroalkanes and the same technique was utilized as with the alkali metals (Noller, 1956). Activation energies varied from 11 Kcal/mole for 2-chloro-2-methylpropane on TaC to 50 Kcal/mole for 1-chloropropane on Ta_2O_5. The same mechanism as for the alkali metals was suggested with the surface acting to facilitate heterolytic carbon-halogen bond breaking.

The adsorption and reaction of chloromethane on films of nickel, palladium, platinum, tungsten, cobalt, manganese and titanium were studied by Anderson (1968) between 0 and 250°C. All the chlorine was retained by each film but the gas phase products differed. Methane, ethane and ethylene evolved from titanium, methane and ethane from palladium and methane and hydrogen from the others. Rapid retentive adsorption occurred at 0°C on clean films but, on lightly halided surfaces this decreased markedly.

Several studies of hydrogenolysis of haloalkanes by transition metal surfaces have been conducted but, will not be discussed in detail (Addy and Bond, 1957; Kemball and Campbell, 1961 and 1963; Anderson, 1968).

Radio tracer and deuterium labelling experiments designed to determine the reversibility of dissociative haloalkane adsorption on transition metal surfaces

have been performed. Using a mixture of ^{35}Cl and ^{13}C labelled chloromethane, Anderson (1968) concluded that carbon-chlorine bond rupture was irreversible on titanium. Cockelbergs (1955 and 1959), also using radio tracer techniques found that exchange occurred between chloromethane and hydrogen chloride on tungsten and molybdenum surfaces.

Deuterium exchange during hydrogenolysis of haloalkanes on transition metals surfaces has also been investigated (Campbell and Kemball 1961 and 1963; Anderson, 1967; Addy and Bond 1957; Morrison and Krieger, 1968). In no case was deuterated parent haloalkane detected initially; however, as hydrogenolysis proceeded, deuterated products and some deuterated haloalkane were formed. Campbell suggested that deuterated products arose from reversible rupture of the carbon-chlorine bond allowing deuterated isobutane to equilibrate with the parent haloalkane. Morrison and Krieger also showed for iodoalkanes that exchange occurred.

I-G-2) Harrod and Summers

Dehydrohalogenation of gaseous haloalkanes on atomically clean titanium films have recently been studied in this laboratory (Harrod and Summers, 1971; Summers and Harrod, 1972). Films were deposited under ultra-high vacuum and reactions on both clean and succesively halided surfaces were investigated. For a given haloalkane, reaction differed markedly between unreacted films and halided surfaces.

Four series of haloalkanes were investigated: 1-methyl substituted chloroethanes, 2-methyl substituted chloroethanes, the four 1-halopropanes and some dichloropropanes. Among these materials, three distinct types of reactions were discovered on halided surfaces.

Reactions on clean films involved introducing 10^{-2} Torr (probably less than one monolayer) of reactant to the freshly deposited metal. In each case, the reaction proceeded too rapidly for kinetic investigation, producing primarily a surface chloride and the paraffin and/or olefin resulting from dehydrohalogenation. However, they varied markedly with regard to products, degree of retentive adsorption, extent of reaction and amount of film deactivation. For example, products varied from 100% olefin for 2-chloro-2-methylpropane to 90% paraffin for 1-chloro-2,2-dimethylpropane, the degree of retentive adsorption from nearly 100% for 1-chloro-2,2-dimethylpropane to none for most of the reactants, the extent of reaction from 100% for 1-fluoropropane to 30% for 2-chloroethane, and the amount of film deactivation from 100% for most of the reactants to almost none for 1-fluoropropane.

In addition, clean film reactivity was inversely proportional to reaction temperature, with films studied at 200°C being extremely unreactive. Generally, reactivity was related more to the C-X bond strength than to the formation of an impermeable surface layer.

Anomalous behavior was found for 1-chloro-2,2-dimethylpropane which was almost completely adsorbed without subsequent production of gas phase products and 1-fluoropropane which displayed continuing reactivity even after several 10^{-2} Torr aliquots had reacted. The latter was explained in terms of the small size of the fluoride ion and the large TiF bond strength, encouraging facile removal of the surface fluoride into the bulk of the metal and the rapid regeneration of active surface sites.

Subsequent reactions on halided surfaces proceeded at constant rate with consistent products generally between 150 and 250°C. The three observed reaction schemes differed in products, in rate and in activation parameters.

For the first scheme(non-catalytic) the surface did not act as a true catalyst since it retained all the chloride and some of the hydrogen, generating a gaseous mixture of olefin and paraffin. Reaction continued throughout the deposition of a cohesive titanium halide layer, yet exhibited no dependence on its thickness. It followed half order kinetics throughout the explored temperature range with the activation parameters shown in Table I-1. 1-Chloroethane, 1-chloro, bromo and iodopropane, 1,2-dichloropropane and 1,3-dichloropropane reacted in this manner. Both olefin and paraffin were formed by half order kinetics with the paraffin fraction increasing both with increased film reaction and for higher reactant pressures.

TABLE I-1

Some Properties of Dehydrohalogenation Reactions of Haloalkanes on Titanium

reactant	temp. range (°C)	$P_Q \times 10^2$ (Torr)	activ. energy (Kcal)	$\log_{10} A$	relative reactivity
hydrogen chloride	235	1.0	-	-	1
chloromethane	200	0.5	-	-	10
chloroethane	200-240	1.0	23.5	5.7	50
1-chloropropane	180-220	1.0	23.0	6.0	50
1-bromopropane	195-225	1.0	27.5	7.8	50
1-iodopropane	190-220	1.0	29.5	9.0	50
1-fluoropropane	60-100	1.0	20.5	10.2	10^8
2-chloropropane	100-180	1.0 25.0	8.7 15.2	1.3 4.6	10^3
1-chloro-2-methyl propane	160-205	1.0 5.0	12.6 15.2	2.4 4.9	150
2-chloro-2-methyl propane	30-70	2.8	15.4	7.5	10^9
1-chloro-2,2-dimethylpropane	160-210	1.0 2.5	13.9 15.0	4.0 3.3	500
1,2dichloropropane	165-205	1.0	24.0	6.6	50
1,3dichloropropane	200-230	1.0	27.0	8.0	50
1,3dichloro-2,2-dimethylpropane	245	1.0	-	-	500

The half order kinetics were explained by the mechanism shown in Equations I-2 to I-6.

$$RCH_2CH_2X + 2* \underset{k_{-1}}{\overset{k_1}{\rightleftharpoons}} RCH_2CH_2* + X* \qquad \text{I-2}$$

$$RCH_2CH_2* \xrightarrow{k_2} RCH{=}CH_2 + H* \qquad \text{I-3}$$

$$X* \xrightarrow{k_3} * + X_{lattice} \qquad \text{I-4}$$

$$RCH_2CH_2* + H* \xrightarrow{k_4} RCH_2CH_3 + 2* \qquad \text{I-5}$$

$$H* \xrightarrow{k_5} * + H_{lattice} \qquad \text{I-6}$$

Assuming that the dissociative equilibrium was rapid and the diffusion of hydride rapid and reversible, rate control was ascribed to the production of surface sites (*) by reactions I-2, I-3 and I-4. Hydride adsorption could be either competitive or non-competitive and diffusion either a rapid equilibrium with a lattice or a steady state without affecting reaction order.

The resultant rate expression is shown in Equation I-7.

$$\frac{-d[RCH_2CH_2X]}{dt} = \left[\frac{k_1 k_3 (k_2 + k_4 d[H*])}{k_{-1}}\right]^{\frac{1}{2}} \frac{[*][RCH_2CH_2X]}{} \qquad \text{I-7}$$

A second type of non-catalytic behavior was found for the dehydrofluorination of 1-fluoropropane. This generated the same products as the previous non-catalytic

reaction, but by first order kinetics. Reaction was very rapid with both the clean film and subsequent reactions producing about 80% olefin. Activation parameters and reaction temperatures are again listed in Table I-1.

In this case, rate control was attributed to a non-equilibrium dissociation onto the surface with all subsequent steps proceeding rapidly. As with the clean film, the extreme reactivity was attributed to the ready availability of surface sites facilitated by the rapid diffusion of fluoride into the metal lattice.

Thirdly, a first order catalytic dehydrochlorination producing an equi-molar mixture of HCl and olefin was observed. This generally proceeded on more heavily halided films at lower temperature and with lower activation energy than non-catalytic decompositions (Table I-1). 2-Chloropropane, 1-chloro-2-methylpropane, 2-chloro-2-methylpropane and 1-chloro-2,2-dimethylpropane followed this path. Before settling into the catalytic pattern, each of these reactions proceeded through a brief non-catalytic stage during which paraffin and surface halide were formed.

The kinetics have been explained by various mechanisms. Most simply, the surface might facilitate a concerted elimination of HCl in much the same manner as proposed for homogeneous dehydrohalogenations (Maccoll, 1964).

However, another interpretation would be that the haloalkane was first dissociated as in Equation I-2 followed by a rate controlling reactive desorption of adjacent surface alkyl and surface halide (Summers, 1970).

Hydrogen chloride was found to decompose very slowly into hydrogen and surface chloride by first order kinetics. Chloromethane also decomposed with difficulty generating surface chloride, methane and traces of ethane.

Some insight into the reasons for the various mechanisms resulted from comparing the properties of the reagents proceeding by the different schemes. The tendency to react catalytically was not related to the free energy for homogeneous dehydrohalogenation. Thus, the differences in behavior must be attributed to kinetic control and the two types of reaction must have proceeded by different mechanisms.

The variation in rates of catalytic reactions was due to changes in Arrhenius pre-exponential factors rather than to activation energies. 1-Halopropanes proceeded by the non-catalytic scheme and branched molecules by the catalytic path, suggesting that the presence of readily available hydrogens on methyl branches may be required for catalytic behavior.

At elevated temperatures, 2-chloropropane generated paraffin suggesting that the two types of reaction were competitive and at lower temperatures the reaction with a lower activation energy predominated. In addition, as opposed to the non-catalytic reaction, activation energies for catalytic reactions increased with initial pressure, possibly due to the decrease in heat of adsorption as the surface became more fully covered.

I-H) Surface Site Specificity and the Multiplet Hypothesis

As postulated by Balandin (1929), the multiplet theory states that adsorption of a gas onto a surface frequently involves more than one site on the gas molecule and a specific geometrical arrangement on the surface. Hence, lattice spacing is critical to effective adsorption. Geometrical factors, in addition to electronic considerations, have been utilized consistently to account for specific catalytic behavior (Balandin, 1969).

Geometrical considerations have been employed to explain the specific decomposition of ethanol to either ethylene and water or acetaldehyde and hydrogen Beeck (1939a, 1939b) found that the activity of nickel surfaces toward the hydrogenation of ethylene depended upon the specific crystal face exposed. A five fold increase in activity was detected changing from polycrystalline catalyst to only the (110) face. As mentioned in Section I-F, Noller

(1956,1959) evoked the same reasoning to explain activation energies among the alkali metal catalyzed dehydrochlorinations of chloroalkanes.

Adsorption specificity in the form of domains has been detected for simple gases chemisorbed on metal surfaces. Domains of geometrically different orientations were detected for the adsorption of carbon monoxide on palladium (Park, 1968) and possibly for oxygen and nitrogen on all the transition metals (May, 1970).

I-I) Reactions on Non-uniform Surfaces

Except for carefully prepared single crystals, metal surfaces are structurally heterogeneous. Films prepared by evaporation onto clean surfaces are particularly heterogeneous, containing lattice defects such as grain boundaries, point defects as well as the variety of crystal planes present on even the most carefully prepared surfaces. The results of these heterogeneities are manifest in different thermodynamic and kinetic properties on different parts of the same surface.

Short of determining the properties of each type of surface site, surfaces have been treated as containing continuous distributions of surface activities. This latter approach has been used most extensively since identification of individual sites is generally impossible (Halsey and Taylor, 1947; Young and Crowell, 1962).

On different sections of a heterogeneous surface, both heats and entropies of adsorption will change. The general trend is that a high heat of adsorption is associated with a large lossin entropy. Thus, there is a compensating effect and the free energy of adsorption changes less than either of its components.

Kinetic effects are more pertinent to the present discussion and result from the distribution of activation parameters over the surface. The rate constant, rather than being described in terms of a single set of activation parameters, must be described in terms of many different sets. As for heats and entropies of adsorption, there is generally a compensating effect of energies and entropies of activation on a given surface.

Halsey (1949) has shown that on heterogeneous surfaces the kinetics may be different from those normally expected for the same reaction on a uniform surface. Recognizing that on various parts of a non-uniform surface, different processes may be rate controlling (adsorption, reaction or desorption), he concluded that on a specific site the greater the heat of adsorption of reactant the less the activation energy for reaction and the greater the activation energy for desorption of products. The first conclusion is irrefutable; however, the latter is not generally true It would be true only if adsorption and desorption were occurring

without surface rearrangement. However, where there is a significant difference between the adsorbed and desorbed species this need not generally be true.

Halsey derived an expression for unimolecular decomposition of a molecule on a surface. This expression contained proportionality constant, r, between the activation energies for adsorption and desorption. This proportionality constant is treated as an adjustable parameter and is used to bring the theory into accord with experimentally observed kinetics. Thus, it seems that any kinetics could be explained by judicious choice of 'r'. In addition, this treatment does not apply to reactions for which reactants and products are not competitively adsorbed since a relationship must be obtained between $\theta_{reactant}$ and $\theta_{product}$. The same theory is used by Halsey (1963) to explain the kinetics for the reaction of hydrogen with ethylene; however, all the same assumptions were made and 'r' was chosen to bring the theory into agreement with the observed kinetics.

II) EXPERIMENTAL PROCEDURES

II-A) Ultrahigh Vacuum Apparatus

All experiments conducted on atomically clean surfaces were performed in a standard ultrahigh vacuum system (Roberts, 1963). As shown schematically in Figure II-1, this was constructed from four types of components: a pumping system, valves for isolating gases, analytical devices and a reaction vessel. The section enclosed within dotted lines was baked at 300°C to facilitate rapid production of ultrahigh vacuum. Except for metal components the system was constructed entirely of pyrex glass.

Only a general outline of the apparatus is presented here, since it is described in detail elsewhere (Summers, 1970). However, all variations are thoroughly delineated. Abbreviations for vacuum components refer to Figure II-1.

II-A-1) Pumping System

Pumping was performed by a three stage mercury diffusion pump backed by a mechanical pump. These were isolated from the reaction manifold by two liquid nitrogen cooled traps in series, T1 and T2, the latter being bakeable and filled only after bakeout.

II-A-2) Valves

Manipulation of gases within the

FIGURE II-1

Schematic Representation of Ultrahigh Vacuum Apparatus

CM = Capacitance Manometer

GP = Glass Port

IG = Ionization Gauge

MS = Mass Spectrometer

RV = Reaction Vessel

T = Trap

V = Valve

VL = Variable Leak

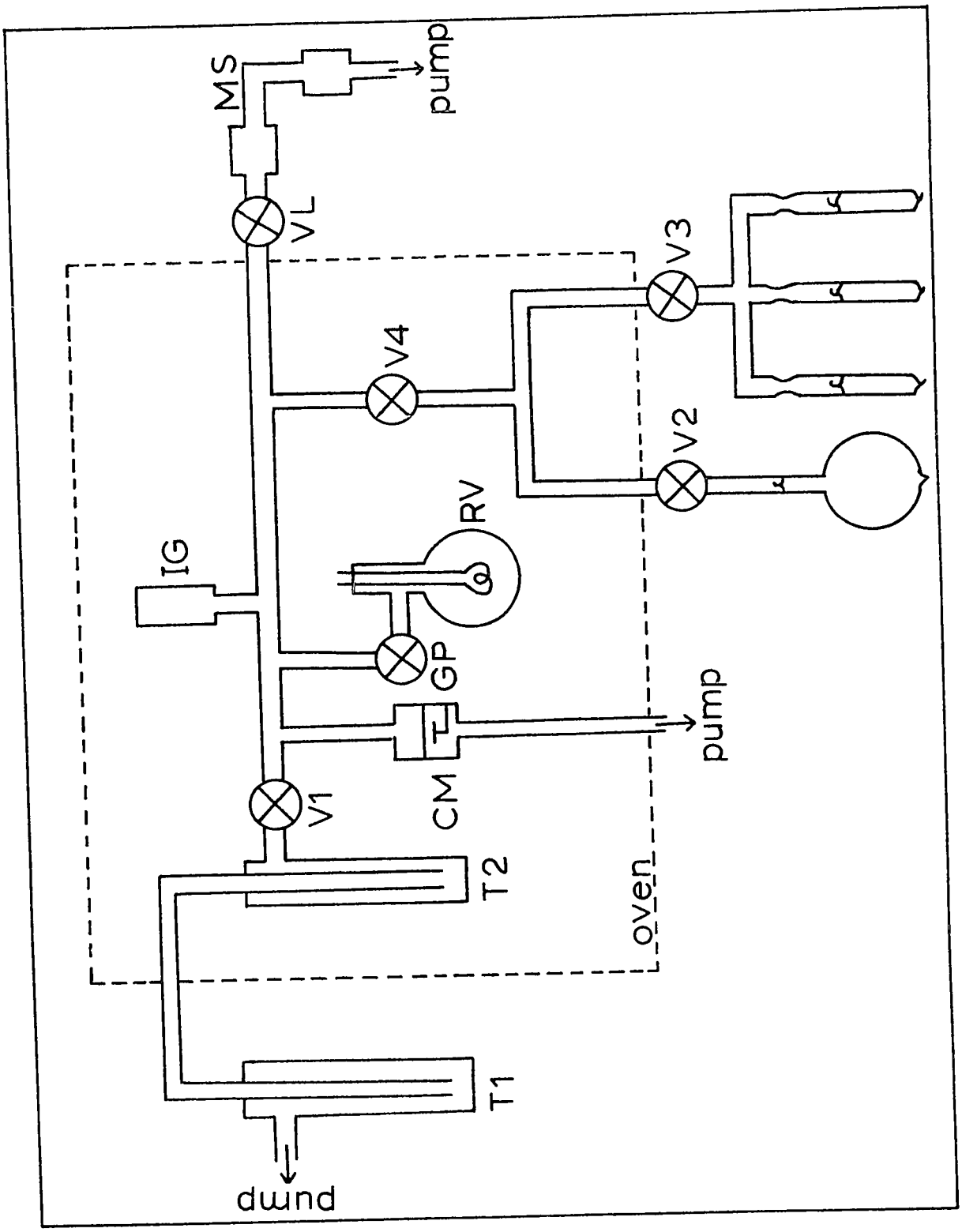
MS
pump
VL
V3
V4
V2
RV
IG
GP
pump
CM
V1
T2
oven
T1
dwnd

system was facilitated by five types of valves. A magnetically operated glass port was used for limited durations to isolate the reaction vessel at pressures up to 10^{-1} Torr. Break seals isolated gas sources during transport to the system and enabled them to be sequentially introduced.

In addition to glass valves, three types of bakeable metal valves were employed. Valves V1, V2, V3 and V4 comprised Granville Phillips type 'C' valve bodies, the former three being operated by standard drivers and the latter by a low torque driver. A Granville Phillips variable leak, CVL, was used to transmit very small aliquots of gas into the residual gas analyzer, MS.

II-A-3) Analytical Devices

Measurement of pressures within two ranges was required in the present study. Those below 10^{-4} Torr were detected by a bakeable Bayard-Alpert type ionization gauge, IG. Those between 10^{-2} and 1.0 Torr were monitored by a bakeable Granville Phillips capacitance manometer, CM.

Calibration of the capacitance manometer against a McLeod gauge for pressures between 5×10^{-3} and 10^{-1} Torr (using dry nitrogen) is shown in Figures II-2 and II-3. In some pressure ranges the McLeod gauge was not particularly sensitive and approximate error bars are indicated. Similar calibrations were conducted at higher pressures but were not

used extensively and are not included here. Performance was checked regularly and the calibration found to be consistent. It differed from that of Summers because a different sensing head was used.

Reaction products were analyzed mass spectrometrically using a residual gas analyzer, MS, with a range of 2-100 AMU. This was operated dynamically such that the desired peaks were scanned while a small amount of reaction mixture was admitted at a constant rate and removed by a pumping system. Each analysis required an immeasurably small quantity of reaction mixture.

II-A-4) Reaction Vessel

Reaction vessels, RV, were 300 ml round bottom flasks attached to the manifold by a sidearm. Manifold volumes were approximately 500 ml on each side of the glass port. Three tungsten electrical feedthroughs permitted resistive heating of filaments composed of the desired metal either pure or suspended on a support (Section II-D).

Constant temperature baths maintained temperatures from 0 to 250°C to within ± 1°C.

II-A-5) Protective Circuitry

In addition to electrical relays

FIGURE II-2

Calibration of Capacitance Manometer

Against McLeod Gauge

J-Scale

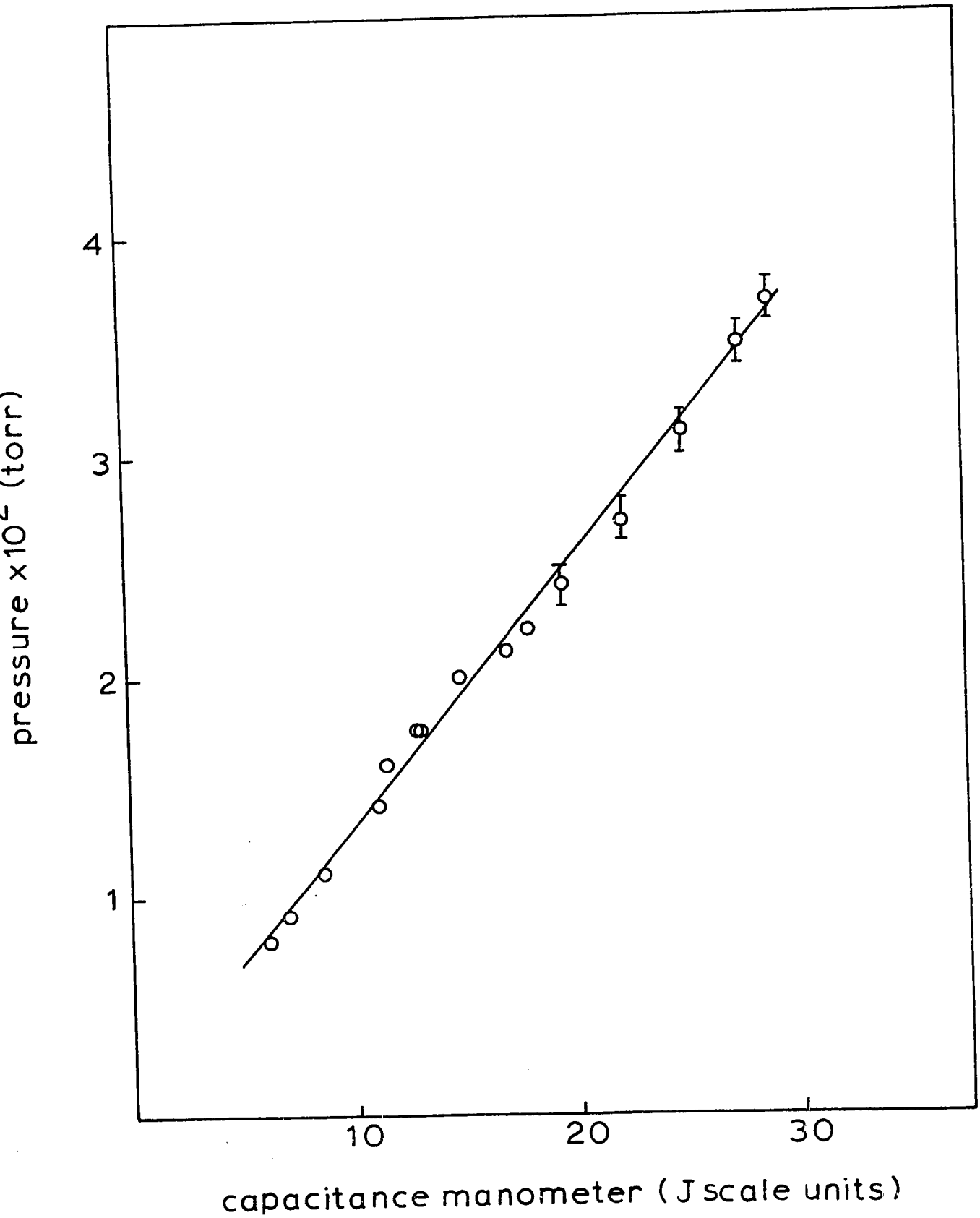
4
3
2
1
pressure x10^2 (torr)
10
20
30
capacitance manometer (J scale units)

FIGURE II - 3

Calibration of Capacitance Manometer

Against McLeod Gauge

H-Scale

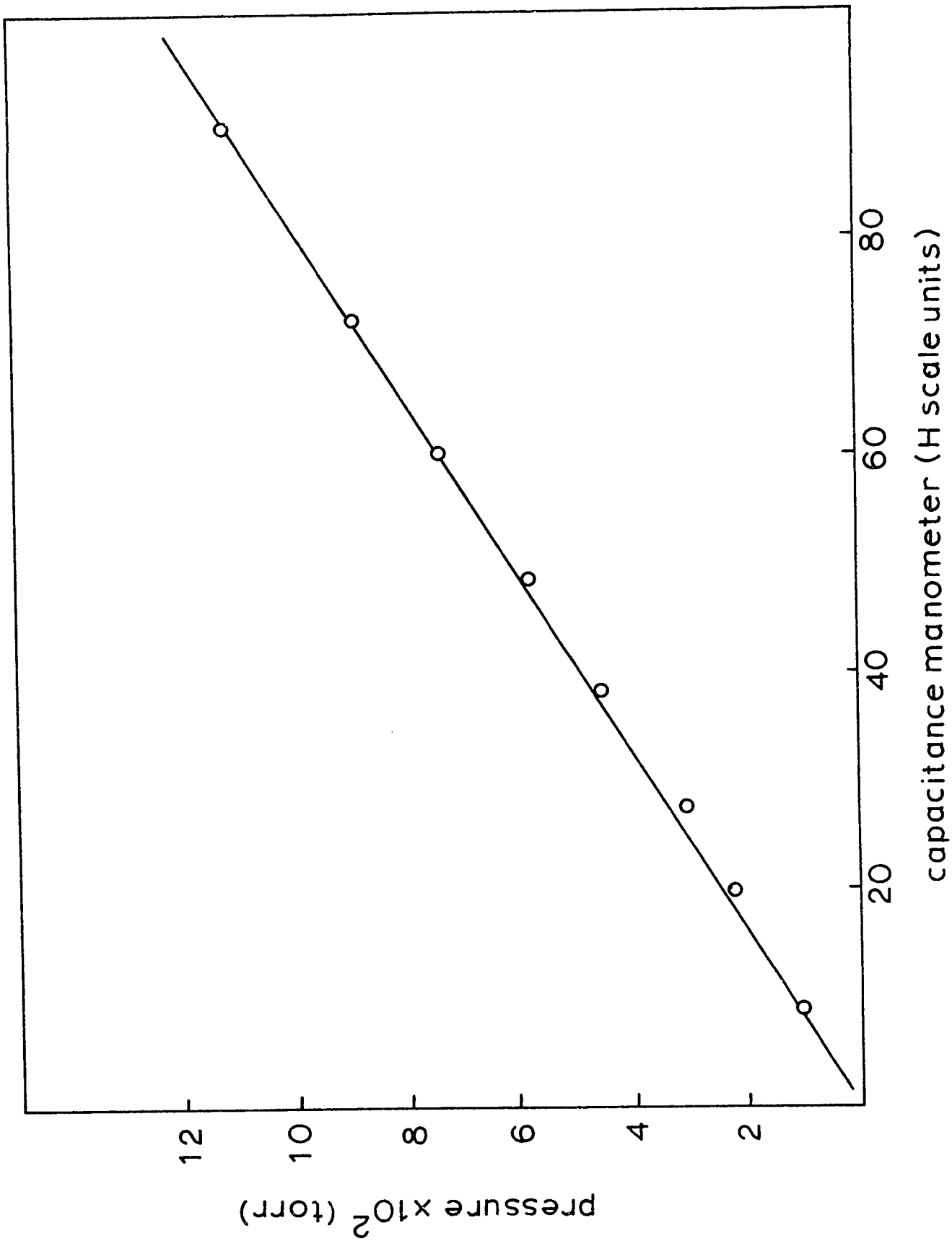
pressure x10^2 (torr)
12
10
8
6
4
2
20
40
60
80
capacitance manometer (H scale units)

designed to minimize damage in the event of a large pressure increase during bakeout, a United Electronic Controls J40X-271 water activated microswitch was incorporated to protect the apparatus against the frequent water shutdowns. Thus, both diffusion pumps would shut off at water pressures below 20lbs/in^2, about 1/3 the normal value.

II-B) Procedure for Reactions on Atomically Clean Surfaces

II-B-1) Sample Preparation and Residual Gas Analyzer Calibration

Samples were placed on the ultra-high vacuum apparatus both as gases and as volatile liquids. Each was contained in a pyrex vial and isolated from the reaction manifold by a break seal and valve V2 or V3. During calibration, several vials were on the line concurrently, yet the contents of each was studied individually by smashing the appropriate break seal, bleeding the gas into the reaction manifold and withdrawing the unused portion into its vial. A used vial could then be removed at a constriction placed above the break seal and the next sample studied in similar fashion. However, on a given film only two gases could be studied simultaneously since each was thoroughly outgassed before bakeout and isolated only by the metal valve.

Liquid samples were purified by vacuum

distillation from calcium hydride followed by thorough outgassing and sealing under vacuum. Gases were introduced into vials directly from the lecture bottle again followed by outgassing and sealing under vacuum. Prior to examination, each sample was outgassed to around 10^{-6} Torr on the ultrahigh vacuum line.

All gases were Matheson of Canada Limited C.P. grade (99% pure). Liquids were supplied by Eastman Kodak or Aldrich Chemical Companies and were the highest purity possible. Their purity was further verified by gas chromatography.

With a sample of each gas of a given reaction system (i.e. 1-chloropropane, propene and propane) attached to the gas inlets, the mass spectral fragmentation pattern and relative sensitivity was determined for each component (Appendix C). Sensitivities of product gases relative to the reactant alkyl halide were calculated from gas mixtures of known composition (Appendix A).

II-B-2) Preparation of the Ultrahigh Vacuum System

To prepare the system for an experiment, a new reaction vessel was attached and the entire system evacuated and leak tested. When the pressure reached about 10^{-6} Torr, the residual gas analyzer was calibrated. Then the

reactant gases were isolated from the manifold by valves V2 and V3 and the metal filaments outgassed by resistive heating. Filaments were maintained below their evaporation temperature but at red heat for at least 24 hours, at which time the pressure was usually on the 10^{-7} Torr scale.

While continuing to heat the filaments, the ion gauge grid was outgassed, non-bakeable portions of valves V1 and V4 removed, and the valves locked open. The electronics were removed from the capacitance manometer sensing head, the protective circuitry activated, and the oven frame installed. The system was baked at 300°C for about 15 hours. After cooling, both traps were filled with liquid nitrogen, valve V4 closed, and the system allowed to pump for about one hour. Using this technique, pressures around 10^{-9} Torr were obtained routinely.

A film of the desired metal was then deposited by resistive heating of the filaments (Section II-D).

II-B-3) Reaction and Analysis

After film deposition, the ionization gauge was shut off and the reaction vessel equilibrated for ten minutes at the desired temperature. With the glass valve closed, the desired quantity of reactant was admitted through

valve V4. The glass port was opened, the amount of reactant irreversibly adsorbed determined, and the subsequent reaction followed mass spectrometrically. The reaction manifold was then evacuated and the procedure repeated until no further reaction occurred at low temperature.

Reactions at elevated temperatures were studied in similar fashion, usually with the reaction vessel thermostatted between 150 and 250°C. When more than one reactant was studied on a given film, samples were withdrawn behind their respective valves by cooling with liquid nitrogen.

Kinetics were followed by recording mass spectra of the reaction mixture at various extents of reaction and analyzing these for composition as described in Appendix A. In addition, certain reactions were followed by characteristic changes in distinctive peaks as will be described separately in each case.

To collect data for Arrhenius plots, reactions were performed at various temperatures in a random manner with the first and last runs performed at the same temperature to assure that no alteration in film activity or reaction products had occurred during the series. Similar precautions were taken with a series of reactions at varying

pressures.

II-C) Experimental Limitations

II-C-1) Manifestations of Rate Controlling Diffusion

When analyzing devices are remote from a site of reaction, the apparent rate may be controlled by movement of products from the site of reaction to the analyzer. For gaseous systems, the reaction would then be temperature insensitive since gaseous diffusion is not an activated process. Likewise, were diffusion of reactant from the gas phase to the surface the slow step, a similar zero activation energy should be observed.

In the ultrahigh vacuum apparatus, the residual gas analyzer is separated from the reaction vessel by a manifold at ambient temperature. The reaction rates at which diffusion became slower than reaction were calculated for the first order dehydrochlorinations of 2-chloro-2-methylpropane and 2-chloropropane by determining the rate constant at which Arrhenius plots leveled out, indicating a large decrease in activation energy (Summers, 1970). For the former the rate was 8×10^{-4} Torr/sec and for the latter 4.4×10^{-4} Torr/sec.

For none of the present reactions did the slope of the Arrhenius plot drop off suddenly and approach

zero at higher temperatures. By this criterion, it is assumed that the rate controlling step occurs at the site of reaction and the calculated activation energy is a manifestation of this process.

II-C-2) Time Correction For Kinetic Studies

For a given set of reactions there was a constant time differential between the beginning of a mass spectral scan and the appearance of the desired peaks. Since time was designated as the start of a scan, each reaction would appear overly advanced for a given time.

As shown in Figure II-4, among other things, this caused the intercept for time order plots to be greater than zero. In this case, the first order reaction of 2-chloropropane on titanium was studied at 200 °C and 10^{-2} Torr. The residual gas analyzer scanned from 24 to 44 AMU and peaks 41 and 43 were used for analysis. The time between peaks 24 and 42 was 42 sec. Adding 42 sec to each time reading generated the lower line which intercepts the pressure axis at .008 compared to .042 for the uncorrected curve. That this was a consistent phenomenon was verified for several half and first order reactions.

Slopes of time order plots remained unaltered by the correction. The concentration order was likewise, unaffected since the correction was constant through-

out. However, it explains the consistently low intercept of time-pressure curves (Figure II-4). Thus, in no case were any kinetic parameters altered due to the use of uncorrected time readings.

II-D) Deposition of Metallic Films in Ultrahigh Vacuum

Films were deposited by evaporation either from wires of the pure metal or from electrolytically coated tungsten wires. Where possible, the former technique was used; however, wires of some of the metals were not available.

Films several thousand angstroms thick were deposited in around thirty minutes. Film thickness was not generally measured directly, but was estimated from the opacity of the bulb compared with films of known thickness.

II-D-1) Deposition from Pure Metal Wires

The approximate evaporation and melting temperatures for the metals deposited from pure wires are shown in Table II-1 (Roberts, 1963). Judging from their thermal characteristics, some of these should have been impossible to deposit by resistive heating. However, by carefully controlling filament temperature and using large surface areas, all were suitably evaporated.

FIGURE II-4

Time Correction For Kinetic Studies

○ time as recorded

△ time as recorded + 42 sec

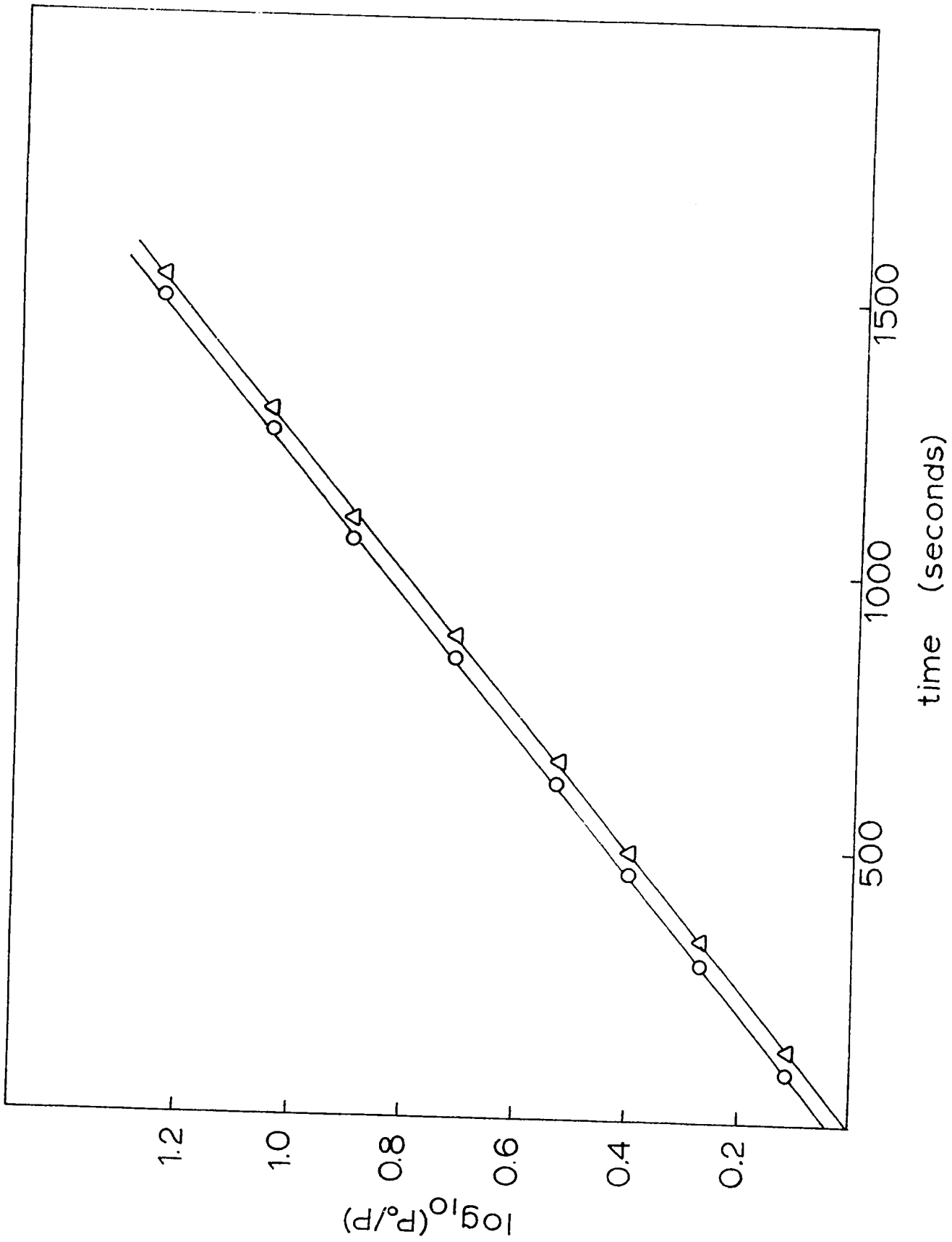
1.2
1.0
0.8
0.6
0.4
0.2
log10(P°/P)
500
1000
1500
time (seconds)

TABLE II-1

Thermal Properties of Metals Deposited From Pure Wires

Metal	T (melt) (°C)	T (evap) (°C)
titanium	1727	1546
vanadium	1697	1888
iron	1535	1447
cobalt	1478	1649
nickel	1455	1510

Listed below are some of their outgassing and deposition characteristics. Each 'U' shaped filament was 10 mil in diameter and about 3 in long. Wire (99.9% pure) was supplied by either A.D. MacKay Inc. or Alfa Inorganics Inc. For each metal, the pressure after deposition was around 10^{-9} Torr.

a) Titanium - Outgassing for two days was sufficient to keep the pressure around 10^{-9} Torr during evaporation. Deposition from two filaments was complete in twenty minutes.

b) Vanadium - Even after outgassing for four days the pressure increased to 10^{-7} Torr at the outset of evaporation. However, most deposition occurred with the pressure below 10^{-8} Torr. Four filaments were used and the evaporation required about 40 minutes.

c) Iron - After two days of outgassing, the pressure increased onto the 10^{-8} Torr scale at the start of evaporation. It rapidly decreased onto the 10^{-9} Torr scale for the remainder and deposition from two filaments was complete in twenty minutes.

d) Cobalt - Outgassing for two days was sufficient to keep the pressure on the 10^{-9} Torr scale during evaporation. Deposition from two filaments was complete in 20 minutes.

e) Nickel - Outgassing for two days was sufficient to keep the pressure in the 10^{-9} Torr scale during evaporation. Deposition from four filaments was complete in twenty minutes.

II-D-2) Deposition from Metal Coated Tungsten Wires

To investigate the possibility of tungsten contamination in films evaporated from coated tungsten wires, an uncoated tungsten wire was heated to temperatures far exceeding those used during deposition. After several hours no deposit was visible. On this basis, films deposited from electrolytically coated wires were assumed to be free from tungsten.

a) Chromium

Approximately 0.085 grams of chromium was electrolytically deposited on about 3 inches of U shaped tungsten wire. This filament was outgassed for two

days at constant temperature then heated to evaporation temperatures for short intervals to further drive off gas. During deposition, pressure remained below 10^{-8} Torr and for the latter part was around 10^{-9} Torr. Evaporation from a single filament was generally complete in about twenty minutes producing a film of standard thickness.

Electrolytic deposition was conducted with a circuit comprising 5-1½ volt batteries attached in series, an ammeter, a variable resistance and the stirred electrolyte bath. The bath contained 80 gm Cr_2O_3, 0.8 gm H_2SO_4 and 320 ml water. The anode was a lead sheet. The optimum current density was determined for each run separately but was generally around 2.65×10^5 ma/in^2 (4.11×10^4 ma/cm^2). Below this current density, deposition was too slow and above it, deposits were flakey and could be readily peeled from the wire. Using this technique, deposits were virtually pure chromium (Moore, 1945).

b) Manganese

Techniques similar to those described for chromium were used to electrolytically deposit and evaporate manganese. However, outgassing was more difficult and even after several days of both constant and variable temperature treatment the pressure at the outset of deposition rose to about 10^{-7} Torr. Nevertheless, it decreased rapidly and most

evaporation occurred at about 10^{-9} Torr. Deposition from a single filament was complete in about twenty minutes.

The electrolyte solution consisted of 218 gm $MnCl_2 \cdot 4H_2O$, 134 gm NH_4Cl, 67 gm $(NH_4)_2SO_4$, 1.4 gm KCNS and 670 gm water. The pH of the bath was maintained at 6-6.5. The circuit was the same as with chromium; however, the anode was a manganese platelet and the optimum current density was around $1.06 \times 10^5 ma/in^2$ ($1.65 \times 10^4 ma/cm^2$). Since manganese was more readily oxidized than chromium, air was kept away from the deposit by deeply immersing the cathode and avoiding any circulation. Taking these precautions, it was possible to obtain coherent deposits capable of being evaporated.

c) Copper

Although copper wires are readily available, they melt before evaporating at a significant rate. Consequently, copper films have been deposited from filaments consisting of 10 mil tungsten wire wrapped with 5 mil copper wire. Since copper does not wet tungsten, melting the copper by heating the filament caused it to form beads.

The filament was outgassed by heating it just below the melting point of copper. However, during deposition the copper melts and beads, initially

increasing the pressure to about 10^{-6} Torr. Deposition from a single filament was complete in ten minutes as the pressure gradually decreased.

Electrolytically coated wires also beaded and evolved more gas during evaporation.

II-E) Preparation of Deuterated Halocarbons

Deuterated 1-halopropanes and 1-halo-2-methylpropanes were required for halide exchange experiments (Section IV-B-3). To prepare 1-haloalkanes by reaction of DX with a terminal olefin would require anti-Markownikoff addition. Thus, they were synthesized by reduction of the appropriate aldehyde with lithium aluminum deuteride to the alcohol-1-d_1 and subsequent halo substitution. The resulting materials were 1-halopropanes-1-d_1 and 1-halo-2-methylpropanes-1-d_1.

The purity of each product was verified by gas chromatography and nmr as described in Section II-E-4.

II-E-1) Preparation of Alcohols-1-d_1

The deuterated alcohols 1-propanol-1-d_1 and 2-methyl-1-propanol-1-d_1 were prepared by the reaction of a 50% molar excess of lithium aluminum deuteride with propanal and methylpropanal respectively (Brown, 1951). Any excess lithium aluminum deuteride and the intermediate

tetraalkoxy aluminum(III) complex were subsequently hydrolyzed by sulfuric acid. The reactions are shown in Equation II-E-1 and II-E-2.

$$LiAlD_4 + 4RCH_2\text{-}CHO + 2H_2SO_4 \longrightarrow 4RCH_2CHDOH + \tfrac{1}{2}Li_2SO_4 + \tfrac{1}{2}Al_2(SO_4)_3 \qquad \text{II-E-1}$$

$$LiAlD_4 + 2H_2SO_4 \longrightarrow \tfrac{1}{2}Li_2SO_4 + \tfrac{1}{2}Al_2(SO_4)_3 + 4H_2 \qquad \text{II-E-2}$$

Reactions were conducted in a two necked flask fitted with a water cooled condenser and a dropping funnel. Aldehyde and ether were added to the dropping funnel and lithium aluminum deuteride and ether to the flask. The funnel was then slowly discharged into the stirred lithium aluminum deuteride slurry causing mild reflux. After addition was complete, (about one hour) 10 ml of water was added to destroy the excess lithium aluminum deuteride. The resulting thick white paste was dissolved by 20% sulfuric acid and the aqueous layer extracted several times with ether. Ether extracts were dried over potassium carbonate, distilled, and the alcohol dried over calcium hydride and vacuum distilled.

1-Propanol-1-d_1 was prepared from 3 gm lithium aluminum deuteride and 12.5 gm propanal with a 75% yield. 2-Methyl-1-propanol-1-d_1 was prepared from 2 gm lithium aluminum deuteride and 10.3 gm methylpropanal with a 70% yield.

Lithium aluminum deuteride was supplied by Stohler Isotope Chemicals and the aldehydes by Eastman Kodak. Aldehydes were distilled, propanal at 48-49°C and methylpropanal at 63-64°C.

II-E-2) Preparation of Bromoalkanes-1-d_1

Both bromoalkanes-1-d_1 were prepared from the previously deuterated alcohols by reaction with excess phosphorous tribromide as shown in Equation II-E-3 (Org. Syn. 1932a). In turn, phosphorous tribromide was prepared in situ by the reaction of yellow phosphorus with bromine (Equation II-E-4).

$$3RCHDOH + PBr_3 \longrightarrow 3RCHDBr + H_3PO_4 \qquad \text{II-E-3}$$

$$2P + 3Br_2 \longrightarrow 2PBr_3 \qquad \text{II-E-4}$$

The reaction was conducted in a 10ml two necked flask fitted with a water cooled condenser and a dropping funnel, and heated with an oil bath. Phosphorus and alcohol were placed in the flask and bromine in the dropping funnel. The mixture was heated under gentle reflux and bromine admitted slowly. Addition was complete in about one hour and the oil bath temperature increased about 15°C for another hour to insure completion of the reaction. The reaction mixture was distilled, the distillate extracted with 5% NaOH and water then vacuum distilled from $CaCl_2$.

1-Bromopropane-1-d_1 was prepared from 2.0 gm 1-propanol-1-d_1, 0.12 gm yellow phosphorous and 1.5 gm bromine with the oil bath at 115°C for reflux and 130-135°C to complete the reaction. The product was distilled at 70°C with a yield of 2.0 gm (50%).

1-Bromo-2-methylpropane-1-d_1 was prepared from 1.5 gm 2-methyl-1-propanol-1-d_1, 0.08 gm yellow phosphorus and 1.0 gm bromine with the oil bath at 125°C for reflux and at 135-140°C to complete the reaction. The product was distilled at 90°C with a yield of 0.9 gm (32%).

II-E-3) Preparation of Chloroalkanes-1-d_1

a) 1-Chloropropane-1-d_1

1-Chloropropane-1-d_1 was prepared by the zinc chloride catalyzed reaction of HCl with 1-propanol-1-d_1 as shown in Equation II-E-5 (Org. Syn., 1932b). The lack of specificity of this reaction led to formation of both 1-chloropropane and 2-chloropropane, necessitating separation of the product.

$$CH_3CH_2CHDOH + HCl \xrightarrow{ZnCl_2} CH_3CH_2CHDCl + H_2O \qquad \text{II-E-5}$$

The reaction was conducted in a 25 ml distilling flask heated by an oil bath, and the product distilled continuously. A solution of 13.6 gm zinc chloride,

8.7 gm 37% HCl and 3.1 gm 1-propanol-1-d_1 was placed in the flask and heated to 110°C. Product was distilled into an ice cooled flask. Reaction was complete in about one hour. The distillate was extracted with water, cold concentrated sulfuric acid, and 10% sodium carbonate, then dried over calcium chloride and vacuum distilled.

The mixture of chloroalkanes was separated using a 20% Carbowax 20M on AW Chrom 'P' 45/60 mesh column in a Hewlett Packard 775 Prepmaster gas chromatograph. The yield was 1.0 gm (30%).

b) 1-Chloro-2-methylpropane-1-d_1

1-Chloro-2-methylpropane could not be prepared by the afore mentioned procedure since the reaction product contained 80% of the rearranged material 2-chloro-2-methylpropane. Hence, phosphorous pentachloride was used to chlorinate the alcohol as shown in Equation II-E-6. Although this technique produced only 25% of the rearranged material, the product still required separation.

$$PCl_5 + 4(CH_3)_2CHCHDOH \longrightarrow 4(CH_3)_2CHCHDCl + HCl + H_3PO_4 \qquad \text{II-E-6}$$

The reaction was conducted in a 10 ml ice cooled flask fitted with a water cooled condenser. A two-fold molar excess of phosphorous pentachloride (8.7 gm) was carefully added through the condenser into 5.6 gm

2-methyl-1-propanol-1-d_1. This was accompanied by violent fizzing and was complete in 30 minutes. After warming to ambient temperature for one hour, the product was distilled, extracted with water and 10% sodium carbonate, and vacuum distilled from $CaCl_2$.

The mixture was separated using the same gas chromatograph with a 10% SE-30 on AW Chrom 'W' 30/60 mesh column. The yield was 0.82 gm (15%).

II-E-4) Analysis of Products

The composition and purity of each of the alcohols and halocarbons was determined by gas chromatography and nmr. While nmr revealed the overall structure, the presence of deuterium and the possible presence of major impurities, gas chromatography provided a semiquantitative measure of purity and verified the nature of both the desired product and impurities.

a) Alcohols

By gas chromatography, both were found to contain less than 1% ether as the only impurity. Retention times agreed with those for the pure alcohols. The nmr spectra agreed with the proposed structures and integration verified the presence of a single hydrogen atom on the 1-carbon atom.

b) Bromoalkanes

The nmr traces verified the presence of a single hydrogen atom on the 1-carbon atom. About 3% 2-bromopropane-1-d_1 in the 1-bromopropane-1-d_1 and about 4% 2-bromo-2-methylpropane-1-d_1 in the 1-bromo-2-methylpropane-1-d_1 were detected with both nmr and gas chromatography. Retention times agreed with those for the pure bromoalkanes.

c) Chloroalkanes

The nmr traces verified the presence of a single hydrogen atom on the 1-carbon atom. Both nmr and gas chromatography revealed less than 1% 2-chloropropane-1-d_1 in the 1-chloropropane-1-d_1 and 1% 2-chloro-2-methylpropane-1-d_1 in the 1-chloro-2-methylpropane-1-d_1 as the only impurities. Retention times agreed with those for the pure chloroalkanes.

III) REACTIONS OF HALOALKANES WITH THE FIRST ROW TRANSITION METALS

III-A) General Comments

The reactions of several haloalkanes with clean titanium surfaces were investigated in this laboratory (Summers, 1970) and have been reviewed in Section I- G . All the reactions studied were grouped in three general categories according to their overall characteristics and designated as listed below:

1) initial reactions on clean films,
2) non-catalytic reactions on halided surfaces, and
3) catalytic reactions on halided surfaces.

The first category refers to the initial few reactions on the freshly deposited film. Conducted at low temperatures, these produced paraffin and olefin with the same carbon skeleton as the parent haloalkane while the film retained all the chloride. The rate of low temperature reaction rapidly decreased and the film was heated to generate the reactions in the second and third groupings.

Under these reaction conditions, non-catalytic dehydrochlorination proceeded to the same paraffin and olefin while the film retained all the chloride and some hydrogen. The catalytic reaction, on the other hand,

generated an equimolar mixture of hydrogen chloride and olefin. Both schemes resulted in much greater reaction rates than those for homogeneous dehydrohalogenation; however, in the former the surface did not act as a true catalyst but formed a surface chloride as one of the products.

This chapter describes studies of the reactions of typical haloalkanes for both the non-catalytic and catalytic categories with the first row transition metals from vanadium through copper. While several haloalkanes fell into each category, 1-chloropropane was selected to typify the non-catalytic scheme and 1-chloro-2-methylpropane the catalytic reaction.

As several of the properties of the reactions with the other metals have been similar to those of titanium, the afore mentioned groupings have been retained and used to divide the experimental results in this chapter. Following this is an integrated discussion of the various modes of behavior. More detailed accounts of individual reactions are presented immediately prior to the particular section to serve as a more direct reference. Where necessary, some reactions with titanium have been re-examined. A distinction between this and the prior work of

Harrod and Summers is emphasized.

Throughout this chapter and Chapter IV, P_o refers to an initial reactant pressure and P to the actual reactant pressure. Unless specified otherwise, the reactant is a haloalkane.

The mathematical techniques used to analyze the data are described in Appendix A and the mass spectral patterns are listed in Appendix C. Each reaction was studied by the procedures outlined in Section II unless specifically stated.

The term, rate constant, must be qualified for these reactions. Since this constant contains a term for the concentration of surface sites and is sometimes likely a combination of individual rate constants, these are not rate constants in a strict sense. A term like pseudo rate constant or rate coefficient might be substituted but, realizing these limitations, rate constant has been used throughout for the sake of simplicity. Likewise, the activation energies may be complex and undoubtedly contain heats of adsorption.

III-B) Experimental Results

III-B-1) Initial Reactions

III-B-1-a) Introductory Comments

The initial low temperature reactions of 1-chloropropane and 1-chloro-2-methylpropane with atomically clean films of the first row transition metals are reported in this section. As outlined in Section I- G , these and several other haloalkanes had been examined in similar fashion with titanium (Summers, 1970). Titanium retained all the chloride and some hydrogen from the reacted molecules while the gas phase products were paraffin and olefin both with the same carbon structure as the reactant haloalkane (total pressure constant). About 3.5×10^{17} molecules reacted before the film was rendered inactive at low temperatures.

Similarly, on the metals from vanadium through copper all the chloride from reacted molecules was retained by the surface and the gaseous products were paraffin and olefin. However, during the initial reactions with these metals, as many as three distinct phenomena were observed:

1) dehydrochlorination
2) instantaneous adsorption without subsequent release of gas phase products (retentive adsorption), and
3) hydrogenation of the olefin generated by dehydrochlorination.

The properties of each of these reactions are summarized in Table III-3.

Since they were reacted at low temperatures, each haloalkane was examined at the lowest temperature studied (-78°C for 1-chloropropane and 0°C for 1-chloro-2-methylpropane) to confirm that no condensation was occurring.

At 10^{-2} Torr and 25°C the reaction manifold contained about 3.2×10^{17} molecules.

Due to similarities in mass spectral patterns, traces of butane and the straight chain butenes could have avoided detection in mixtures of methylpropene and methylpropane, the major hydrocarbon products of the reactions of 1-chloro-2-methylpropane. However, at concentrations greater than about 10% they would be detectable. Therefore, they cannot be ruled out as trace products particularly in initial reactions.

b) Vanadium

1-Chloropropane

During its low temperature initial reactions with vanadium, large quantities of 1-chloropropane were retentively adsorbed. For the first few reactions, the major gaseous product was propane; however, during sub-

sequent runs the proportion of propene gradually increased. During these reactions no hydrogen was generated; however, heating the film to 200°C liberated large quantities of hydrogen and traces of hydrocarbon cracking products.

The conditions and properties of these reactions are listed in Table III-1. The first four occurred instantaneously whereas the fifth and sixth proceeded at a measurable rate. The sixth reaction produced a mixture of propane and propene, while the total pressure remained constant at about 1×10^{-3} Torr. As shown in Figure III-1, 1-chloropropane seemed to disappear by first order kinetics. However, as explained in Section III-C, this is likely a result of compensating effects and is not indicative of the true kinetic order of the reaction.

TABLE III-1

Initial Reactions of 1-Chloropropane with Vanadium

reaction	initial pressure $\times 10^{3}$ (Torr)	film temp(°C)	% retentively adsorbed	products
1	5	0	100	none
2	5	0	99	propane/methane
3	10	0	95	propane
4	10	-78	99	propane
5	5	-78	99	propane/propene
6	5	0	85	propane/propene
7	1000	0	0	no reaction
8	10	0	0	no reaction

In addition, propene was gradually converted to propane independent of the production of both from halide. This phenomenon was manifested by an increase in the ratio of propane to propene both during and after dehydrochlorination (Figure III-2). After completion of dehydrohalogenation, the rate of change in this ratio decreased suddenly from $2.9 \times 10^{-4} sec^{-1}$ to $1.7 \times 10^{-4} sec^{-1}$. By extrapolation, to zero time, the ratio at zero extent of reaction was found to be 0.60.

Although followed for only about 10% reaction, the hydrogenation appeared to be approximately first order in propene with a rate constant of $5.7 \times 10^{-5} sec^{-1}$ (Figure III-3). The olefin concentration at completion of dehydrohalogenation was taken as 100%; thus, the line in Figure III-3 intersects the time axis not at zero but at 1691, the time from which the hydrogenation was studied.

One Torr of 1-chloropropane was then admitted to the film at $0^{o}C$ with no adsorption or reaction over several hours. Following this, the film remained completely inactive toward subsequent doses at $0^{o}C$. About 1.3×10^{18} molecules of reactant were retained by the film.

FIGURE III - 1

TABLE IV-I Reaction 6

Disappearance of 1-Chloropropane

on Vanadium

Plotted as a First Order Reaction

$T = 0^{o}C$

P_{o}(1-chloropropane) = 1×10^{-3} Torr

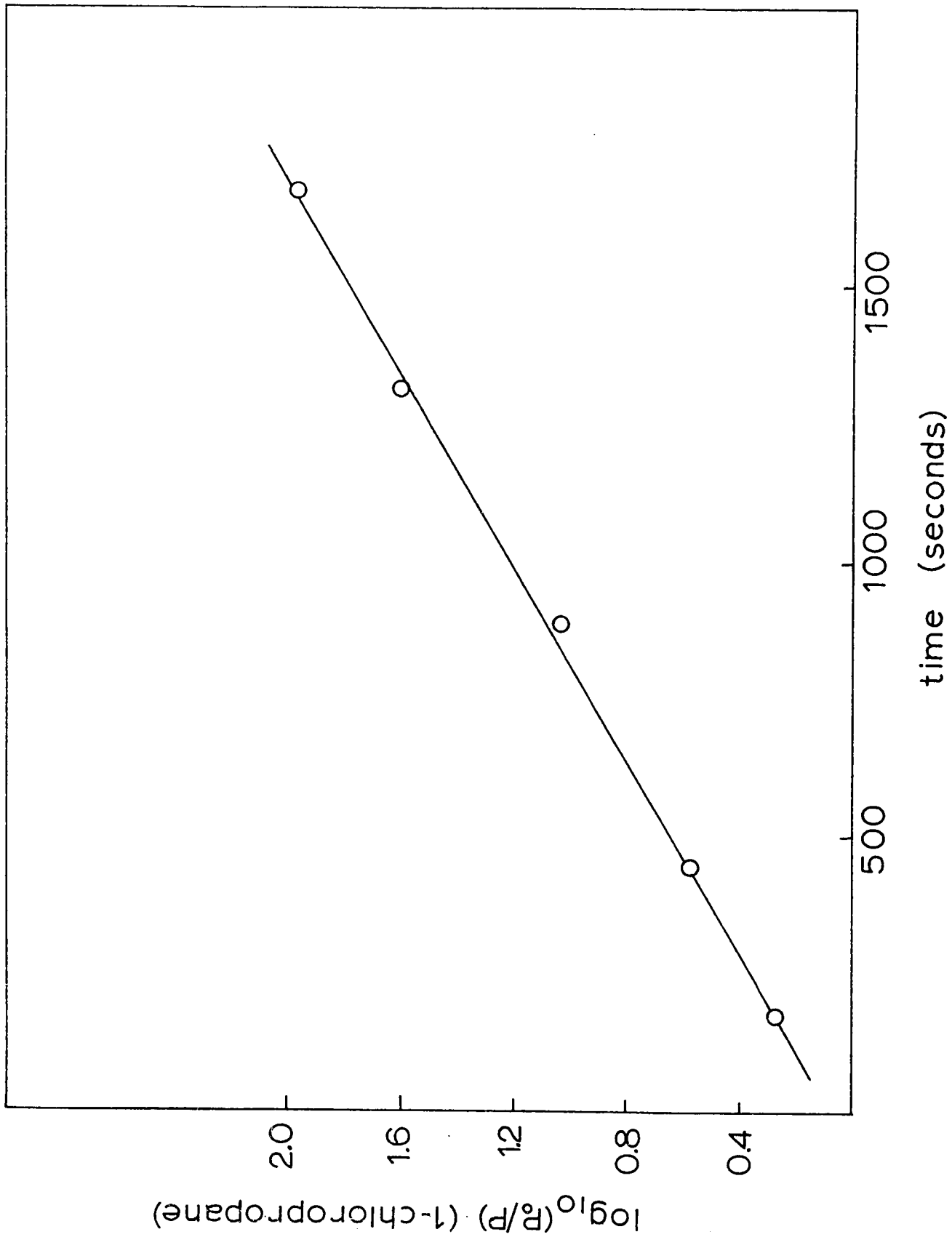
2.0
1.6
1.2
0.8
0.4
log10(R0/P) (1-chloropropane)
500
1000
1500
time (seconds)

FIGURE III - 2

Variation in (Paraffin)/(Olefin) Ratio

With Time During Initial Reaction of

1-Chloropropane on Vanadium

$T = 0^{o}C$

P_{o}(1-chloropropane) = $1x10^{-3}$ Torr

□ - Completion of Dehydrochlorination

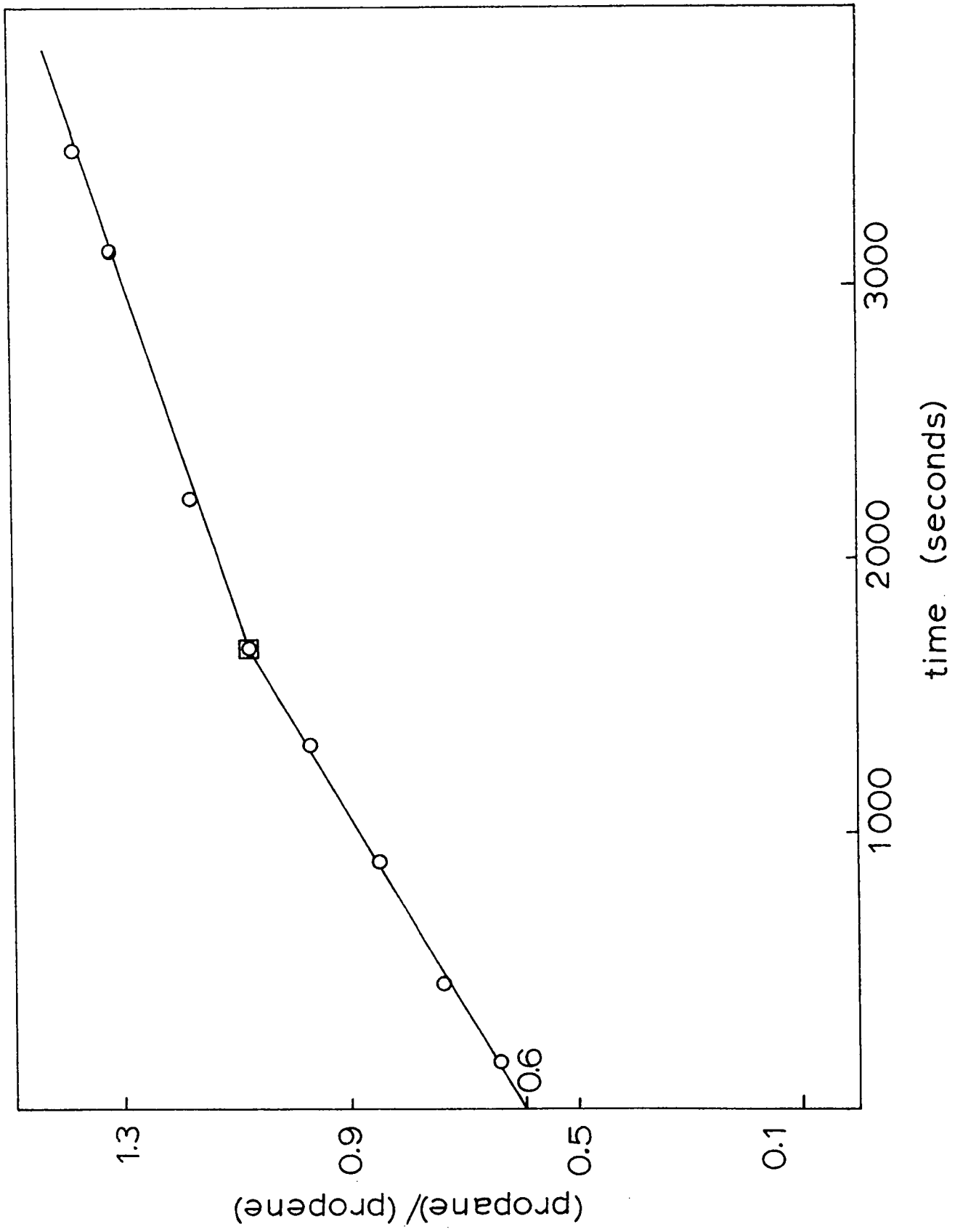
1.3
0.9
0.5
0.1
(propane)/ (propene)
0.6
1000
2000
3000
time (seconds)

FIGURE III - 3

TABLE IV-I Reaction 6

Disappearance of Propene

With Time Following Initial Reaction of

1-Chloropropane on Vanadium

Plotted as a First Order Reaction

$T = 0^{o}C$

$P_{o}(\text{propene}) = 4.3 \times 10^{-4}$ Torr

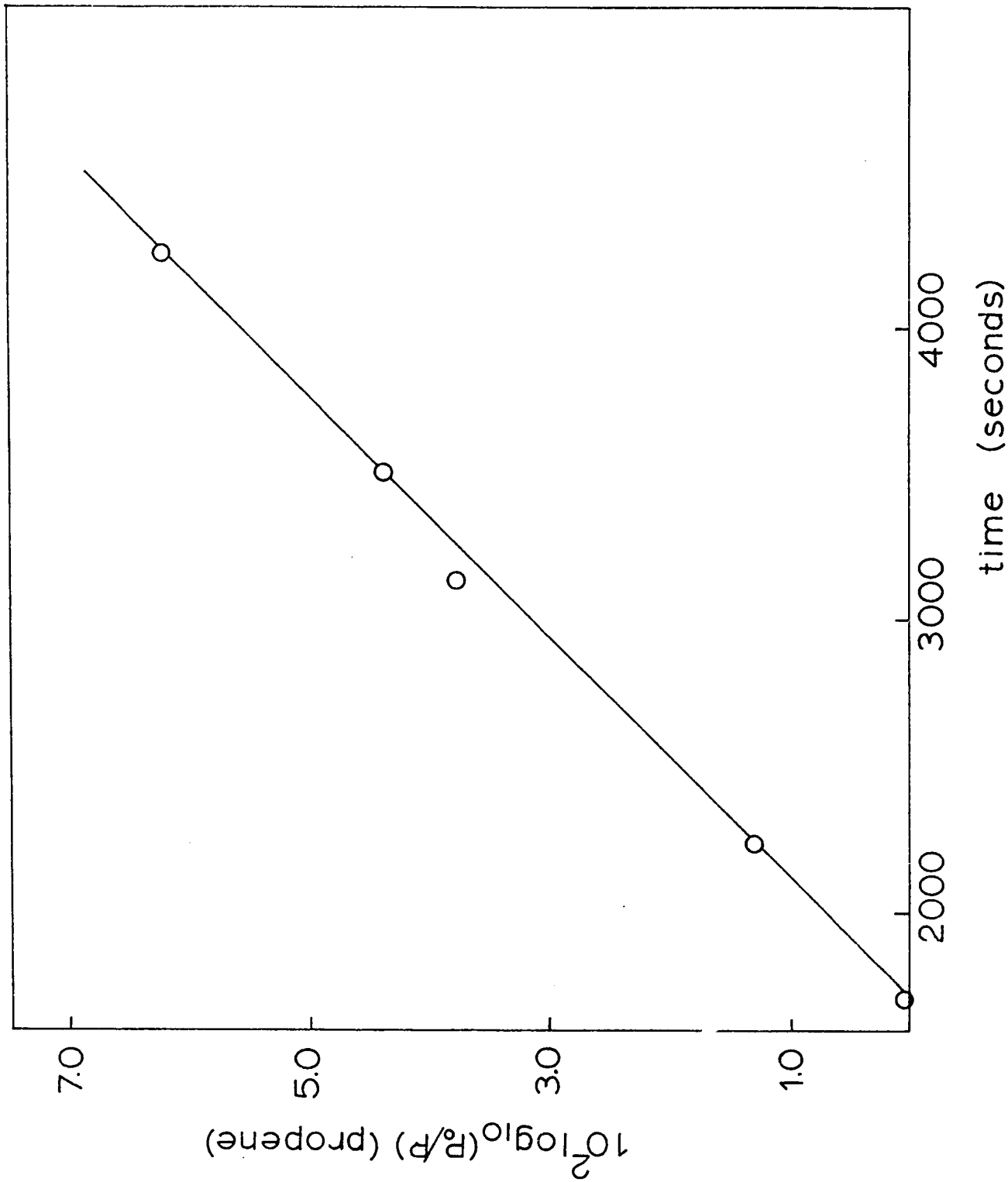
$10^2 \log_{10}(P_o/P)$ (propene)
7.0
5.0
3.0
1.0
2000
3000
4000
time (seconds)

1-Chloro-2-methylpropane

As with 1-chloropropane, large quantities of 1-chloro-2-methylpropane were retentively adsorbed. However, in this case, the film was successively reacted with small doses until both reaction and adsorption ceased at low temperatures. The first few reactions generated methylpropane and traces of methane whereas the percentage of methylpropene increased in subsequent runs; throughout the entire series no hydrogen gas was evolved.

The conditions and properties of the initial reactions are listed in Table III-2. The first six dehydrochlorination reactions occurred instantaneously; however, the subsequent hydrogenation of methylpropene was studied for reactions 5 and 6. As shown in Figure III-4, olefin again seemed to disappear by first order kinetics, although only 20% reaction was followed. However, the rate of hydrogenation decreased markedly between the two consecutive reactions ($k=3.1\times10^{-4}sec^{-1}$ for five and $1.5\times10^{-4}sec^{-1}$ for six). In this case, since dehydrochlorination was instantaneous the curve passes through the origin.

Throughout the remaining reactions, the rate of dehydrochlorination and the degree of retentive adsorption decreased. Methylpropane content, likewise,

decreased to 17%. As expected, dehydrochlorination rate increased at higher temperatures. However, adsorption was inversely related to film temperature. Between reactions nine and ten the film equilibrated in vacuum for several hours rather than the usual 15-30 minutes. This resulted in a major increase in both dehydrochlorination rate and degree of retentive adsorption.

About 3.2×10^{18} molecules of reactant were retained by the film before both retentive adsorption and low temperature reaction ceased. No significant adsorption occurred in subsequent reactions.

TABLE III-2

Initial Reactions of 1-Chloro-2-methylpropane with Vanadium

reaction	initial pressure, $\times 10^2$(Torr)	film temp	% retentively adsorbed	product
1	1.1	0	100	none
2	0.6	0	90	MP*, trace methane
3	0.9	0	90	MP*, trace methane
4	1.1	0	80	87^+
5	1.0	0	80	65^+
6	1.0	0	80	64^+
7	1.0	0	80	38^+
8	0.5	0	30	-

TABLE III-2 (continued)

reaction	initial pressure $x10^{2}$(Torr)	film temp (^{o}C)	% retentively adsorbed	product
9	0.4	0	30	-
10	1.1	0	95	38+
11	1.0	30	70	39+
12	1.0	73	40	28+
13	1.1	73	25	17+
14	1.1	30	60	-
15	1.1	71	25	10+

* MP - methylpropane

\+ approximate percent methylpropane in product of methylpropane and methylpropene

c) Chromium

1-Chloropropane

The initial doses of 1-chloropropane on chromium underwent a brief period of retentive adsorption and rapid reaction at 0^{o}C. The first aliquot of $5x10^{-3}$ Torr was instantaneously 60% retentively adsorbed, rapidly generating propane and traces of methane. A second reaction with $2x10^{-1}$ Torr proceeded without any appreciable pressure change slowly producing a mixture of propane and propene. No further reaction or retentive adsorption occurred

FIGURE III - 4

Disappearance of Methylpropene

With Time Following Initial Reaction of

1-Chloro-2-methylpropane on Vanadium

Plotted as a First Order Reaction

$T = 0^{o}C$

(TABLE IV-2) Reaction	P_o(methylpropene) Torr
Δ - 5	4.49×10^{-4}
O - 6	4.64×10^{-4}

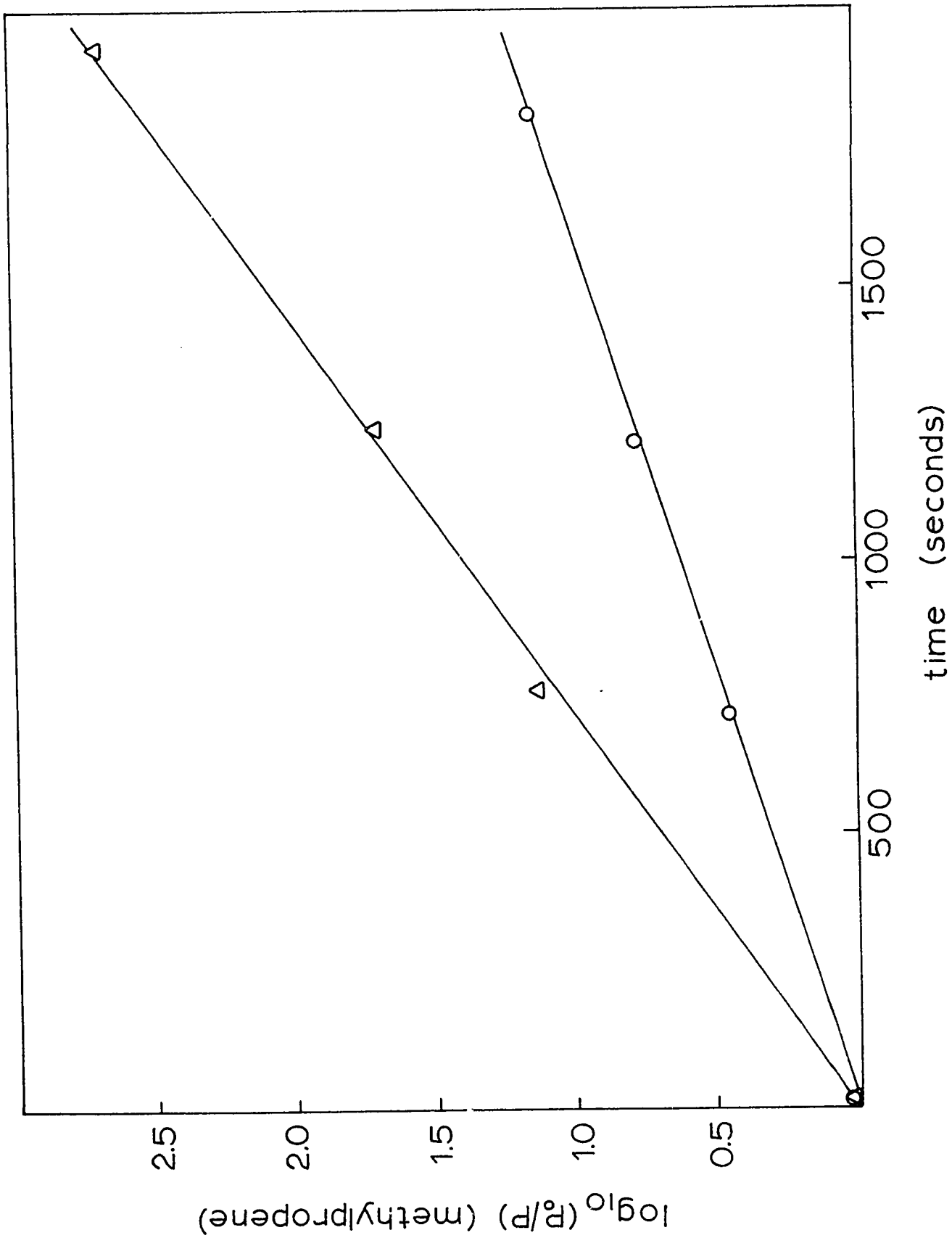
2.5
2.0
1.5
1.0
0.5
log10 (R°/P) (methylpropene)
500
1000
1500
time (seconds)

at low temperature. Although no appreciable hydrogen was released during these reactions, heating the film to 138°C evolved both hydrogen and traces of hydrocarbon cracking products. About 1.6×10^{17} molecules of 1-chloropropane were retained in the film.

1-Chloro-2-methylpropane

At low temperatures, a slightly more extended period of reaction and retentive adsorption occurred with 1-chloro-2-methylpropane than with 1-chloropropane. The first aliquot of 5×10^{-3} Torr was completely retained without generating any detectable gas phase products. The next identical dose was 80% retained and instantaneously generated 100% methylpropane.

The third was 70% retained and reacted at a measurable rate producing a mixture of methylpropane and methylpropene. While the pressure remained constant, 1-chloro-2-methylpropane seemed to disappear by approximately first order kinetics (Figure III-5). As for vanadium, this does not reflect the kinetic order of the reaction and its significance will be explained in Section III-C.

The resulting methylpropene was hydrogenated to methylpropane both during and after

FIGURE III - 5

Disappearance of 1-Chloro-2-methylpropane

on Chromium

Plotted as a First Order Reaction

$T = 0^{o}C$

P_{o}(1-chloro-2-methylpropane) = $2x10^{-3}$ Torr

2.4
2.0
1.6
1.2
0.8
0.4
log10(P°/P) (1-chloro-2-methylpropane)
250
500
750
time (seconds)

FIGURE III - 6

Variation in (Paraffin)/(Olefin) Ratio

With Time During Initial Reaction of

1-Chloro-2-methylpropane on Chromium

$T = 0^{o}C$

P_{o}(1-chloropropane) = 1×10^{-3} Torr

□ - Completion of Dehydrochlorination

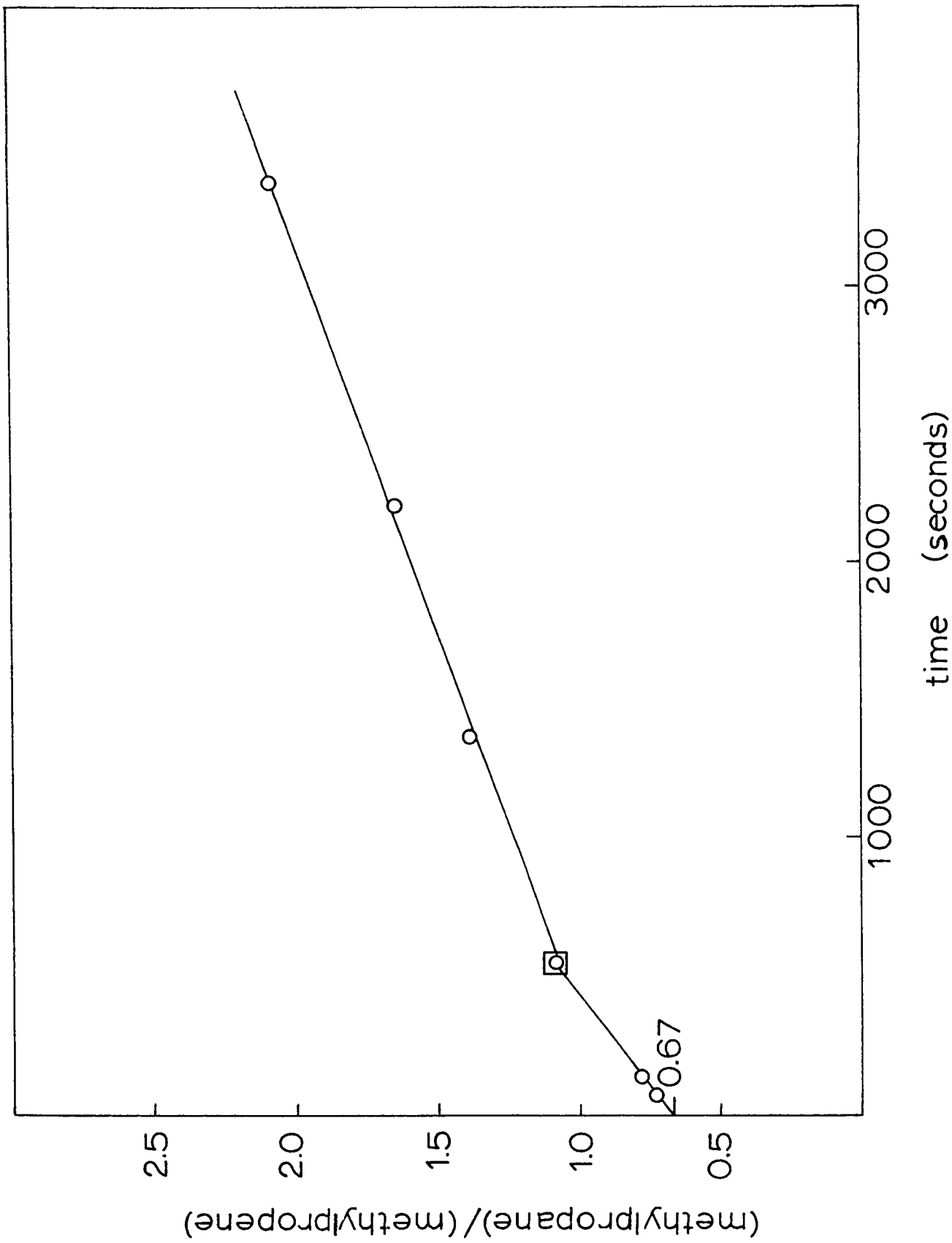
(methylpropane)/ (methylpropene)
2.5
2.0
1.5
1.0
0.5
0.67
1000
2000
3000
time (seconds)

FIGURE III - 7

Disappearance of Methylpropene

With Time Following Initial Reaction of

1-Chloro-2-methylpropane on Chromium

Plotted as a First Order Reaction

$T = 0^{o}C$

P_{o}(methylpropene) = 1×10^{-3} Torr

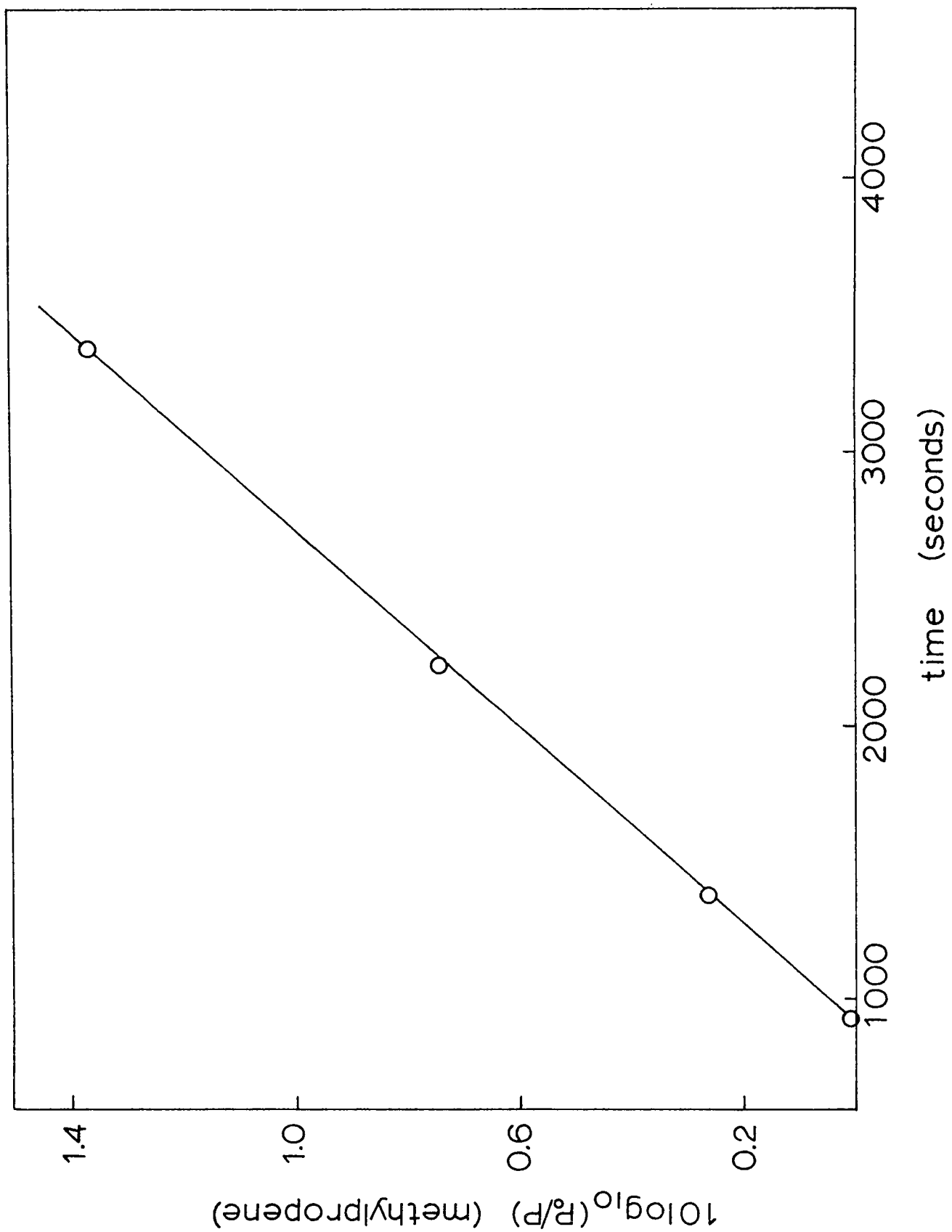
1.4
1.0
0.6
0.2
1000
2000
3000
4000
time (seconds)
10log10(R0/P) (methylpropene)

both during and after dehydrochlorination. After completion of the dehydrochlorination the rate of increase of the (paraffin)/(olefin) ratio decreased abruptly from 5.9×10^{-4} sec^{-1} to $3.6 \times 10^{-4} sec^{-1}$. By extrapolation to zero time, at zero extent of reaction the ratio was 0.67. Again olefin was converted to paraffin apparently by first order kinetics with a rate constant of $5.6 \times 10^{-5} sec^{-1}$ (Figure III-7). The curve intersects the time axis at 913 seconds, the time at which dehydrohalogenation ceased and hydrogenation was studied.

Slow reaction to a mixture of methylpropane and methylpropene occurred with the next dose and subsequently reaction at 0°C and retentive adsorption ceased. Heating to 118°C evolved hydrogen and small amounts of hydrocarbon cracking products. About 5.8×10^{17} molecules of reactant were retained in the film.

d) Manganese

Unlike vanadium and chromium, manganese retained only about 15% of the first dose of 1-chloro-2-methylpropane and only the first reaction proceeded rapidly enough for kinetic study at 0°C. During this reaction, the pressure remained constant at 10^{-2} Torr as the halide was

FIGURE III - 8

Disappearance of 1-Chloro-2-methylpropane

on Manganese

Plotted as a First Order Reaction

$T = 0^{o}C$

P_{o}(1-chloro-2-methylpropane) = 1×10^{-2} Torr

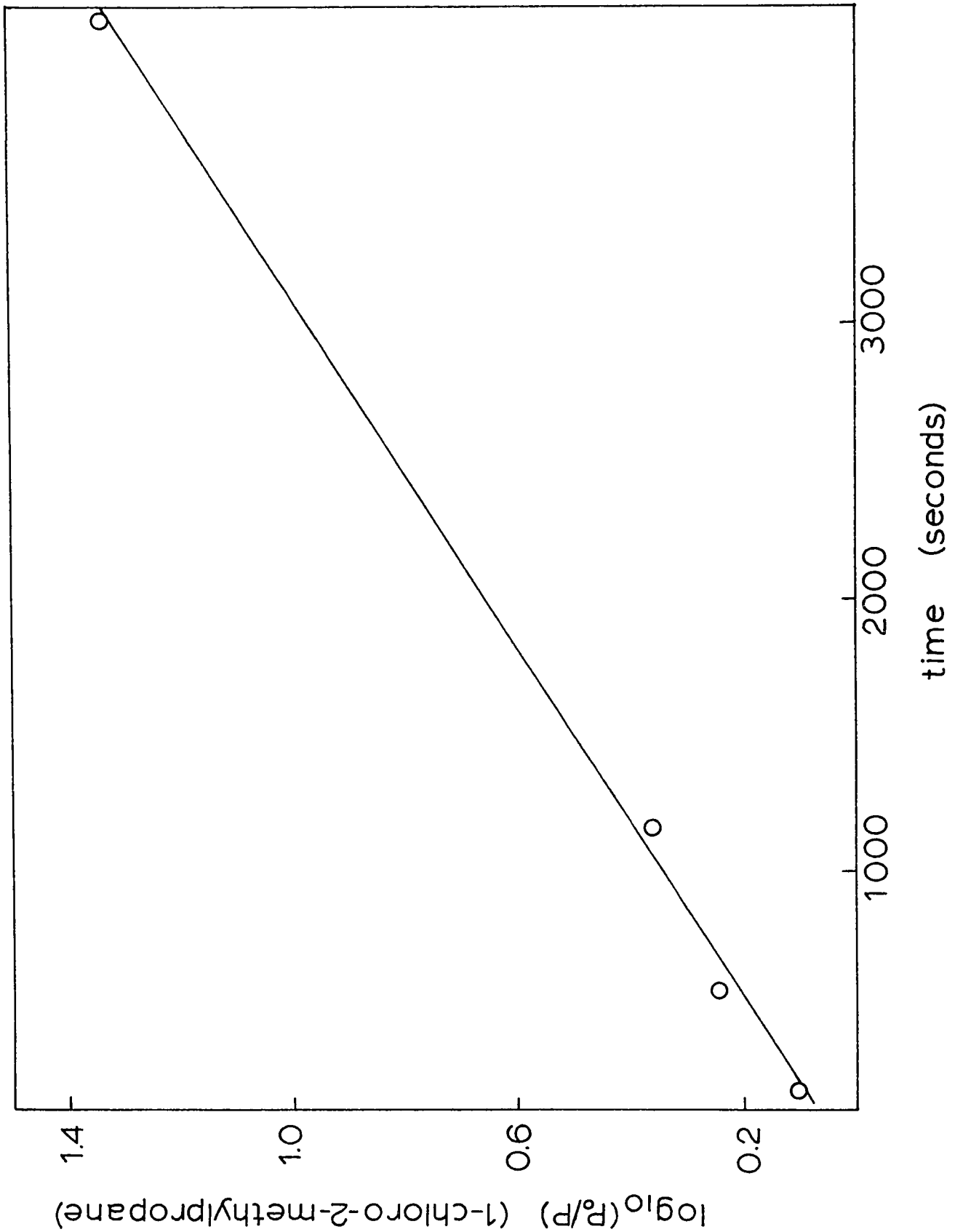
1.4
1.0
0.6
0.2
1000
2000
3000
time (seconds)
log10(P°/P) (1-chloro-2-methylpropane)

slowly converted into methylpropane and methylpropene, apparently by first order kinetics (Figure III-8). As described in Section III-C, this is probably not indicative of the kinetic order of the reaction but likely results from the superposition of compensating effects. The ratio of paraffin to olefin increased throughout the reaction to a final value of 0.42 at 95% completion.

About 4.4×10^{16} molecules of reactant were retained by the film. Heating evolved small amounts of hydrogen.

e) Iron

1-Chloropropane

The initial low temperature reactions of iron with 1-chloropropane proceeded through a brief period of rapid dehydrohalogenation and retentive adsorption. At $0^{o}C$, the first aliquot was approximately 15% retained while the remaining 1×10^{-2} Torr reacted instantaneously, at constant pressure, to a mixture of 80% propane, 20% hydrogen and a trace of methane. A second reaction proceeded very slowly to a mixture of propene and propane. Neither was amenable to kinetic study.

About 4.8×10^{16} molecules of 1-chloropropane were retained on the surface. Heating the film to $65^{o}C$ evolved hydrogen and traces of hydrocarbon cracking products.

1-Chloro-2-methylpropane

A more extensive initial period of dehydrohalogenation and retentive adsorption occurred at 0°C with 1-chloro-2-methylpropane than with 1-chloropropane. The first 10^{-2} Torr dose was 80% retentively adsorbed and instantaneously generated methylpropane with traces of hydrogen. A second aliquot, reacted under identical conditions, was 25% retained as the remaining reactant was converted rapidly, at constant pressure, to a mixture of methylpropane and methylpropene. Following this rapid dehydrochlorination, the methylpropene was isobarically hydrogenated to methylpropane by first order kinetics with a rate constant of 4.0×10^{-4} sec^{-1} (Figure III-9). This was followed to 90% completion.

A third reaction at 0°C and 10^{-2} Torr was extremely slow with no appreciable retentive adsorption. Heating the film to 60°C evolved hydrogen and traces of methane. About 3.2×10^{17} molecules of 1-chloro-2-methylpropane were retained by the surface.

f) Cobalt

1-Chloropropane

At 0°C, 2.5×10^{-1} Torr of 1-chloropropane was admitted to the clean film. Neither dehydrochlorination nor retentive adsorption was observed. The film remained entirely inert at low temperatures.

FIGURE III - 9

Disappearance of Methylpropene

With Time Following Initial Reaction of

1-Chloro-2-methylpropane on Iron

Plotted as a First Order Reaction

$T = 0^{o}C$

P_{o}(methylpropene) = 5.3×10^{-3} Torr

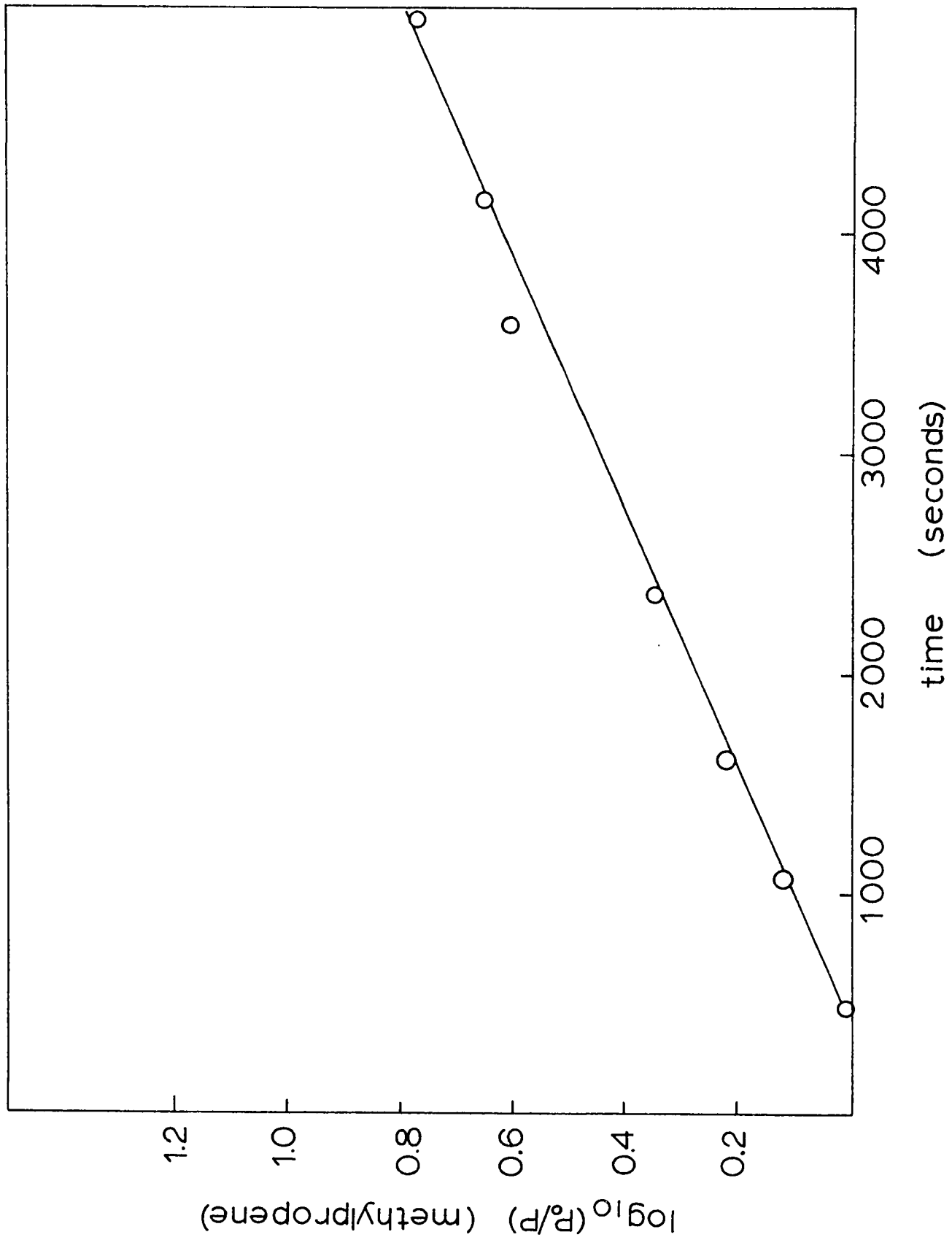
1.2
1.0
0.8
0.6
0.4
0.2
$\log_{10}(P_o/P)$ (methylpropene)
1000
2000
3000
4000
time (seconds)

1-Chloro-2-methylpropane

Along with being 30% retentively adsorbed, the initial 10^{-2} Torr dose of 1-chloro-2-methylpropane reacted very rapidly at 0°C generating a mixture of methylpropane and methylpropene.

A second 10^{-2} Torr aliquot remained both unadsorbed and unreacted for more than one hour. Heating the film to 80°C evolved only hydrogen. About 9.0×10^{16} molecules were retentively adsorbed.

g) Nickel

1-Chloropropane

At 0°C, 10^{-2} Torr of 1-chloropropane was admitted to the film with no dehydrochlorination or retentive adsorption.

1-Chloro-2-methylpropane

At 0°C, 10^{-2} Torr of 1-chloro-2-methylpropane was admitted to the film with 20% retentive adsorption but no dehydrochlorination. Toward a second identical dose, the film was totally inactive at low temperature.

About 7.0×10^{16} molecules were retained in the film. Heating to 90°C evolved hydrogen.

h) Copper

At 0°C, 10^{-2} Torr of 1-chloropropane was admitted to the film. No retentive adsorption and very slow dehydrochlorination resulted with propene as

the primary product. No appreciable gas evolved on heating the film to 184°C.

i) Titanium

The initial reactions of titanium with 1-chloro-2-methylpropane were re-examined since previous reports that the only product was methylpropene and reaction was incomplete were entirely inconsistent with the findings for the other metals (Summers, 1970). Contrary to these reports, 1-chloro-2-methylpropane was 35% retentively adsorbed into the film while the remaining reactant generated a mixture of 60% methylpropene and 40% methylpropane. However, the ratio of methylpropane to methylpropene remained constant at 0.68 both during and after the dehydrochlorination. Thus, methylpropene was not hydrogenated.

The film was completely inactive toward subsequent doses. About 5.1×10^{16} molecules of 1-chloro-2-methylpropane were retained by the film. Heating the film to 170°C evolved no appreciable quantities of gas.

TABLE III-3

Properties of the Initial Reactions of 1-Chloropropane and 1-Chloro-2-methylpropane with the First Row Transition Metals

Metal /reactant+	P/O*at time=0	$\frac{d}{dt}$(P/O)*during dehydrochlo $x10^4(sec^{-1})$	$\frac{d}{dt}$(P/O)*after dehydrochlo $x10^4(sec^{-1})$	k(hydrog) $x10^4(sec^{-1})$	pressure retentively adsorbed $x10^2$ (Torr)	molec retent adsorb $x10^{-17}$
Ti/C_4H_9Cl	0.68				0.16	0.5
V/C_3H_7Cl	0.60	2.9	1.7	0.57	4.1	13
V/C_4H_9Cl				3.1 and 1.5	10	32
Cr/C_3H_7Cl					0.5	1.6
Cr/C_4H_9Cl	0.67	5.9	3.4	0.56	1.8	5.8
Mn/C_4H_9Cl					.12	0.4
Fe/C_3H_7Cl					.16	0.5
Fe/C_4H_9Cl				4.0	1.0	3.2
Co/C_3H_7Cl					0	0
Co/C_4H_9Cl					0.3	0.9
Ni/C_3H_7Cl					0	0
Ni/C_4H_9Cl					0.2	0.7
Cu/C_3H_7Cl					0	0

+ C_3H_7Cl = 1-Chloropropane, C_4H_9Cl = 1-chloro-2-methylpropane

* P/O = paraffin/olefin ratio, $\frac{d}{dt}$ (P/O) = rate of change of paraffin/olefin ratio

III-B-2) Reactions on Halided Surfaces

III-B-2-a) Non-Catalytic Reactions

i) Introductory Comments

The non-catalytic reactions of 1-chloropropane and 1-chloro-2-methylpropane with halided surfaces of the first row transition metals are reported in this section.

The reactions of 1-chloropropane with halided titanium surfaces (Section I-G) differed from those with all the other metals. Whereas on titanium, successive reactions proceeded at constant rate after a settling down period, with the other metals reaction rate decreased between successive runs until the film ceased to induce dehydrochlorination even at 240°C.

During non-catalytic dehydrochlorination of both chloroalkanes each of the metals retained all the chloride and no gaseous hydrogen chloride was detected. However, for 1-chloropropane, propene and hydrogen were generated by all the metals except titanium which produced propene and propane, and retained some of the hydrogen. Whereas 1-chloropropane reactions remained non-catalytic, the non-catalytic period with 1-chloro-2-methylpropane was transitory between its initial reactions and subsequent catalytic behavior.

ii) 1-Chloropropane

Vanadium

The initial low temperature reactions of 1-chloropropane on vanadium underwent extensive retentive adsorption and dehydrochlorination before the film deactivated (Section III-B-1). After low temperature reaction ceased, dehydrochlorination continued at elevated temperatures producing propene as the only hydrocarbon product while the film retained the chloride. Hydrogen was continually released from the film to the extent that for a given interval about equal quantities were liberated both in the presence and absence of a reaction. After the reaction settled into a period of consistent products, consecutive reactions were studied allowing about thirty minutes between runs for the film to recover.

The rate of dehydrochlorination decreased consistently between runs at both 185 and 230°C. A series of five reactions at 230°C and about 1.3×10^{-2} Torr were studied in detail. For each reaction, the initial rate of disappearance of 1-chloropropane was determined by calculating the equations for the pressure-time curves (Figure III-10) using the program CURFIT. Thus, successive values were determined for the reaction rate at 1.3×10^{-2} Torr on a progressively halided surface. Each reaction was carried to completion.

FIGURE III - 10

Disappearance of 1-Chloropropane

With Time

on Vanadium

$T = 230^{o}C$

$P_o = 1.3 \times 10^{-2}$ Torr

Reaction

□ - 1

○ - 2

△ - 3

○ - 5

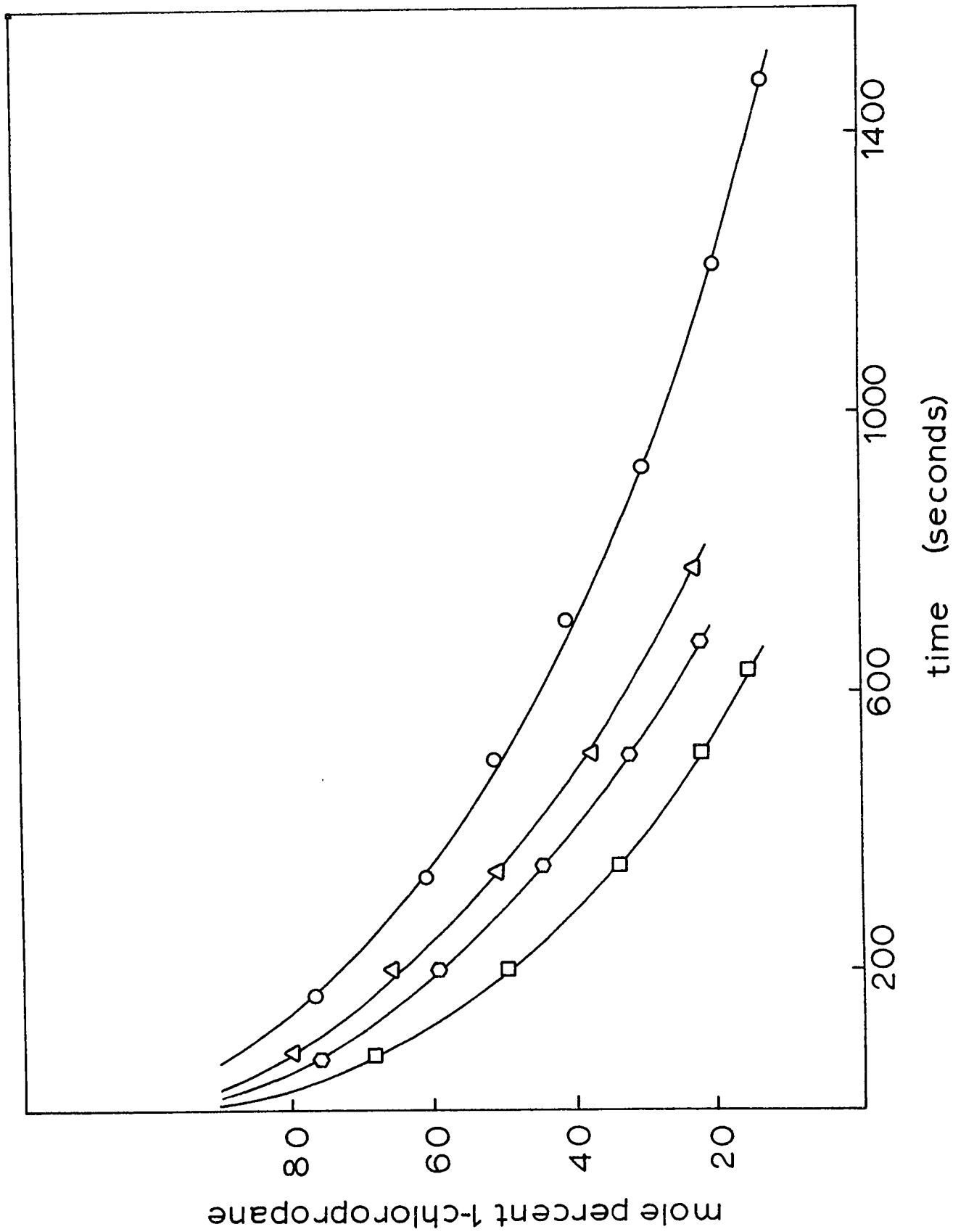
mole percent 1-chloropropane
20
40
60
80
200
600
1000
1400
time (seconds)

Due to technical difficulties during the fourth reaction, it has been omitted from the following calculations; however, the halide deposited has been included.

In spite of the impossibility of maintaining constant reactant pressure in the apparatus, by this method it was possible to measure directly the extent of retardation of reaction rate caused by the development of the surface halide layer at constant pressure. Although the film had been reacted with about 1.3×10^{-1} Torr 1-chloropropane prior to this series of runs, the beginning of the first reaction in the series was established as an arbitrary zero of surface halide concentration. Extrapolating back to the clean film would only introduce a constant into the calculations and have no effect on the results.

Initial reaction rate, $-(dP/dt)_o$, plotted against total pressure of 1-chloropropane initially reacted (P_o^T) is shown in Figure III-11. The expression for the resultant straight line is shown in Equation III-1. The extent of the surface halide layer was proportional to the pressure of 1-chloropropane reacted since each reacted molecule deposited chloride in the film.

$$-(dP/dt)_o = 0.003123 - 0.033P_o^T \qquad \text{III-1}$$

Thus, for individual reactions, two effects combine to determine the kinetics, decreasing reactant pressure and formation of the surface halide layer. Both half and first order plots of the first and fifth reactions in the

FIGURE III - 11

Change in Initial Rate of Reaction

With Total Pressure Reacted

for 1-Chloropropane

on Vanadium

$T = 230^{o}C$

$P_o = 1.3 \times 10^{-2}$ Torr

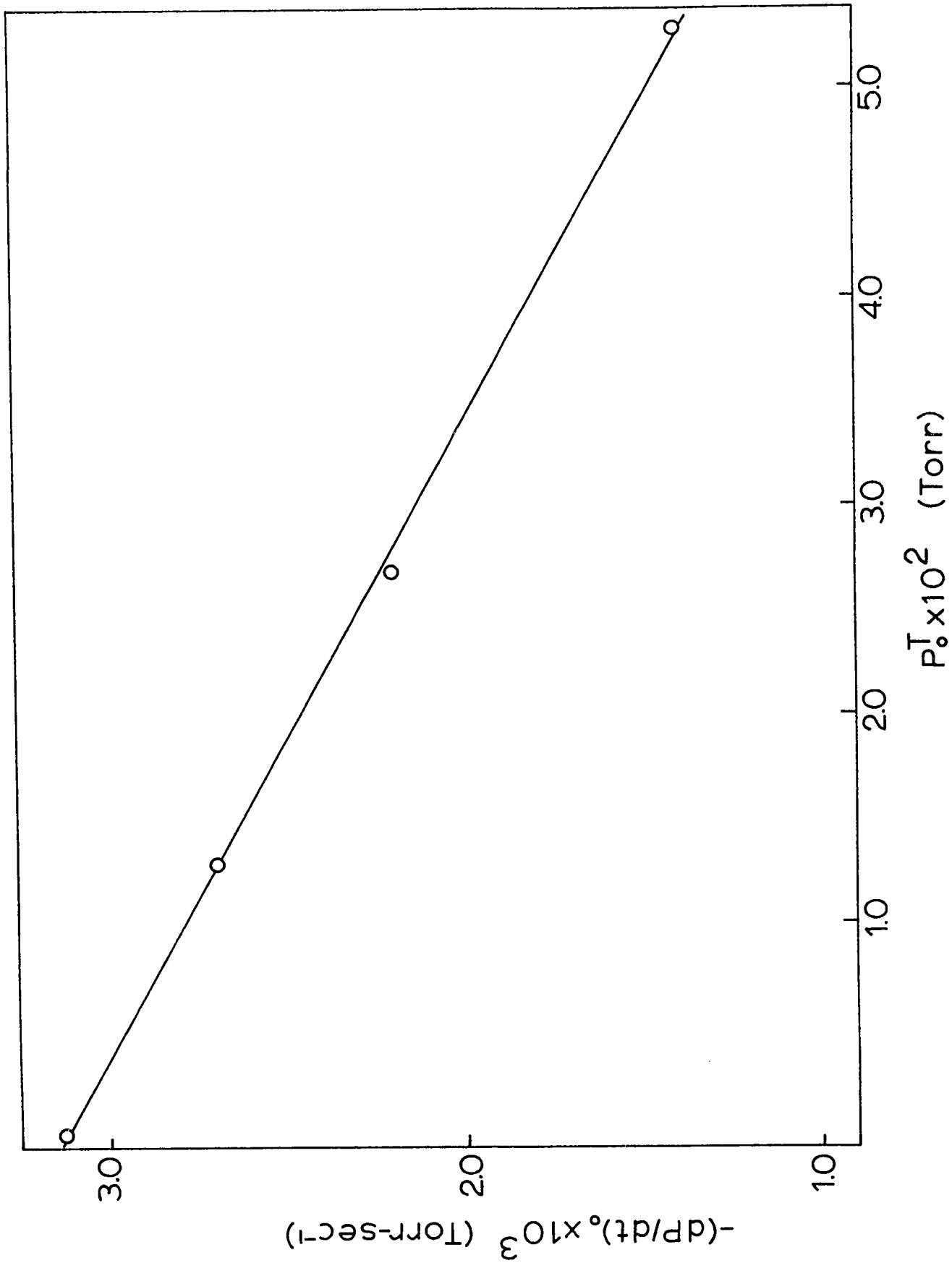
-(dP/dt)$_o$ x10^3 (Torr-sec^{-1})
3.0
2.0
1.0
1.0
2.0
3.0
4.0
5.0
P_o^T x10^2 (Torr)

series are shown in Figures III-12 and III-13. Ignoring the inhibitory effect, the order appears to be slightly less than one.

To account for inhibition due to formation of the surface halide during an individual run, Equation III-1 must be included in the kinetic expression. However, in this case, -dP/dt is the rate at any extent of reaction and P^T is the total pressure of 1-chloropropane reacted including that during the particular reaction. A normal expression is used to represent the concentration effect (Equation III-2).

$$-\frac{dP}{dt} = kP^n \qquad \text{III-2}$$

The total kinetic expression is

$$-\frac{dP}{dt} = kP^n(0.003123-0.033P^T) \qquad \text{III-3}$$

where $P^T = P_O^T + (P_o-P)$

with P_o = initial 1-chloropropane pressure for the individual reaction.

For $n = \frac{1}{2}$ this reduces to

$$-\frac{dP}{dt} = kP^{\frac{1}{2}}\left[0.003123-0.033(P_O^T + P_o - P)\right]. \qquad \text{III-4}$$

FIGURE III - 12

Disappearance of 1-Chloropropane

on Vanadium

Plotted as Half and First Order Reactions

First Reaction

$T = 230^{o}C$

$P_o = 1.3x10^{-2}$ Torr

Δ - Half Order

O - First Order

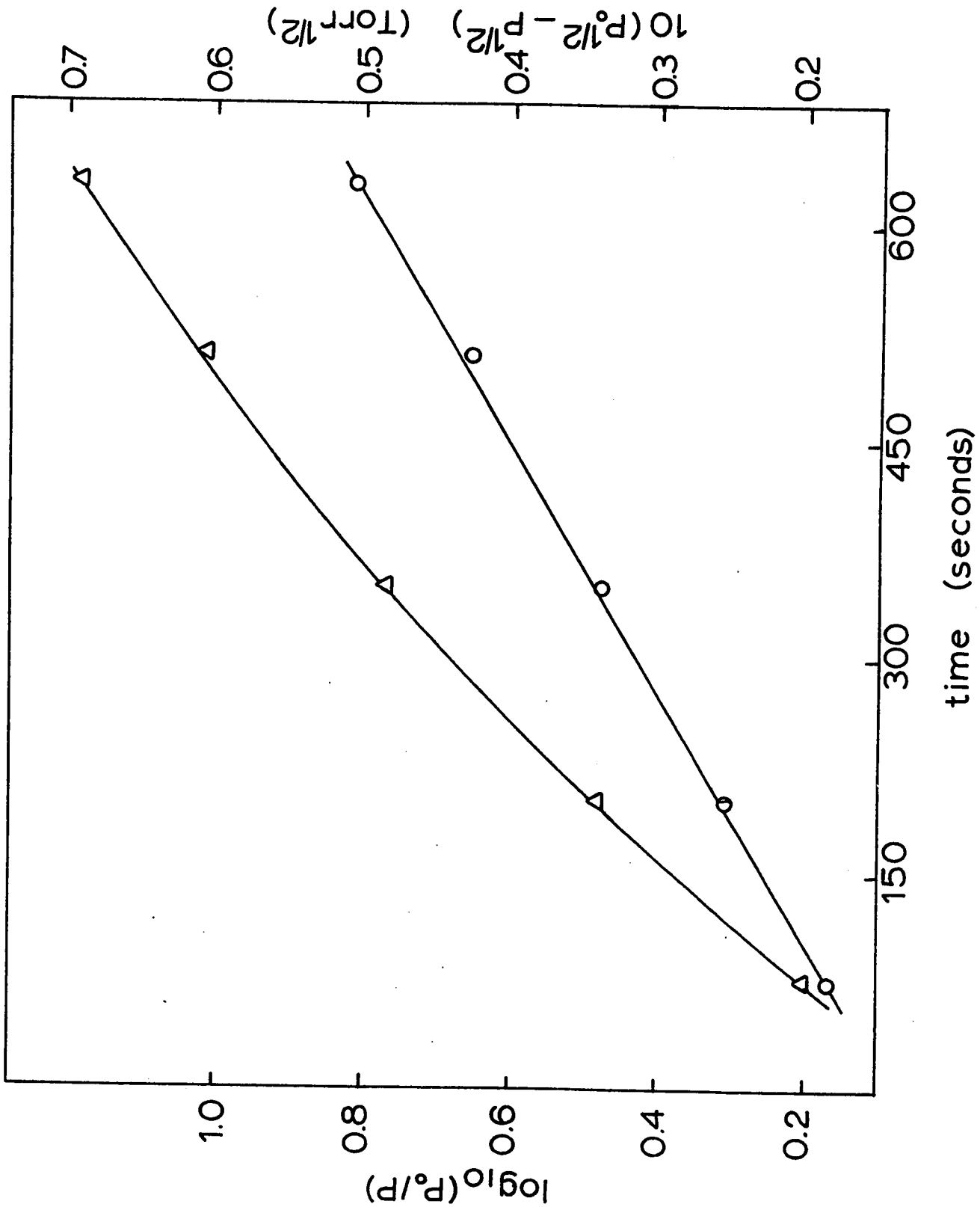
log10(P°/P)
1.0
0.8
0.6
0.4
0.2
time (seconds)
150
300
450
600
10 (P°1/2 − P1/2) (Torr1/2)
0.7
0.6
0.5
0.4
0.3
0.2

FIGURE III - 13

Disappearance of 1-Chloropropane

on Vanadium

Plotted as Half and First Order Reactions

Fifth Reaction

$T = 230^{o}C$

$P_o = 1.4 \times 10^{-2}$ Torr

Δ - Half Order

O - First Order

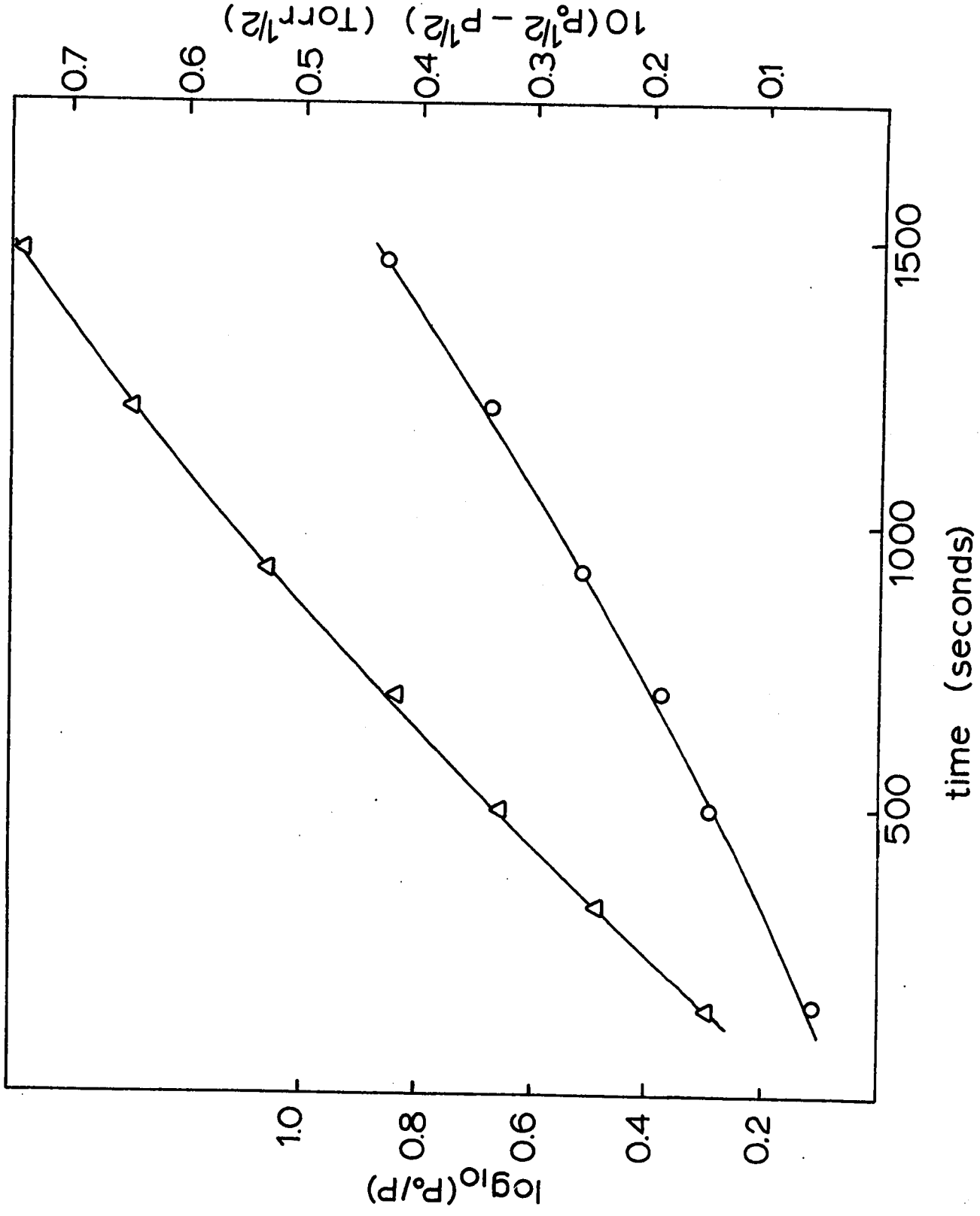
0.7
0.6
0.5
0.4
0.3
0.2
0.1
10 (P°1/2 − P1/2) (Torr1/2)
1.0
0.8
0.6
0.4
0.2
log10(P°/P)
500
1000
1500
time (seconds)

Integration gives

$$t = \frac{2}{(\alpha\beta)^{\frac{1}{2}}}\left\{\mathrm{Tan}^{-1}\left[(\beta/\alpha)^{\frac{1}{2}}P_o^{\frac{1}{2}}\right] - \mathrm{Tan}^{-1}\left[(\beta/\alpha)^{\frac{1}{2}}P^{\frac{1}{2}}\right]\right\} \qquad \text{III-5}$$

where $\alpha = k\left[0.003123 - 0.033(P_o^T + P_o)\right]$

$\beta = 0.033k$

Plots of this expression against time are shown in Figures III-14 and III-15 for the first and fifth reactions respectively. The straight lines indicate that the concentration effect is, indeed, half order and the first order disappearance in Figures III-12 and III-13 is misleading. Plots of the other two reactions showed the same effect. Slopes of these lines progressively increased by a total of 30% between the first and last reactions from 0.06 to 0.08. The intercept, which would be expected to be zero was randomly scattered around 9. This positive intercept is likely due to the time lag in mass spectral readings as explained in Section II-C and was found with all time order plots.

FIGURE III - 14

Disappearance of 1-Chloropropane

on Vanadium

Plotted as Combined Half Order

and Surface Chloride Inhibition

First Reaction

$T = 230^{o}C$

$P_o = 1.3 \times 10^{-2}$ Torr

$$\text{Tan}^{-1}P^{\frac{1}{2}} \text{ term} = 212.12 \left[\text{Tan}^{-1}(3.500P_o^{\frac{1}{2}}) - \text{Tan}^{-1}(3.500P^{\frac{1}{2}})\right]$$

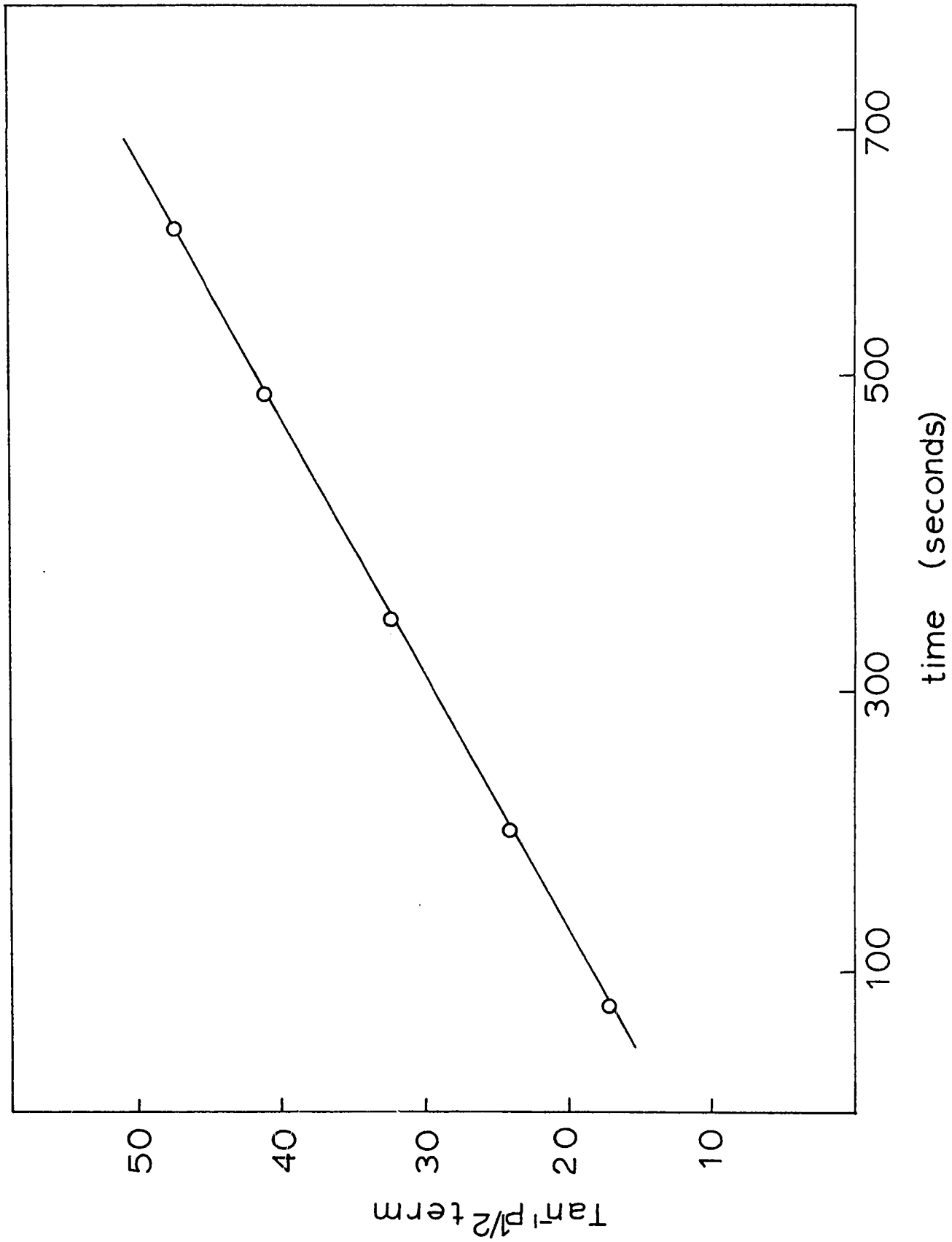
50
40
30
20
10
Tan⁻¹ pl/2 term
100
300
500
700
time (seconds)

FIGURE III - 15

Disappearance of 1-Chloropropane

on Vanadium

Plotted as Combined Half Order

and Surface Chloride Inhibition

Fifth Reaction

$T = 230^{o}C$

$P_o = 1.4X10^{-2}$ Torr

$$\text{Tan}^{-1}P^{\frac{1}{2}} \text{ term} = 357.43 \left[\text{Tan}^{-1}(5.9937P_o^{\frac{1}{2}}) - \text{Tan}^{-1}(5.9937P^{\frac{1}{2}})\right]$$

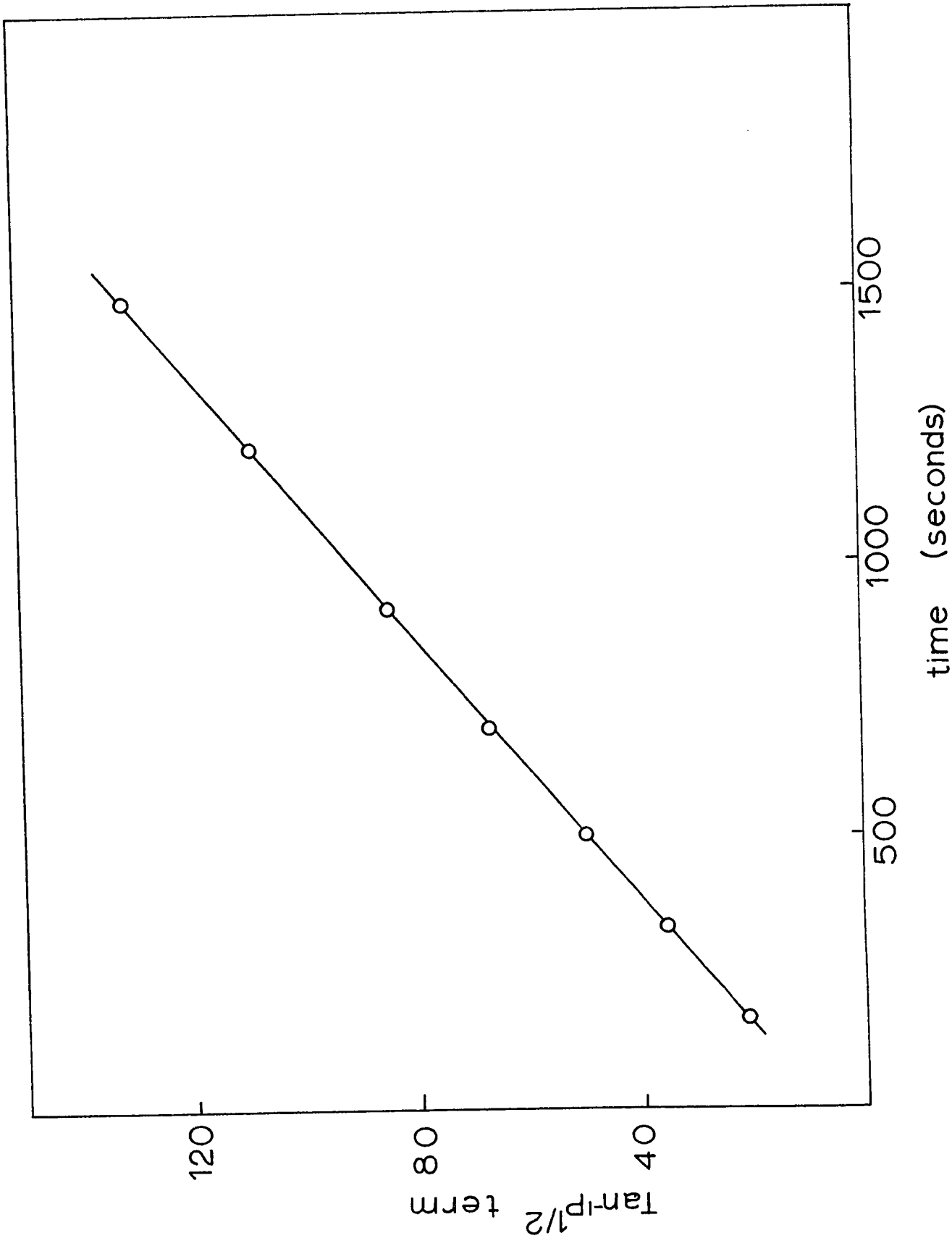
120
80
40
$\tan^{-1}p^{1/2}$ term
500
1000
1500
time (seconds)

Chromium

The first elevated temperature reaction of 1-chloropropane on chromium proceeded according to the pattern frequently detected during initial low temperature reactions - rapid dehydrochlorination followed by hydrogenation of the resulting olefin . As shown in Figure III-16 at 138°C and 1.7×10^{-2} Torr, hydrogenation of propene proceeded by first order kinetics (reaction studied to 50% completion). The rate constant was 7.89×10^{-4} sec^{-1}. Dehydrochlorination was complete within the first 382 seconds and this is designated as 100% propene with respect to hydrogenation. Thus, the line intersects the time axis at 382 sec.

A second similar reaction at 138°C also dehydrochlorinated rapidly but without subsequent hydrogenation. Heating the film from 0 to 138°C evolved a considerable quantity of hydrogen. While this evolution continued throughout the first reaction at 138°C only small quantities of hydrogen were liberated during the second.

Reactions studied between 159 and 189°C consistently produced 70% propene and 30% hydrogen according to Equation III-6. In the absence of reaction, no hydrogen was evolved from the film.

$$2CH_3CH_2CH_2Cl + 2* \longrightarrow 2CH_3CH{=}CH_2 + H_2 + 2*Cl \qquad \text{III-6}$$

* is a surface site

FIGURE III - 16

Disappearance of Propene

With Time Following Reaction of

1-Chloropropane on Chromium

Plotted as a First Order Reaction

$T = 138^{o}C$

$P_{o}(\text{propene}) = 1.7 \times 10^{-2}$ Torr

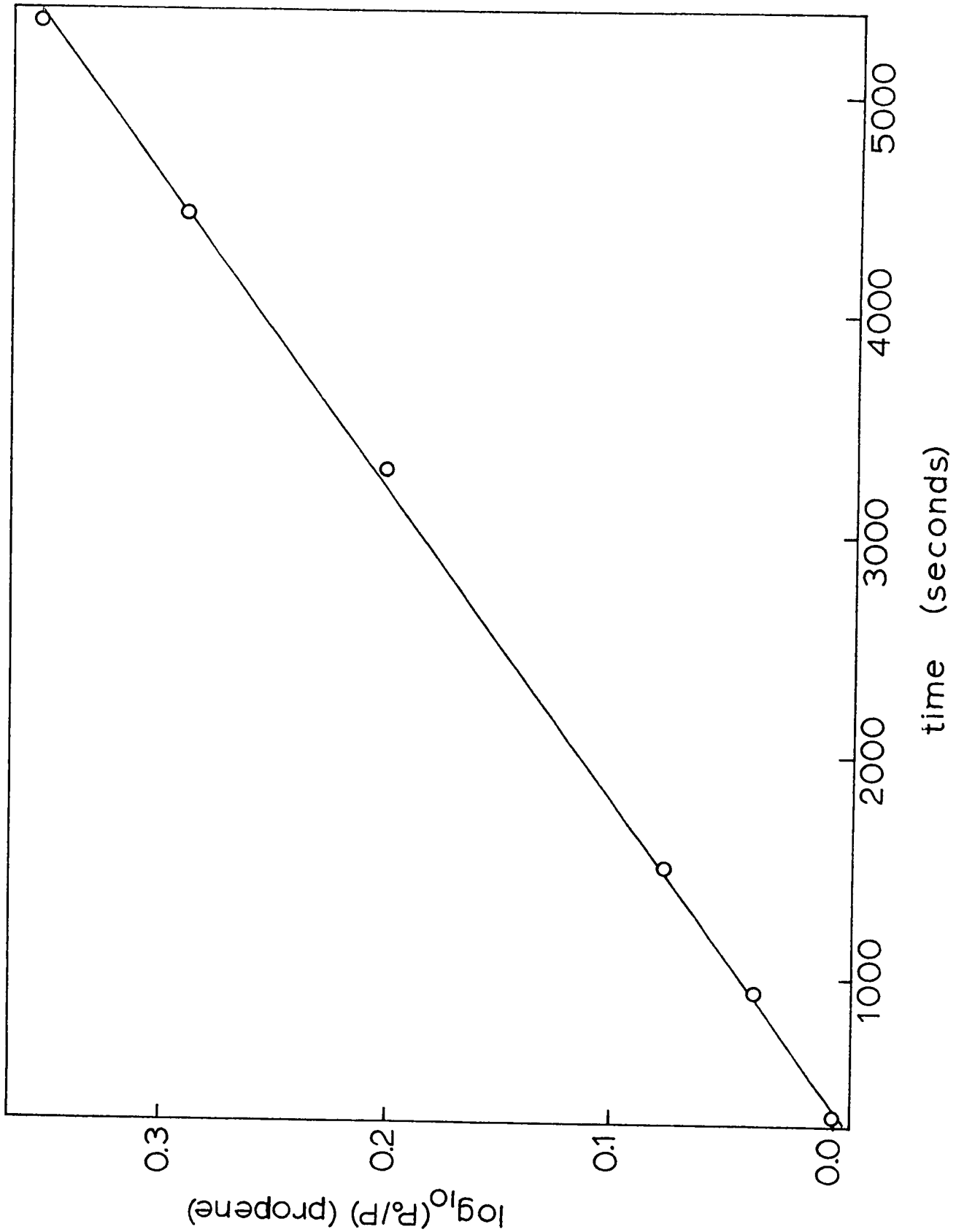
0.0
0.1
0.2
0.3
$\log_{10}(P_o/P)$ (propene)
1000
2000
3000
4000
5000
time (seconds)

For five consecutive reactions at $3x10^{-3}$ Torr 1-chloropropane seemed to disappear by first order kinetics (Figure III-17). However, over the course of these reactions film reactivity decreased by about 45% as a total 1-chloropropane pressure of $1.5x10^{-10}$ Torr reacted. Thus, the kinetic order was definitely less than one and may well have approached one half as with titanium, vanadium and manganese.

Manganese

During the high temperature reactions of 1-chloropropane with manganese, six consecutive reactions at 10^{-2} Torr caused no detectable decrease in film activity. However, at a 1-chloropropane pressure of $5x10^{-2}$ Torr the film deactivated noticeably between runs.

As with most of the other metals, the products of the manganese reactions were consistently propene and hydrogen with no traces of propane. All the chloride remained on the surface. Hydrogen evolved both during and between reactions making it impossible to accurately determine the quantity arising from each chloroalkane decomposition.

As shown in Figure III-18, at $1x10^{-2}$ Torr 1-chloropropane disappeared according to a half order rate law between 159 and 200°C. An activation energy of 17.2 ± 0.6 Kcal/mole and $\log_{10}A$ of 4.9 ± 0.3 were determined from an Arrhenius plot (Figure III-19).

FIGURE III - 17

Disappearance of 1-Chloropropane

on Chromium

Plotted as Half and First Order Reactions

$T = 167^{o}C$

$P_o = 3x10^{-3}$ Torr

Δ - Half Order

O - First Order

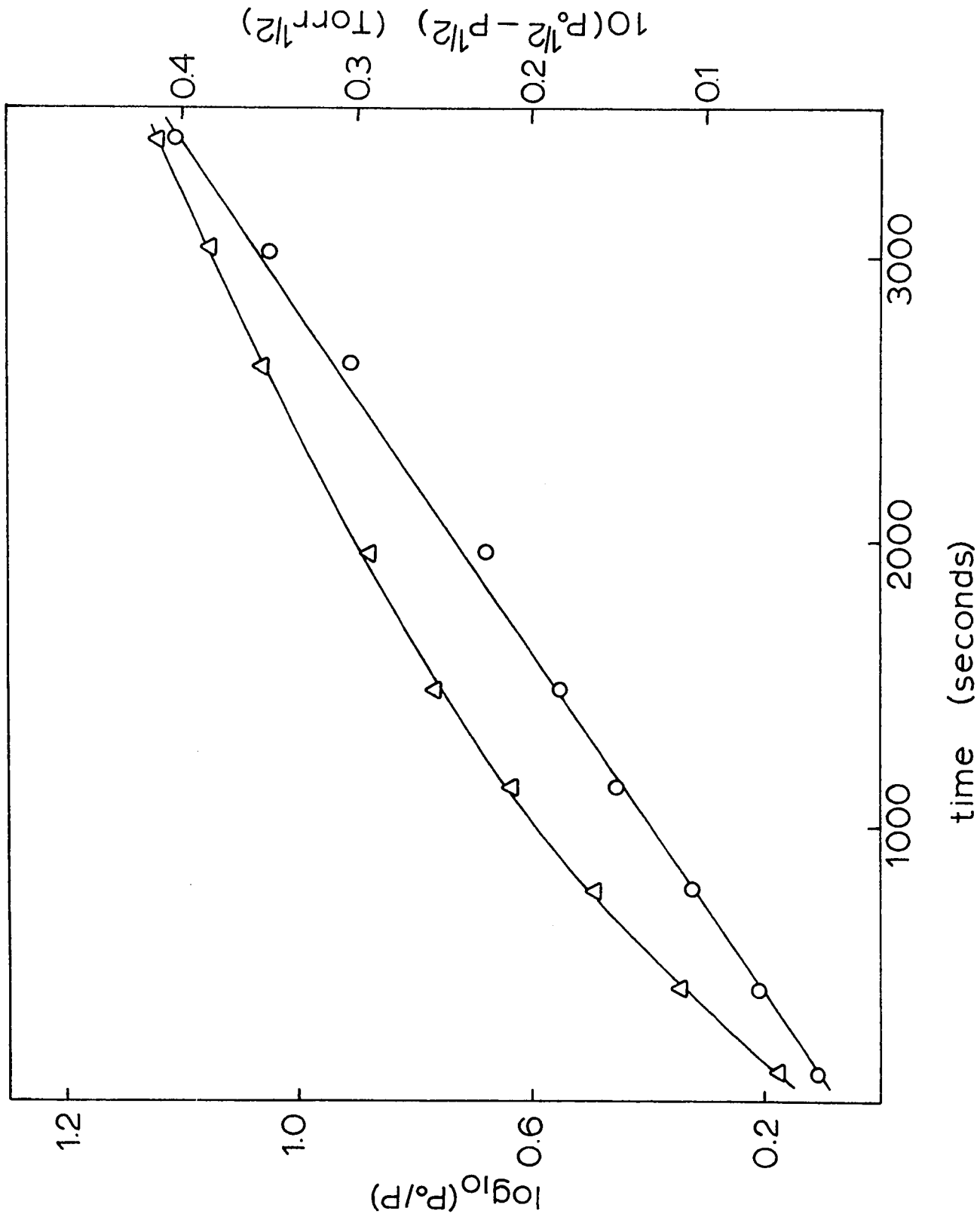
1.2
1.0
0.6
0.2
log10(P°/P)
1000
2000
3000
time (seconds)
0.4
0.3
0.2
0.1
10(P°1/2 − P1/2) (Torr1/2)

FIGURE III - 18

Disappearance of 1-Chloropropane

on Manganese

Plotted as a Half Order Reaction

for $P_o = 1x10^{-2}$ Torr

○ - 158°C

○ - 169°C

□ - 177°C

◇ - 189°C

▽ - 198°C

△ - 200°C

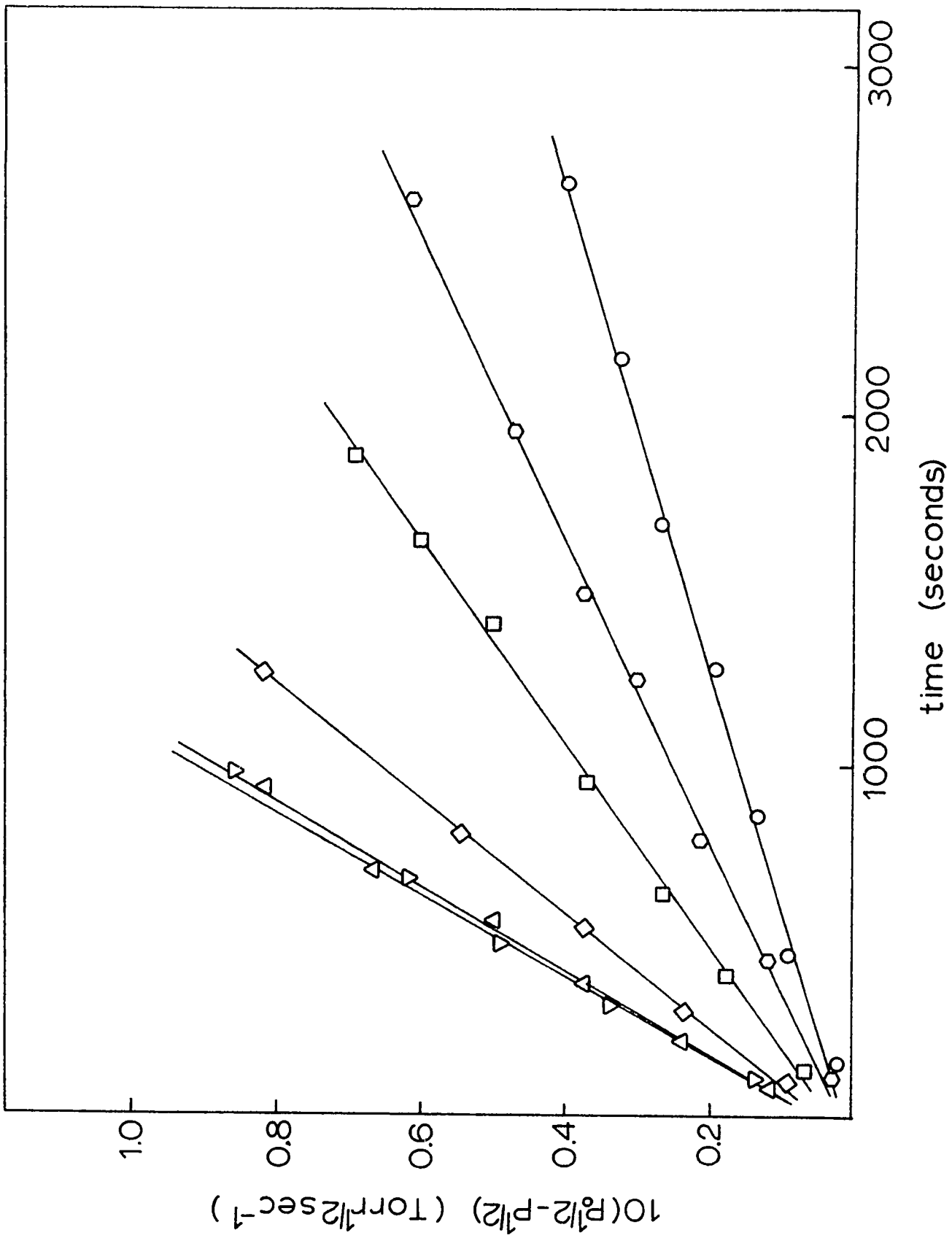
1.0
0.8
0.6
0.4
0.2
1000
2000
3000
time (seconds)
10(P$_0$1/2-P1/2) (Torr1/2sec^{-1})

FIGURE III - 19

Arrhenius Plot of Rate Data for Half Order

Disappearance of 1-Chloropropane

on Manganese

for $P_o = 1 \times 10^{-2}$ Torr

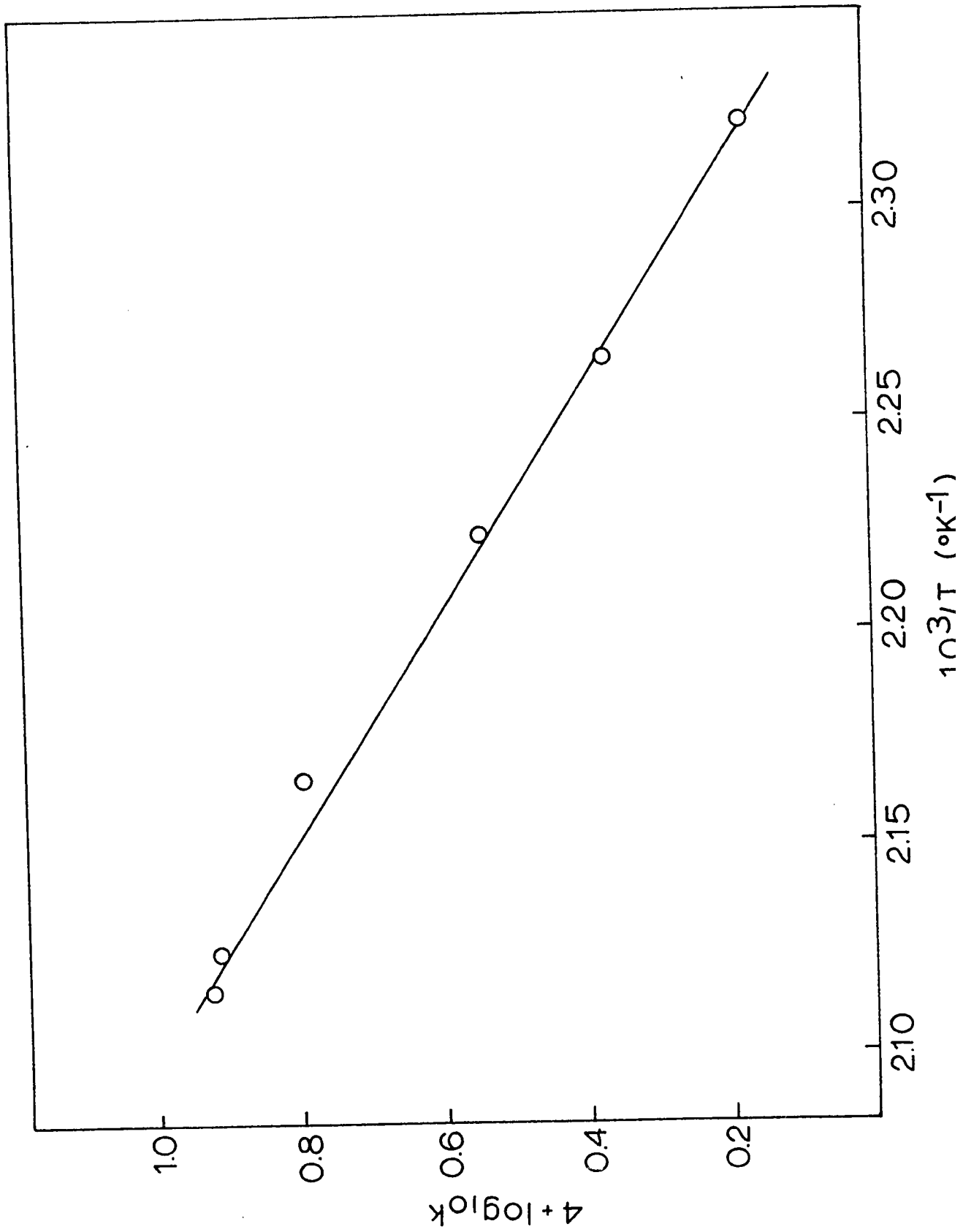
1.0
0.8
0.6
0.4
0.2
A + log10k
2.10
2.15
2.20
2.25
2.30
10^3/T (°K^-1)

Iron

High temperature reactions of 1-chloropropane with halided iron surfaces were characterized by rapid surface deactivation. Successive reactions were conducted at increasing temperatures between 65 and 212°C until the film became totally inactive. The products were consistently propene and hydrogen while all the chloride remained in the film. Each temperature increase caused hydrogen evolution from the film. Rate decreased so rapidly that no meaningful kinetics could be determined. Reaction with only 2.5×10^{-2} Torr of 1-chloropropane was sufficient to totally deactivate the film.

Cobalt

The same behavior for reactions of 1-chloropropane was found with cobalt as with iron. In this case the reaction was studied up to 234°C and a total of 4.5×10^{-2} Torr of 1-chloropropane was reacted prior to total film deactivation.

Nickel

As with iron and cobalt, nickel films were rapidly poisoned by reactions of 1-chloropropane.

After the reaction of $6x10^{-2}$ Torr of 1-chloropropane the film was totally inactive even at 240°C. The gas phase products were, likewise, propene with a continual release of hydrogen as all the chloride was retained by the film.

iii) 1-Chloro-2-methylpropane

Between the initial low temperature reactions and the onset of catalytic behavior, the reactions of 1-chloro-2-methylpropane with all the metals passed through periods of high temperature non-catalytic behavior similar in products to those found with 1-chloropropane. During this period, no hydrogen chloride was produced and the products were olefin with gradually decreasing quantities of paraffin and hydrogen. To be discussed at the end of this chapter, the kinetics were both inconsistent and complex.

An approximation to the length of this non-catalytic interval is shown in the third column of Table III-4. The first column lists the total pressure of 1-chloro-2-methylpropane reacted during the low temperature initial reactions and second the total pressure reacted prior to the appearance of hydrogen chloride. The difference between these two, the pressure reacted during the high temperature non-catalytic stage, is listed in the third.

However, this is only a rough approximation to the length of this interval since hydrogen chloride adsorbs onto the walls of the reaction manifold before appearing in the gas phase.

TABLE III - 4

Pressures of 1-Chloro-2-methylpropane Reacted With The First Row Transition Metals Prior to The Appearance of Hydrogen Chloride

metal	pressure initially reacted $x10^2$(Torr)	pressure reacted before HCl $x10^2$(Torr)	pressure reacted high T non-catalytic interval $x10^2$(Torr)
Ti	0.5	15.7	15.2
V	15.1	18.9	3.8
Cr	2.7	6.8	4.1
Mn	0.5	7.8	7.3
Fe	1.9	3.8	1.9
Co	1.0	4.1	3.1
Ni	0.9	3.8	2.9

III-B-2-b) Catalytic Reactions of 1-Chloro-2-methylpropane

Introductory Comments

As described previously, two general types of reactions were detected on halided surfaces: catalytic and non-catalytic. These designations distinguish between the former where the surface acted as a true catalyst releasing olefin and hydrogen chloride and the latter during which chloride and some hydrogen was retained in the surface. As 1-chloropropane was used to exemplify the non-catalytic reaction, 1-chloro-2-methylpropane was selected to typify the catalytic scheme. On titanium (Summers, 1970), the latter reacted to an equimolar mixture of hydrogen chloride and methylpropene. Its characteristics have been reviewed in Section I-G.

This section describes the reactions of 1-chloro-2-methylpropane on the first row transition metals from vanadium through nickel. Each reaction generated an equimolar mixture of hydrogen chloride and methylpropene as the pressure doubled. No side reactions were observed.

Before proceeding catalytically each reaction passed through a period of non-catalytic behavior. This settling down or induction period varied in duration among the metals and is described in detail in

Section III-B-2-a. In the absence of a metal film, hydrogen chloride was adsorbed onto the reaction manifold. This, along with the observation that reaction became first order before any hydrogen chloride was detected, suggests that part of the induction period may have involved saturation of the walls with hydrogen chloride.

The time order of each reaction has been determined. Since the activation parameters were pressure sensitive, concentration order could not be established (Section IV-B-2).

Vanadium

After an extensive period of non-catalytic reaction the dehydrochlorination of 1-chloro-2-methylpropane on vanadium progressed catalytically generating an equimolar mixture of methylpropene and hydrogen chloride as the pressure doubled. The reaction was conveniently studied at 10^{-2} Torr between 180 and 220°C. As shown in Figure III-20, 1-chloro-2-methylpropane disappeared by first order kinetics. An Arrhenius plot of these reactions is shown in Figure III-21 giving an activation energy of 8.1 ± 0.3 Kcal/mole and a $\log_{10}A$ of 1.1 ± 0.1.

Chromium

The reactions of both 2-chloropropane and 1-chloro-2-methylpropane on chromium have been

FIGURE III - 20

Disappearance of 1-Chloro-2-methylpropane

on Vanadium

Plotted as a First Order Reaction

for $P_o = 1 \times 10^{-2}$ Torr

□ - 186°C

○ - 200°C

▽△ - 214°C

○ - 221°C

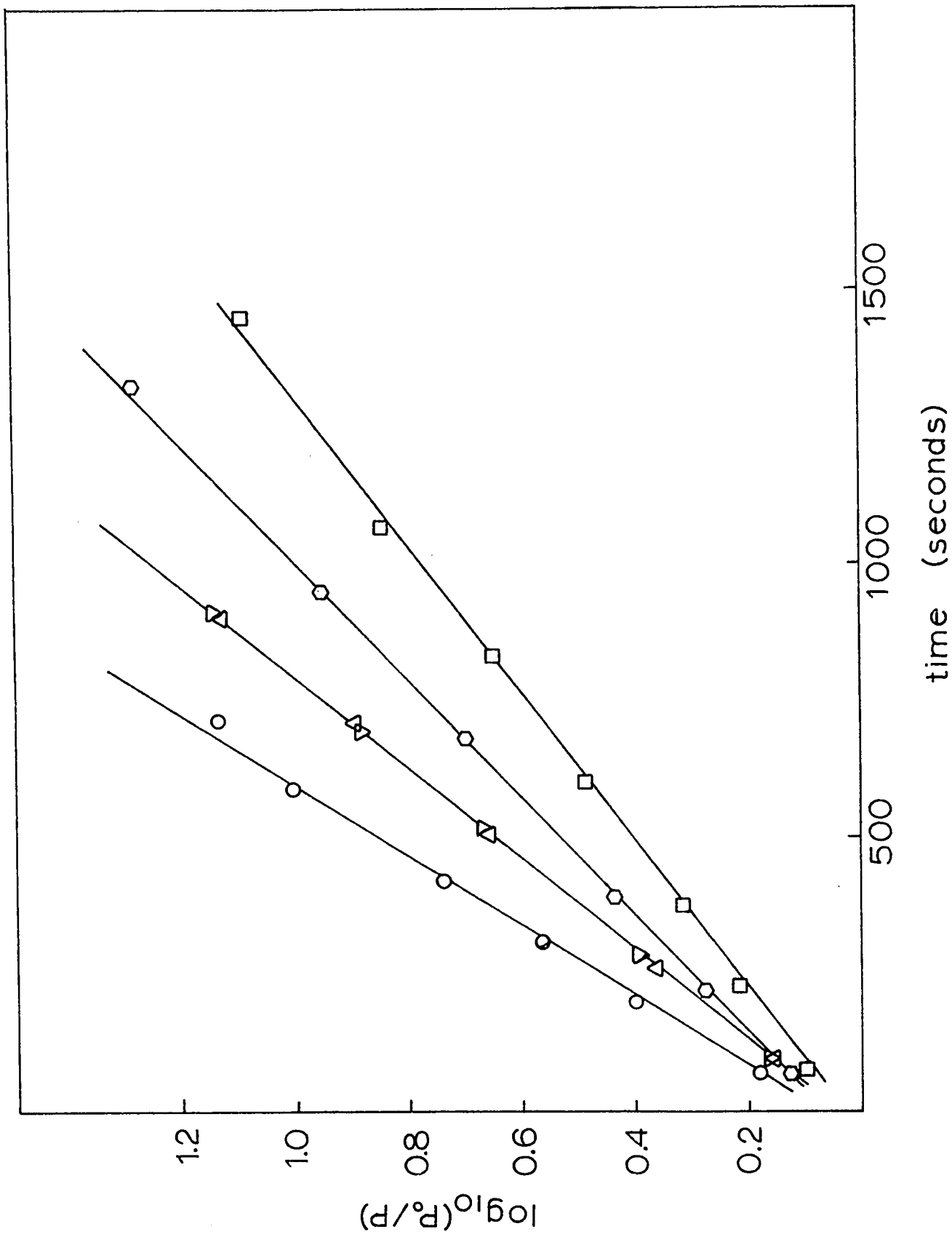
1.2
1.0
0.8
0.6
0.4
0.2
log10(P°/P)
500
1000
1500
time (seconds)

FIGURE III - 21

Arrhenius Plot of Rate Data for First Order

Disappearance of 1-Chloro-2-methylpropane

on Vanadium

for $P_o = 1 \times 10^{-2}$ Torr

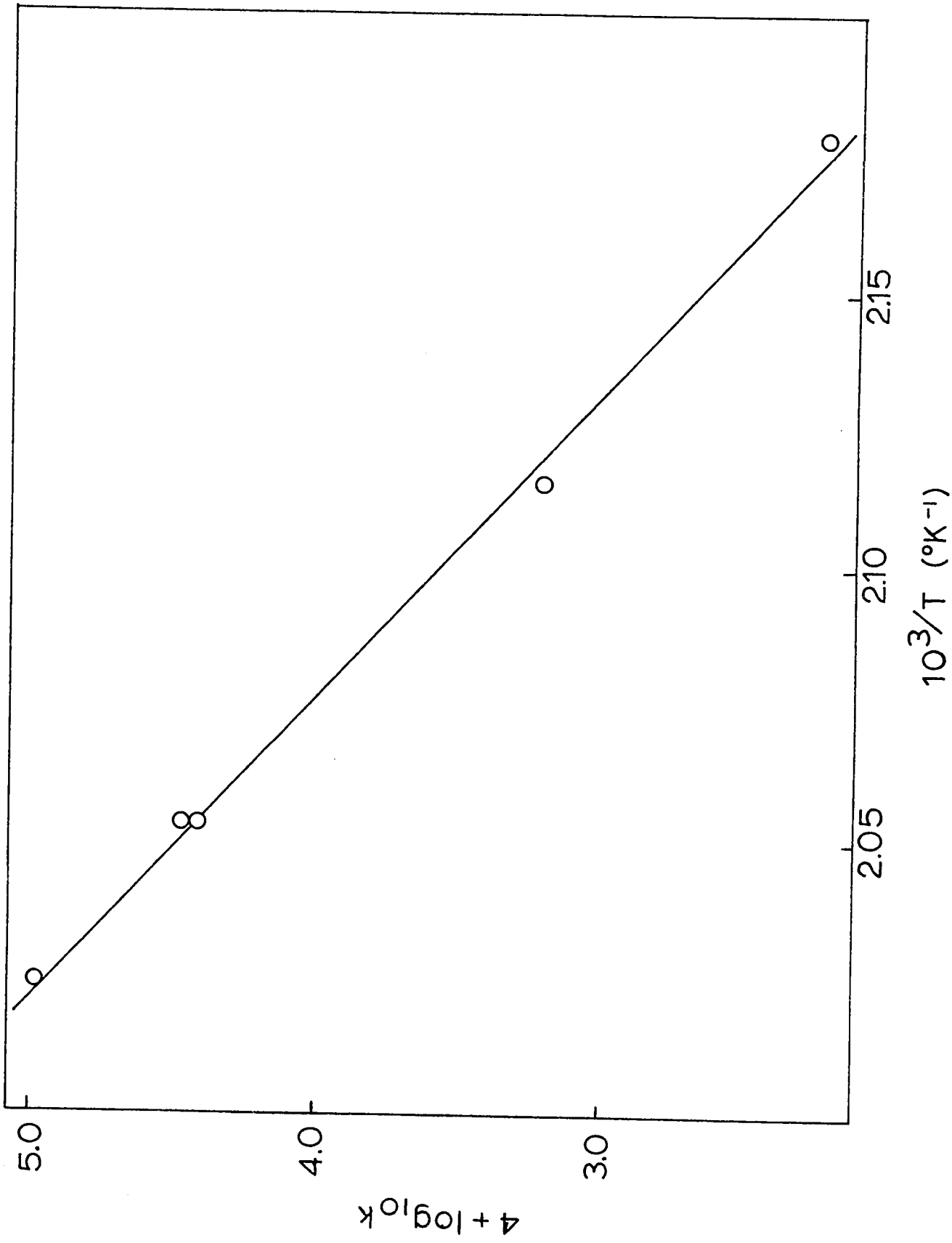
5.0
4.0
3.0
4 + log10k
2.05
2.10
2.15
10^3/T (°K^-1)

studied. The latter manifested an extended period of non-catalytic behavior before settling into the stoichiometric reaction to olefin and hydrogen chloride.

The reaction with 1-chloro-2-methylpropane was studied at 10^{-2} Torr between 150 and 200°C. As shown in Figures III-22, III-23, it was first order in 1-chloro-2-methylpropane with an activation energy of 6.6 ± 0.2 Kcal/mole and a $\log_{10}A$ of 0.3 ± 0.1. During reaction, the total pressure doubled.

On a film previously reacted with 1-chloro-2-methylpropane, the catalytic reaction of 2-chloropropane was studied. As described in detail in Section IV- C , pretreatment with 1-chloro-2-methylpropane likely altered the behavior of the film toward 2-chloropropane. As shown in Figures III-24, III-25, III-26, and III-27, the reaction followed first order kinetics between 150 and 200°C. Both $\log_{10}A$ and activation energy increased with pressure, the former from 0.95 ± 0.08 to 2.0 ± 0.1 and the latter from 8.0 ± 0.2 to 10.6 ± 0.3 for a pressure change from 1×10^{-2} to 5×10^{-2} Torr. Although these values likely differ from those for a film reacted exclusively with 2-chloropropane, they certainly indicate the trend in Arrhenius parameters with reactant pressure.

FIGURE III - 22

Disappearance of 1-Chloro-2-methylpropane

on Chromium

Plotted as a First Order Reaction

for $P_o = 1x10^{-2}$ torr

○ - 150°C

○ - 171°C

◇ □ - 183°C

△ ▽ - 198°C

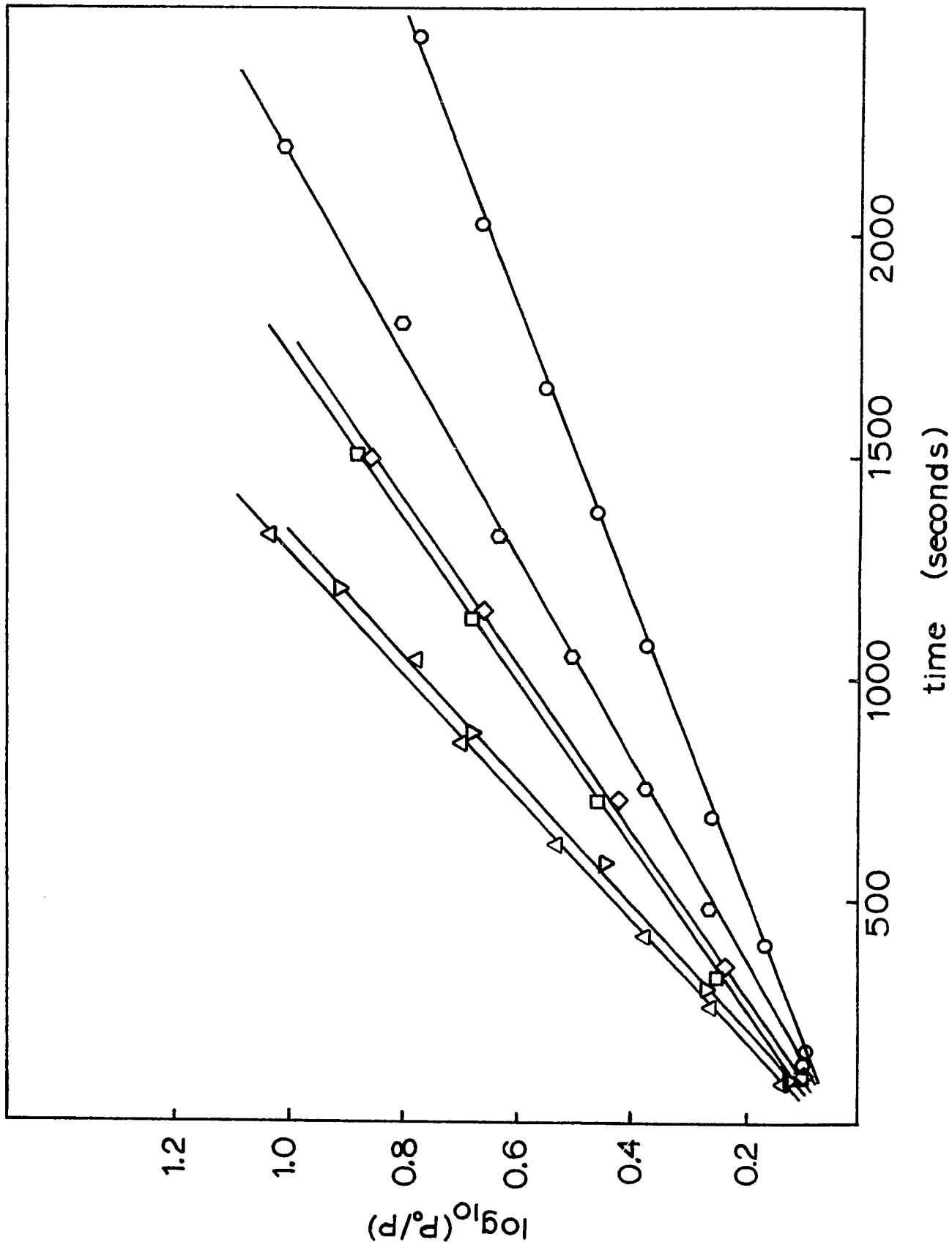
1.2
1.0
0.8
0.6
0.4
0.2
$\log_{10}(P_o/P)$
500
1000
1500
2000
time (seconds)

FIGURE III - 23

Arrhenius Plot of Rate Data for First Order

Disappearance of 1-Chloro-2-methylpropane

on Chromium

for $P_o = 1 \times 10^{-2}$ Torr

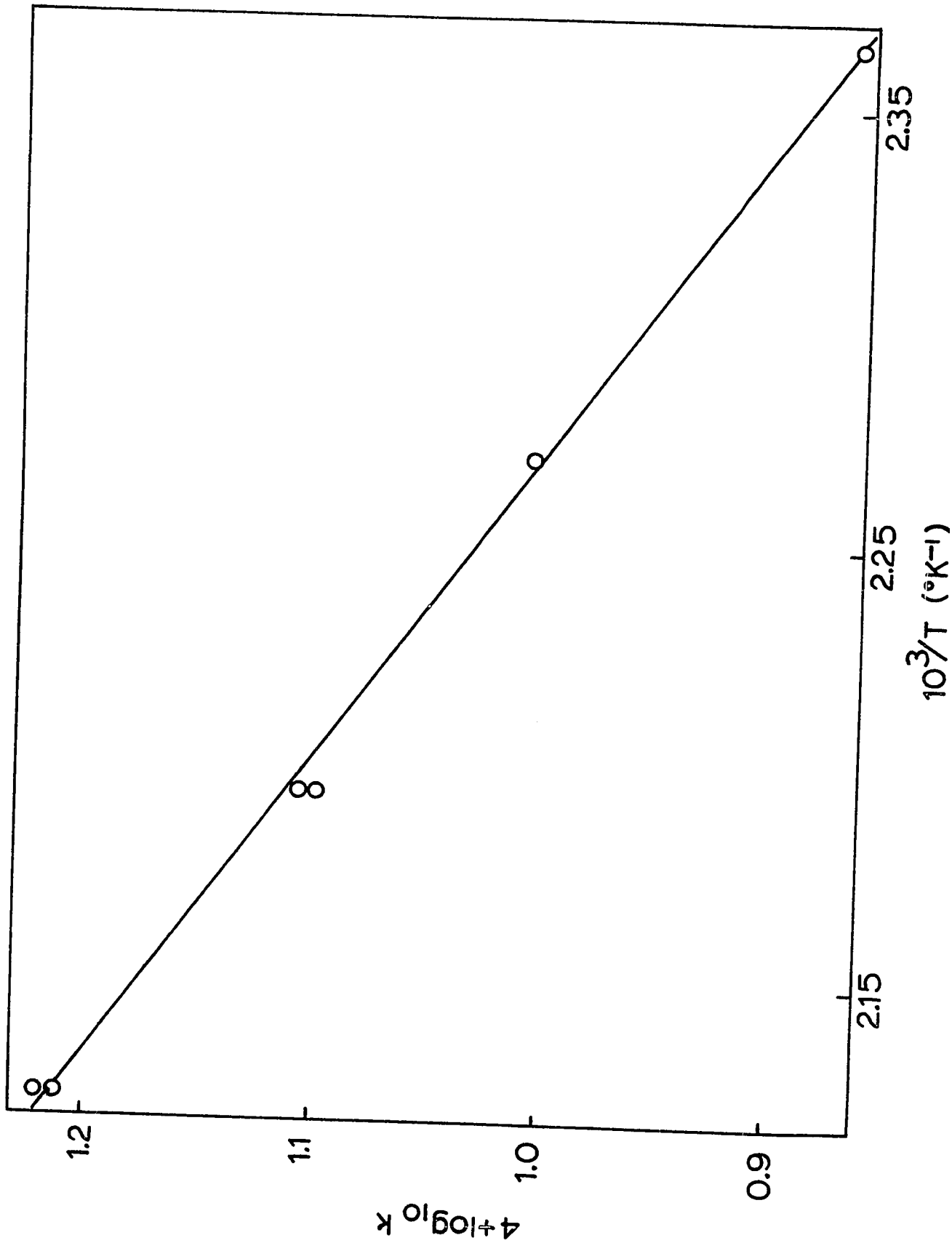
4+log10 k
1.2
1.1
1.0
0.9
2.15
2.25
2.35
10^3/T (°K-1)

FIGURE III - 24

Disappearance of 2-Chloropropane

on Chromium

Plotted as a First Order Reaction

for $P_o = 1 \times 10^{-2}$ torr

o - 153°C

◇ - 170°C

⬡ - 179°C

▽△ - 193°C

□ - 202.5°C

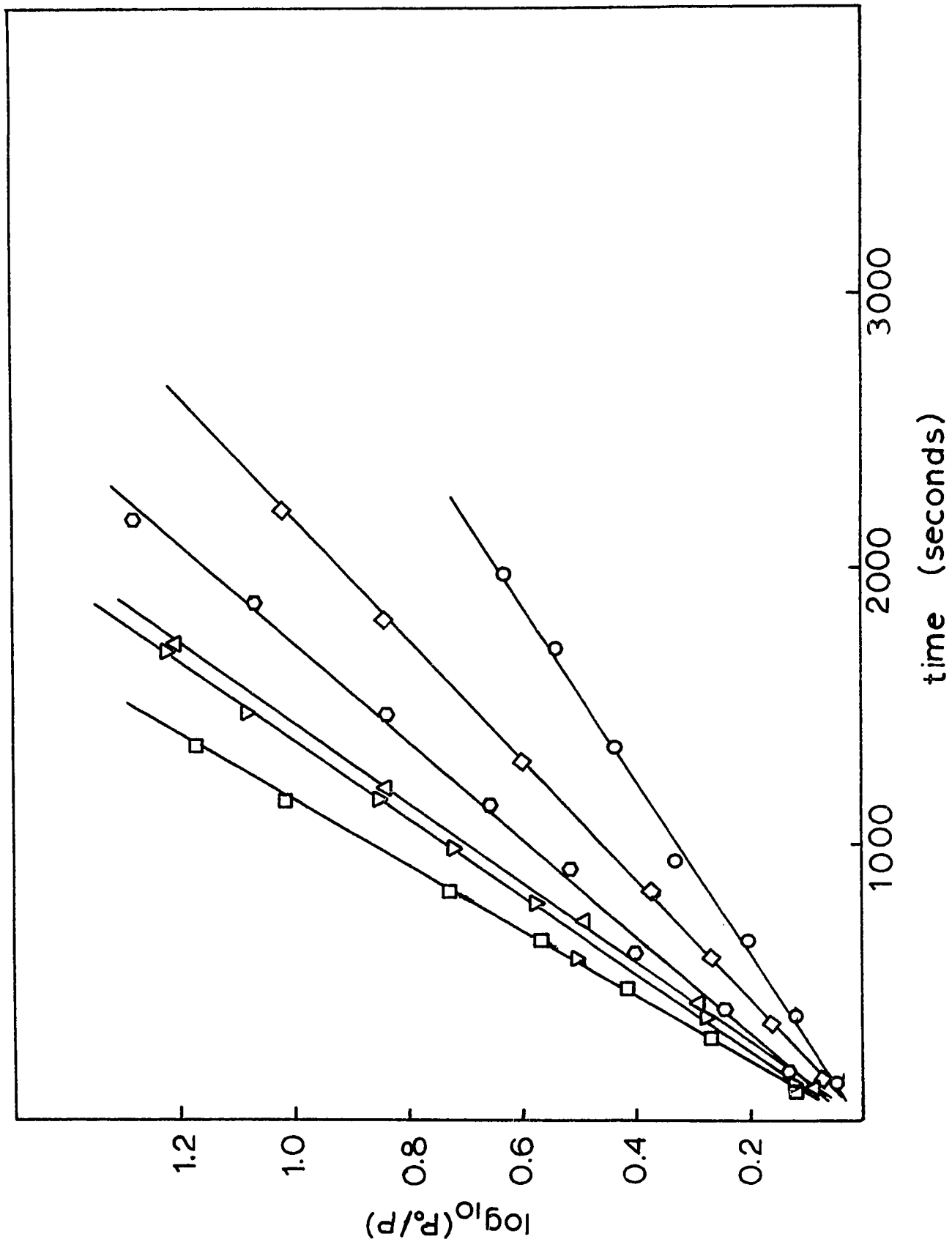
1.2
1.0
0.8
0.6
0.4
0.2
log10(P°/P)
1000
2000
3000
time (seconds)

FIGURE III - 25

Arrhenius Plot of Rate Data for First Order

Disappearance of 2-Chloropropane

on Chromium

for $P_o = 1 \times 10^{-2}$ Torr

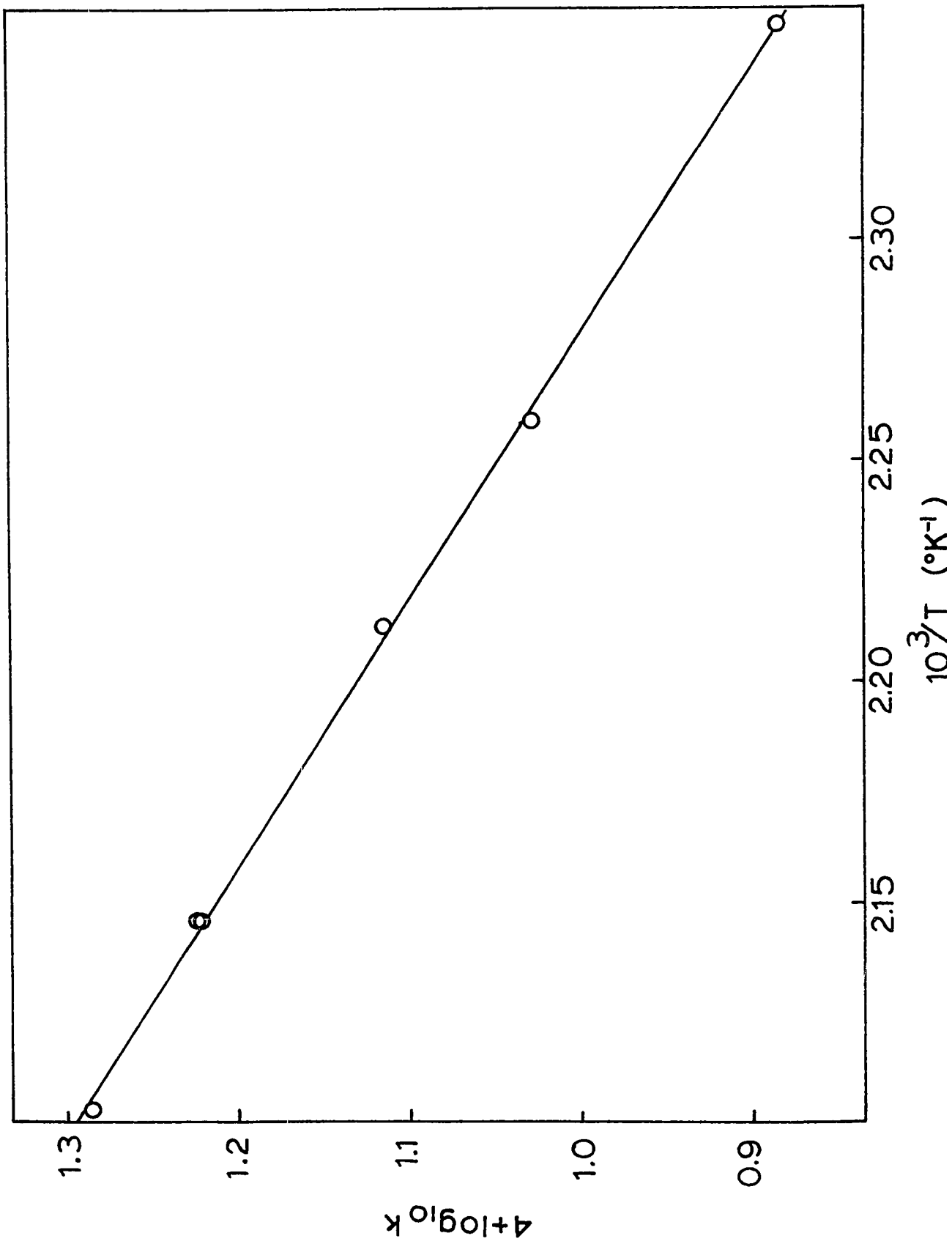
4+log10 k
1.3
1.2
1.1
1.0
0.9
2.15
2.20
2.25
2.30
10^3/T (°K^-1)

FIGURE III - 26

Disappearance of 2-Chloropropane

on Chromium

Plotted as a First Order Reaction

for $P_o = 5x10^{-2}$ torr

○ - 169°C

□ - 183°C

△ - 201°C

▽ - 201.5°C

⬡ - 210°C

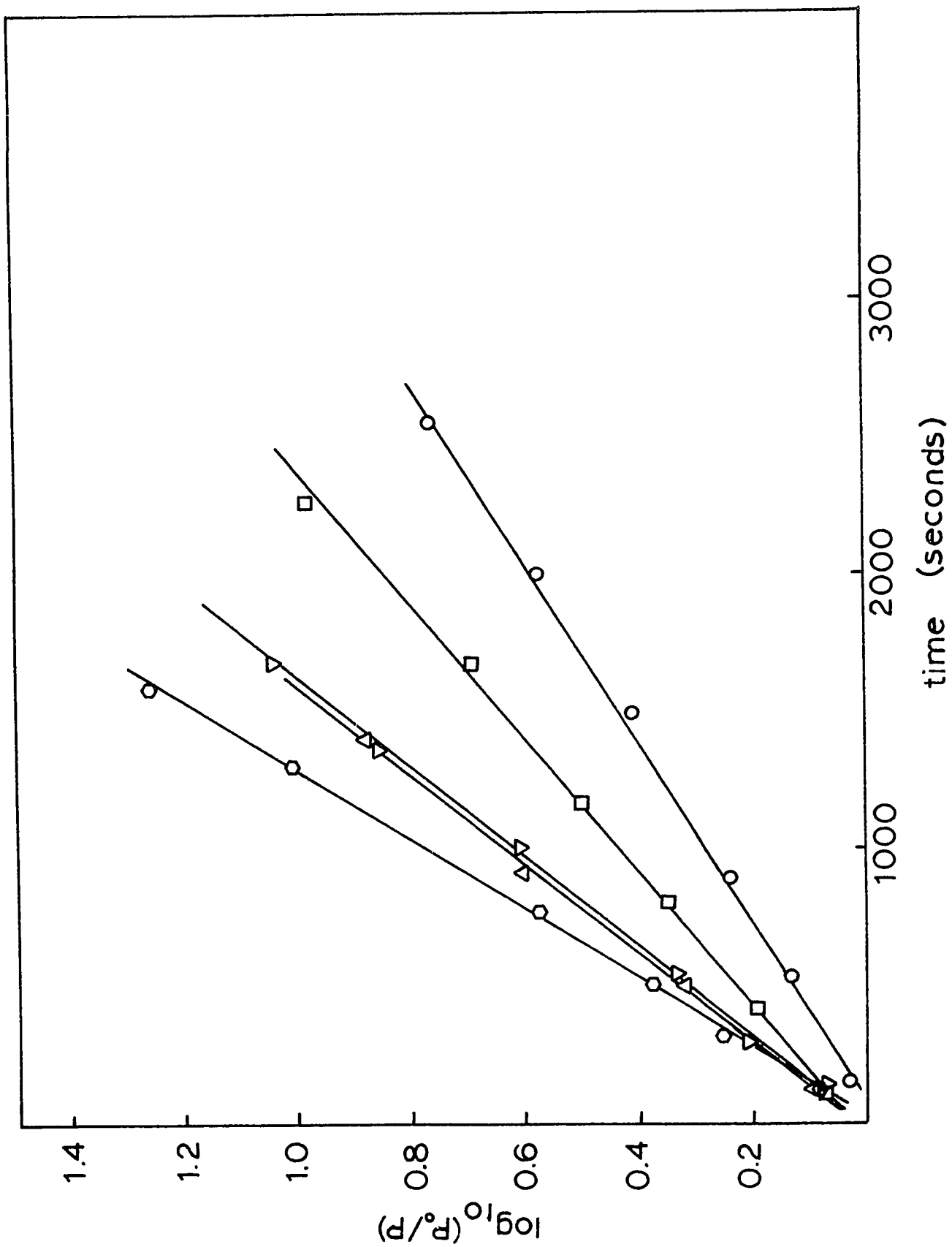
1.4
1.2
1.0
0.8
0.6
0.4
0.2
log10(P°/P)
1000
2000
3000
time (seconds)

FIGURE III - 27

Arrhenius Plot of Rate Data for First Order

Disappearance of 2-Chloropropane

on Chromium

for $P_o = 5 \times 10^{-2}$ Torr

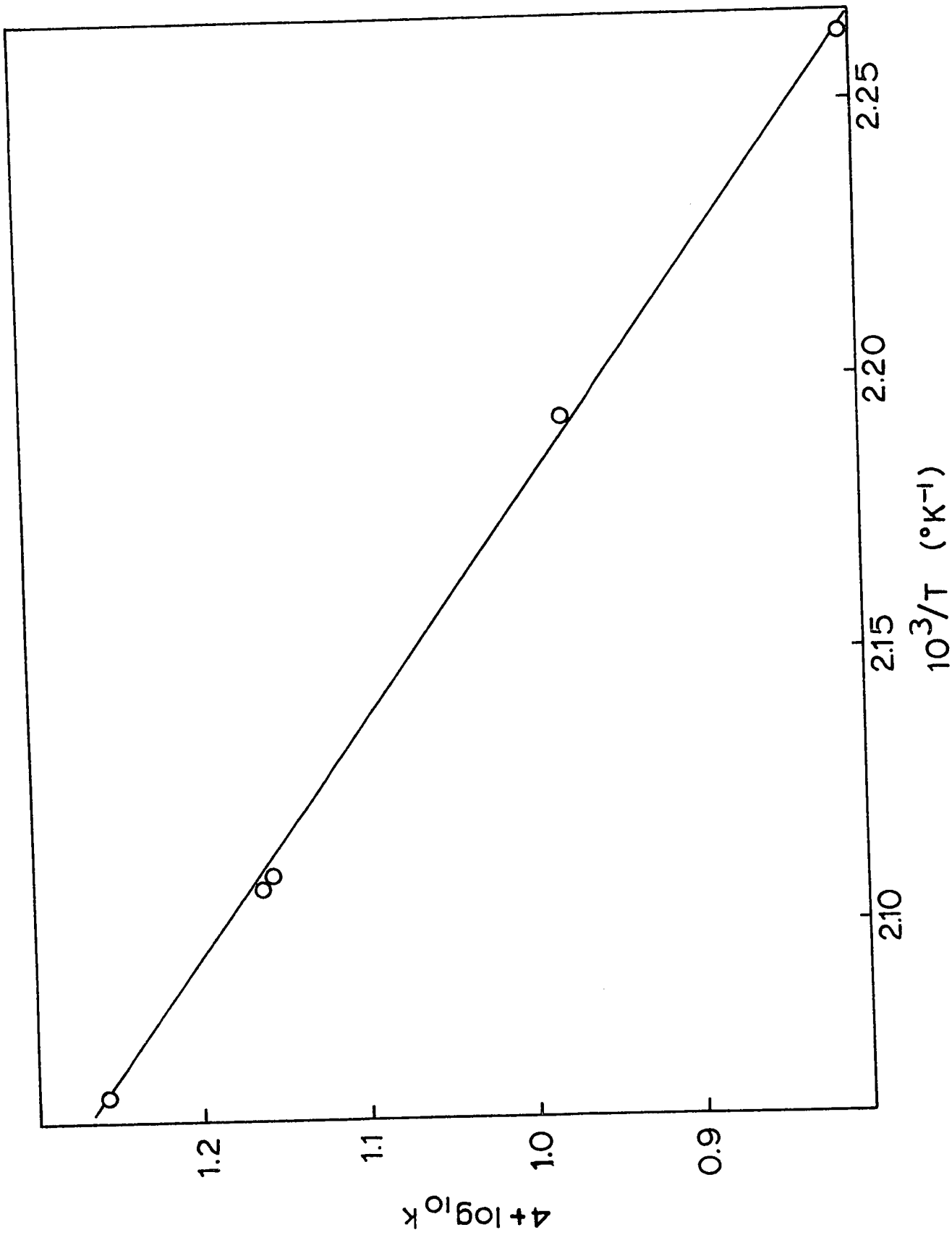
4 + log10 k
1.2
1.1
1.0
0.9
2.10
2.15
2.20
2.25
10^3/T (°K^-1)

Manganese

After experiencing a standard period of non-catalytic behavior, the dehydrochlorination of 1-chloro-2-methylpropane on manganese to methylpropane and hydrogen chloride proceeded normally with a two fold pressure increase. Between 175 and 235°C, reactant disappeared by first order kinetics at both $1x10^{-2}$ and $5x10^{-2}$ Torr (Figures III-28 and III-30).

Figure III-29 shows an Arrhenius plot of the data at $1x10^{-2}$ Torr with an activation energy of 2.9 ± 0.2 Kcal/mole and a $\log_{10}A$ of -1.6 ± 0.1. At $5x10^{-2}$ Torr, both increased to an activation energy of 3.5 ± 0.2 Kcal/mole and a $\log_{10}A$ of -1.4 ± 0.1 (Figure III-31).

Iron

The reactions of 1-chloro-2-methylpropane on iron proceeded through a period of non-catalytic behavior. Eventually, however, a catalytic reaction to olefin and hydrogen chloride was achieved. At $1x10^{-2}$ Torr, 1-chloro-2-methylpropane disappeared by first order kinetics between 210 and 240°C as the pressure doubled (Figure III-32). The Arrhenius parameters were 6.2 ± 0.4 Kcal/mole and -0.1 ± 0.2 for the activation energy and $\log_{10}A$ respectively (Figure III-33).

FIGURE III - 28

Disappearance of 1-Chloro-2-methylpropane

on Manganese

Plotted as a First Order Reaction

for $P_o = 1x10^{-2}$ Torr

○ - 177°C

□ - 192°C

▽ △ - 207°C

⬡ - 220°C

◇ - 234°C

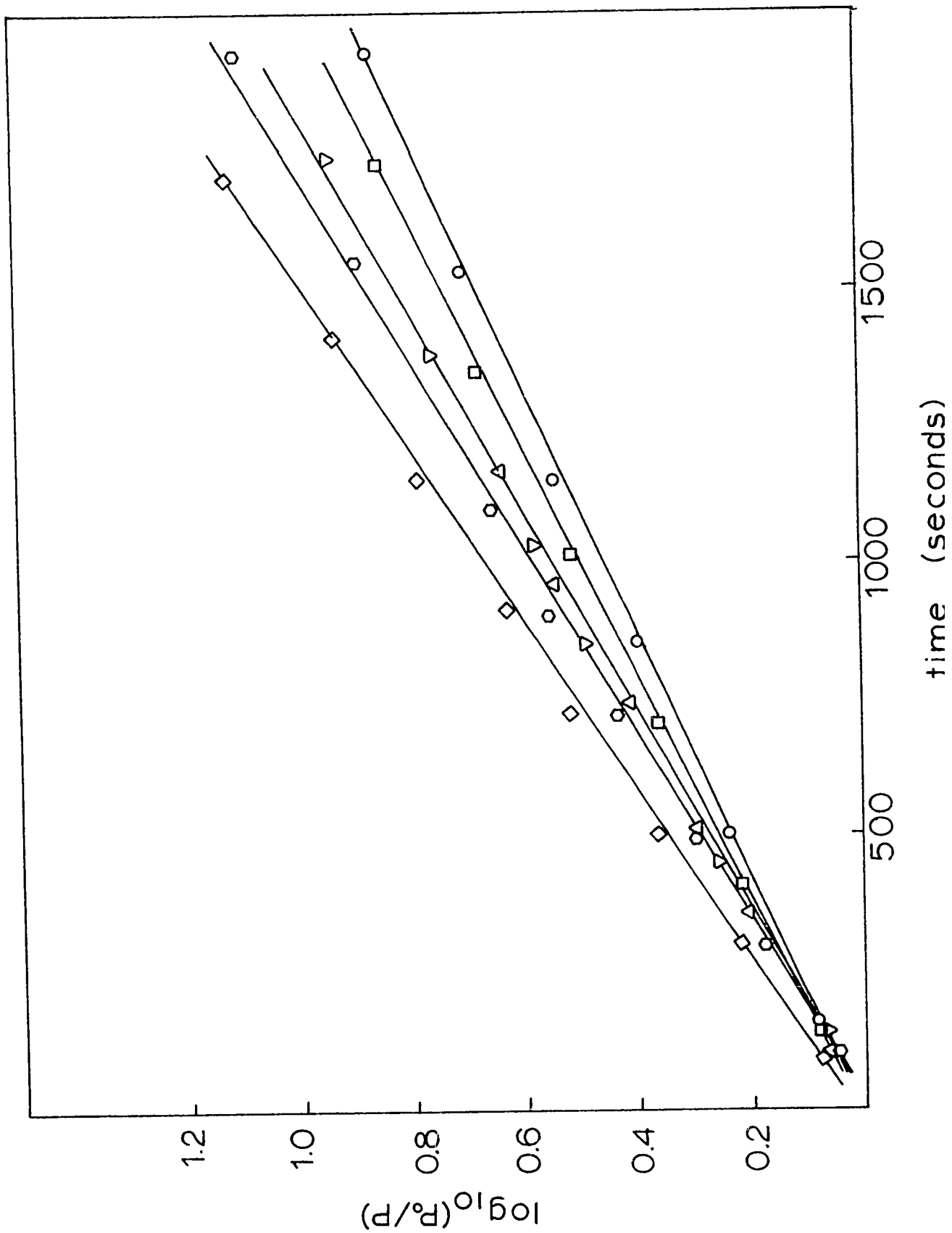
1.2
1.0
0.8
0.6
0.4
0.2
log10(P°/P)
500
1000
1500
time (seconds)

FIGURE III - 29

Arrhenius Plot of Rate Data for First Order

Disappearance of 1-Chloro-2-methylpropane

on Manganese

for $P_o = 1 \times 10^{-2}$ Torr

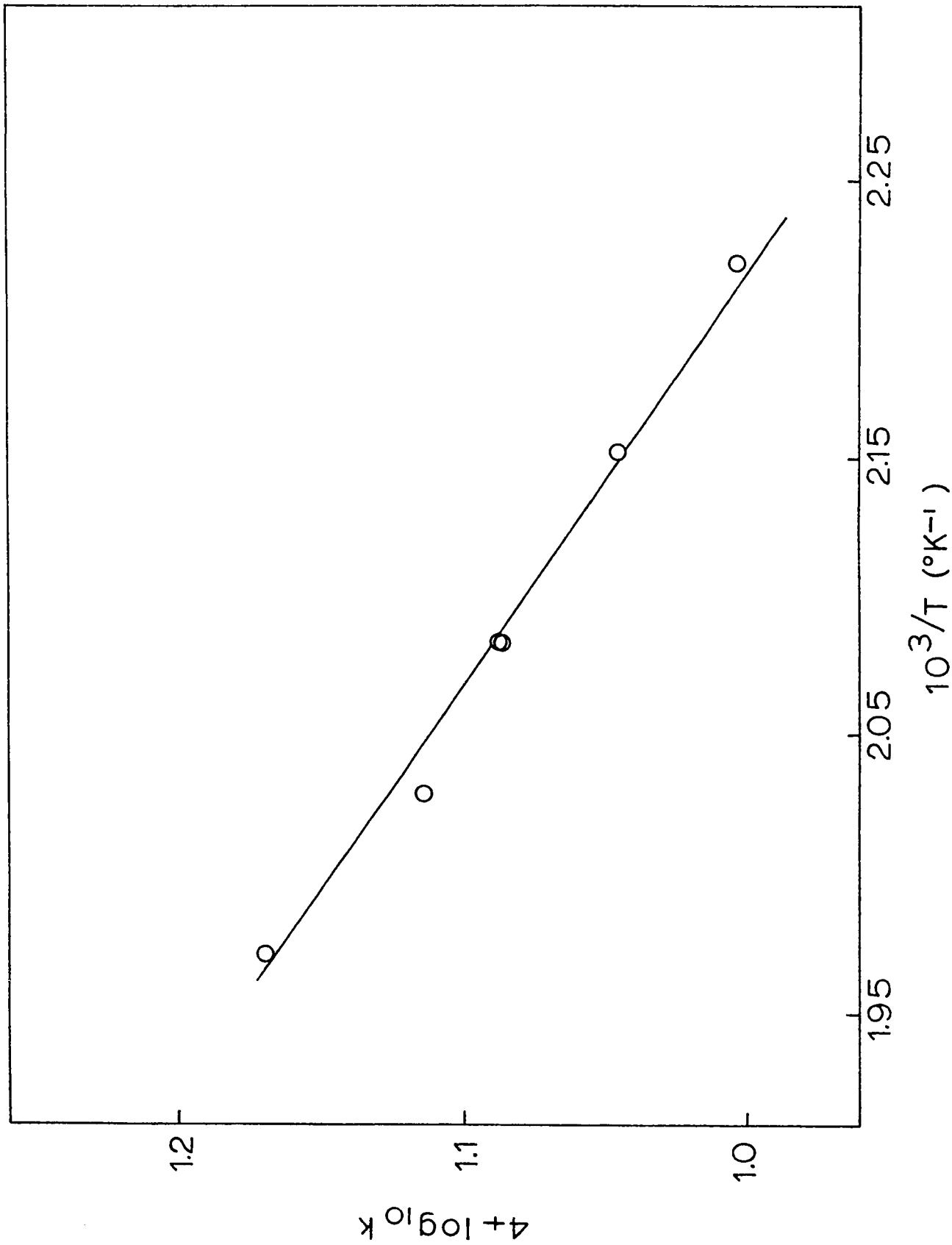
4+ log10 k
1.2
1.1
1.0
1.95
2.05
2.15
2.25
10^3/T (°K^-1)

FIGURE III - 30

Disappearance of 1-Chloro-2-methylpropane

on Manganese

Plotted as a First Order Reaction

for $P_o = 5x10^{-2}$ Torr

○ - 177°C

○ - 178°C

△ - 196°C

□ - 224°C

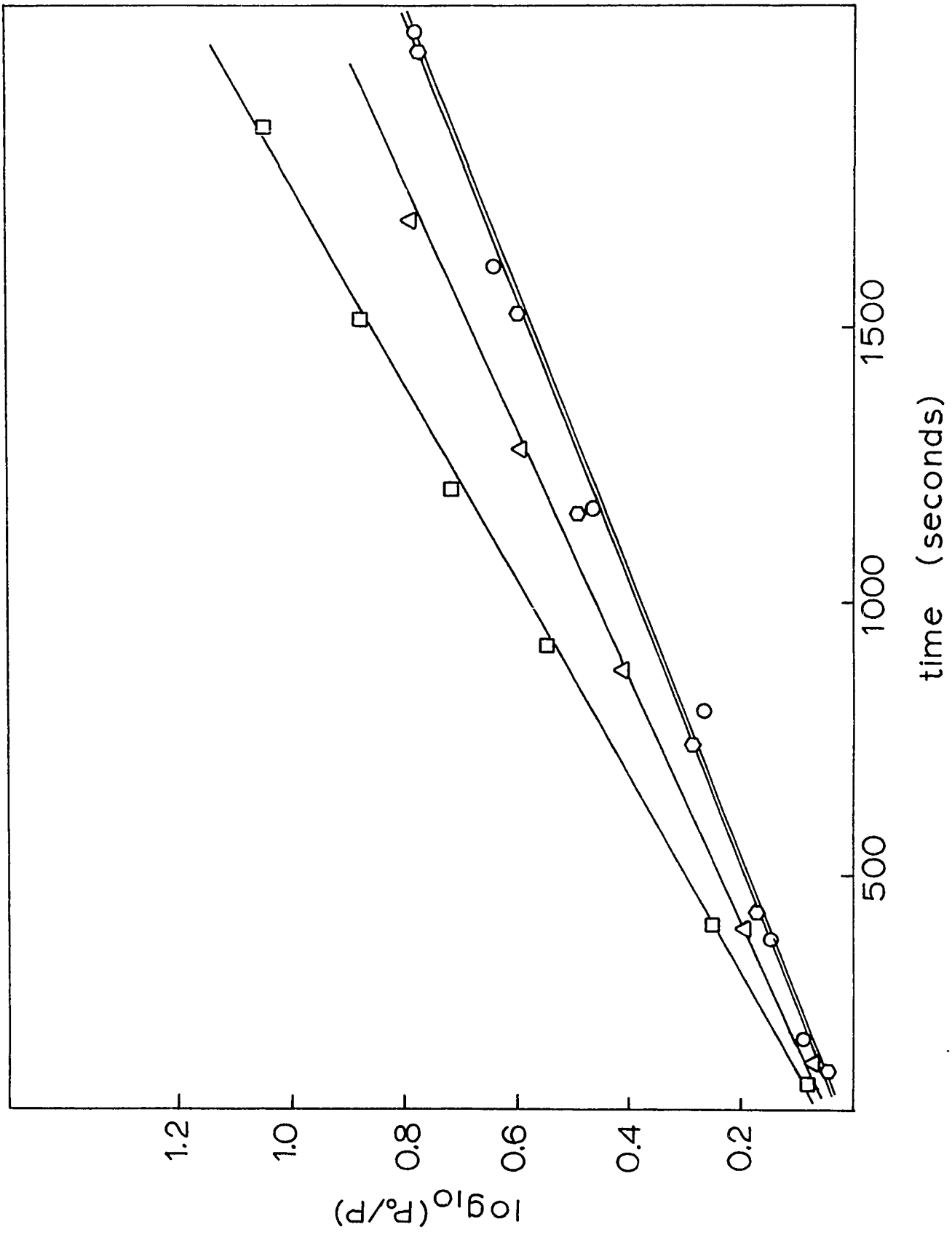
1.2
1.0
0.8
0.6
0.4
0.2
log10(P°/P)
500
1000
1500
time (seconds)

FIGURE III - 31

Arrhenius Plot of Rate Data for First Order

Disappearance of 1-Chloro-2-methylpropane

on Manganese

for $P_o = 5 \times 10^{-2}$ Torr

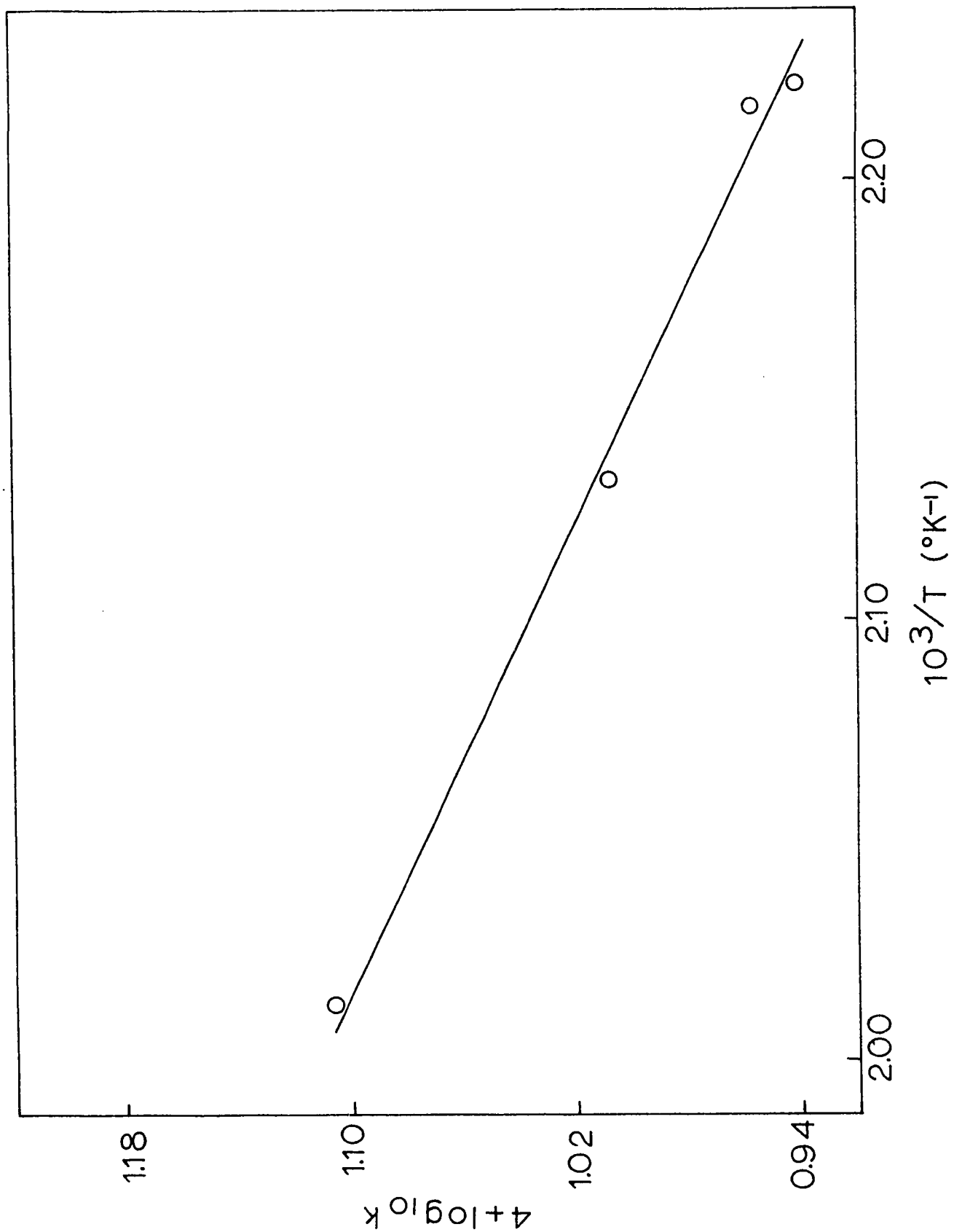
1.18
1.10
1.02
0.94
4 + log10 k
2.00
2.10
2.20
10^3/T (°K-1)

FIGURE III - 32

Disappearance of 1-Chloro-2-methylpropane

on Iron

Plotted as a First Order Reaction

for $P_o = 1 \times 10^{-2}$ Torr

▽△ - 210°C

○ - 226°C

□ - 241°C

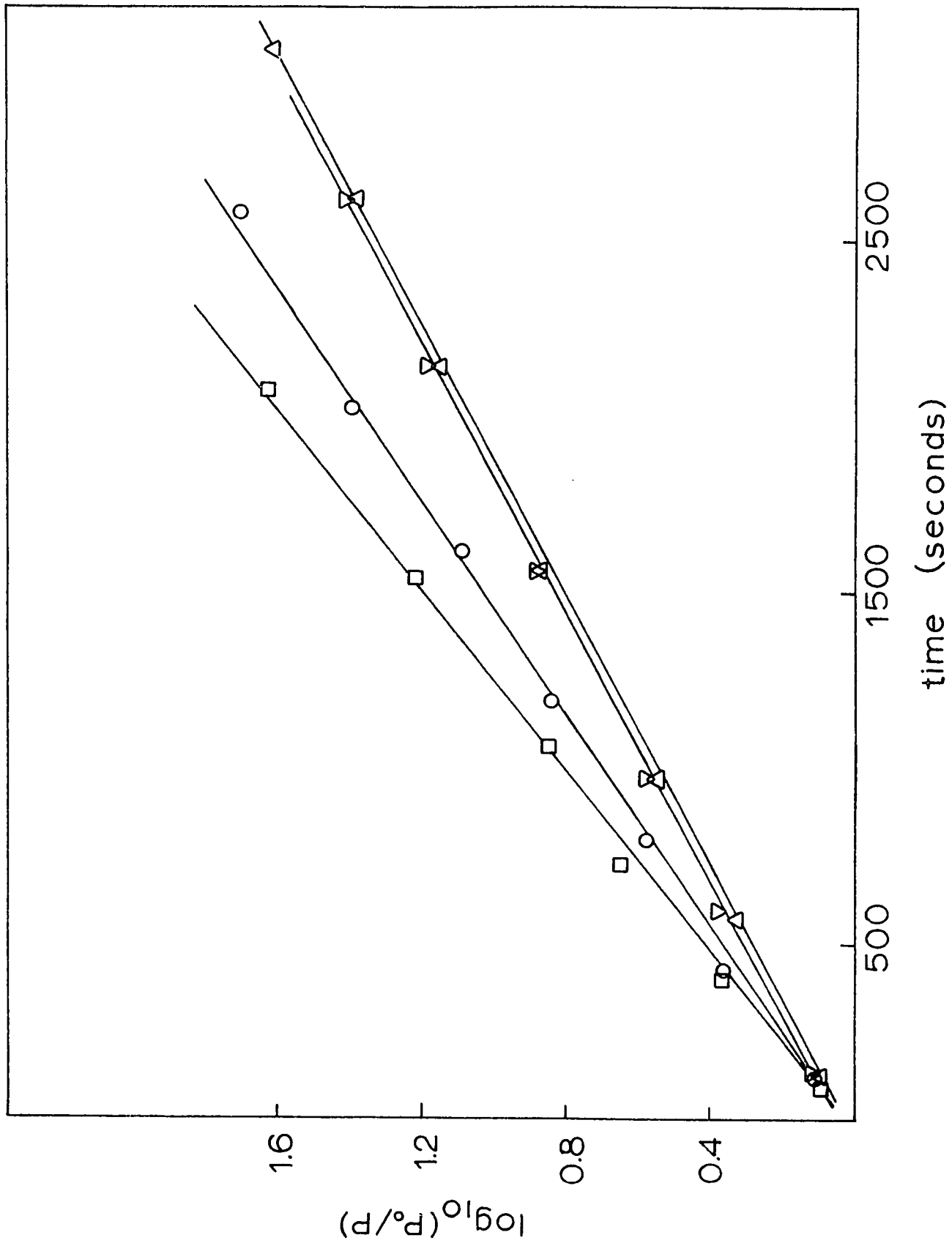
1.6
1.2
0.8
0.4
log10(P°/P)
500
1500
2500
time (seconds)

FIGURE III - 33

Arrhenius Plot of Rate Data for First Order

Disappearance of 1-Chloro-2-methylpropane

on Iron

for $P_o = 1 \times 10^{-2}$ Torr

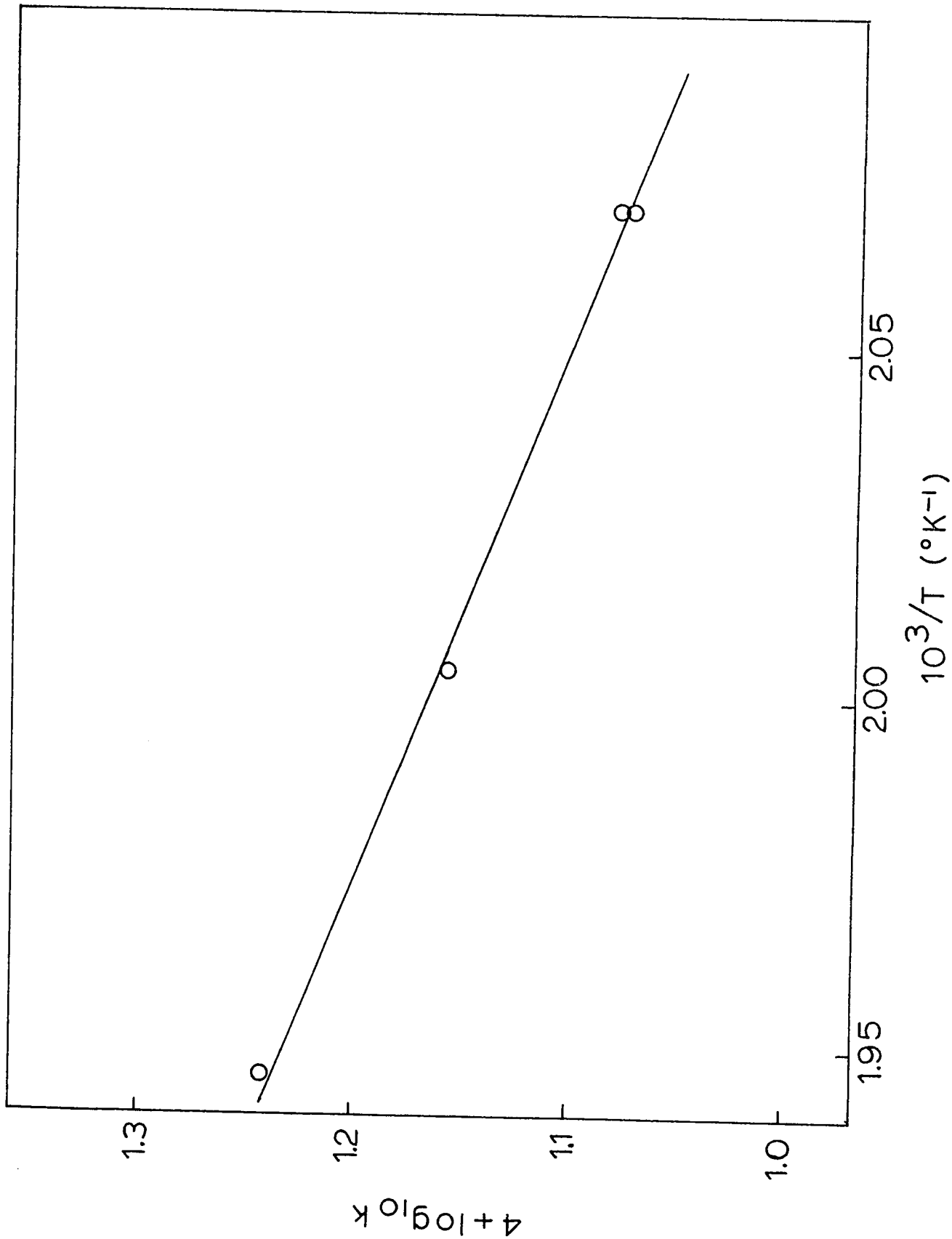
4 + log10 k
1.3
1.2
1.1
1.0
1.95
2.00
2.05
10^3/T (°K^-1)

Cobalt

As with the other metals, the reaction of 1-chloro-2-methylpropane on cobalt to an equimolar mixture of olefin and hydrogen chloride occurred after a period of non-catalytic behavior. At $1x10^{-2}$ Torr, reactant disappeared by first order kinetics between 200 and 245°C as the pressure doubled (Figure III-34). From the Arrhenius plot (Figure III-35), the activation energy was 8.3 ± 0.4 Kcal/mole and $\log_{10}A$ was 1.5 ± 0.2.

Nickel

The reactions of 1-chloro-2-methylpropane with nickel required a standard non-catalytic induction period before proceeding to an equimolar mixture of hydrogen chloride and methylpropane with consequent doubling of the pressure. At $1x10^{-2}$ Torr, this catalytic reaction proceeded by first order kinetics between 190 and 240°C (Figure III-36), the activation energy was 7.6 ± 0.4 Kcal/mole and $\log_{10}A$ was 0.3 ± 0.2 (Figure III-37).

FIGURE III-34

Disappearance of 1-Chloro-2-methylpropane

on Cobalt

Plotted as a First Order Reaction

for $P_o = 1 \times 10^{-2}$ Torr

△ - 202°C

○ - 214°C

□ - 223°C

⬡ - 234°C

▽ - 246°C

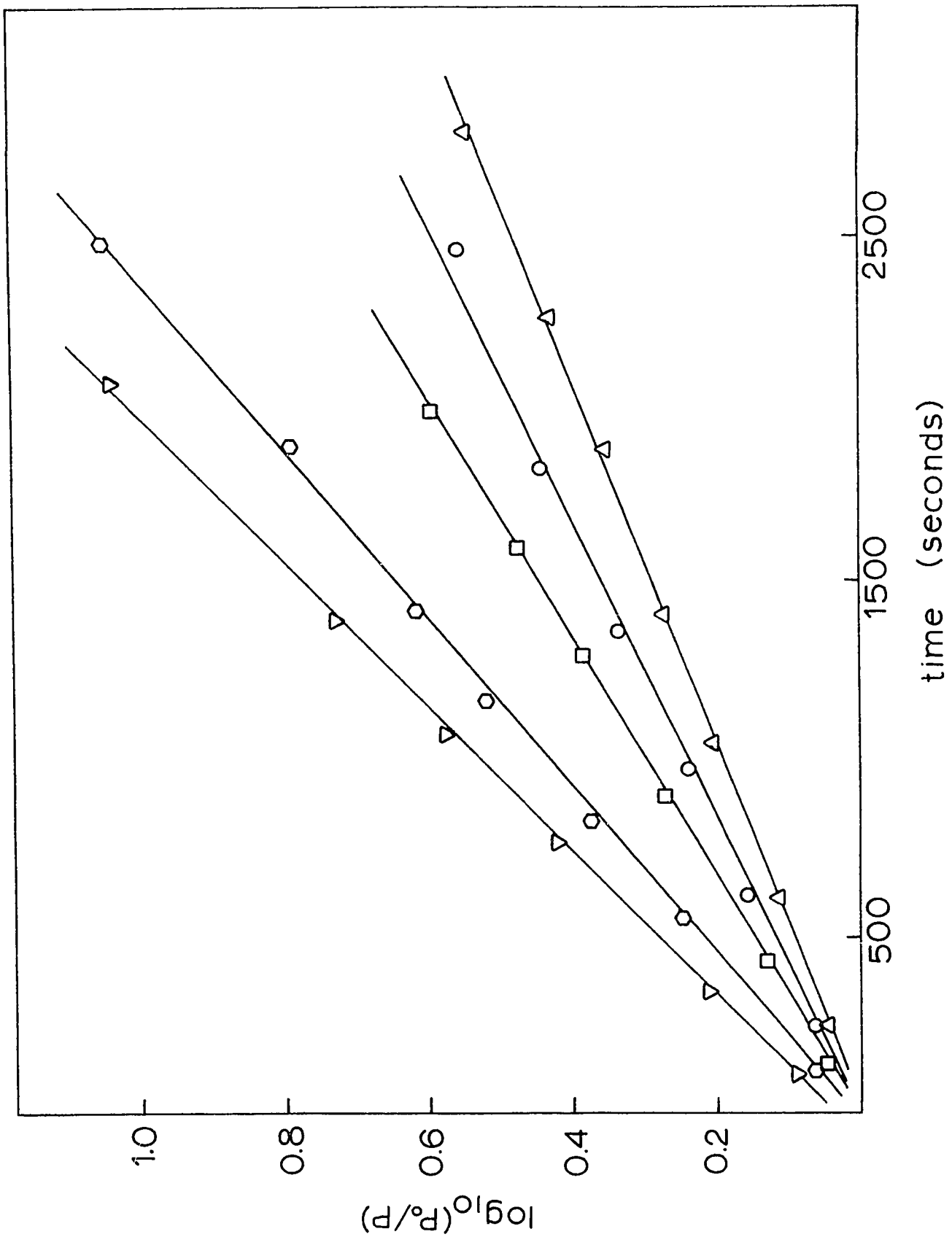
1.0
0.8
0.6
0.4
0.2
log10(P°/P)
500
1500
2500
time (seconds)

FIGURE III - 35

Arrhenius Plot of Rate Data for First Order

Disappearance of 1-Chloro-2-methylpropane

on Cobalt

for $P_o = 1 \times 10^{-2}$ Torr

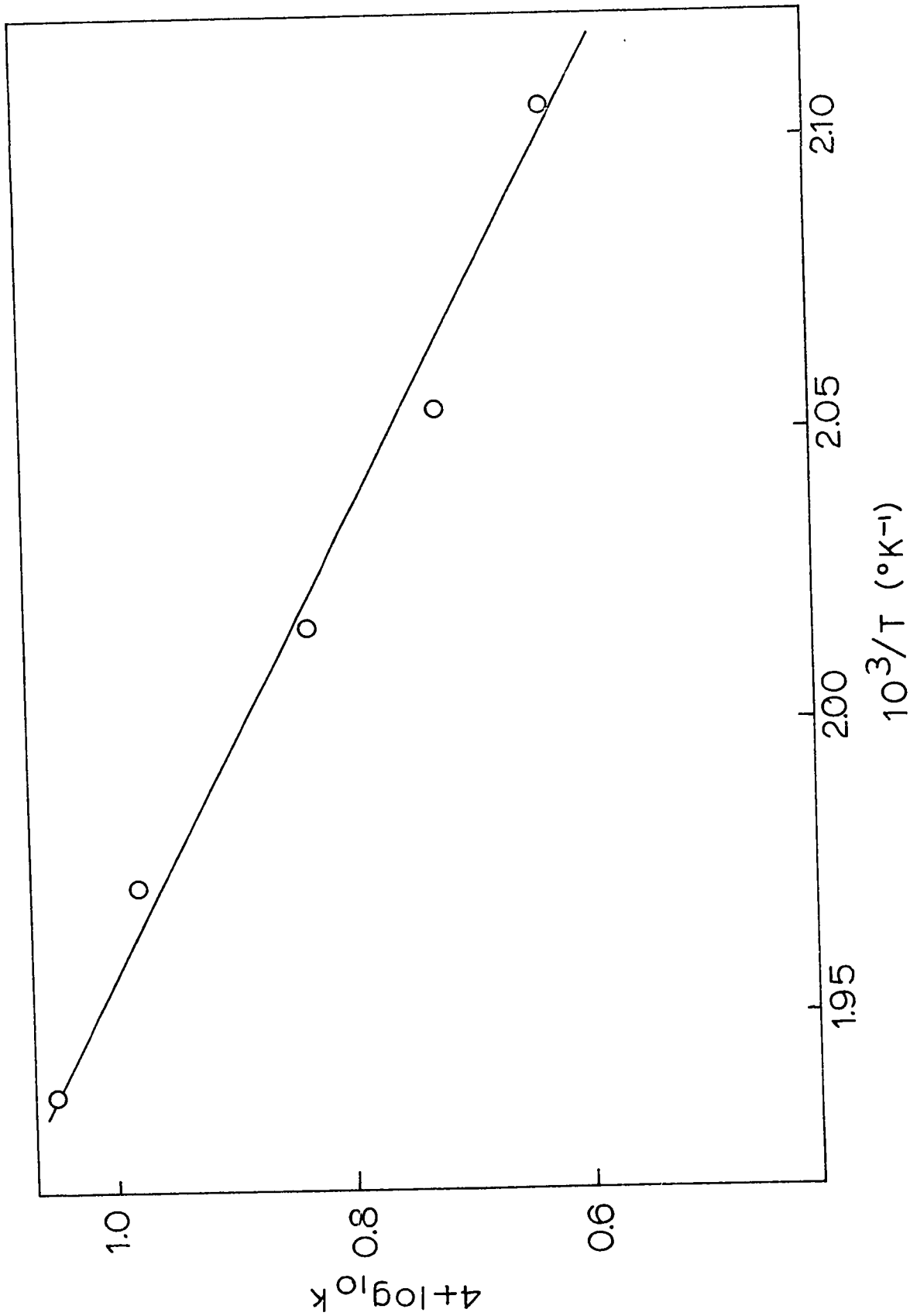
4+log10 k
1.0
0.8
0.6
1.95
2.00
2.05
2.10
10^3/T (°K^-1)

FIGURE III - 36

Disappearance of 1-Chloro-2-methylpropane

on Nickel

Plotted as a First Order Reaction

for $P_o = 1x10^{-2}$ torr

▽△ - 190°C

□ - 209°C

○ - 218°C

○ - 230°C

◇ - 239°C

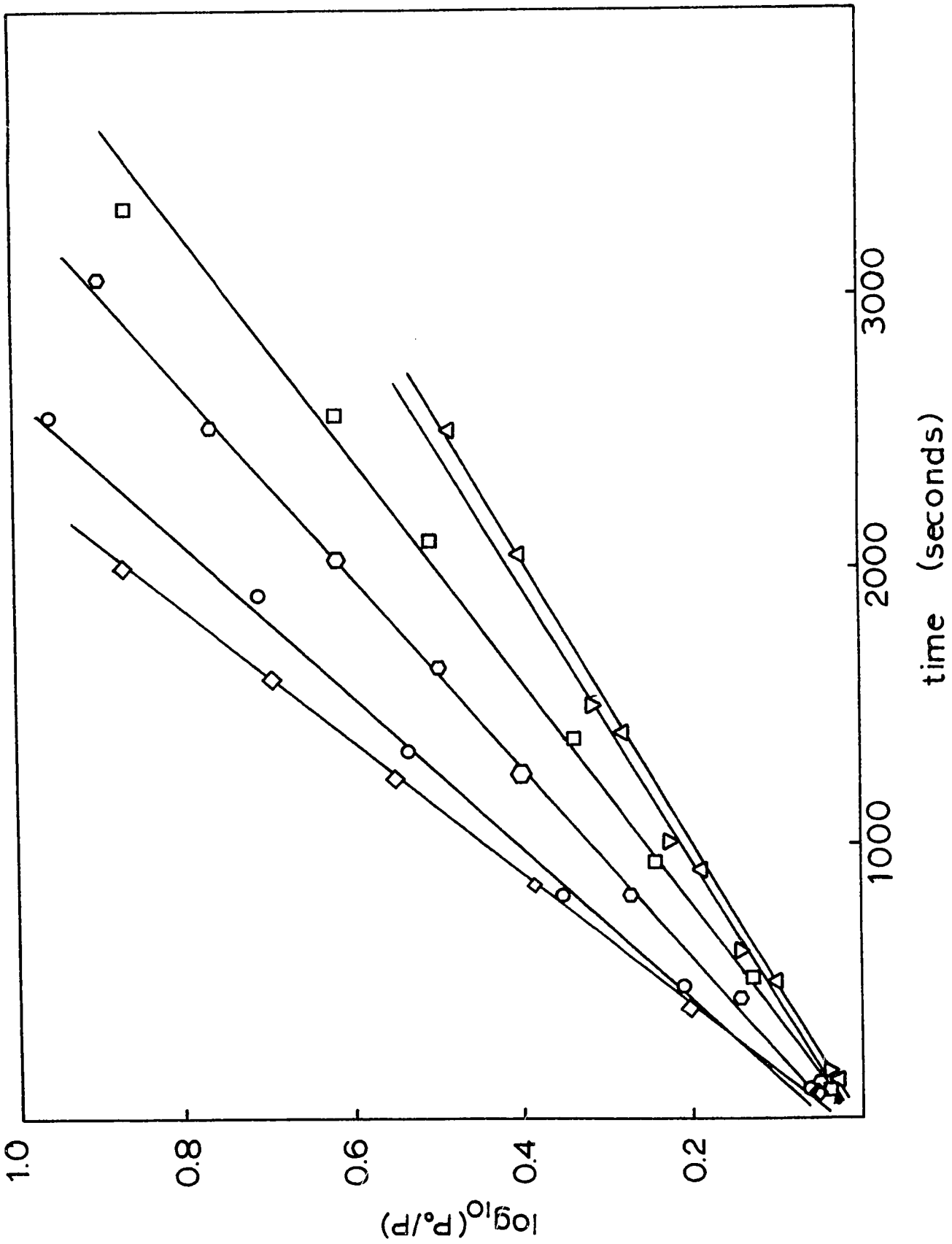
1.0
0.8
0.6
0.4
0.2
log10(P°/P)
1000
2000
3000
time (seconds)

FIGURE III - 37

Arrhenius Plot of Rate Data for First Order

Disappearance of 1-Chloro-2-methylpropane

on Nickel

for $P_o = 1x10^{-2}$ Torr

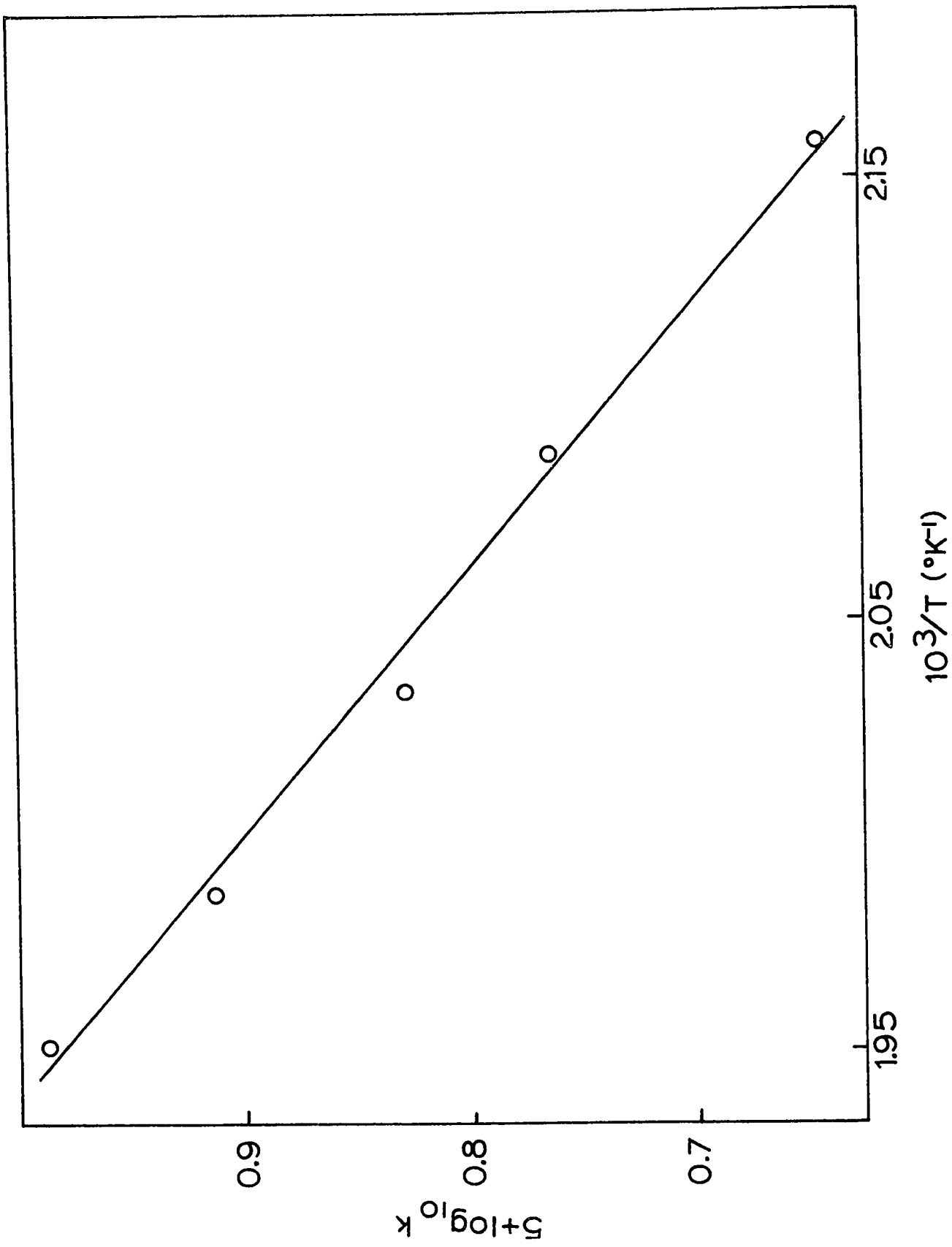
0.9
0.8
0.7
5+log10 k
1.95
2.05
2.15
10^3/T (°K^-1)

TABLE III-5

Kinetic Data For the Reactions of 1-Chloro-2-methylpropane on Halided Surfaces of the First Row Transition Metals

Metal	temp. range (°C)	pressure x10^2 (Torr)	E_a(Kcal/mole)	$\log_{10}A$
Titanium*	160-210	1	12.6 ± 0.3	2.4
	140-180	5	15.5 ± 0.5	4.1
Vanadium	180-220	1	8.1 ± 0.3	1.1 ± 0.1
Chromium	150-200	1	6.6 ± 0.2	0.3 ± 0.1
Manganese	175-235	1	2.9 ± 0.2	-1.6 ± 0.1
	175-225	5	3.5 ± 0.2	-1.4 ± 0.1
Iron	210-240	1	6.2 ± 0.4	-0.1 ± 0.2
Cobalt	200-245	1	8.3 ± 0.4	1.5 ± 0.2
Nickel	190-240	1	7.6 ± 0.4	0.3 ± 0.2

* Summers (1970)

III-C) Discussion

III-C-1) Introductory Comments

Reactions of haloalkanes with films of the first row transition metals have been categorized as 1) initial reactions, 2) non-catalytic reactions on halided surfaces and 3) catalytic reactions on halided surfaces. These classifications are based on the extent to which the surface was halided and on the products of dehydrohalogenation. Throughout much of this discussion, the first two catagories are combined since both led to the formation of a metal halide layer and both manifested many of the same properties.

Based on their behavior on titanium, 1-chloropropane was selected to typify non-catalytic reactions whereas 1-chloro-2-methylpropane exemplified the catalytic scheme. Most allusions to reactivity patterns will be with regard one of these two chloroalkanes. During their initial reactions, both behaved similarly.

This discussion will deal primarily with comparative reactions among the metals, whereas mechanisms will be discussed in detail in Chapter IV. Although titanium frequently behaved differently from the other metals, it often emphasises the factors governing various phenomena.

Due to unsatisfactorily large filament outgassing during film deposition, the reactions on copper may not have been representative of the clean metal

and will not be discussed in detail. The low reactivity of copper may have resulted from either innate inactivity or impurities in the film.

Although for the sake of discussion, reactions have been divided into various catagories, there was, in fact, a continuous progression between the characteristic types of behavior as the film became halided. Initial low temperature reactions occurred on both clean and slightly reacted films followed by high temperature non-catalytic reactions on more heavily halided surfaces. Some haloalkanes progressed to a period of catalytic behavior while some continued to dehydrohalogenate non-catalytically until the film deactivated. Thus, only the first reaction involved the pure metal and all subsequent reactions occurred on halided surfaces.

Three phenomena were observed during initial and non-catalytic reactions:

1) retentive adsorption - retention of complete haloalkane molecules by the surface without subsequent release of gas phase products (total pressure decrease),

2) dehydrohalogenation - removal of chlorine and hydrogen from the haloalkanes generating gas phase hydrocarbons and surface halide and, in some cases, hydrogen and

3) hydrogenation of the olefin produced during dehydrohalogenation.

Hence, this discussion is divided into four sections, the three mentioned above and one for catalytic reactions.

III-C-2) Retentive Adsorption

During initial reactions of many first row transition metals, some haloalkane molecules were completely adsorbed without subsequent release of gas phase products (retentive adsorption). 1-Chloro-2-methylpropane was retentively adsorbed to varying degrees on surfaces of the metals from titanium through nickel whereas 1-chloropropane was retained by only vanadium, chromium and iron.

Excluding titanium and manganese, retentive adsorption decreased across the row with both chloroalkanes. Both titanium and manganese showed very little retentive adsorption. Furthermore, the amount of retentive adsorption was minimal on metals which displayed little tendency to participate in low temperature dehydrochlorination.

Retentive adsorption of ethylene on surfaces of many transition metals has been reported (see Section I-E). It proceeded equally well with titanium, nickel, tungsten, palladium, and iridium and appeared to be a general tendency for all the transition metals. On nickel, these hydrocarbon residues have been removed by reaction with gaseous hydrogen (Jenkins and Rideal, 1955). There seems to be little correlation between the general phenomenon of ethylene

retention and the specific retention of haloalkanes.

Throughout both our studies and those of Anderson and McConkey (1968), chlorine adsorbed onto transition metal surfaces remained there at elevated temperatures and in the presence of gas phase hydrocarbons and hydrogen. During the present studies, heating films which had retentively adsorbed significant quantities of chloroalkane liberated traces of methane and large quantities of hydrogen.

The surface halide layer formed during these initial reactions was likely responsible for determining the extent of retentive adsorption as well as that of dehydrochlorination. This could have arisen from competitive adsorption of hydrocarbon residues and halide. The strongly bound halide would progressively block sites otherwise available for retentive adsorption and dehydrochlorination. Differences among the metals could have been due to variations either in the number of initially available sites or their ability to regenerate active sites. At low temperature, it is more difficult for surfaces to regenerate active sites as evidenced by the rapid film deactivation.

III-C-3) Dehydrohalogenation

On each metal film, dehydrohalogenation was the principal reaction studied. Frequently, a surface halide was formed with the liberation of hydrocarbons and possibly hydrogen. This section will discuss these reactions

whereas those generating hydrogen halide will be described in Section III-C-5. Reactions which formed surface halide are subdivided into those proceeding at low temperature (initial) and those at high temperature (non-catalytic). In the sense that the metal surface entered into the reaction stoichiometry, both the low and high temperature reactions were non-catalytic.

At both temperatures, surface halide inhibited the activity of the film toward further dehydrohalogenation. Inhibition varied markedly among the metals. Although not detected previously for titanium (Summers, 1970), experiments with large aliquots of 1-chloropropane have shown that there was a loss of activity even in this case (Section IV-B-5). However, for both 1-chloropropane and 1-chloro-2-methylpropane, the extent of inhibition induced by a given aliquot of halide was entirely different within the two temperature ranges.

a) Initial Low Temperature Dehydrochlorinations

During their initial dehydrochlorination reactions at low temperatures, both 1-chloropropane and 1-chloro-2-methylpropane were converted into gaseous hydrocarbons while chlorine remained on the surface. Although 1-chloro-2-methylpropane was consistently more reactive than 1-chloropropane, the trend in reactivity among the metals was

identical for both. Dehydrochlorination was frequently but not necessarily accompanied by retentive adsorption and hydrogenation. On a given surface, the rates of all three types of low temperature behavior decreased concurrently.

Although on vanadium and chromium the first aliquot introduced to the clean film was entirely retentively adsorbed, the relative rates of the first observable dehydrohalogenation reactions were:

$$Ti \simeq V \simeq Cr > Fe > Mn > Co \simeq Ni.$$

In contrast to the initial rates, the extent to which the metals promoted low temperature dehydrochlorination varied irregularly across the row as shown below.

$$V > Cr > Fe > Ti > Mn > Co \simeq Ni.$$

These conform neither to trends in work function nor heat of sublimation (Table III-6). Work function is a measure of the ability of the metal to release electrons and heat of sublimation the binding energy of the metal lattice.

Titanium and manganese, the two metals which reacted extensively with 1-chloropropane at elevated temperature showed an anomalously small extent of reaction at low temperature. Whereas their high temperature activity has been attributed to small dihalide lattice energies, this could not account for their low temperature behavior. However, although titanium was rapidly inactivated, reaction

was rapid as with vanadium and chromium. Indeed, there is a general decrease in reaction rate with atomic number such that more electropositive metals reacted more rapidly.

TABLE III-6

Work Functions and Heats of Sublimation for the First Row Transition Metals

metal	Work function* (electron volts)	Heat of Sublimation+ (Kcal/mole)
Ti	3.95	112
V	4.12	123
Cr	4.58	95
Mn	3.83	70
Fe	4.31	95
Co	4.41	102
Ni	4.50	103

* Krishnan (1952)

\+ Smithelles (1967)

For all the initial reactions studied, chloroalkane seemed to disappear according to a first order rate law. However, reaction rate also decreased as the surface was progressively halided. This product inhibition would cause a concave downward curvature in time order plots (Figure IV-9). In addition, reactions plotted as too high an order curve concave upward (ie. a half order reaction

plotted as first order).

As was undoubtedly the case for these reactions, a product inhibited reaction of order less than one could exhibit a straight line when plotted as first order. Hence, the first order plots indicate only that the actual reaction order was generally less than one. Segregation of the two effects, as was done for the high temperature reactions of 1-chloropropane on vanadium, was not attempted since rate was generally measurable over too limited a range to quantitatively determine the inhibition effect.

b) Non-catalytic High Temperature Dehydrochlorinations

On halided surfaces at elevated temperatures, 1-chloropropane and 1-chloro-2-methylpropane behaved differently. The former continued to react non-catalytically whereas the latter proceeded catalytically after a brief settling down period. Only the former will be discussed here.

The ability to effect dehydrochlorination of 1-chloropropane differed dramatically among the metals, ranging from very little with cobalt and nickel to almost indefinite with titanium. In the region of 200°C, the amount of dehydrochlorination required to induce a given decrease in activity varied as shown below.

Ti>Mn>V>Cr>Fe>Co≈Ni

As discussed in detail in Appendix E and Section III-C-5, it is most probable that all surface species were dichlorides, in which case they would also all be anionic layer lattices with cations occupying half the octahedral holes. There is a strong correlation between the lattice energies for these structures (Table III-7, p.140) and the extent of film activity. Thus, the lattice energy of the metal halide is very likely responsible for determining the rate of poisoning for a given amount of halide deposition.

Harrod and Summers (1971) previously proposed that rate control for the non-catalytic reactions of haloalkanes with titanium could be ascribed to the appearance of surface sites by liberation of hydrocarbon fragments into the gas phase and by diffusion of halide into the bulk of the metal. No surface deactivation was noted and translocation of cations across the metal-metal halide boundary was suggested as the rate controlling step.

In the present work, film deactivation by products was observed for all the metals except titanium and manganese. By analogy with numerous oxidation reactions (Hauffe, 1965), diffusion through the metal halide lattice to generate fresh surface sites is probably the slow step in the solid phase since larger lattice energies could make penetration more difficult. In accord with this hypothesis, films allowed to equilibrate for extended periods tend to

regain some, but not all, of their original reactivity.

On titanium and manganese a sufficient number of reactions could be conducted without noticeable film deactivation to determine activation parameters. However, on the other metals both film deactivation and changes in haloalkane concentration determined the kinetics during a given reaction. For the reaction of 1-chloropropane on vanadium these two effects were separated and analyzed individually.

This was accomplished by studying first the decrease in film activity at constant 1-chloropropane pressure. The mechanics of this are outlined in Section III-B-2-a-ii. The initial rate, dP/dt, was related to the pressure of haloalkane reacted, P_o^T, by an expression of the form $-dP/dt = A - BP_o^T$. Since the extent of the halide layer, w, is directly proportional to the amount of halide reacted, integration gives Equation III-7 for experimentally determined constants.

$$w = 0.095 - 0.095e^{-t} \qquad \text{III-7}$$

This is not in agreement with the expression found previously with either thick or thin surface layers (reviewed by Hauffe, 1965). Coherent surface layers thicker than 1000 Å generally obey a parabolic rate law of the type $dw/dt = k/w$, whereas several expressions have been found for thin surface layers. The most common are the

logarithmic law, $w = w_o \ln(t - t_o)$ - const, and the reciprocal logarithmic law, $1/w = A - B\ln t$. These two have been experimentally observed and theoretically explained.

Incorporating both the inhibition and concentration effects into a single rate law gave an expression which could be integrated for various values of the reaction order, n, in the absence of surface inhibition. The expression obtained for $n = \frac{1}{2}$ gave a straight line when plotted against time. Thus, the reaction order in the absence of surface deactivation is approximately $\frac{1}{2}$. It would be expected that the slope of the line for each reaction would have been constant; however, it increased steadily by about 25%. Although inexplicable, it seems too consistent to be an artifact. Nevertheless, it does not detract from the overall conclusion that the order of the reaction of 1-chloropropane on vanadium was close to one half rather than one as it appeared before accounting for surface deactivation.

Since the non-catalytic reactions of 1-chloropropane on titanium, vanadium and manganese followed a half order rate law, this is likely true for the other metals. Reactions of 1-chloropropane on chromium were also inhibited by surface halide formation yet appeared first order. As with vanadium, this was the result of compensating effects with the true reaction order less than one.

The products of high temperature

dehydrochlorinations of 1-chloropropane are explicable in terms of the ability of the film to retain hydrogen (Appendix D). The solubility of hydrogen in titanium is very large compared with the other metals. Thus, while titanium retained hydrogen and generated only hydrocarbon products, chromium, which has almost no hydrogen solubility, released hydrogen throughout each reaction. The other metals with low hydrogen solubilities also released hydrogen during dehydrochlorination. Vanadium, with an intermediate solubility, gradually released hydrogen causing a continuous hydrogen evolution even between reactions. On the other hand, titanium produced a mixture of paraffin and olefin whereas the other metals generated olefin as the only hydrocarbon product. Hydrogen held by the film was probably utilized to hydrogenate surface alkyls on titanium. With the rapid release of hydrogen from the other metals this was not possible.

During the non-catalytic reactions of 1-chloro-2-methylpropane, the kinetics were complex due to the superposition of several effects. Firstly, with most of the metals the non-catalytic reaction was probably slowing down due to film deactivation. In addition, as catalytic behavior replaced the non-catalytic scheme, reaction rate increased steadily. The superposition of these two effects renders any quantitative consideration of the kinetics impossible.

III-C-4) Hydrogenation

Throughout some initial and non-catalytic dehydrochlorination reactions, there was a continual increase in the ratio of paraffin to olefin in the products. This occurred for both 1-chloropropane and 1-chloro-2-methyl-propane on slightly reacted surfaces during the period when dehydrochlorination was proceeding very rapidly. No trend in hydrogenation activity was observed as vanadium, chromium, and iron catalyzed hydrogenation whereas titanium, manganese, cobalt and nickel did not.

The products released during the first reaction on each reactive metal (titanium through iron) were higher in paraffin content than subsequent sets of reaction products. Since these reactions were so rapid, it was impossible to distinguish the mode of paraffin production. As the surface was halided, hydrogenation rate decreased more rapidly than dehydrochlorination rate. Most likely, a similar hydrogenation process occurred for each reaction including those that were too rapid to study.

The paraffin/olefin ratio increased both during and after dehydrochlorination. Since the latter reaction occurred at constant pressure in the absence of gaseous hydrogen, olefin must have been hydrogenated to paraffin by surface hydride. On vanadium and chromium the rate of increase of the paraffin/olefin ratio decreased by about 50%

after completion of dehydrochlorination.

Hydrogenation of 1-chloro-2-methylpropane on iron at 0°C and 1-chloropropane on chromium at 138°C were first order in olefin after completion of dehydrochlorination. Other hydrogenations were not studied sufficiently to ascertain their order. However, it was less than three halves, greater than one half and has been approximated as one. Since hydrogenation rate was so dependent upon the extent of surface reaction, the apparent rate constants are of little value.

During a given reaction, for paraffin to exceed olefin the film must release previously acquired hydrogen. Since the gas phase products detected from reactions on clean films were invariably high in paraffin content (100% for vanadium and chromium), the excess hydrogen must have derived from retentively adsorbed molecules. Metals such as titanium and manganese which did not retentively adsorb haloalkane, never produced paraffin in excess of olefin. However, the inability of titanium to promote hydrogenation may have resulted from either its inability to retentively adsorb haloalkane or the high solubility of hydrogen in titanium (Appendix D).

The initial paraffin/olefin ratio for the three reactions during which it could be determined was about 2/3, indicating the reaction shown in Equation III-8

(* is a surface site). For all the metals except titanium, this ratio increased both during and after dehydrochlorination and, as with 1-chloro-2-methylpropane on iron, would probably have continued to do so in each case until all the olefin was consumed.

$$5R_2CHCH_2Cl + 6* \longrightarrow 2R_2CHCH_3 + 3R_2C{=}CH_2 + 5Cl* + H* \qquad \text{III-8}$$

The kinetics can be interpreted in terms of two hydrogenation mechanisms, direct production of paraffin during decomposition of haloalkane and hydrogenation of gaseous olefin by surface hydrogen. During dehydrochlorination, both would occur whereas after only the latter would continue. Hence, the rate would decrease. At the point when dehydrochlorination terminated, the concentrations of paraffin and olefin were approximately equal indicating that all the hydrogen from reactant molecules had been utilized in product formation (Figures III-2 and 6). Thus, hydrogen from reactant molecules may have been used to generate paraffin at the site of dehydrochlorination whereas surface hydrogen was used to hydrogenate olefin.

At no time during low temperature hydrogenation reactions was hydrogen detected in the gas phase. However, heating liberated hydrogen from all the metals except titanium. This was due to the high solubility of hydrogen

in titanium even at elevated temperatures.

A chromium film, reacted only once with 1-chlorporopane at low temperature, evolved hydrogen when heated to 138°C. At 138°C, the film functioned as a hydrogenation catalyst as long as the surface was liberating hydrogen. Holding the film at 138°C until it no longer evolved hydrogen destroyed its ability to effect hydrogenation. Most likely, no hydrogen capable of combining with olefin remained; however, it is possible in this case that the observed hydrogenation reaction occurred between gaseous hydrogen and olefin and no more gaseous hydrogen was available.

Hydrogenation was generally measurable over a very limited range of film reaction, usually one reaction of 10^{-2} Torr (3.2×10^{17} molecules). However, with vanadium, two consecutive hydrogenation reactions were studied and the rate found to decrease by about 50%. Since the only surface change between the two was due to retentive adsorption or dehydrochlorination, either adsorbed chlorine or hydrocarbon fragments must have induced the rate change. Since hydrogenation rate decreased rapidly even in the absence of significant quantities of retentive adsorption (iron with 1-chloro-2-methylpropane at 0°C), chlorine deposition was the most likely cause.

This halide layer is also responsible for retarding the rate of dehydrochlorination, and films which

underwent a rapid decrease in dehydrochlorination activity behaved similarly toward hydrogenation. Whether loss of surface activity was due to changes in the surface characteristics or the formation of a barrier to diffusion is not known. However, since so little surface contamination was necessary to completely inhibit reaction, the former seems most likely

Self hydrogenation of ethylene on transition metal surfaces has been studied by Beeck (1950), Jenkins and Rideal (1955), Trapnell (1952), Stephens (1959) and Roberts (1963). In support of the above hypothesis, these studies indicated that in spite of significant retentive adsorption, hydrogenation continued for many reactions.

For these surfaces to catalyze hydrogenation, they must satisfy two conditions.

1) They must be either clean or only slightly halided.

2) They must be capable of retaining hydrogen strongly enough to have it available for hydrogenation but not so strongly that it cannot be released.

III-C-5) Catalytic Reactions

The sequence of reactions for 1-chloro-2-methylpropane was similar on all the first row transition metals. After a period where chlorine was retained by the surface (initial and non-catalytic), hydrogen chloride appeared in the gas phase. Eventually, equimolar quantities of olefin and hydrogen chloride were produced and the surface

acted as a true catalyst increasing the reaction rate without entering into the stoichiometry. Although the initial reactions and the extent of the non-catalytic period varied among the metals, behavior in the catalytic region was uniform in terms of both products and kinetics.

On the other hand, 1-chloropropane did not react catalytically with any of the metals. Hence, the final reaction scheme (catalytic versus non-catalytic) was dependent on the haloalkane and not on the metal. It, therefore, seems most likely that haloalkanes which reacted catalytically on titanium (Summers, 1970) would react similarly on the other first row transition metals. This was verified for 2-chloropropane on chromium which behaved catalytically.

The order with respect to time for the disappearance of 1-chloro-2-methylpropane appeared to be close to one for all the catalytic reactions studied. However, for the same chloroalkane on chromium the concentration order was 0.76 ± 0.08 (Section IV-B-2). This discrepancy will be discussed in detail in Section IV-C-3.

In addition, no halo-exchange occurred during catalytic reactions on titanium and nickel (Section IV-B-3), strongly suggesting that reaction did not proceed via a rapid dissociative equilibrium. It is, therefore, proposed that each catalytic reaction involved a surface assisted internal rearrangement similar to an Ei mechanism (Section IV-C). For

a given haloalkane, variations in behavior are attributed to differences in the properties of the metal rather than to mechanistic changes.

As shown in Table III-7 (page 140), the activation energy for catalytic dehydrochlorination of 1-chloro-2-methylpropane at 10^{-2} Torr decreased steadily from 12.6 Kcal/mole on titanium to 2.9 Kcal/mole on manganese then increased again to 6.2 Kcal/mole on iron, 8.3 Kcal/mole on cobalt and 7.6 Kcal/mole on nickel. Increased activation energies were accompanied by increased frequency factors with a linear relationship between Ea and $\log_{10}A$ (Figure IV-27, page 223). As described in Section IV-C-3, this compensation effect is not uncommon.

All the apparent activation energies contain both the true activation energy for dehydrochlorination and the heat of adsorption of the haloalkane. Thus, changes in either of these quantities would alter the observed activation energy. Essential to any discussion of either of these parameters is knowledge of the crystal structure of the surfaces.

From thermodynamic considerations, structures of all the surfaces are likely very similar (Appendix E). In the presence of excess metal, the most stable arrangement is the dichloride and the crystal structures for dichlorides are very similar - CdI_2 or $CdCl_2$. These two

structures are almost identical, both being layer lattices of close packed anions with cations occupying half the octahedral holes. Cations are spaced such that all the holes between every second layer are fully occupied with spaces between the other layers devoid of cations. However, the anionic layers are stacked so that CdI_2 structures are hexagonal close packed and $CdCl_2$ are cubic close packed. Chromium dichloride, on the other hand, is an exception due to Jahn-Teller distortions.

Based on the similarity in structures, surface properties could have been dependent solely on lattice energies. Table III-7 lists the dichloride lattice energies and apparent activation energies at 10^{-2} Torr for the series of metals studied. Lattice energies followed the usual double humped pattern detected for most thermodynamic properties of the first row transition metals (Dunn, 1965). On the other hand, activation energies did not and there is little correlation between the two.

For the chemisorption of ethylene, carbon monoxide and hydrogen on transition metals, a similar lack of correlation with lattice energies has been observed (Hayward, 1971).

The true activation energy for dehydrochlorination, could also induce variations in apparent activation energies. In the metal dichlorides, the cations would have been in octahedral environments. Since chloride

is a weak field ligand (Orgel, 1960), each surface chloride likely contained high spin octahedrally coordinated divalent metal ions.

TABLE III-7

Lattice Energies and Activation Energies at 10^{-2} Torr

metal chloride	lattice energy(Kcal/mole)*	activation energy(Kcal/mole)
$TiCl_2$	592	12.6 ± 0.3
VCl_2	608	8.1 ± 0.3
$CrCl_2$	612	6.6 ± 0.2
$MnCl_2$	602	2.9 ± 0.2
$FeCl_2$	623	6.2 ± 0.4
$CoCl_2$	638	8.3 ± 0.4
$NiCl_2$	658	7.6 ± 0.4

* (Dunn, 1965)

By comparing the crystal field splitting energies for octahedral and pentagonal bipyramidal structures, Basolo and Pearson (1968) have calculated the crystal field activation energies (CFAE) for expansion of the coordination sphere by one ligand. The conclusion for high spin complexes was that for d^1, d^2, d^5, d^6 and d^7 the CFAE would not contribute to the activation energy. However, for d^3, d^4, d^8 and d^9 there would be an increase in activation energy due to the CFAE.

Hence, for divalent complexes, titanium, manganese, iron and cobalt should have lower activation energies than vanadium, chromium and nickel.

Again there is little correlation between CFAE effects and apparent activation energies. The lack of correlation with either lattice energies or CFAE and activation energies is not surprising in light of the many undetermined reaction parameters. Two such effects are changes in activation energy with reactant pressure and the influence of geometrical factors on adsorption. The latter is discussed in detail in Section IV-C-4.

Regarding the former, it has been shown that activation energy increased with reactant pressure for 1-chloro-2-methylpropane on titanium and manganese (Section III-B-2-b). Most likely, this is a general phenomenon for all the systems. Metals may have varied considerably with respect to their sensitivity toward reactant pressure changes and at a given reactant pressure may have differed also in their relative ability to adsorb haloalkane molecules. To make a valid comparison, it would be necessary to assure that each surface had a similar specific reactivity which is impossible without extensive examination of the surface itself. On the basis of the change in activation energy for the reaction of 2-chloropropane on titanium from 8.7 Kcal/mole at 10^{-2} Torr to 12.2 Kcal/mole at 5×10^{-2} Torr these variations could possibly

have outweighed the other parameters in determining activation energies.

IV) MECHANISMS FOR THE REACTIONS OF HALOALKANES WITH THE FIRST ROW TRANSITION METALS

IV-A) General Comments

Possible mechanisms for the reactions of several haloalkanes on titanium surfaces have been proposed (see Section I-G). According to their general characteristics, these reactions have been classified in three categories:

1) initial reactions on clean surfaces,
2) non-catalytic reactions on halided surfaces, and
3) catalytic reactions on halided surfaces.

The first designation is self explanatory whereas the second and third refer to the reaction products. Non-catalytic reactions proceeded according to a half order rate law generating propene and propane while all the halide and some hydrogen was retained by the surface. Catalytic reactions, on the other hand, produced an equimolar mixture of hydrogen halide and olefin according to a first order rate law. These designations have been retained for reactions with the other first row transition metals, all of which behaved similarly to titanium (Section III).

Reported in this section are the results of some experiments designed to further elucidate the mechanism involved in these reactions. All were conducted on titanium or chromium with 1-chloropropane, 2-chloropropane

or 1-chloro-2-methylpropane. The validity of generalizing these findings will be discussed in more detail at the end of this chapter.

Of particular interest were the mechanisms on halided surfaces. Along these lines, five types of experiment have been performed:

1) the effects of products

2) concentration order determination

3) examination of the hypothesis of dissociative equilibria,

4) studies of surface specificity for certain reaction schemes, and

5) determination of surface alterations induced by reactions of large aliquots of chloroalkane.

Based on these experiments and the general studies with all the first row transition metals, the possibility of various mechanisms for and mechanistic differences between the reactions of haloalkanes on surfaces of the first row transition metals will be discussed.

An outline of the nomenclature is presented in the introduction to Chapter III. All films studied were deposited according to the specifications stated in Section II. The peculiarities of each experiment are described in prefaces immediately prior to the individual section.

IV-B) Experimental Results

IV-B-1) The Effect of Propene on the Reaction of 1-Chloropropane with Halided Titanium Surfaces

To investigate the effect of propene, the primary gas phase product, on the kinetics of the 1-chloropropane dehydrochlorination, the reaction was studied in the presence of excess propene.

1-Chloropropane was reacted on titanium until the film settled down and the reaction proceeded at constant rate with consistent products for several consecutive runs. The gaseous products of the reaction were about 90% propene and 10% propane while all the chloride and some hydrogen were retained by the film.

Consecutive reactions at 1.35×10^{-2} Torr of 1-chloropropane were run at 222°C. The first and last in the series contained no excess propene whereas the second initially contained 1.30×10^{-2} Torr and the third 4.45×10^{-2} Torr excess.

Each reaction was followed to greater than 95% completion and found to obey strict half order kinetics both with and without excess propene (Figure IV-1). To better display the half order kinetics, each reaction is offset vertically +0.1 unit from its predecessor. Although no legend is shown on the vertical axis, the unit size is designated and the final value of $10(P_o^{\frac{1}{2}} - P^{\frac{1}{2}})$ was about 1.0 for each run.

The effect of excess propene on the half order rate constant for the disappearance of 1-chloropropane is shown in Figure IV-1. Surface activity remained constant throughout the series and the rate constant stayed between 1.11 and 1.14×10^{-4} $Torr^{\frac{1}{2}}\text{-}sec^{-1}$ even in the presence of a three fold initial excess of propene.

FIGURE IV - 1

Disappearance of 1-Chloropropane

on Titanium

Plotted as a Half Order Reaction

T = 222°C

P_o(1-chloropropane) = 1.35×10^{-2} Torr

	reaction number	offset	P_o(propene) $\times 10^{+2}$(Torr)
○ -	1	0	0
□ -	2	+0.1	1.30
○ -	3	+0.2	4.45
△ -	4	+0.3	0

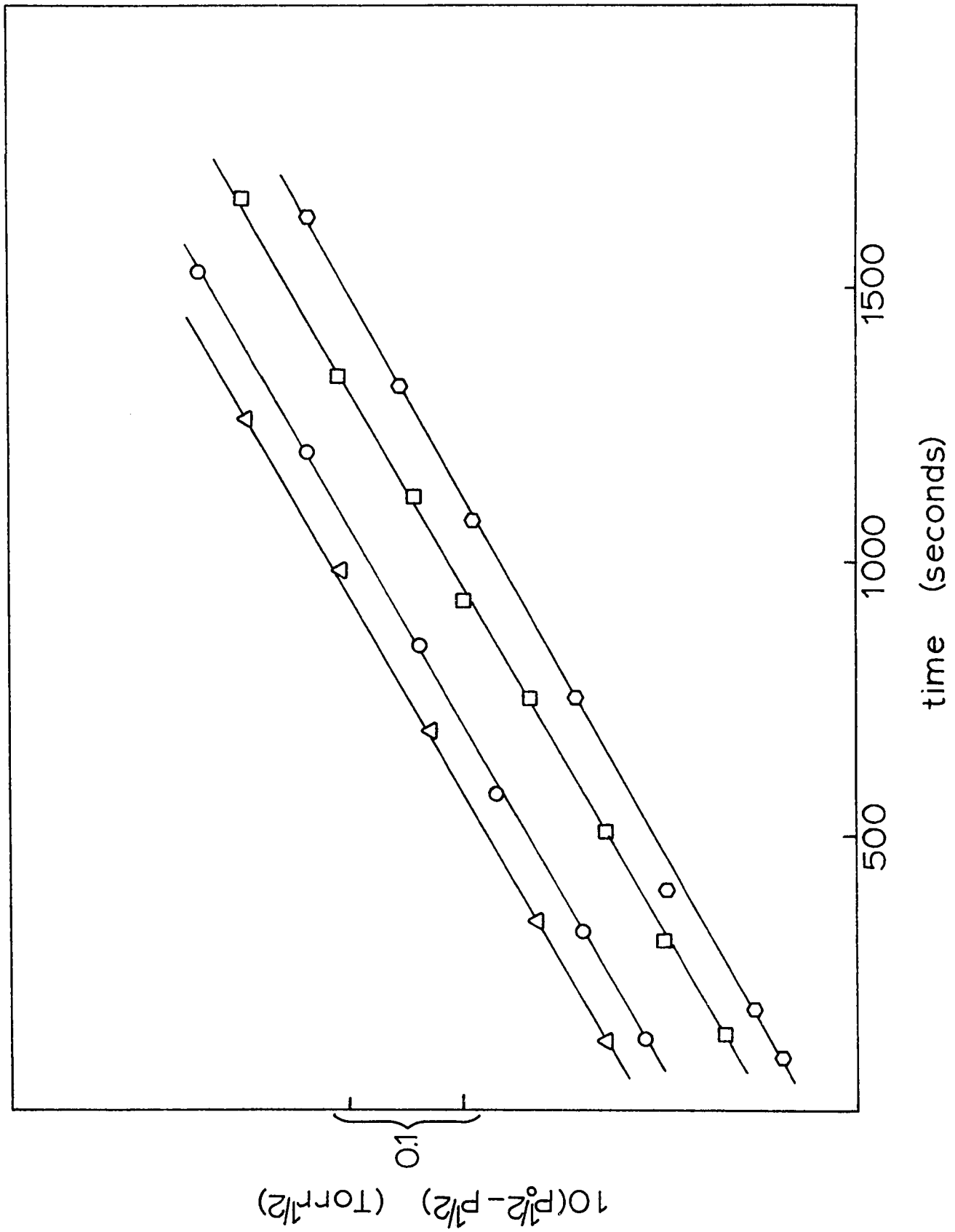
500
1000
1500
time (seconds)
0.1
10(P°½ - P½) (Torr½)

FIGURE IV - 2

The Effect of Propene on the

Half Order Rate Constant for the

Disappearance of 1-Chloropropane

P_o (1-chloropropane) = 1.35×10^{-2} torr

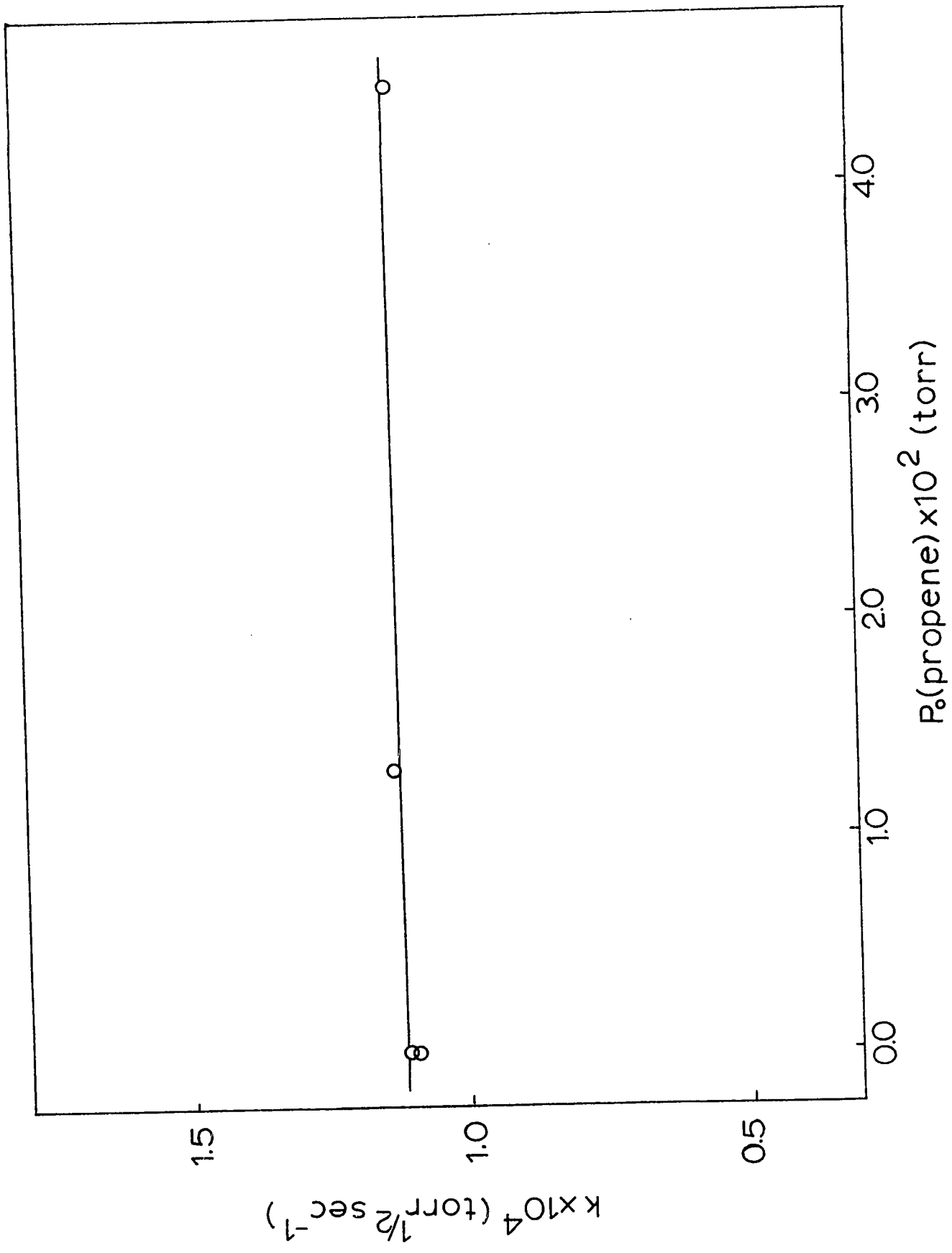
k x10^4 (torr^1/2 sec^-1)
1.5
1.0
0.5
0.0
1.0
2.0
3.0
4.0
P°(propene) x10^2 (torr)

IV-B-2) Determination of Concentration Orders on Halided Surfaces

Previously quoted reaction orders for haloalkanes on titanium were based solely on time order plots (Harrod and Summers, 1971; Summers and Harrod, 1972). Since there is often an effect of product on rate for surface catalyzed reactions, this could possibly be misleading. Hence, the concentration order (true order) has been established for representative examples of both catalytic and non-catalytic reactions. The reaction of 1-chloropropane on titanium typifies the non-catalytic reaction scheme and 1-chloro-2-methylpropane on chromium the catalytic type.

Non-catalytic Reaction

On a clean titanium film, about 5×10^{-2} Torr of 1-chloropropane was reacted before characteristic non-catalytic behavior was established; 1-chloropropane disappeared by half order kinetics generating propene and propane while the film retained all the chloride and some hydrogen.

With consecutive reactions proceeding consistently, the concentration order was determined at 221°C between about 10^{-2} and 10^{-1} Torr. Figure IV-3 shows the decrease in reactant pressure with time for each of the reactions. An equation for each set of points was generated by the program CURFIT. From these equations, the slope at

FIGURE IV - 3

Disappearance of 1-Chloropropane With

Time on Titanium

T = 221°C

$P_o \times 10^2$ (Torr)

△ - 1.23

▽ - 1.34

□ - 3.70

○ - 6.00

● - 11.10

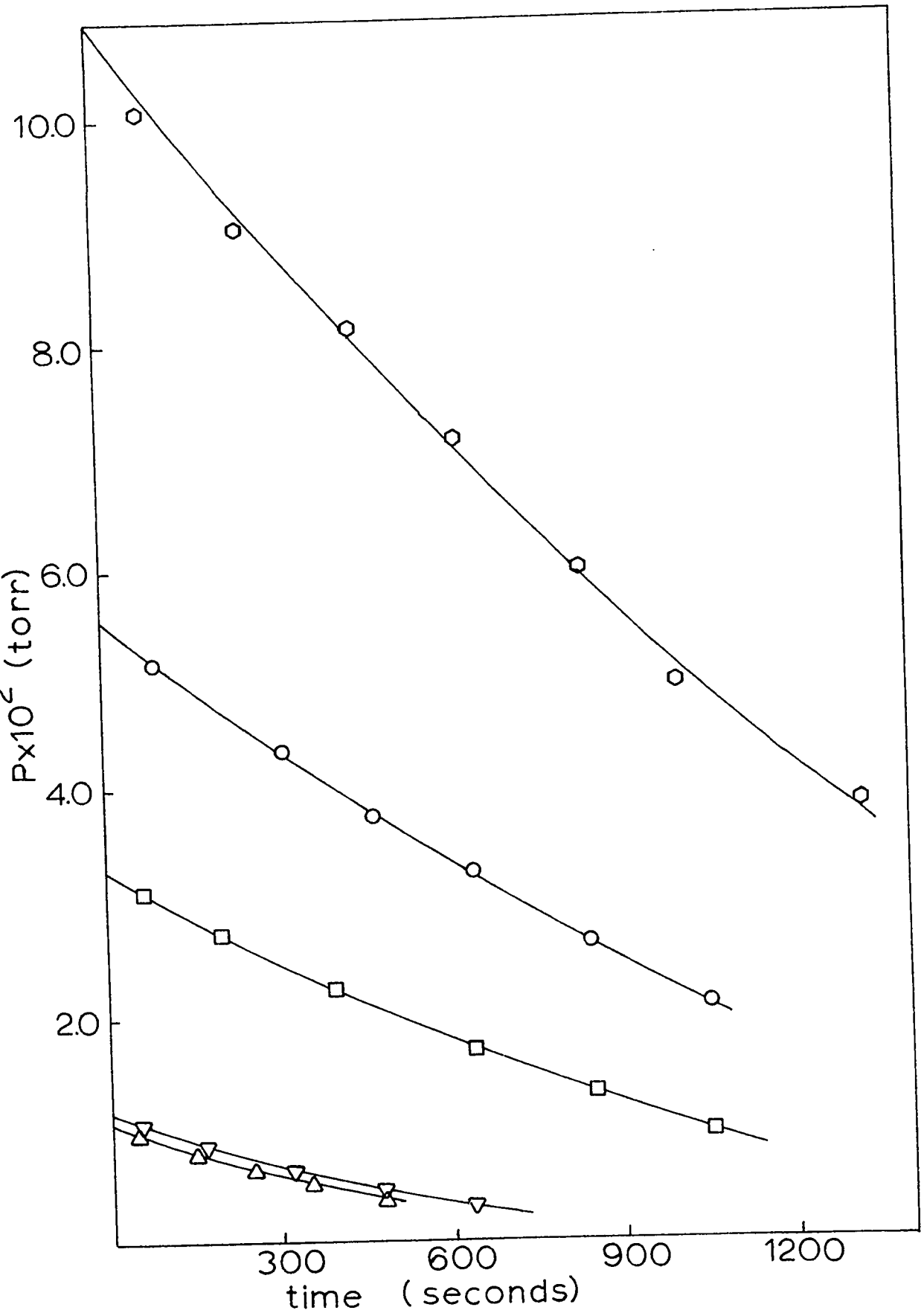
10.0
8.0
6.0
4.0
2.0
Px10^2 (torr)
300
600
900
1200
time (seconds)

zero time (v_o) was calculated. The intercept on the pressure axis was consistently less than the initial pressure. As explained in Section II-C this was due to the time lag in mass spectrometer readings and would not alter the results.

Figure IV-4 shows the log-log plot of v_o versus initial pressure. As calculated from the slope and intercept respectively, the concentration order was 0.49 ± 0.02 and the rate constant $1.6 \pm 0.1 \times 10^{-4}$ $Torr^{\frac{1}{2}}sec^{-1}$.

By plotting each reaction as half order, the individual rate constants were determined. As seen from Table IV-1, rate constant was independent of initial reactant pressure with an average value of about 1.7×10^{-4} $Torr^{\frac{1}{2}}$-sec^{-1}, in good agreement with that found along with the concentration order.

TABLE IV-1

The Effect of Initial Reactant Pressure on the Rate Constant for the Reactions of 1-Chloropropane on Titanium

initial pressure (Torr) $\times 10^{+2}$	rate constant ($Torr^{\frac{1}{2}}$-sec^{-1})
1.23	1.66
1.34	1.60
3.70	1.62
6.00	1.71
11.10	1.72

FIGURE IV - 4

Determination of the Order

With Respect to Concentration

for the Reaction of

1-Chloropropane

on Titanium

$T = 221^{o}C$

$v_o = -(\frac{dP}{dt})_o$

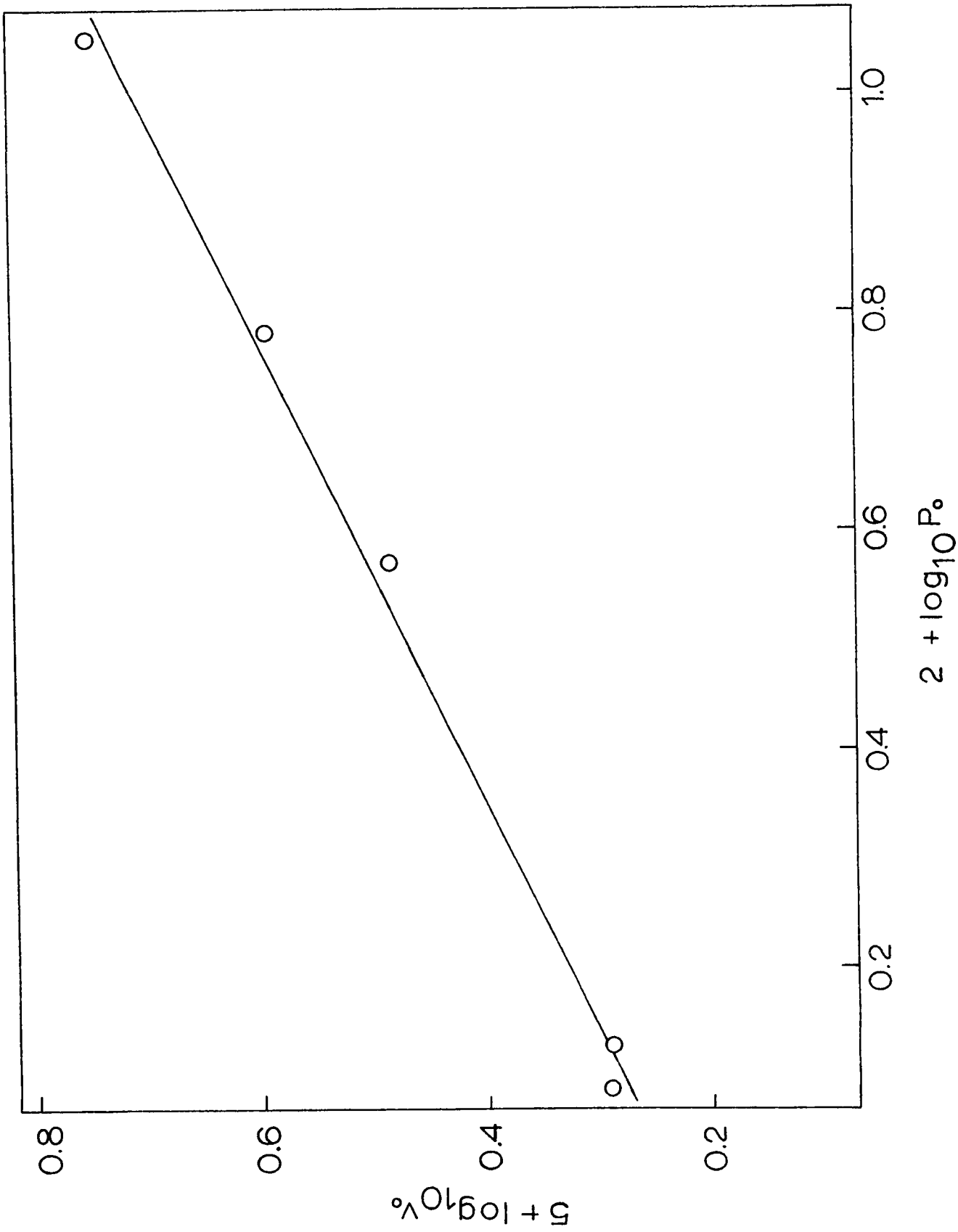
0.8
0.6
0.4
0.2
5 + log10Vo
0.2
0.4
0.6
0.8
1.0
2 + log10Po

Since the reactions used to determine the concentration order were followed to only about 60% completion, additional runs were conducted to confirm that the time order was one half. Figure IV-5 shows two of these, performed with markedly different film conditions (Section IV-B-5). Followed through 95% reaction they obeyed half order rate laws.

Catalytic Reaction

The reaction of 1-chloro-2-methylpropane was studied at various pressures on a chromium film which had settled into consistent catalytic behavior. Reaction proceeded by first order kinetics producing an equimolar mixture of hydrogen chloride and methylpropene with a doubling of total pressure.

Reactions between 10^{-2} and 10^{-1} Torr were conducted at 179°C. The decrease in haloalkane pressure with time is shown in Figure IV-6 for each of the reactions. Again an equation for each set of points was generated by the program CURFIT and the initial slope determined. However, in this case, very little lag time in mass spectrometer readings was permitted so the intercepts of the equations were very close to the actual initial pressure.

A log-log plot of v_o versus initial reactant pressure is shown in Figure IV-7. This gave a concentration order of 0.76 ± 0.08 and a rate constant of $3.6 \pm 0.3 \times 10^{-4} sec^{-1}$.

FIGURE IV - 5

Disappearance of 1-Chloropropane

on Titanium

Plotted as a Half Order Reaction

$T = 221^{o}C$

$P_o = 1.35 \times 10^{-2}$ Torr

△ - before large reactant dose

○ - after large reactant dose

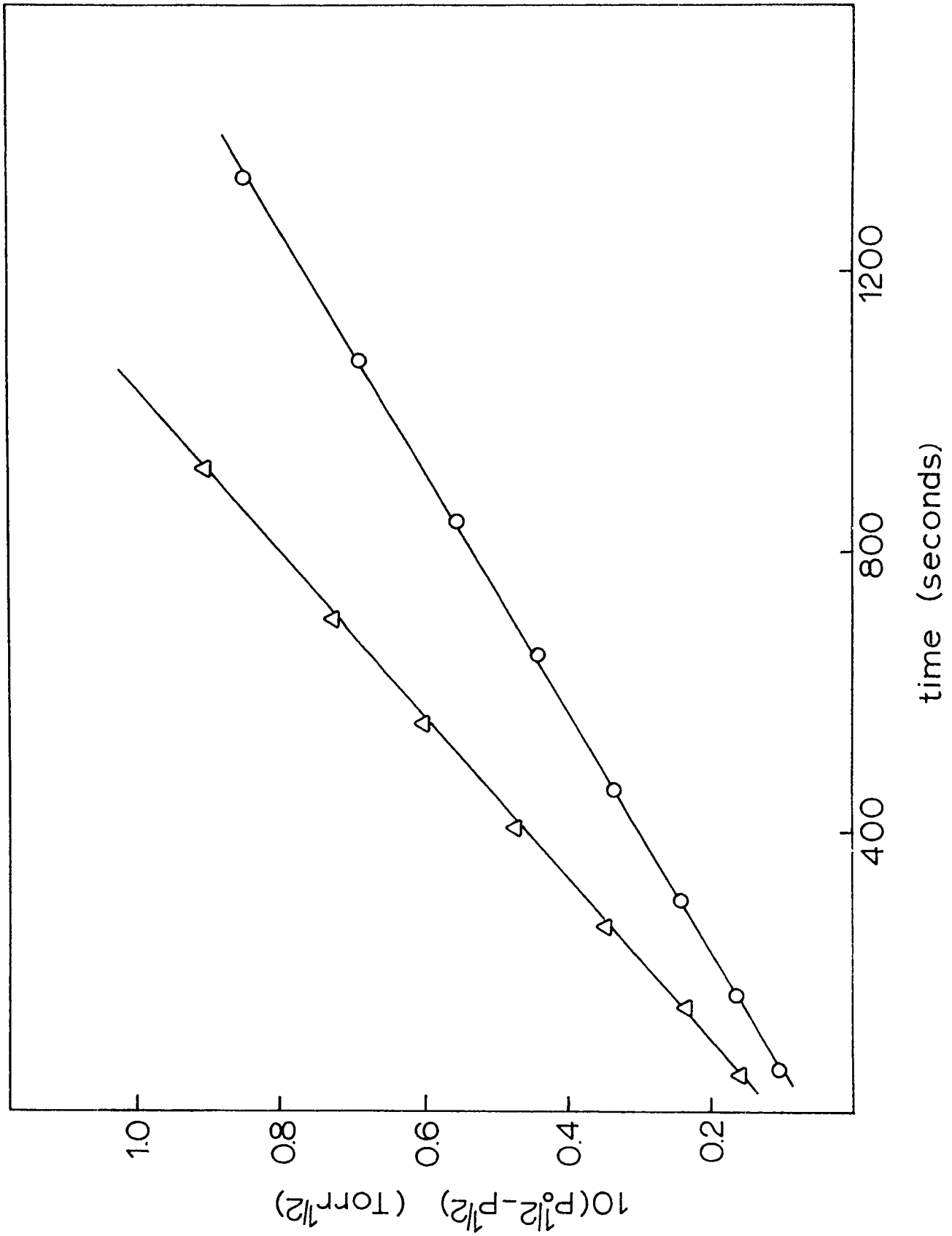
1.0
0.8
0.6
0.4
0.2
$10(P_i^{1/2} - P^{1/2})$ (Torr$^{1/2}$)
400
800
1200
time (seconds)

FIGURE IV - 6

Disappearance of 1-Chloro-2-methylpropane With

Time on Chromium

$T = 179^{o}C$

$P_o \times 10^2$ (Torr)
⬡ - 1.32
○ - 1.99
□ - 3.51
▽ - 5.48
△ - 7.58

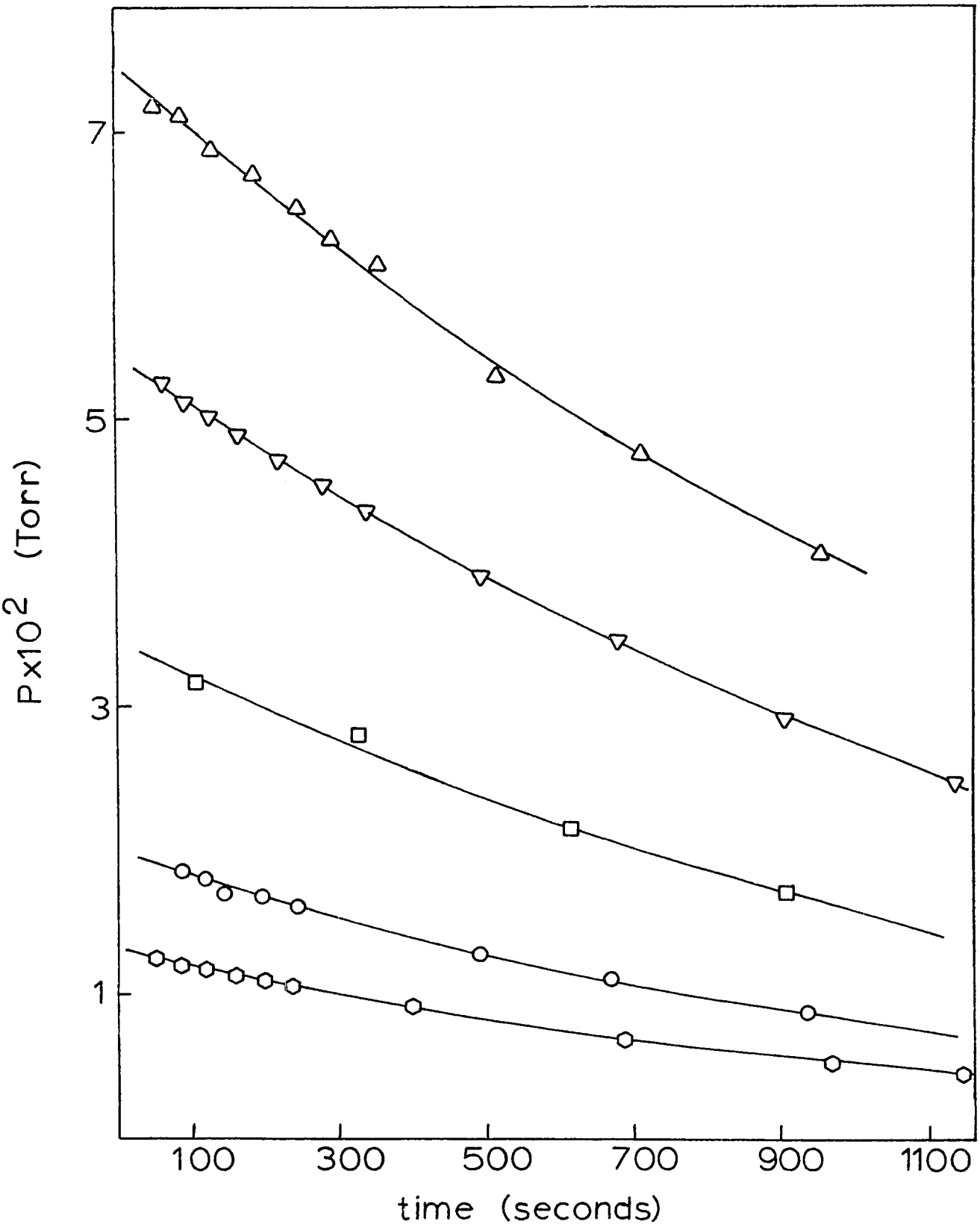
7
5
3
1
Px10^2 (Torr)
100
300
500
700
900
1100
time (seconds)

FIGURE IV - 7

Determination of the Order

With Respect to Concentration

for the Reaction of

1-Chloro-2-methylpropane

on Chromium

$T = 179^{o}C$

$v_o = -(\frac{dP}{dt})_o$

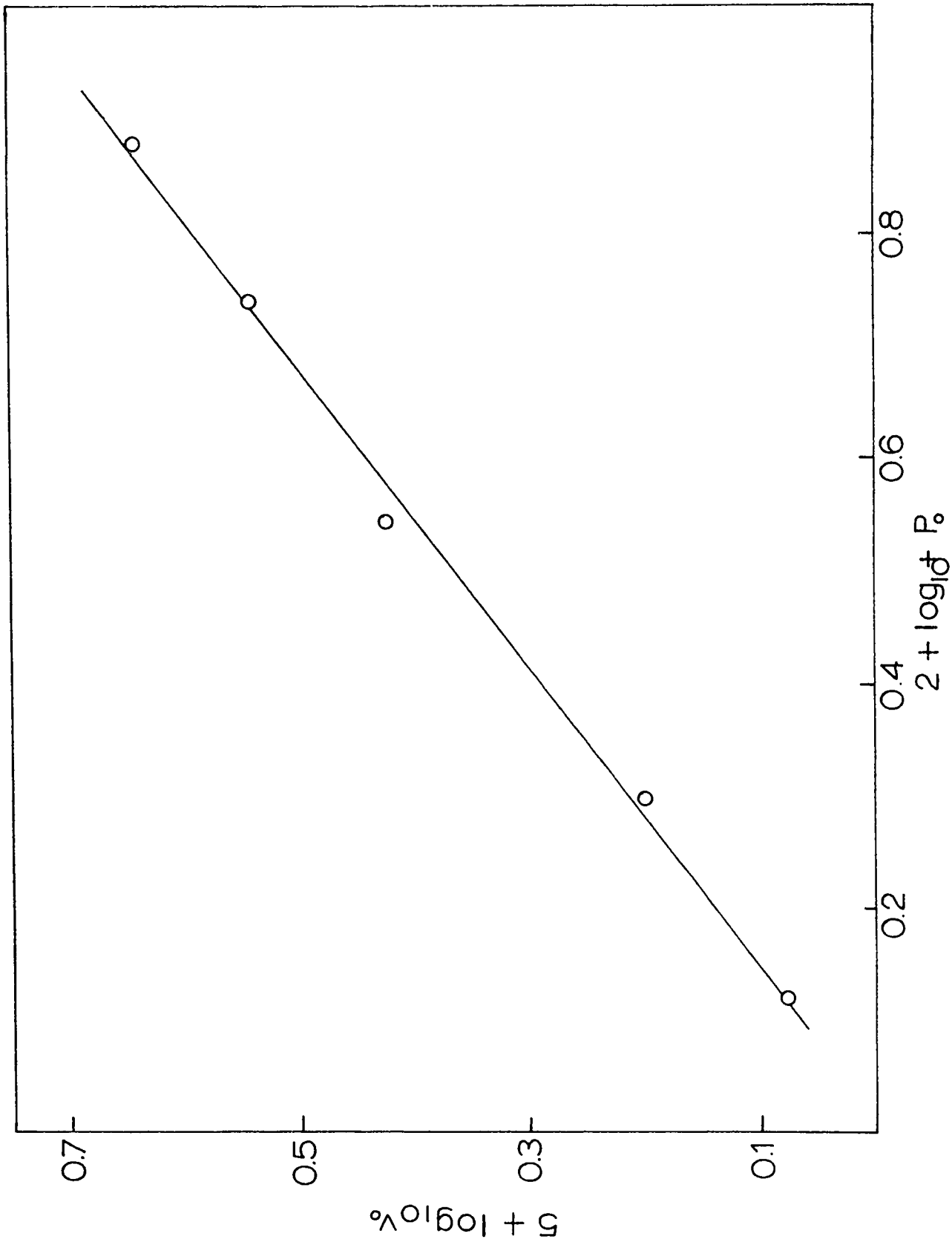
0.7
0.5
0.3
0.1
5 + log10v∘
0.2
0.4
0.6
0.8
2 + log10 P∘

Plotting each reaction as first order gave the individual rate constants which were found to decrease linearly with increasing initial reactant pressure as shown in Figure IV-8. About 40% decrease in rate constant for about an 8 fold increase in initial reactant pressure was observed. Each of these reactions was followed to about 70% completion and obeyed a first order rate law.

An interpretation of this behavior will be presented in the discussion at the end of this chapter. Two sample reactions which followed very closely a first order rate law, were plotted according to a 0.75 order rate law to determine whether a curvature in the line would be detectable. The reactions chosen were those at 201 and 220°C for 1-chloro-2-methylpropane on titanium (Figure IV-16), both of which were followed to about 90% completion. The plots are shown in Figure IV-9. At both temperatures, there was a very slight downward curvature in the 0.75 order plots. Thus, although the two would be distinguished they appeared very similar and a lower order may have prevailed during the catalytic reactions. However, most of the catalytic reactions studied seemed to adhere more to first than to 0.75 order rate laws.

FIGURE IV - 8

The Effect of Initial Reactant Pressure

on the Rate Constant

for the Reactions of

1-Chloro-2-methylpropane

on Chromium

$T = 179^{o}C$

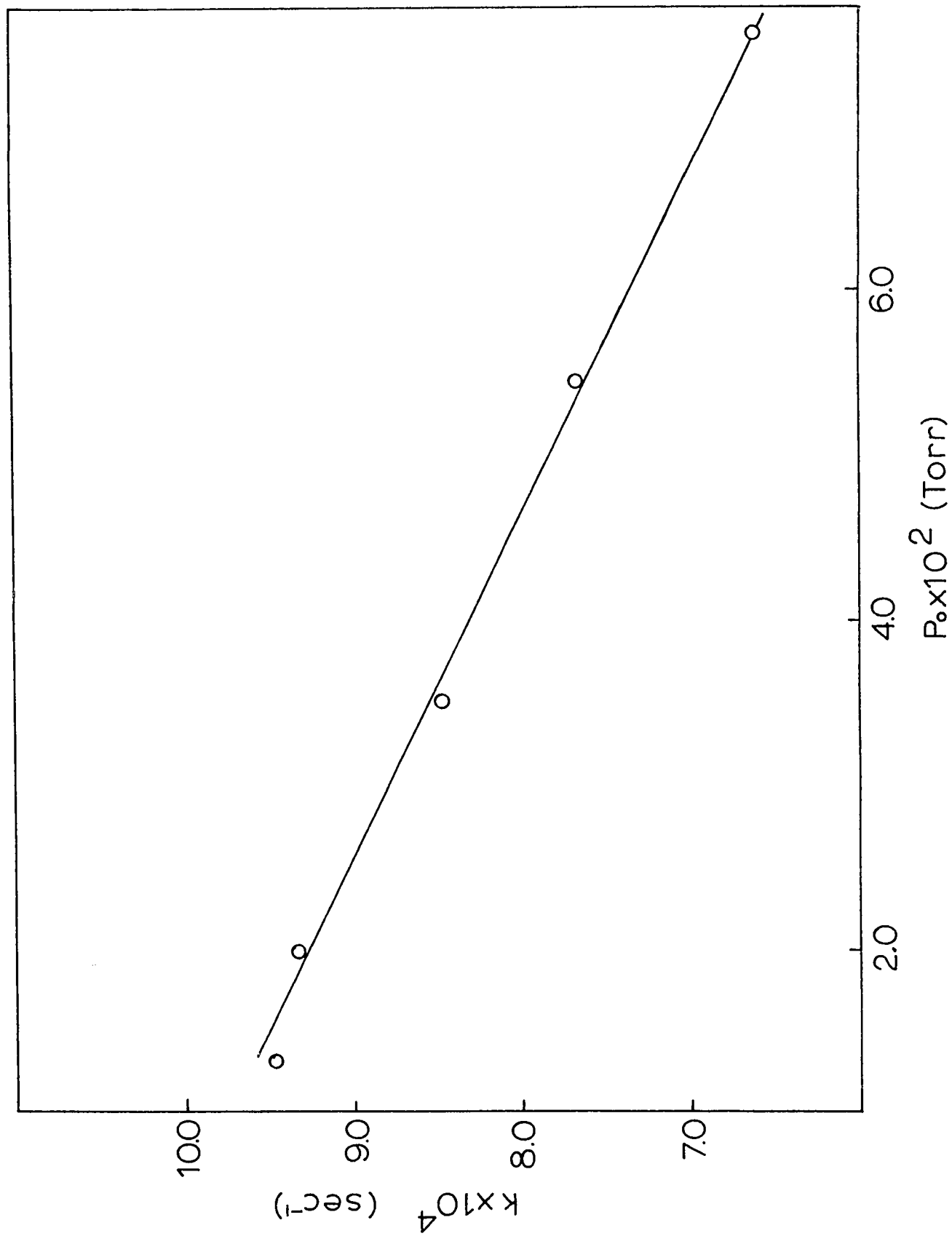
10.0
9.0
8.0
7.0
k x10^4 (sec^-1)
2.0
4.0
6.0
P°x10^2 (Torr)

FIGURE IV - 9

Disappearance of 1-Chloro-2-methylpropane

on Titanium

Plotted as First and 0.75 Order Reactions

$P_o = 1x10^{-2}$ Torr

▽ -	First Order	T = 201
◇ -	First Order	T = 220
△ -	0.75 Order	T = 201
□ -	0.75 Order	T = 220

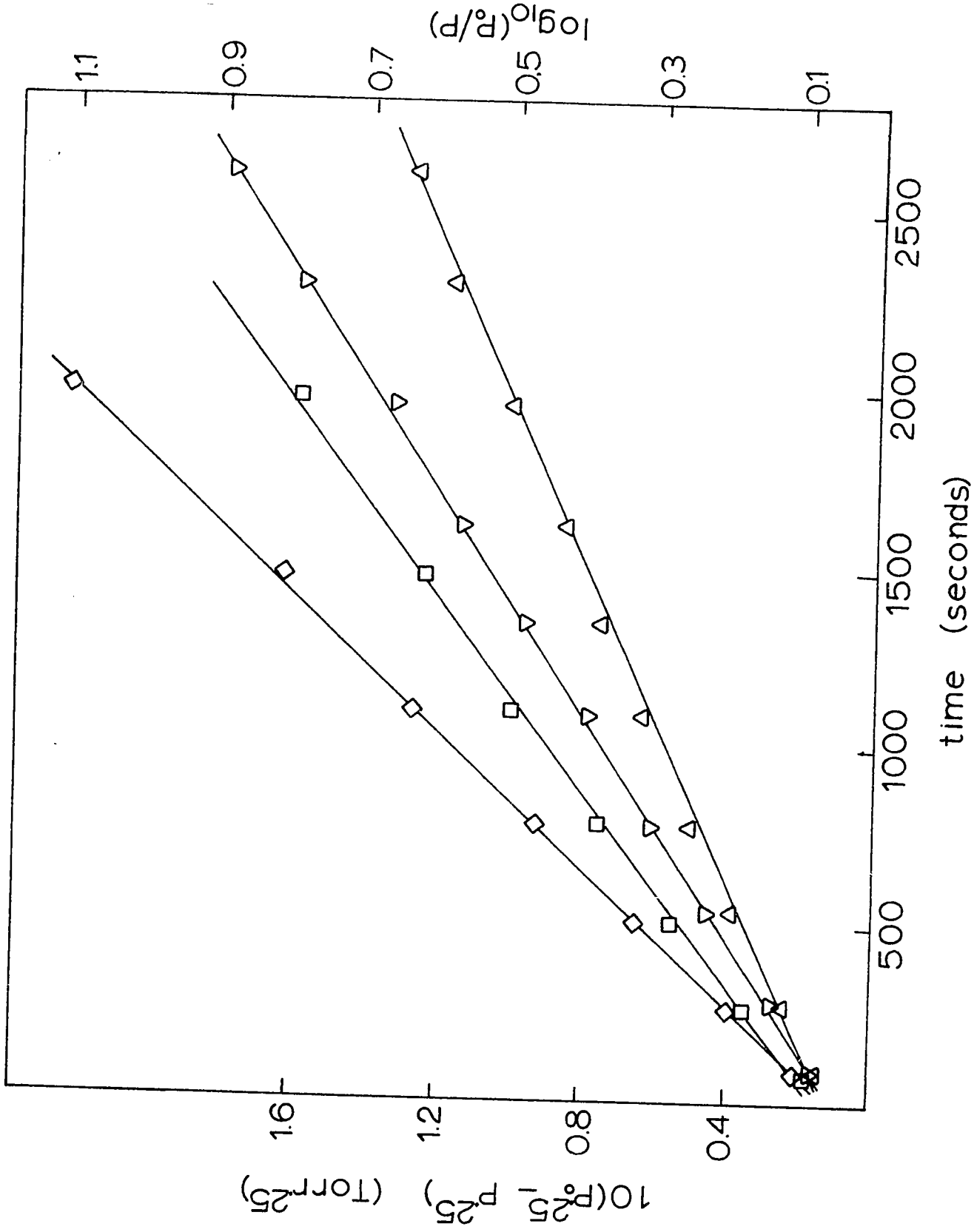
10(P°25 - P25) (Torr25)
1.6
1.2
0.8
0.4
log10(P°/P)
1.1
0.9
0.7
0.5
0.3
0.1
500
1000
1500
2000
2500
time (seconds)

IV-B-3) Examination of Dissociative Equilibria - Halo-exchange Experiments

Theory As outlined in Section I-G , the first step of the reaction mechanism for either the non-catalytic, or catalytic reactions of the haloalkanes could have been a rapid dissociative equilibrium involving reversible, surface-assisted cleavage of the carbon-halogen bond to form a surface alkyl and surface halide. Rate control would then have been governed by subsequent rearrangement of these surface moities. Equilibration required that alkyl and halide groups be continually redistributing on the surface generally resulting in the desorption of alkyl groups bonded to halide atoms other than those to which they were attached before adsorption. Thus, to examine the hypothesis of a dissociative equilibrium, bromo-chloro exchange between haloalkanes with differentiable alkyl groups was studied.

The proposed mechanisms required that halo-exchange proceed much more rapidly than dehydrohalogenation; however, the following experiments were designed to detect exchange at any extent of reaction. Equations IV -1 IV-2 and IV-3 show a schematic depiction of the two processes where X and Y are halogens and * is a surface site.

Catalytic Dehydrohalogenation

$$\begin{array}{l} R_2CHCHDX \\ + R_2CHCH_2Y \end{array} \longrightarrow \begin{array}{l} HX + HY + R_2C = CHD \\ \qquad + R_2C = CH_2 \end{array} \qquad \text{IV-1}$$

Non-catalytic Dehydrohalogenation

$$\begin{matrix} R_2CHCHDX \\ + R_2CHCH_2Y \end{matrix} \longrightarrow \begin{matrix} *X + *Y + R_2C = CHD \\ + R_2C = CH_2 + R_2CHCH_2D + R_2CHCH_3 \end{matrix} \qquad \text{IV-2}$$

Halo-Exchange

$$\begin{matrix} R_2CHCHDX \\ + R_2CHCH_2Y \end{matrix} \longrightarrow \begin{matrix} R_2CHCHDX + R_2CHCHDY \\ + R_2CHCH_2Y + R_2CHCH_2X \end{matrix} \qquad \text{IV-3}$$

By a judicious choice of haloalkanes, halo-exchange could be examined mass specrometrically as dehydrohalogenation proceeded. Lack of information about fragmentation patterns for the deuterated hydrocarbons made it impossible to precisely determine reactant and product concentrations. Instead, as explained below, halo-exchange and dehydrohalogenation were differentiated by characteristic changes in the mass spectral pattern. Olefins may have isomerized in the presence of hydrogen halide and, perhaps, by the surface itself; however, this was of no consequence to the experiments.

To keep extraneous influences to a minimum, several criteria were demanded of the reactants used for these studies.

1) Halo-exchange had to be detectable and distinguishable from dehydrohalogenation by mass spectrometry.

2) Both exchanging halides had to occupy the surface concurrently. This required that both haloalkanes be introduced to the film simultaneously and dehydrohalogenate at about the

same rate.

3) No thermodynamic barrier to exchange could exist. To assure this, haloalkanes with alkyl groups differing only by replacement of one hydrogen by deuterium were employed.

4) Both reactants had to dehydrohalogenate according to the same kinetic scheme.

Two sets of reactants were chosen which met each of these requirements. The non-catalytic reaction was studied with a mixture of 1-bromopropane and 1-chloropropane-1-d_1 and the catalytic with 1-bromo-2-methylpropane and 1-chloro-2-methylpropane-1-d_1. The non-catalytic reaction was studied on titanium and chromium and the catalytic on titanium.

The experiments reported herein represent the culmination of extensive halo-exchange studies conducted by several techniques. Other approaches such as exchange between halides from haloalkanes with different length alkyl groups and reactions on surfaces prepared exclusively with one halide were utilized. However, each of these contained some of the faults mentioned above and will not be discussed further. Nevertheless, they agree completely with the reported results.

Non-catalytic Reactions on Titanium and Chromium

The reactant haloalkanes were 1-bromopropane and 1-chloropropane-1-d_1. Preparation of the latter is described in Section II-E. Listed in Appendix C are the mass spectral patterns of these and the products of halo-exchange, along with the non-deuterated products of dehydrohalogenation. Fragmentation patterns for the possible deuterated products of dehydrohalogenation were not determined; however, these would not influence the results of the study.

On titanium, the kinetic behavior of both 1-bromopropane and 1-chloropropane has been established (Summers, 1970). Both reacted non-catalytically producing a mixture of propane and propene by half order kinetics. The surface retained all the halide and some hydrogen. The rates were comparable and remained constant for many runs.

The reaction of 1-chloropropane on chromium has also been studied (Section III-B). Whereas the titanium reaction continued at constant rate, with chromium the rate decreased slightly between consecutive runs. Nevertheless, it behaved non-catalytically and, for small reactant doses, could be followed for several runs with less than a 50% rate decrease. The gaseous products were propene and hydrogen while the surface retained only the chloride. 1-Bromopropane was not examined on chromium but, from its

behavior on titanium, was assumed to react similarly to 1-chloropropane. These properties were assumed to be unaltered by deuteration.

The same haloalkane mixture was used with both metals. As determined mass spectrometrically, the reactant vapor contained 40% 1-bromopropane and 60% 1-chloropropane-1-d_1. Mass spectral changes due to halo-exchange would be independent of the metal and apply to both experiments. Complete halo-exchange would produce a mixture of 20% 1-bromopropane, 20% 1-bromopropane-1-d_1, 20% 1-chloropropane and 40% 1-chloropropane-1-d_1. As calculated from known peak intensities, increases in the mass spectral peak ratios 42/43 from 0.3 to 0.7 and 44/43 from 0.15 to 0.36 would accompany this exchange. Therefore, in the absence of dehydrochlorination halo-exchange could be detected by changes in these ratios. As explained below, the 44/43 peak ratio was a particularly sensitive monitor throughout the entire dehydrohalogenation reaction.

Without direct knowledge of the fragmentation patterns of deuterated propenes and propanes it was impossible to calculate the fragmentation pattern for the equilibrium mixtures resulting from dehydrohalogenation. However, after the dehydrohalogenation had settled into a period of consistent behavior, it was determined experimentally for several runs. On both metals, the most significant

changes due to dehydrohalogenation occurred in the 42/43 and 27/43 peak ratios. The former was most dramatic changing from 0.3 in the starting material to about 2.2 in the equilibrium mixtures. Between the starting material and the equilibrium mixture the 44/43 ratio increased only slightly from 0.15 to 0.18. This is as expected from crude calculations based on peak intensities for non-deuterated hydrocarbons.

Thus, changes in peak ratios accompany both halo-exchange and dehydrohalogenation would have been the same for both metals. For rapid halo-exchange followed by dehydrohalogenation the 42/43 peak ratio would have increased rapidly from 0.3 to 0.7 then continued to grow gradually to about 2.2. The 44/43 peak ratio would rapidly increase from 0.15 to 0.4, then decrease gradually to about 0.18. In the absence of halo-exchange the former would grow gradually from 0.3 to 2.2 and the latter remain essentially constant.

With both metals, several reactions were followed until consistent equilibrium mixtures were found. On titanium, both products and reaction rate remained constant; however, with chromium products remained constant while rate slowly decreased as expected.

Neither a pressure change nor hydrogen halide production was detected. Thus, the reactions proceeded according to the non-catalytic pattern established

during individual studies.

On titanium reactions were run at $1x10^{-2}$ Torr at both 195 and 165°C. The former enabled study of the entire dehydrohalogenation reaction whereas the latter allowed for better examination of the region of maximum halo-exchange prior to any appreciable dehydrohalogenation. Changes in the 42/43 and 44/43 peak ratios for these two reactions are shown in Figures IV-10 and IV-11 . The dotted lines represent the theoretical curves resulting from rapid halo-exchange followed by gradual dehydrohalogenation.

At both temperatures, there was no indication of halo-exchange. The gradual growth of the 42/43 peak ratio and the slight increase in the 44/43 peak ratio were completely consistent with dehydrohalogenation in the absence of halo-exchange. The 44/43 peak ratio remaining between 0.15 - 0.2 throughout the entire dehydrohalogenation indicated that slow halo-exchange was, also, not occurring.

As shown in Figures IV-12 and IV-13 the same behavior was observed on chromium. The reactions were conducted at $4x10^{-3}$ Torr and 229°C. Again, the gradual increase in the 42/43 peak ratio to 2.2 and the slight increase in the 44/43 peak ratio from 0.15 to 0.18 was completely consistent with dehydrohalogenation in the absence of halo-exchange. Also, the constancy of the 44/43 ratio throughout the entire dehydrohalogenation indicated the absence of slow halo-exchange

FIGURE IV - 10

Change in 42/43 and 44/43 Peak Ratios

With Time For Non-catalytic Reaction

on Titanium

$T = 165^{o}C$

Δ - 42/43 experimental

O - 44/43 experimental

– - 42/43 theoretical

• - 44/43 theoretical

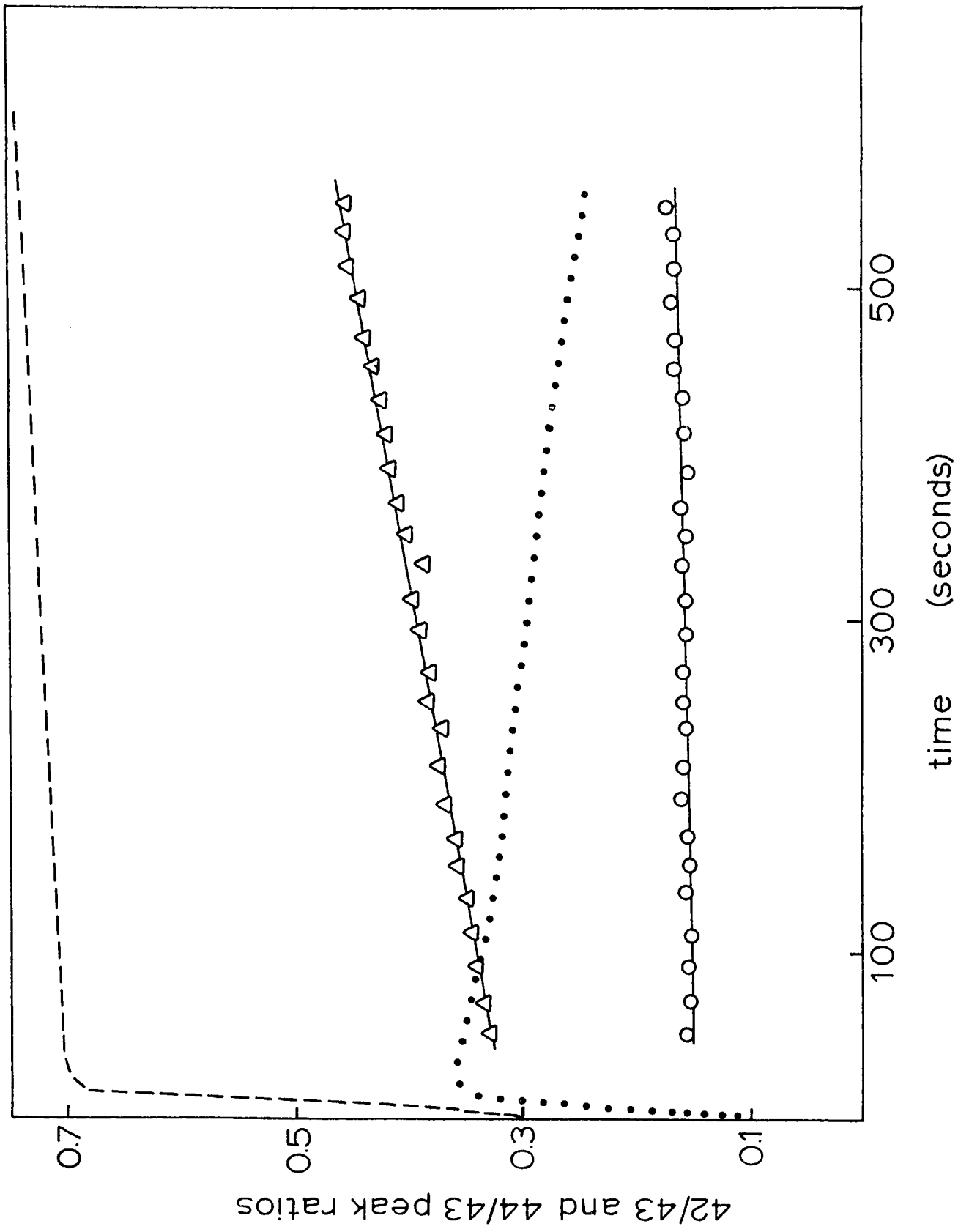
42/43 and 44/43 peak ratios
0.7
0.5
0.3
0.1
100
300
500
time (seconds)

FIGURE IV - 11

Change in 42/43 and 44/43 Peak Ratios

With Time For Non-catalytic Reaction

on Titanium

$T = 195^{o}C$

Δ - 42/43 experimental

O - 44/43 experimental

– - 42/43 theoretical

• - 44/43 theoretical

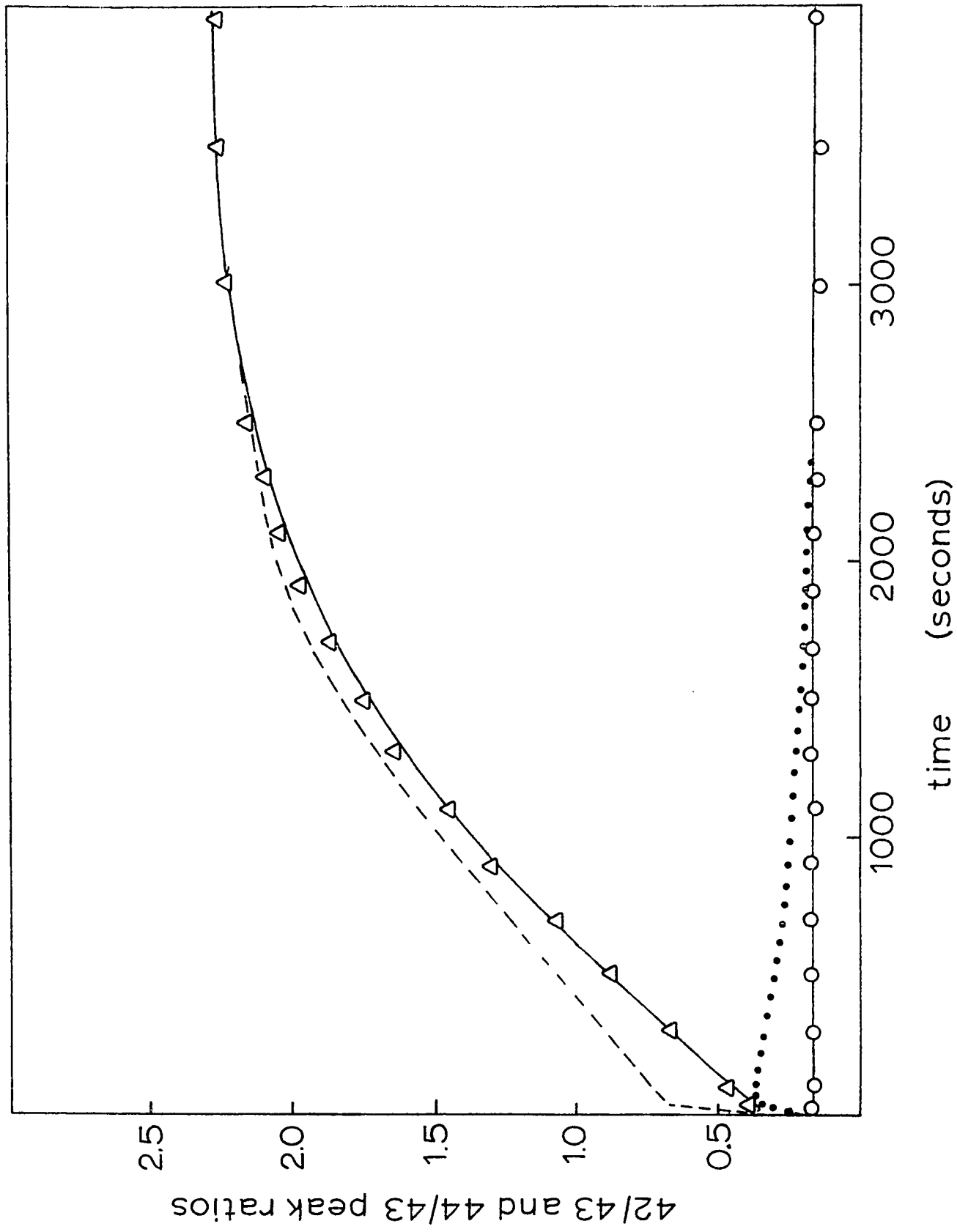
42/43 and 44/43 peak ratios
2.5
2.0
1.5
1.0
0.5
1000
2000
3000
time (seconds)

FIGURE IV - 12

Change in 42/43 and 44/43 Peak Ratios

With Time For Non-catalytic Reaction

on Chromium

$T = 229^{o}C$

Δ - 42/43 experimental

O - 44/43 experimental

_ - 42/43 theoretical

• - 44/43 theoretical

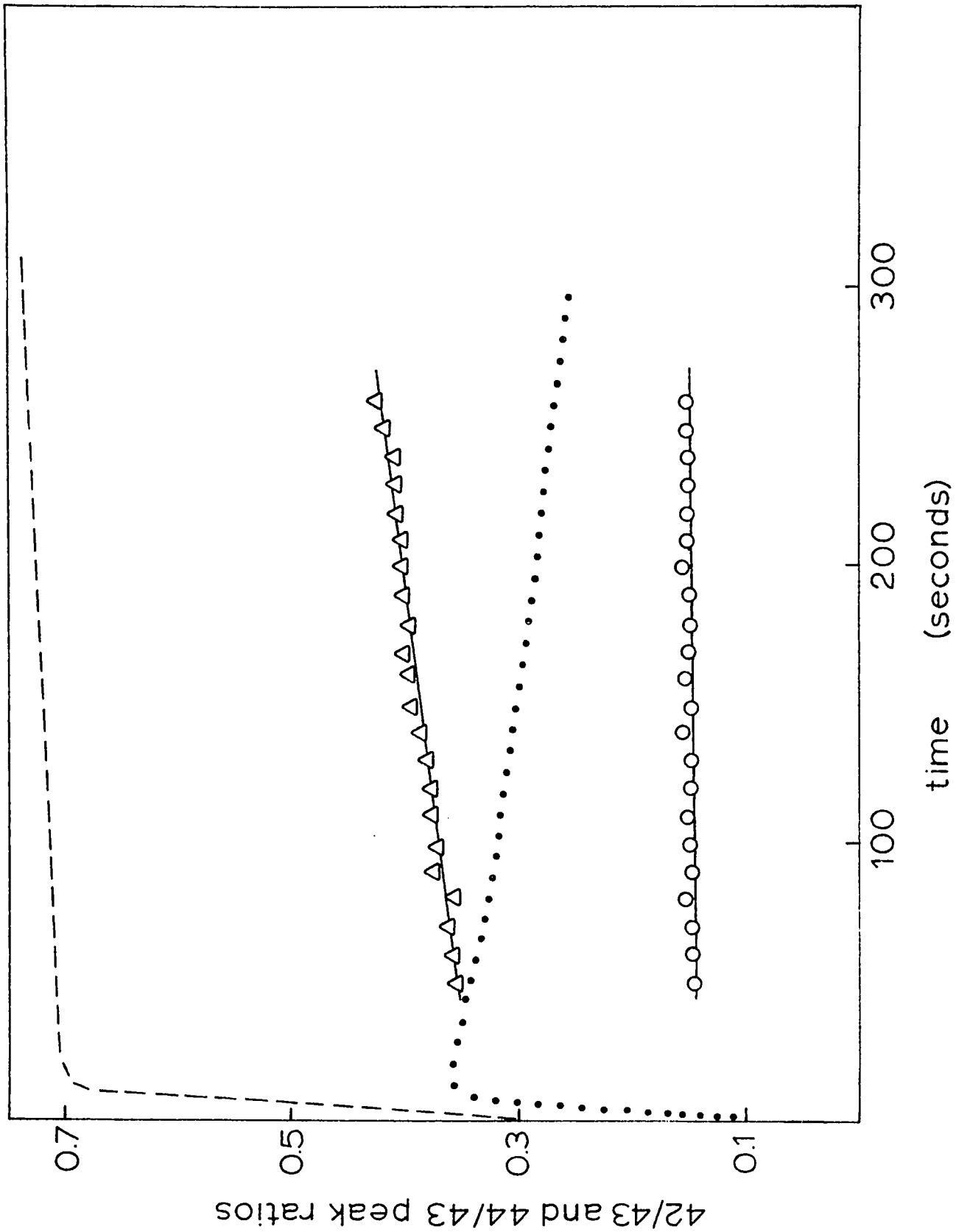
42/43 and 44/43 peak ratios
0.7
0.5
0.3
0.1
100
200
300
time (seconds)

FIGURE IV - 13

Change in 42/43 and 44/43 Peak Ratios

With Time For Non-catalytic Reaction

on Chromium

$T = 229^{o}C$

Δ - 42/43 experimental

O - 44/43 experimental

_ - 42/43 theoretical

. - 44/43 theoretical

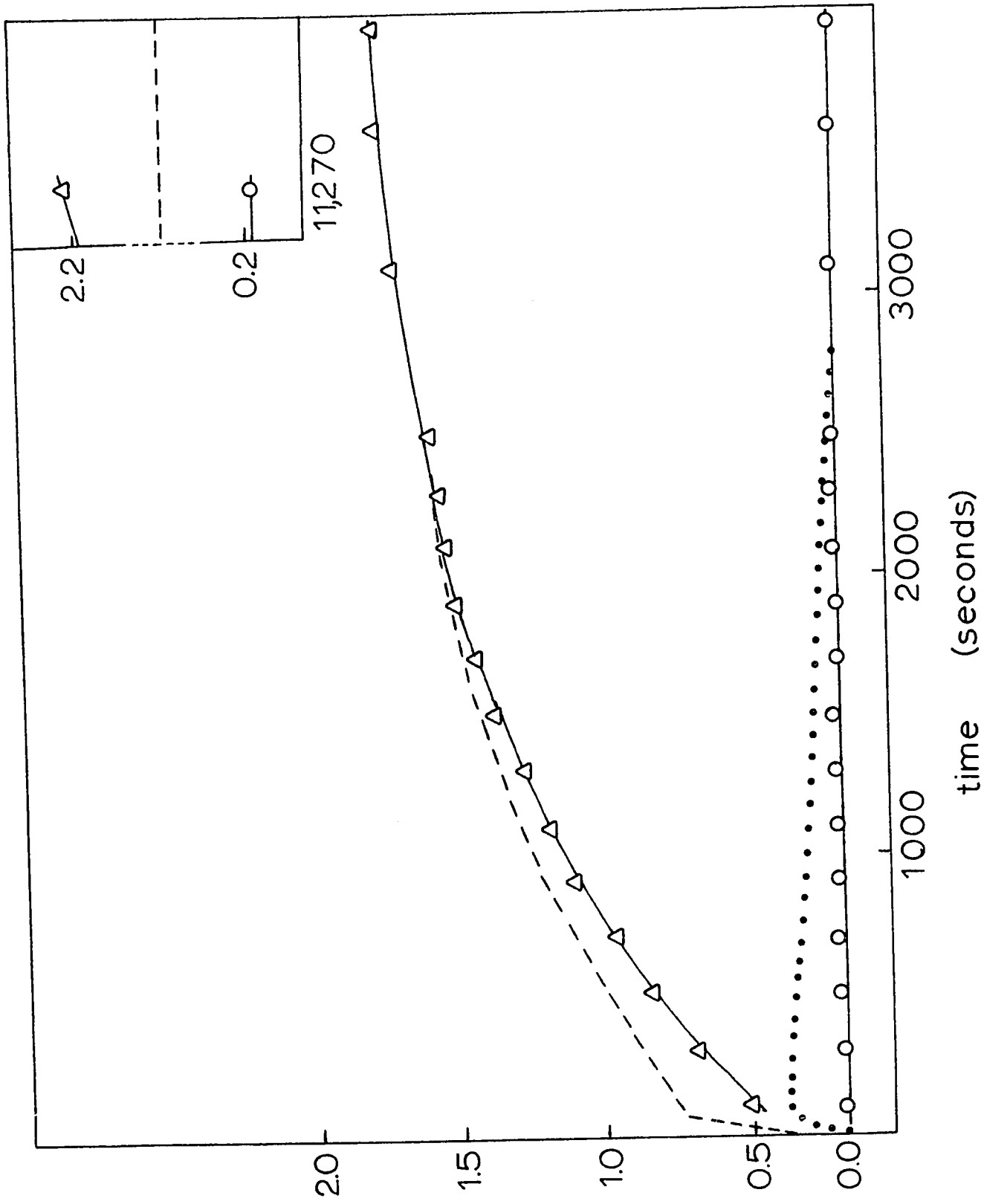
42/43 and 44/43 peak ratios
2.0
1.5
1.0
0.5
0.0
1000
2000
3000
time (seconds)
11,270
2.2
0.2

On both metals, the reactions shown are only examples of many similar runs, all of which were in complete agreement. The peaks displayed were most sensitive to the reactions being examined, but other less sensitive peak changes agreed with the reported findings.

Catalytic Reactions on Titanium and Nickel

The haloalkanes used as reactants were 1-bromo-2-methylpropane and 1-chloro-2-methylpropane-1-d_1, The preparation and analysis of the latter being described in Section II-E. Mass spectral fragmentation patterns of these, the products of halo-exchange, and methylpropene are shown in Appendix C. As in the non-catalytic study, the patterns of deuterated methylpropenes were not determined, but could in no way affect the results.

The kinetic behavior of 1-chloro-2-methylpropane on titanium has been established (Summers, 1970) and that of 1-bromo-2-methylpropane was found to be similar. Both reacted by first order kinetics generating an equimolar mixture of hydrogen halide and methylpropene. Although studied on different films, the rates differed by less than a factor of two. Likewise, the reaction of 1-chloro-2-methylpropane on nickel was found to proceed the same as on titanium, but with different activation parameters (Section III-B). Although not explicitly studied, the reactions of 1-bromo-2-methylpropane on nickel were assumed to behave similarly on

nickel and titanium. It was assumed that deuteration would not cause any appreciably alterations.

Both by mass spectrometry and gas chromatography, the reactant vapor was found to contain equimolar quantities of 1-chloro-2-methylpropane-1-d_1 and 1-bromo-2-methylpropane. This mixture was used with both metals.

Halo-exchange would produce an equimolar mixture of 1-bromo-2-methylpropane, 1-bromo-2-methylpropane-1-d_1, 1-chloro-2-methylpropane and 1-chloro-2-methylpropane-1-d_1. As seen from the fragmentation patterns in Appendix C, this would be accompanied by significant changes in the mass spectral peak ratios 43/41 from 0.8 to 1.4, 58/41 from 0.0 to 0.6 and 58/57 from 0.0 to 0.9. The most sensitive monitor was the 58 peak which was very large in 1-bromo-2-methylpropane-1-d_1 and virtually non-existent in the other three.

The fragmentation patterns of the hydrocarbon products of dehydrohalogenation could not be calculated directly from known individual patterns but were determined by examining the equilibrium mixture from several runs after the reaction had settled into constant catalytic behavior. The most significant changes occurred in the peak ratios 43/41 from about 0.8 in the starting material to about

0.1 and 57/41 from about 0.7 to about 0.2. In the equilibrium mixture, there was no detectable 58 peak.

Halo-exchange could not be induced by the walls of the vessel or by hydrogen halides.

With both metals, several reactions were followed to assure that the behavior of each peak was understood and consistent; each proceeded similarly. Although component concentrations were not known, the behavior of individual peaks was adequate to determine that dehydrohalogenation was proceeding at constant rate with consistent products throughout each study. Total pressure doubled and hydrogen halide was detected mass spectrometrically indicating that the reaction was proceeding catalytically.

On titanium,reactions were conducted in the region of 140°C requiring about 4000 seconds for complete dehydrohalogenation. Several readings were taken within the first 400 seconds to assure that the period of maximum halo-exchange was thoroughly examined. On nickel, reaction proceeded for more than 6500 seconds at 198°C. The results of two such reactions are shown in Figures IV-14 and IV-15 .

As the most sensitive indicators of hydrohalogenation and halo-exchange the peak ratios 43/41 and 58/57 are reported; however, all other peaks indicated the same trend. The dotted lines represent the theoretical curves

for rapid halo-exchange followed by gradual dehydrohalogenation. The continual decrease in the 43/41 ratio and the total absence of a 58 peak throughout both reactions indicated complete lack of halo-exchange while dehydrohalogenation proceeded gradually. The total absence of a 58 peak indicated that no halo-exchange occurred either slowly or rapidly.

Other runs, both slower and faster than that shown in Figures IV-14 and IV-15 demonstrated the same behavior. Lack of proper mass spectral characteristics for the other haloalkanes which reacted catalytically made it impossible to study any system other than that mentioned above.

FIGURE IV - 14

Change in 43/41 and 58/57 Peak Ratios

With Time For Catalytic Reaction

on Titanium

$T = 140^{\circ}C$

Δ - 43/41 experimental

O - 58/57 experimental

— - 43/41 theoretical

• - 58/57 theoretical

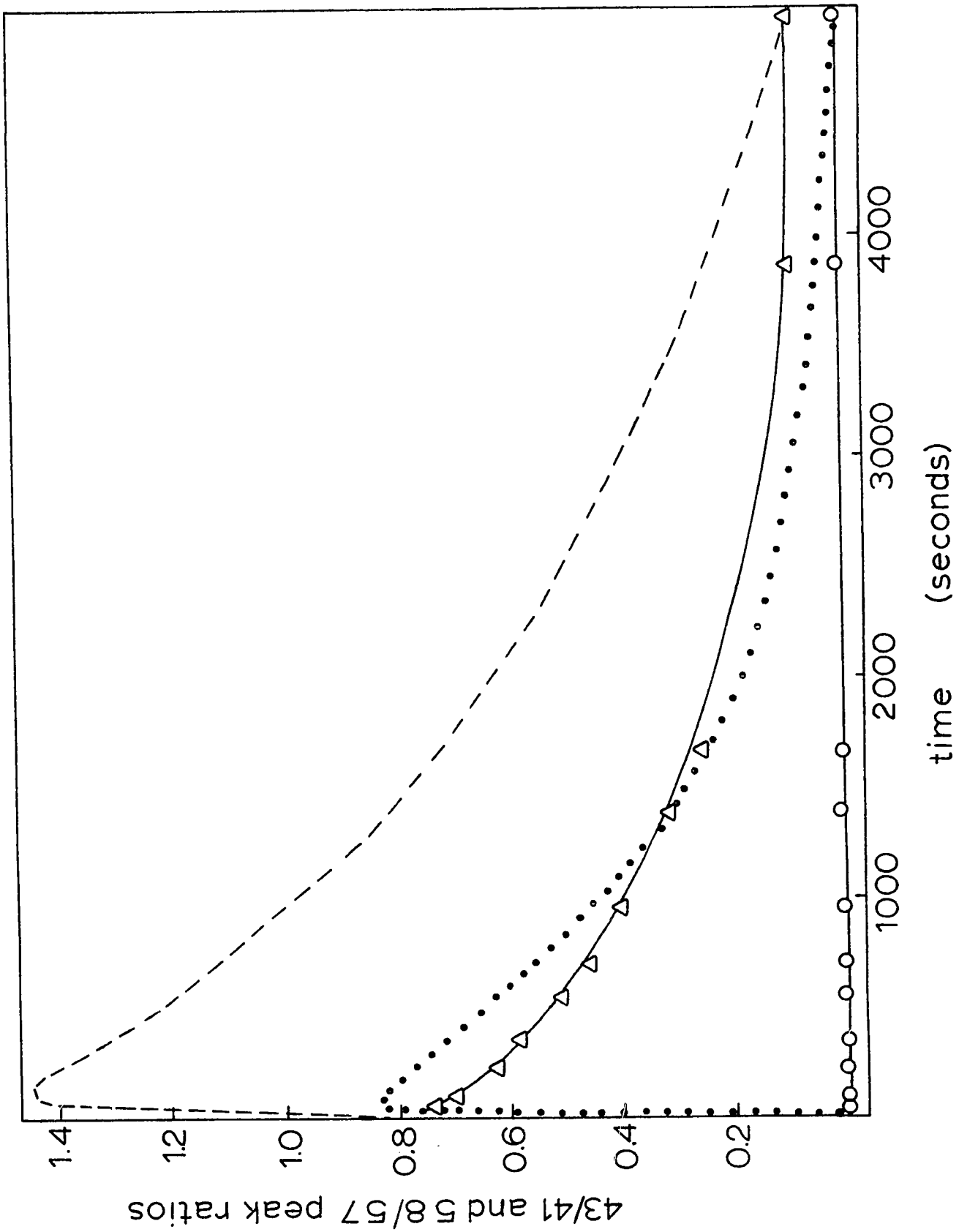
43/41 and 58/57 peak ratios
1.4
1.2
1.0
0.8
0.6
0.4
0.2
1000
2000
3000
4000
time (seconds)

FIGURE IV - 15

Change in 43/41 and 58/57 Peak Ratios

With Time For Catalytic Reaction

on Nickel

$T = 198^{\circ}C$

Δ - 43/41 experimental

O - 58/57 experimental

— - 43/41 theoretical

• - 58/57 theoretical

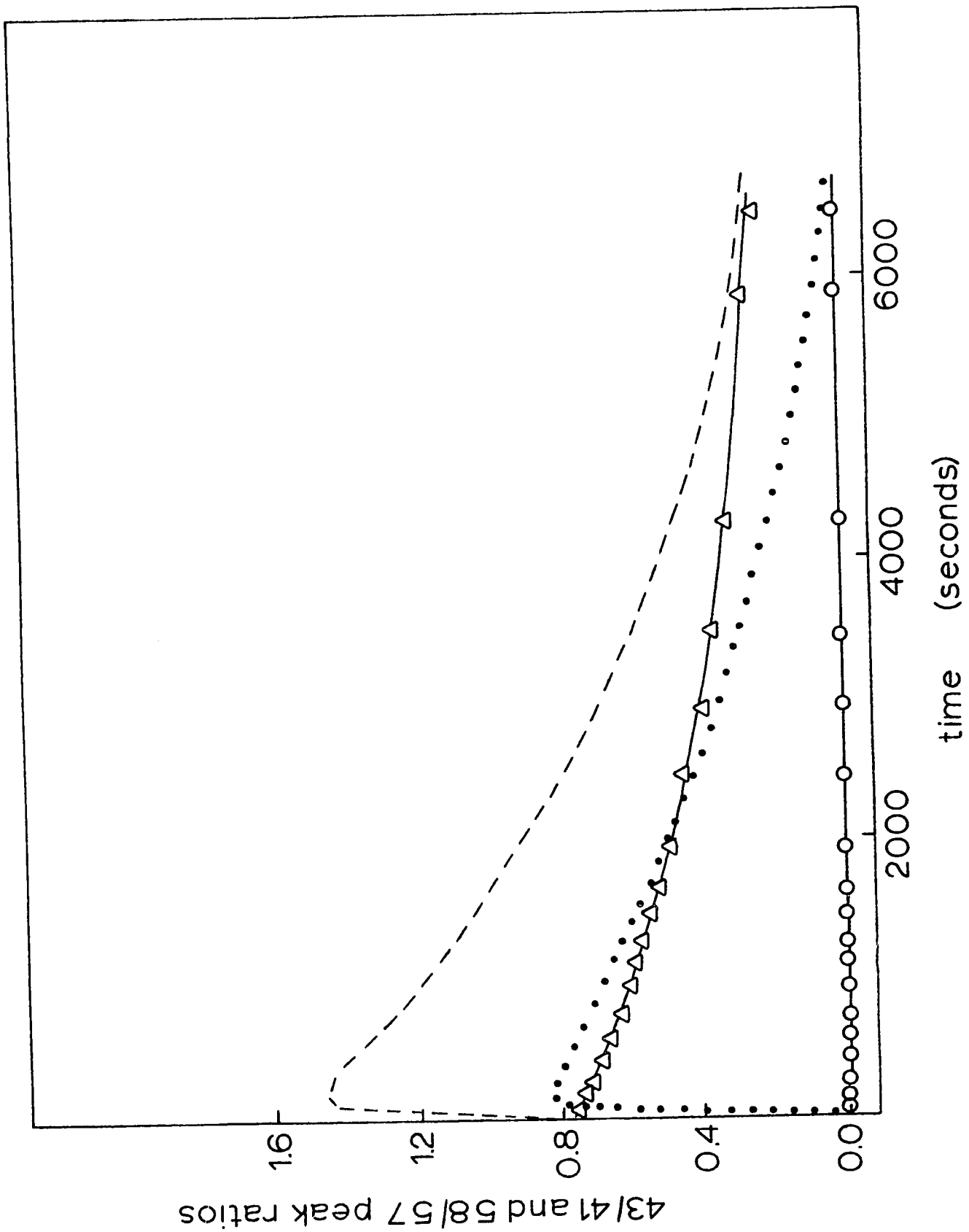
43/41 and 58/57 peak ratios
1.6
1.2
0.8
0.4
0.0
2000
4000
6000
time (seconds)

IV-B-4) Studies of Surface Site Specificity

The possibility that the surface halide layer formed during the reaction of each haloalkane was different and acted as a specific catalyst for that particular reaction was investigated. Both the products and activation parameters of reactions of more than one haloalkane on the same film were studied; reactions of haloalkanes known to proceed catalytically were studied on surfaces initially reacted non-catalytically and vice versa. In addition, the relative rates and activation parameters for two haloalkanes both reacting catalytically on the same film were examined. It was intended that in this manner information bearing on the reasons for the variation in reaction schemes could be generated.

Non-catalytic Reactions on a Catalytic Surface

Reactions of 1-chloropropane were studied on a titanium surface previously reacted exclusively with 1-chloro-2-methylpropane and 2-chloropropane (catalytic reactions).

During the former study, 1-chloro-2-methylpropane was reacted with the freshly deposited surface film until the reaction became catalytic and consistent. Reaction order and activation parameters were determined as shown in Figures IV-16 and IV-17. Equimolar quantities of hydrogen chloride and methylpropene were generated as the

FIGURE IV - 16

Disappearance of 1-Chloro-2-methylpropane

on Titanium

Plotted as a First Order Reaction

for $P_o = 1 \times 10^{-2}$ Torr

○ - 181°C

□ - 196°C

△ - 201°C

○ - 220°C

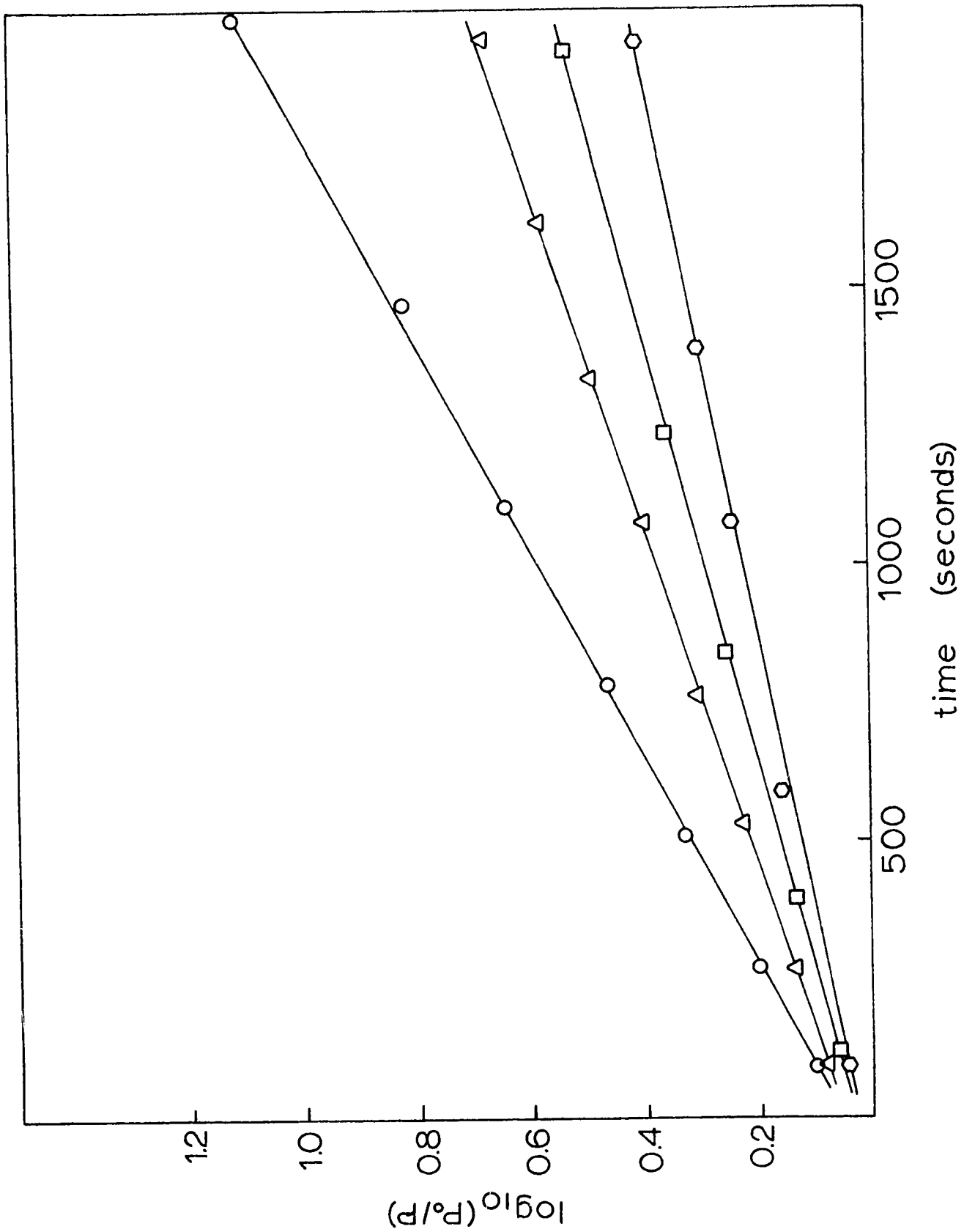
1.2
1.0
0.8
0.6
0.4
0.2
log10 (P°/P)
500
1000
1500
time (seconds)

FIGURE IV - 17

Arrhenius Plot of Rate Data for First Order

Disappearance of 1-Chloro-2-methylpropane

on Titanium

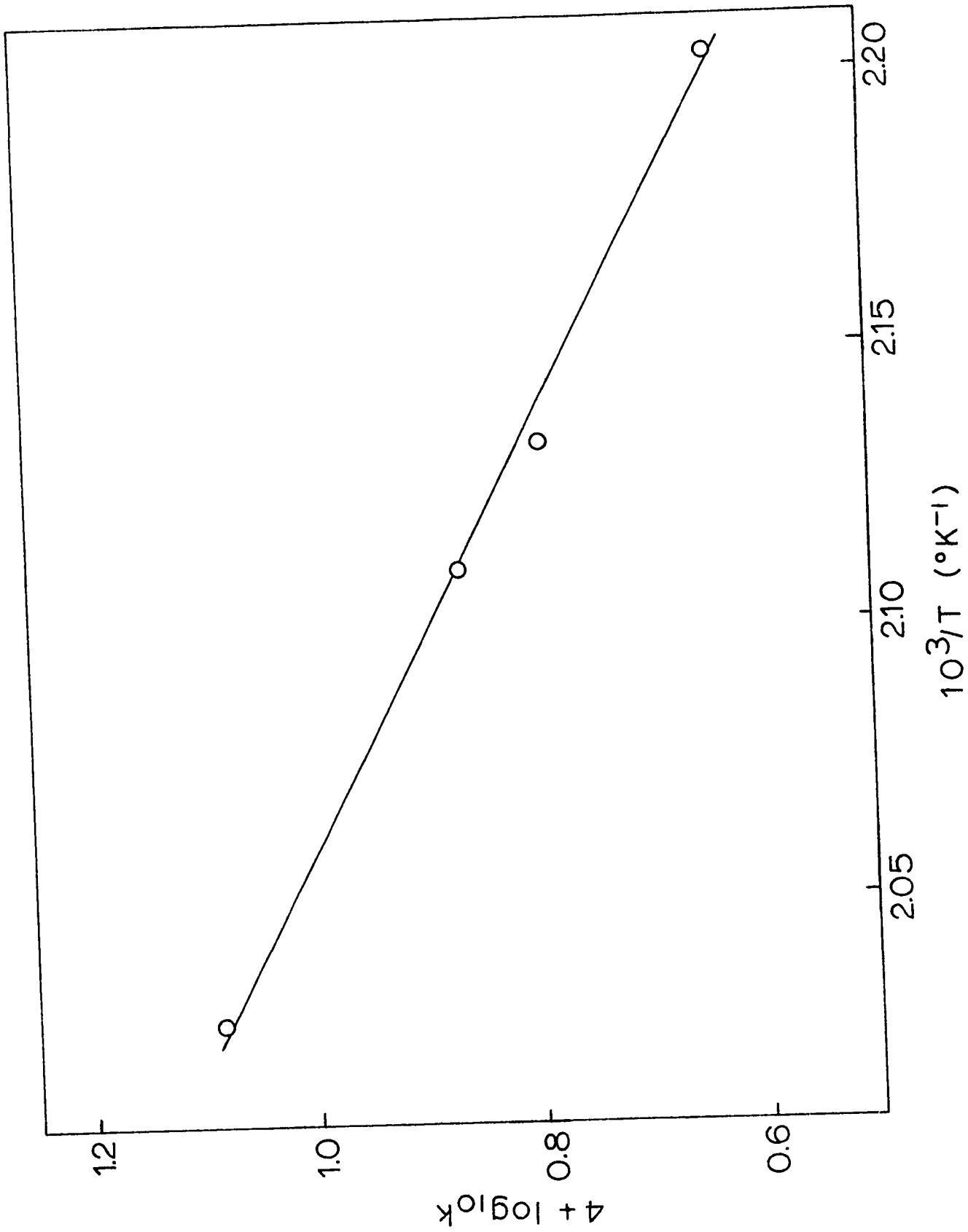
4 + log10k
1.2
1.0
0.8
0.6
2.05
2.10
2.15
2.20
10^3/T (°K^-1)

total pressure in system doubled. 1-Chloro-2-methylpropane disappeared according to a first order rate law with an activation energy of 11.8 ± 0.5 kcal/mole and $\log_{10}A$ of 2.3 ± 0.3, in good agreement with those determined by Summers and Harrod (1972) of 12.6 ± 0.3 and 2.4.

The film was then reacted with 2-chloropropane as reported below and again with 1-chloro-2-methylpropane to confirm that this was still proceeding catalytically with no side products. By isolating the film for two thousand seconds at 240°C it was confirmed that hydrogen chloride would not spontaneously evolve even at the highest temperature studied.

The surface was then reacted three times with 1-chloropropane. The first reaction at 208°C, the temperature at which 1-chloro-2-methylpropane was dehydrochlorinating readily, proceeded only 9% in 2200 seconds giving mainly propene and traces of propane but no hydrogen or hydrogen chloride.

The second reaction at 239°C was also very slow requiring about 10,000 seconds to go to 90% completion. However, hydrogen chloride was detected both mass spectrometrically and by an increase in the total pressure. The total pressure increased about 30% from 1.1 to 1.4×10^{-2} Torr

during the first 50% reaction then remained steady at about 1.4×10^{-2} Torr for the remainder. The disappearance of 1-chloropropane is plotted both as first and half order in Figure IV-18 . The reaction order seemed to decrease at about 3000 seconds (about 50% reaction) as indicated by the disappearance of curvature in the half order plot and the change of curvature in the first order plot.

The third reaction, also at 239°C, proceeded about 30% more rapidly than its predecessor (80% completion in about 6000 seconds), and released no hydrogen chloride. The disappearance of 1-chloropropane was again plotted as first and half order and half order kinetics prevailed throughout (Figure IV-19).

Catalytic Reactant on a Non-catalytic Surface

The reaction of 1-chloro-2-methylpropane was studied on a surface previously reacted only with 1-chloropropane. As shown in Figure IV-5 , this surface was promoting the non-catalytic reaction as usual. 1-Chloro-2-methylpropane passed through the usual settling down period before hydrogen chloride was detected.

However, whereas the appearance of hydrogen chloride was normally accompanied by the disappearance of paraffin from the product mixture, about 10% methylpropane continued to be generated during each reaction and the total

FIGURE IV - 18

Disappearance of 1-Chloropropane

on Titanium Film

Previously Reacted With

1-Chloro-2-methylpropane

Plotted as Half and First Order Reactions

(second reaction)

$T = 239^{o}C$

$P_o = 1.1 \times 10^{-2}$ Torr

Δ - Half Order

O - First Order

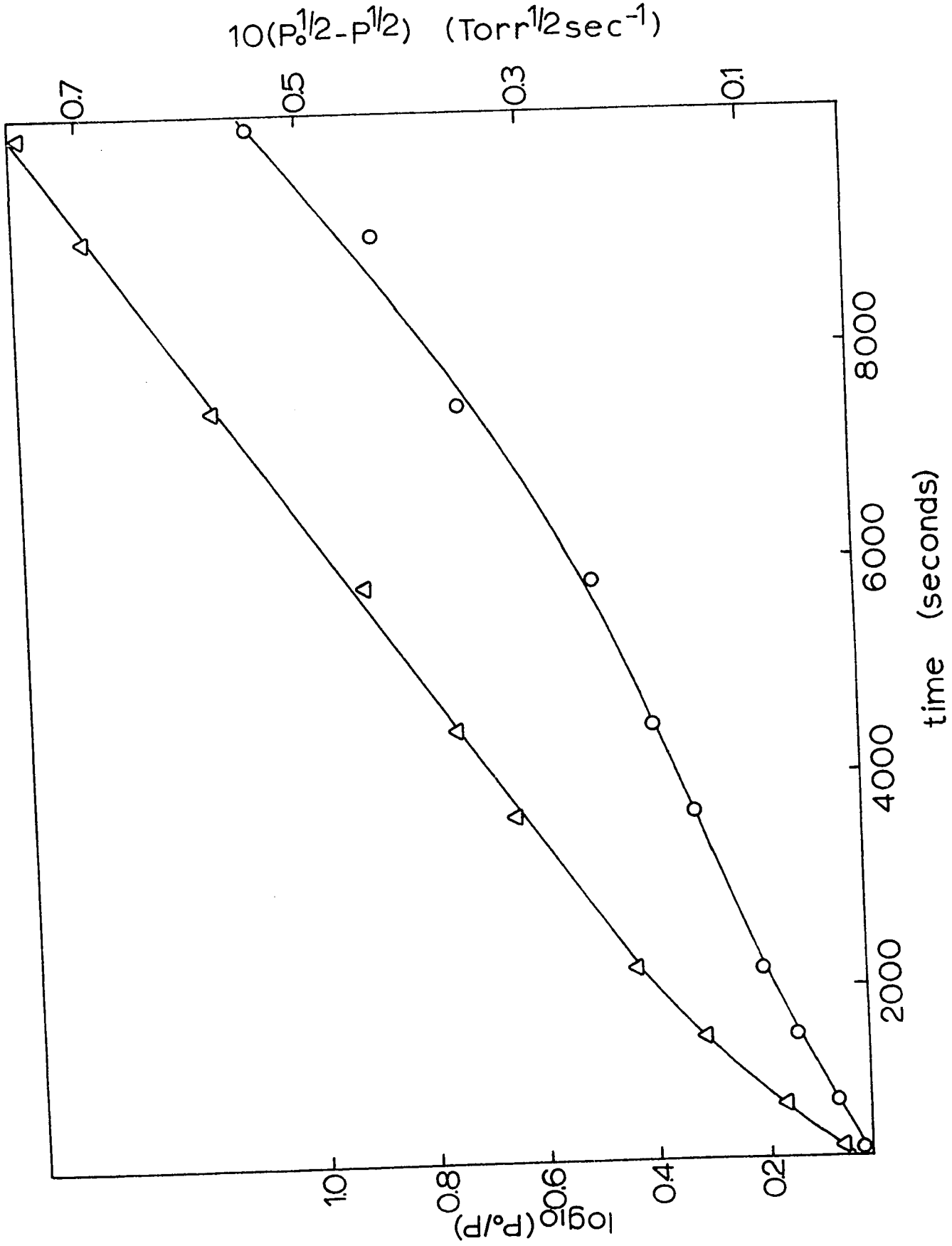
$10(P_o^{1/2}-P^{1/2})$ $(Torr^{1/2}sec^{-1})$
0.7
0.5
0.3
0.1
2000
4000
6000
8000
time (seconds)
1.0
0.8
0.6
0.4
0.2
$\log_{10}(P_o/P)$

FIGURE IV - 19

Disappearance of 1-Chloropropane

on Titanium Film

Previously Reacted With

1-Chloro-2-methylpropane

Plotted as Half and First Order Reactions

(third reaction)

$T = 239^{o}C$

$P_o = 1.0 \times 10^{-2}$ Torr

Δ - Half Order

O - First Order

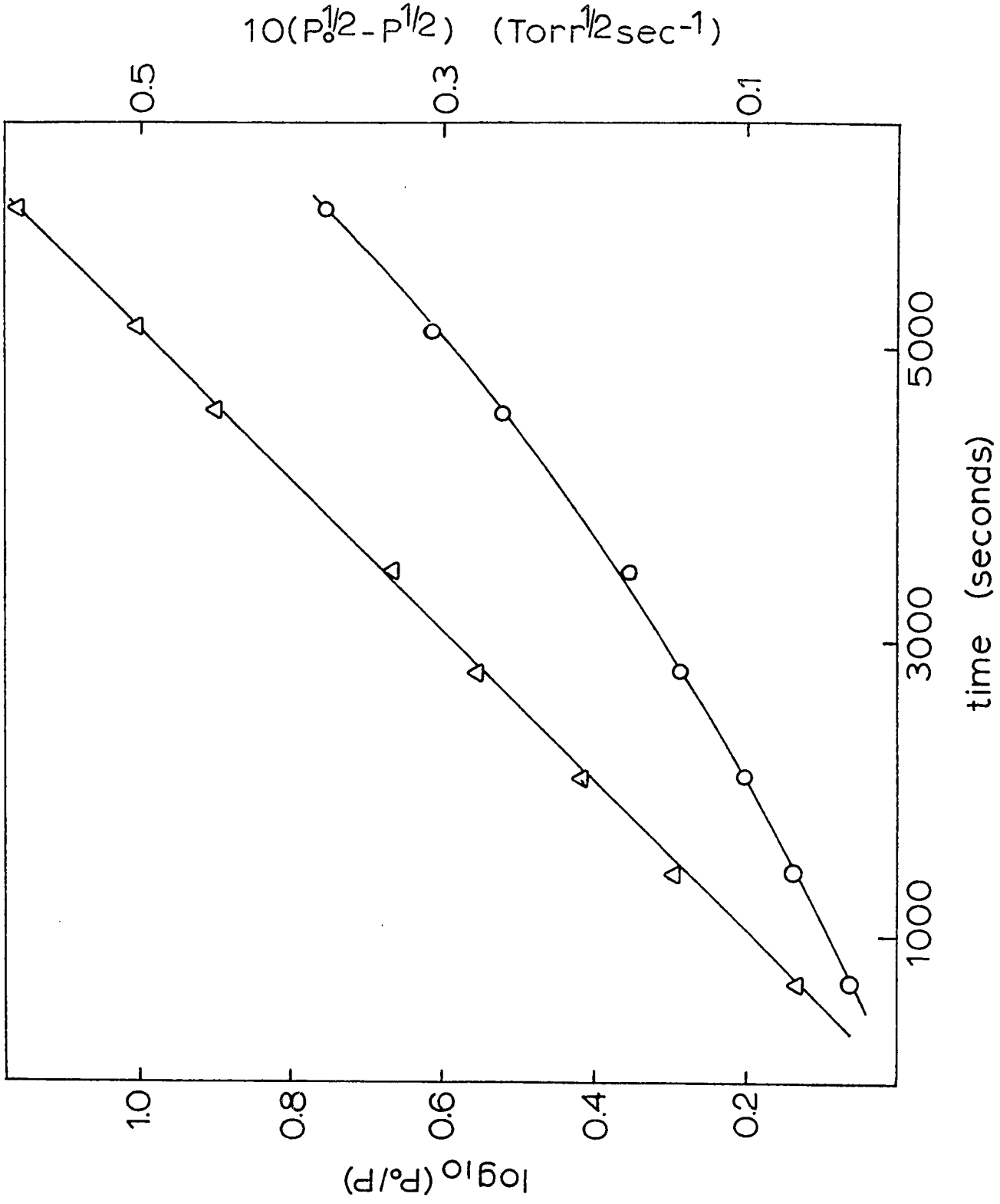
10(P°1/2 - P1/2) (Torr1/2sec-1)
0.5
0.3
0.1
log10 (P°/P)
1.0
0.8
0.6
0.4
0.2
1000
3000
5000
time (seconds)

pressure in the system never increased by more than 80%. This behavior continued even after the catalytic reaction of more than two Torr of 1-chloro-2-methylpropane.

As shown in Figures IV-20 and IV-21 , the reaction followed a first order rate law in 1-chloro-2-methylpropane with an activation energy of 21.2 ± 0.9 Kcal/mole and $\log_{10} A$ of 6.0 ± 0.4.

Catalytic Reactions on a Surface Prepared With Catalytic Reactions of a Different Haloalkane

Reactions of 2-chloropropane were studied on a surface previously reacted only with 1-chloro-2-methylpropane which, as mentioned above, was proceeding normally in terms of both reaction order and activation parameters. The 2-chloropropane reacted catalytically without a settling down period. During all its dehydrochlorinations it disappeared by first order rate lawswith no side reactions.

Relative rates were determined by reacting 2-chloropropane between two 1-chloro-2-methylpropane reactions at 201°C and 10^{-1} Torr. The rate constants were $7.347 \times 10^{-4} sec^{-1}$ and $7.352 \times 10^{-4} sec^{-1}$ for the two 1-chloro-2-methylpropane reactions and $8.550 \times 10^{-4} sec^{-1}$ for that of 2-chloropropane, a 16% increase.

Activation parameters for the

Leaf 185 omitted in page numbering.

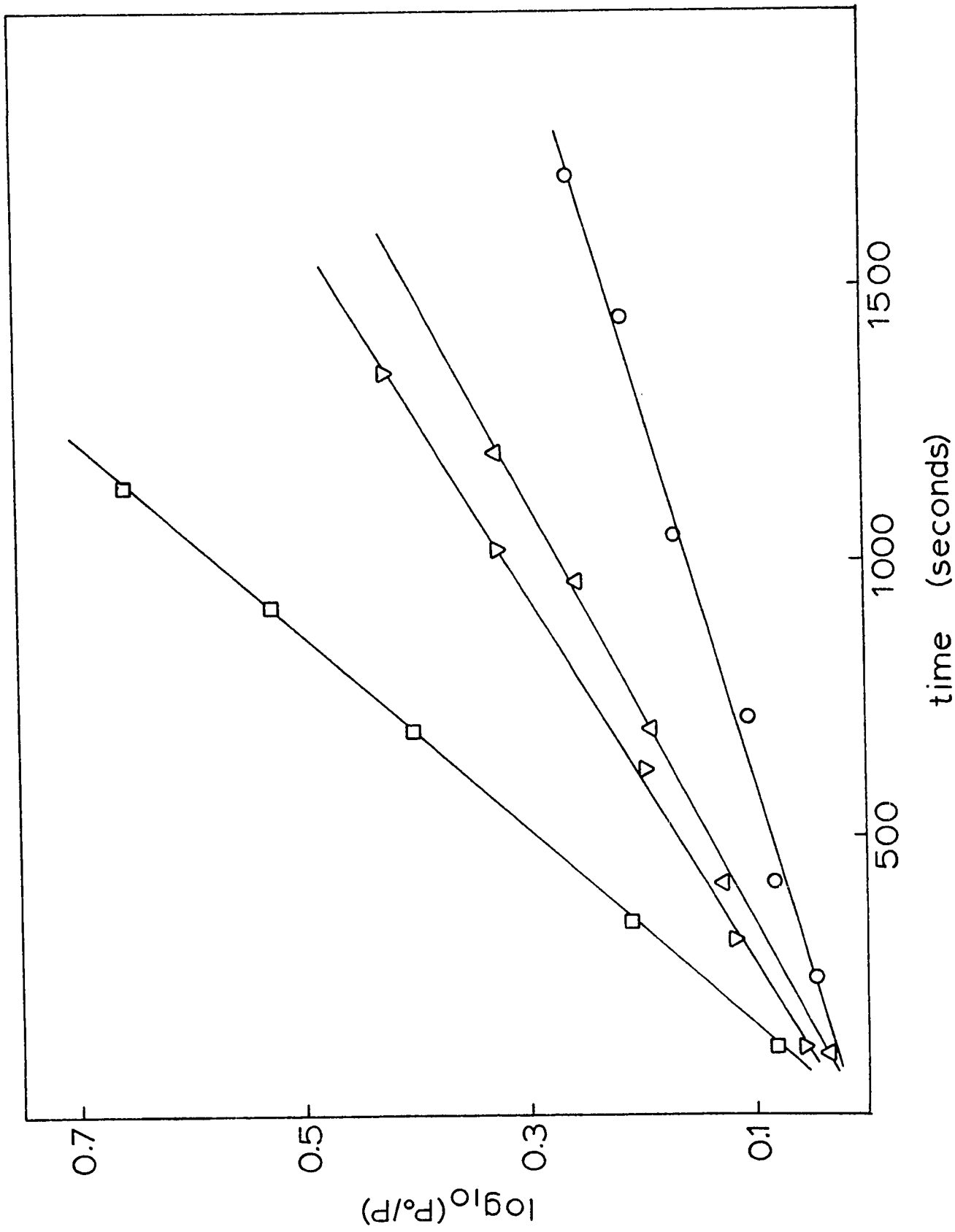
0.7
0.5
0.3
0.1
log10(P°/P)
500
1000
1500
time (seconds)

FIGURE IV - 20

Disappearance of 1-Chloro-2-methylpropane

on Titanium Film

Previously Reacted With

1-Chloropropane

Plotted as a First Order Reaction

for $P_o = 1 \times 10^{-2}$ Torr

○ - 196°C

△ - 212°C

▽ - 213°C

□ - 227°C

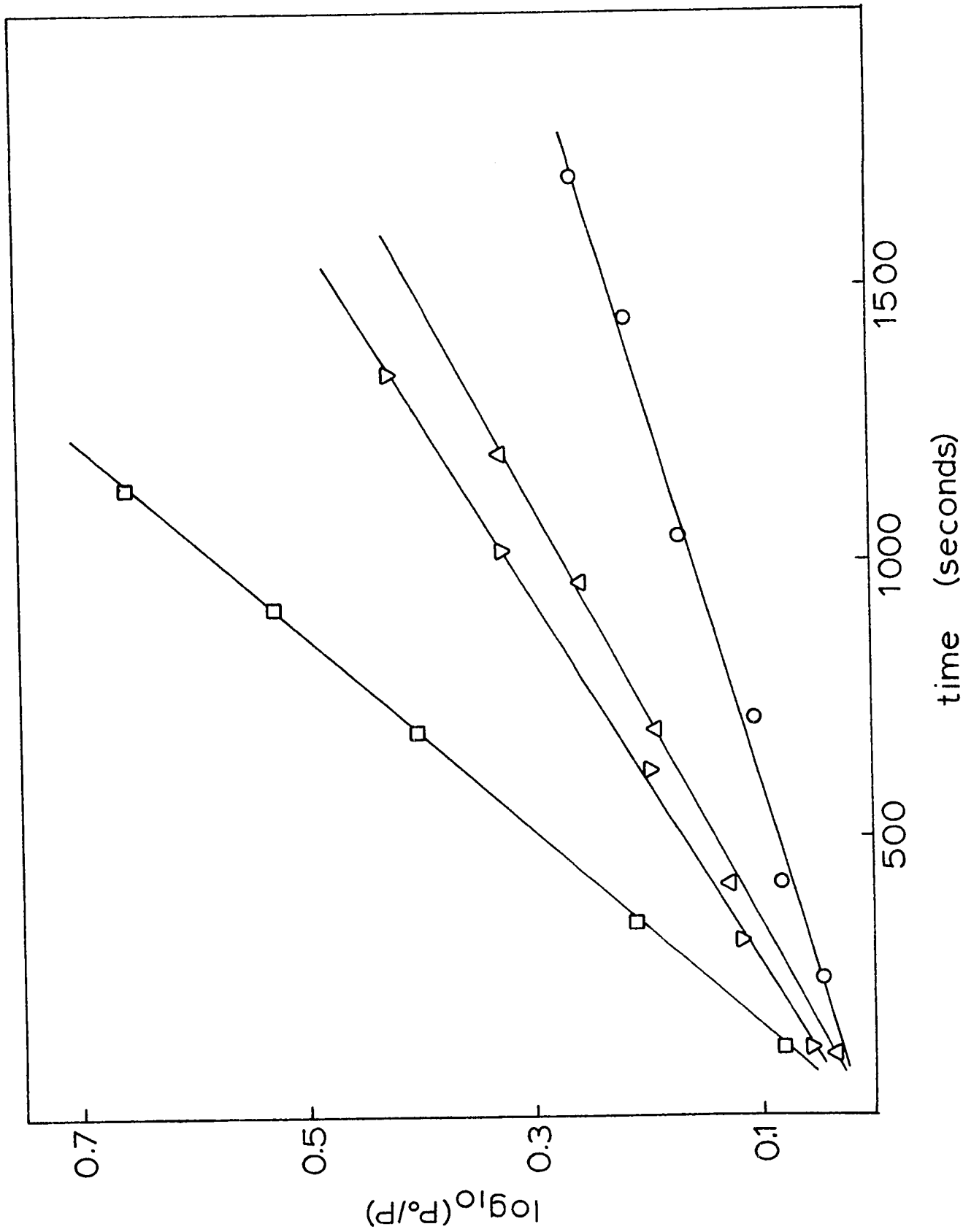
0.7
0.5
0.3
0.1
log10(Po/P)
500
1000
1500
time (seconds)

FIGURE IV - 21

Arrhenius Plot of Rate Data for First Order

Disappearance of 1-Chloro-2-methylpropane

on Titanium Film

Previously Reacted With 1-Chloropropane

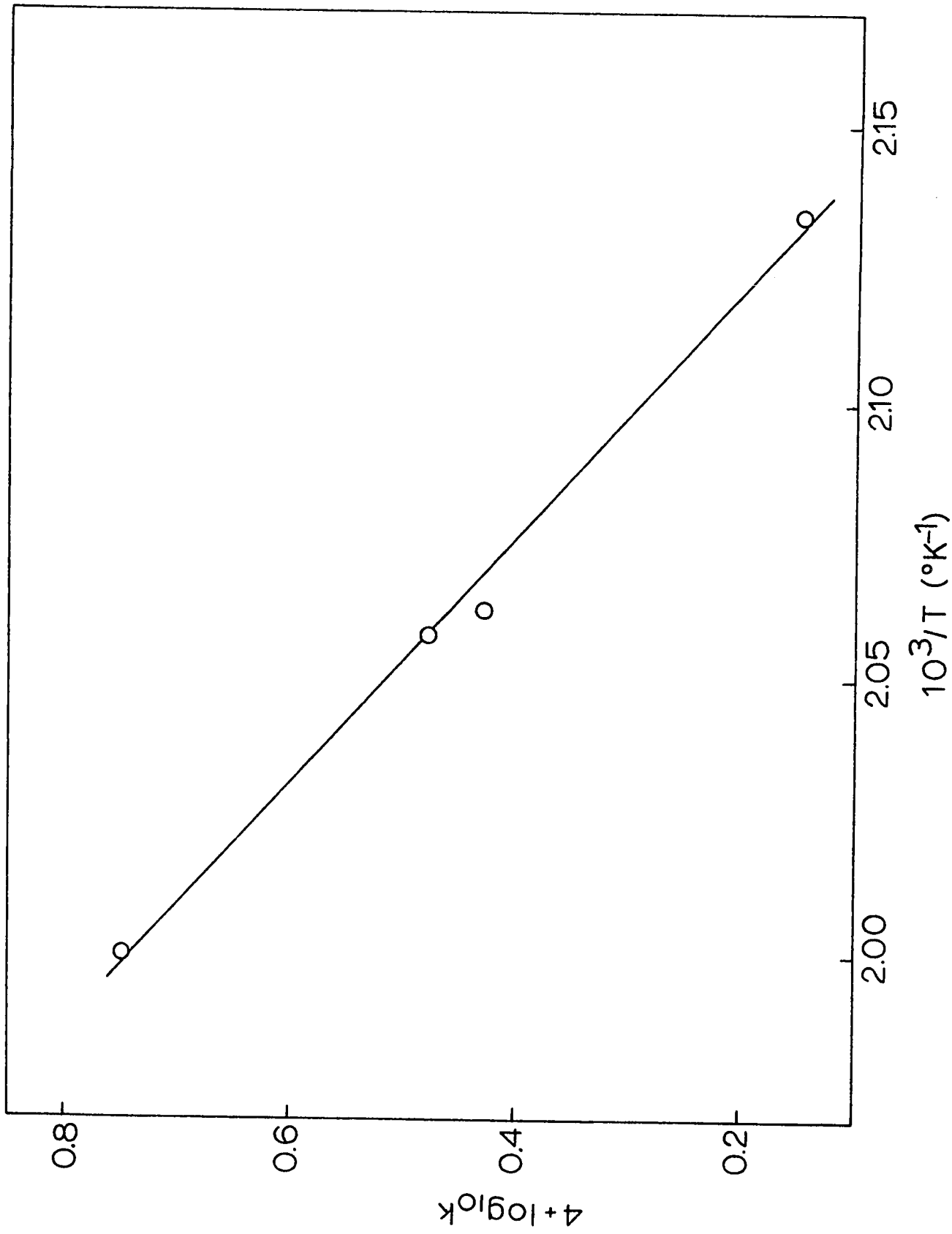
0.8
0.6
0.4
0.2
4 + log10k
2.00
2.05
2.10
2.15
10^3/T (°K^-1)

2-chloropropane reaction were calculated both immediately following the 1-chloro-2-methylpropane reaction (Figures IV-22 and IV-23) and after the surface had been halided with about 1 Torr of 2-chloropropane (Figures IV-24 and IV-25). The former showed an activation energy of 13.7 ± 0.4 Kcal/mole and $\log_{10}A$ of 3.5 ± 0.3 and the latter an activation energy of 14.4 ± 0.2 Kcal/mole and $\log_{10}A$ of 4.0 ± 0.1.

FIGURE IV - 22

Disappearance of 2-Chloropropane

on Titanium Film

Previously Reacted With

1-Chloro-2-methylpropane

Plotted as a First Order Reaction

(immediately following)

for $P_o = 1 \times 10^{-2}$ Torr

□ - 192°C

△ - 207°C

⬡ - 220°C

○ - 220°C

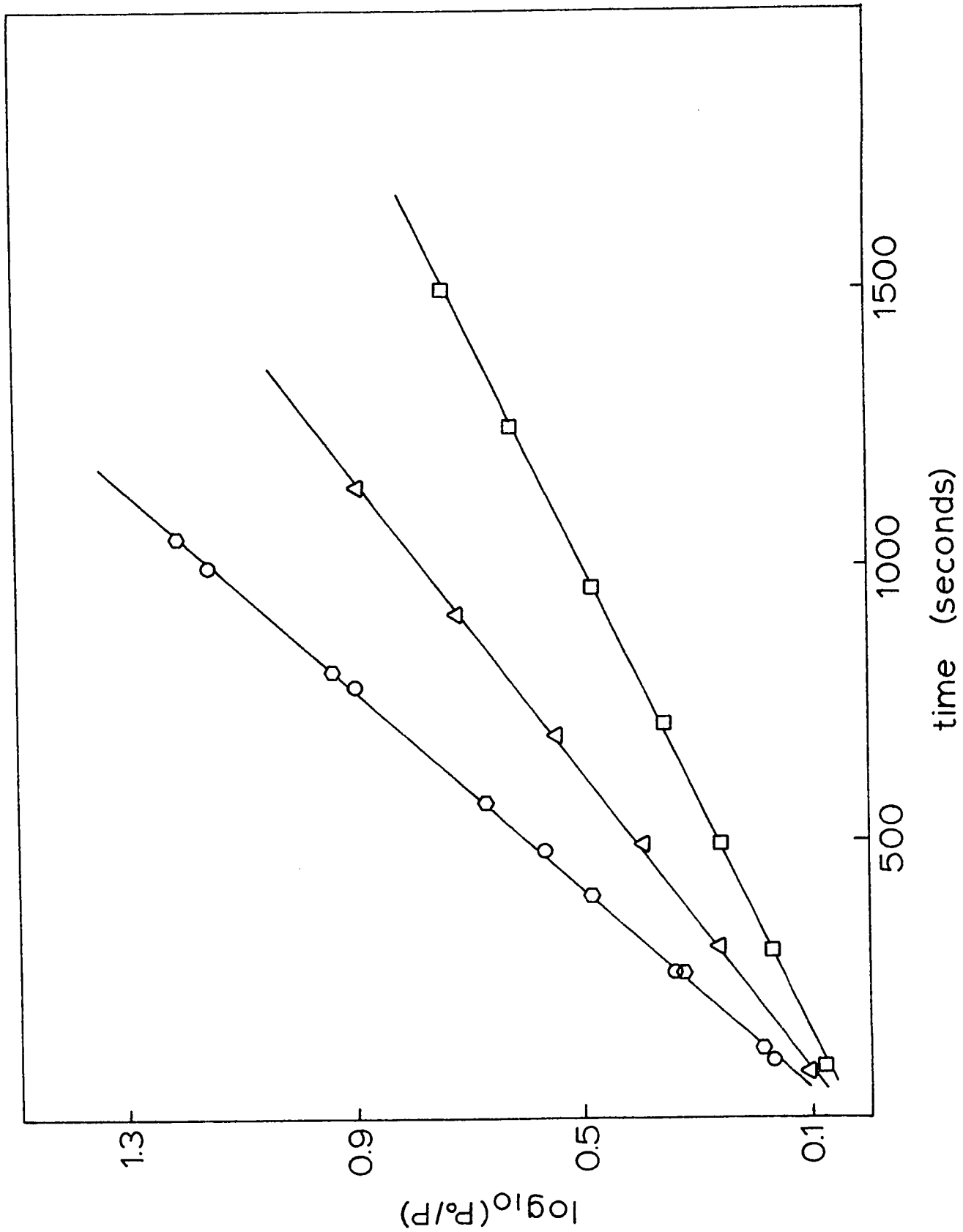
1.3
0.9
0.5
0.1
log10(P°/P)
500
1000
1500
time (seconds)

FIGURE IV - 23

Arrhenius Plot of Rate Data for First Order

Disappearance of 2-Chloropropane

on Titanium Film

Previously Reacted With 1-Chloro-2-methylpropane

(immediately following)

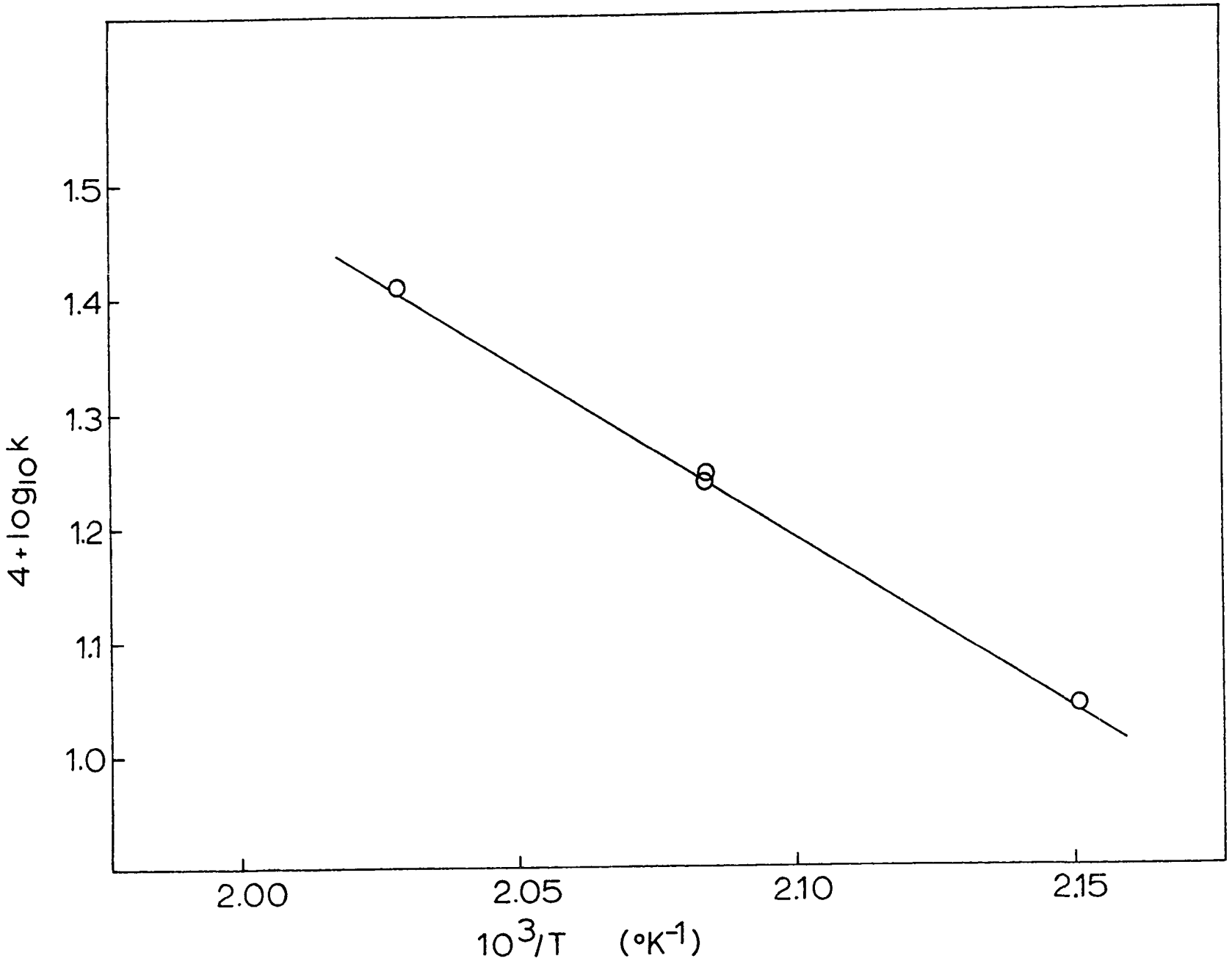
1.5
1.4
1.3
1.2
1.1
1.0
4 + log10 k
2.00
2.05
2.10
2.15
10^3/T (°K^-1)

FIGURE IV - 24

Disappearance of 2-Chloropropane

on Titanium Film

Previously Reacted With

1-Chloro-2-methylpropane

Plotted as a First Order Reaction

(after 1 Torr 2-Chloropropane)

for $P_o = 1 \times 10^{-2}$ Torr

○ - 169°C

□ - 184°C

○ - 201°C

△ - 205°C

▽ - 220°C

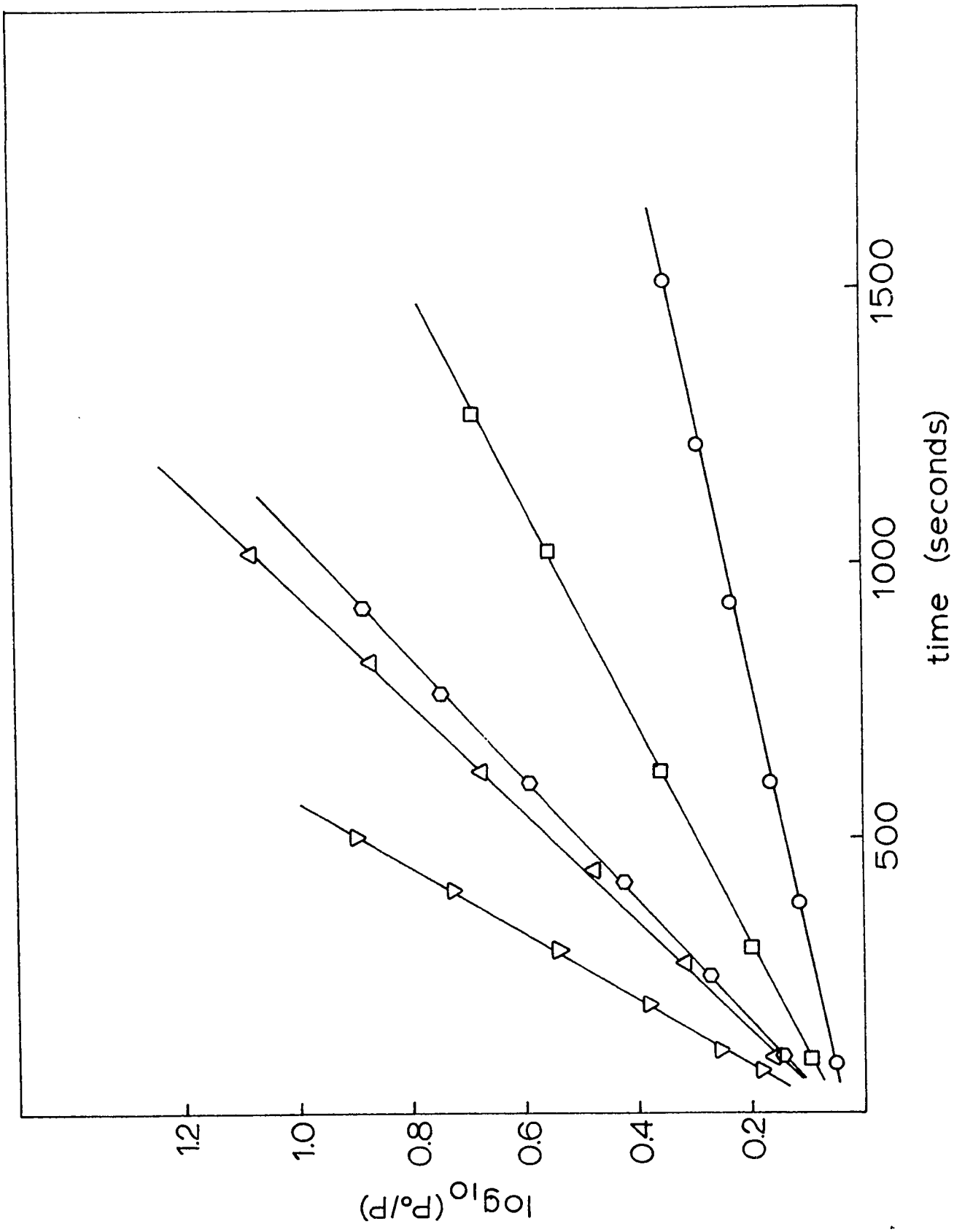
1.2
1.0
0.8
0.6
0.4
0.2
log10 (P°/P)
500
1000
1500
time (seconds)

FIGURE IV - 25

Arrhenius Plot of Rate Data for First Order

Disappearance of 2-Chloropropane

on Titanium Film

Previously Reacted With 1-Chloro-2-methylpropane

(after 1 Torr 2-Chloropropane)

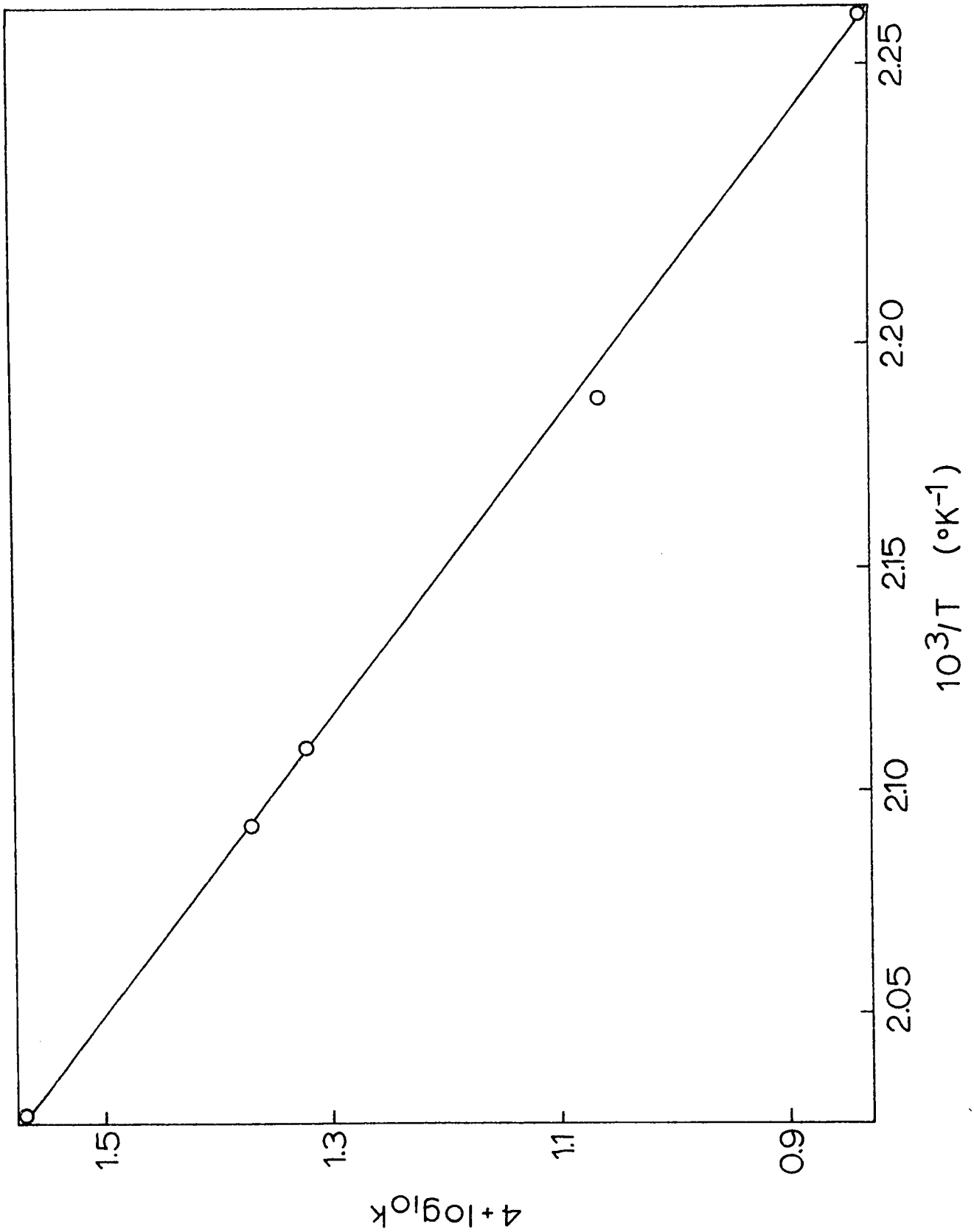
4 + log10k
1.5
1.3
1.1
0.9
2.05
2.10
2.15
2.20
2.25
10^3/T (°K^-1)

IV-B-5) The Effect of Reactant Pressure on Film Activity

The effect of very high reactant pressure on film activity was studied for both catalytic and non-catalytic reactions.

The non-catalytic reaction of 1-chloropropane with titanium was studied between 10^{-2} and 10^{-1} Torr to determine its concentration order (Section IV-B-1). Throughout this range the rate constant was independent of pressure. On the same film, a reaction at 1.34 Torr was followed to 30% completion. As shown in Table IV-2 , its half order rate constant was about 50% of that at 1.35×10^{-2} Torr.

TABLE IV-2

The Effect of High Reactant Pressure on Film Activity for 1-Chloropropane on Titanium

run	$P_o \times 10^2$ (Torr)	rate constant $\times 10^4$ (Torr$^{\frac{1}{2}}$-sec^{-1})
1	1.34	1.60
2	134.0	0.75
3	1.33	0.75
4	1.28	1.18

Subsequent runs (3 and 4) also proceeded slowly although overnight pumping at 10^{-8} Torr caused the film to regain some of its activity (run 4). Both before and after the reaction at 1.34 Torr, 1-chloropropane disappeared according to a half order rate law

through 95% reaction (Figure IV-5).

The catalytic reaction of 2-chloropropane was studied in similar fashion on chromium. In this case, the rate constant was the same both before and after the high pressure reaction. (Table IV-3). The rate constant at 1.3 Torr was much smaller than those at about 5.10^{-2} Torr.

TABLE IV-3

The Effect of High Reactant Pressure on Film Activity for 2-Chloropropane on Chromium

run	$P_o x10^2$ (Torr)	rate constant $x10^4$ (sec^{-1})
1	5.0	3.47
2	130.0	0.60
3	4.7	3.43

IV-C) Discussion

IV-C-1) Preliminary Comments

On each metal film, a series of separate haloalkane decompositions was conducted. Both rate and products sometimes changed noticably between successive reactions due to irreversible alterations in the properties of the surface. For example, during initial reactions, both the amount of paraffin in the products and the rate decreased while the transition between non-catalytic and catalytic behavior was accompanied by the appearance of hydrogen chloride and an increase in rate. Variation in the products most probably indicated changes in reaction mechanism. During these transition periods, it was impossible to make meaningful kinetic measurements.

However, on halided surfaces, behavior often settled into a specific pattern characterized, by constant rate and consistent products throughout many reactions. At this stage, reaction order and Arrhenius parameters were determined. As described in Chapter III, rate decreased continually during initial low temperature reactions. Therefore, only high temperature reactions on previously halided surfaces for which the kinetics can be meaningfully interpreted will be discussed below.

On these surfaces, two patterns of reactivity were detected and have been designated according

to their products:

1) non-catalytic where the surface retained all the chloride releasing olefin and either paraffin or hydrogen into the gas phase and

2) catalytic where the surface performed as a true catalyst releasing equimolar quantities of olefin and hydrogen chloride while not entering into the overall stoichiometry. With the former scheme, haloalkane disappeared according to a half order rate law whereas the latter was approximately first order.

Before reacting catalytically, each film passed through a period during which non-catalytic dehydrohalogenation prevailed. Thus, catalytic behavior was characterized by more extensively halided surfaces. However, some haloalkanes continued to dehydrohalogenate non-catalytically irrespective of the extent to which the surface was reacted.

With titanium surfaces, it was found that branched chloroalkanes eventually reacted catalytically whereas their straight chain counterparts retained non-catalytic behavior (Summers, 1970). To study both patterns of reactivity on surfaces of the other first row transition metals, typical chloroalkanes were selected from each catagory, 1-chloropropane for the non-catalytic case and 1-chloro-2-methylpropane for the catalytic.

Based on the following observations,

it seems most probable that the mechanism for non-catalytic reaction was the same on each metal while a different yet common mechanism prevailed in catalytic cases.

1) That the mechanisms for the two patterns of reaction were different is strongly suggested by their markedly different products, kinetics and Arrhenius activation parameters. While activation parameters varied markedly between the two classes, within each class they were similar both among several haloalkanes on titanium (Summers, 1970) and among the different metals.

2) For a given chloroalkane, a similar sequence of high temperature reactions were observed on each metal. Whereas 1-chloro-2-methylpropane proceeded rapidly through a non-catalytic period followed by consistent catalytic behavior, 1-chloropropane would not react catalytically.

3) For every metal, the products were similar within each class of reaction. Catalytic reactions consistently generated equimolar mixtures of olefin and hydrogen chloride. Although non-catalytic reactions on all the metals except titanium generated olefin and hydrogen while titanium produced olefin and paraffin, this need not indicate significantly differing mechanisms (Section III-C-3). Compared with the other metals, hydrogen is extremely soluble in titanium (Appendix D). Thus, hydrogen gas was readily released along with olefin by all the metals except titanium. The latter retained it

facilitating hydrogenation of surface alkyls with subsequent release of paraffin.

4) The kinetics were also the same for all the reactions within each class. On all the metals, catalytic reactions proceeded approximately according to a first order rate law. In each case where it could be determined, non-catalytic reactions followed a half order rate law. The irreversible decrease in surface activity observed with many of the metals during non-catalytic reactions was due to variations in metal-halide lattice energies without bearing directly on the mechanism (Section III-C-3).

5) Halide exchange experiments on several metals indicated that neither the catalytic, nor the non-catalytic reactions involved a reversible dissociative adsorption step. Although this is not meant to suggest that they, therefore, proceeded by the same mechanism, it does indicate that titanium was not mechanistically unique, reacting in the absence of a dissociative equilibrium while the other metals caused reversible dissociation. This possibility had been suggested by Anderson (1971b).

As described in detail in Section I-G, both patterns of reactivity were explained by Summers (1970) in terms of rapid dissociative equilibria followed by rearrangement and desorption or diffusion into the bulk of

the resulting surface groups. In both cases, rate control was ascribed to the regeneration of active surface sites. For non-catalytic reactions, this included rearrangement and desorption of hydrocarbon fragments with diffusion of surface chloride into the bulk metal. Catalytic reactions, on the other hand, involved only rearrangement and desorption of surface halide and surface alkyl groups without any diffusion into the bulk.

However, in a later publication, Summers and Harrod (1972) described the catalytic reaction in terms of a surface assisted internal rearrangement of haloalkanes similar to the E_i mechanism suggested for gas phase olefin forming reactions (Banthorpe, 1963). Each of these mechanisms would conform to the experimentally determined kinetics.

IV-C-2) Non-Catalytic Mechanisms

Since the proposed mechanism for non-catalytic reactions was experimentally tested only by comparison with time order kinetics (Harrod and Summers, 1971), detailed examination of this and several other alternatives was undertaken. The systems which displayed non-catalytic behavior and half order kinetics were chloroethane, 1-chloropropane, 1-bromopropane and 1-iodopropane on titanium and 1-chloropropane on vanadium and manganese.

Although hydrogen rather than paraffin

was evolved during the reactions on vanadium and manganese, this could be readily incorporated into the previously suggested mechanism without altering the results. Reactions of 1-chloropropane with the remaining first row transition metals exhibited surface deactivation and their reaction order was not determined. The disappearance of 1-chloropropane on titanium conformed very closely to a half order rate law (Figures IV-1 and IV-5). Most of the other reactions were similar, exhibiting almost no curvature in half order plots.

To determine whether autocatalysis or poisoning by products could have contributed to the observed time order, the dehydrochlorination of 1-chloropropane on titanium was studied in the presence of excess propene, the major gas phase product. The rate remained unaltered.

It has been established that surface activity gradually decreased during all non-catalytic reactions including those on titanium. However, it could not have altered the rate expression since in each case where reaction order was determined, it was either negligible or accounted for. Variations in the rate of surface deactivation have been attributed to differences in metal-halide lattice energies (Section III-C) and would alter only the surface activity and not the mechanism of surface alkyl decomposition.

The concentration order (true order) for non-catalytic reactions was determined using the dehydro-

chlorination of 1-chloropropane on titanium as an example. This measured the order in the absence of product and was again strictly one half. The time order for each individual reaction was one half and the rate constants were independent of initial 1-chloropropane pressure.

During non-catalytic dehydrohalogenations, it is clear that haloalkane disappeared according to a strict half order rate law. The usual explanation for reactions which are half order in a reactant, as proposed by Harrod and Summers (1971), is that the reactant rapidly and reversibly dissociated followed by generation of products in the rate controlling step by a first order decomposition of the intermediates.

To test the proposed reversible dissociation, halogen exchange was attempted on titanium and chromium surfaces. This involved monitoring the combined reaction of 1-bromopropane and 1-chloropropane-1-d_1 to detect haloalkanes with interchanged halides. As described in detail in Section IV-B-3, even under optimum conditions no exchange occurred.

A possible interpretation of these results is that reversible dissociation occurred without exchange of halogens. Several experimental precautions were taken to avoid this:

1) using haloalkanes differing only by one deuterium atom so that no thermodynamic barrier to exchange could have

existed,

2) using haloalkanes known to react non-catalytically for which characteristic and easily detected changes in peak height ratios could monitor halo-exchange even in the presence of dehydrohalogenation and

3) reacting both haloalkanes simultaneously to assure that all surface species would be present concurrently.

Dissociation without interaction between fragments from adjacent dissociated molecules must be discounted as an explanation since that situation would not represent a true equilibrium. Equilibration requires that interaction occur between all species present in the equilibrium equation. These concentrations must be interdependent such that variations in one induce changes in the others. However, if chloroalkane was specifically adsorbed only on certain sites and bromoalkane only on others with no interaction between the two, no halo-exchange would occur. Nevertheless, facile interchange among fragments on each type of site would lead to complete reversibility during reaction of a single haloalkane since only one type of site would exist over the entire surface.

Formation of surface halide domains, each composed solely of a single halide, could account for this behavior, with minimal interchange between them yet facile exchange within. During simultaneous reaction of chloro and

bromoalkanes halo-exchange would not have occurred. However, during the reaction of a single haloalkane, isolated domains would not have been formed since only one halide would have occuppied the entire surface and a true dissociative equilibrium could have occurred.

Low energy electron diffraction (LEED) studies have detected domains for gases chemisorbed on metal surfaces. Areas of geometrically different orientations were detected for the adsorption of carbon monoxide on palladium (Park, 1968). Other less clear cut examples for the adsorption of oxygen and nitrogen on specific transition metal crystal faces are reviewed by May (1970). The theoretical aspects of domain formation have also been considered (Lander, 1965; Park, 1969).

With domains detected even during the adsorption of single gases on specific crystal faces, their formation during mixed gas adsorption on polycrystalline surfaces seems a definite possibility. No studies of domain formation during mixed gas adsorption have been reported.

Halo-exchange would also be lacking, even in the absence of domain formation, if different and mutually exclusive sites were required for reactions of chloroalkanes and bromoalkanes. Studies of surface site specificity suggest that this type of behavior could have occurred (Section IV-B-4). These investigations demonstrated that the surface halide layer

formed during the reaction of a given haloalkane acted as a specific catalyst for that particular reaction. Other haloalkanes would then react with difficulty on this surface with the course of reaction being partially determined by the previously formed sites.

This reasoning could possibly be extended to include sites formed by chlorides and bromides. Hence, during the reaction of a mixed sample, chloroalkane would react on sites previously formed by chloroalkanes and likewise for bromoalkanes. No interchange between chloro and bromo sites and consequently no halo-exchange would occur. Reaction of a single haloalkane would occur. Reaction of a single haloalkane could still involve completely reversible dissociation since only one type of site would exist.

Several experiments designed to investigate the adsorption of haloalkanes on transition metal surfaces have been performed (Anderson, 1968; Cockelbergs, 1959; Morrison and Krieger, 1968). These suggest that reversible dissociation may have occurred for iodoalkanes on iron, nickel, palladium, rhodium, and iridium and for chloromethane on tungsten and molybdenum but not for chloromethane on titanium.

Assuming a rapid dissociative equilibrium, reactions which generated olefin and hydrogen according to a half order rate law could be explained by the same mechanism proposed by Harrod and Summers (1971). For

the extreme case of no hydrogen retention, the overall stoichiometry was

$$2RCH_2CH_2X \longrightarrow 2RCH{=}CH_2 + H_2 + 2X_{lattice}. \qquad \text{IV-4}$$

This overall reaction could be explained by the following sequence of steps, where R is an alkyl group, X a halogen * a surface site and $X_{lattice}$ refers to halogen which has left a surface site and diffused into the bulk phase.

$$RCH_2CH_2X + 2* \underset{k_{-1}}{\overset{k_1}{\rightleftharpoons}} RCH2CH2* + X* \qquad \text{IV-5}$$

$$RCH_2CH_2* \xrightarrow{k_2} RCH{=}CH_2 + H* \qquad \text{IV-6}$$

$$X* \xrightarrow{k_3} X_{lattice} + * \qquad \text{IV-7}$$

$$2H* \xrightarrow{k_4} H_2 + 2* \qquad \text{IV-8}$$

Assuming that rate was controlled by the concerted appearance of surface sites and that hydrogen was adsorbed competitively with haloalkane gives

$$\frac{-d[RCH_2CH_2X]}{dt} = \frac{1}{2}\frac{d[*]}{dt} = \frac{1}{2}\left(k_3[X*] + k_4[H*]^2\right). \qquad \text{IV-9}$$

Further, assuming a rapid dissociative equilibrium, steady state hydrogen concentration and equivalent rates of surface site regeneration by gas evolution and halide diffusion gives Equations IV-10 through IV-12 respectively.

$$k_1[RCH_2CH_2X][*]^2 = k_{-1}[RCH_2CH_2*][X*] \qquad \text{IV-10}$$

$$k_2[RCH_2CH_2*] = k_4[H*]^2 \qquad \text{IV-11}$$

$$k_4[H*]^2 = k_3[X*] \qquad \text{IV-12}$$

Substituting Equations IV-11 and IV-12 into Equation IV-9 gives

$$\frac{-d[RCH_2CH_2X]}{dt} = k_2[RCH_2CH_2*]. \qquad \text{IV-13}$$

By substituting Equations IV-11 and IV-12 into Equation IV-10

$$[RCH_2CH_2*] = \left(\frac{k_1k_3[*]^2}{k_{-1}k_2}\right)^{\frac{1}{2}} [RCH_2CH_2X]^{\frac{1}{2}}. \qquad \text{IV-14}$$

Therefore,

$$\frac{-d[RCH_2CH_2X]}{dt} = \left(\frac{k_1k_2k_3}{k_{-1}}\right)^{\frac{1}{2}} [*][RCH_2CH_2X]^{\frac{1}{2}} \qquad \text{IV-15}$$

For $k_{-1} >> k_1$, $[*]$ would remain essentially constant.

The same expression was derived by Summers (1970) to explain the reaction to olefin with both hydrogen and halide retained by the surface. For reaction to an equimolar mixture of paraffin and olefin where all the hydrogen left the surface as hydrocarbon, a similar expression differing only by a factor of two was derived. Although the above expression and the two of Summers were all based on the

steady state hydride hypothesis, Summers assumed that hydrogen adsorption was not competitive with that of haloalkane. The above derivation, on the other hand, assumed that surface hydrogen was in a steady state while permitting competitive adsorption. Nevertheless, assuming non-competitive hydrogen adsorption gave the same final expression.

This facilitated complete analysis without hypothesizing steady state surface hydrogen. As long as the sites of hydrogen adsorption (S) did not become saturated, rate control could be ascribed to the regeneration of sites for haloalkane adsorption (*), and the following sequence of reactions would explain the kinetics.

$$RCH_2CH_2X \underset{k_{-1}}{\overset{k_1}{\rightleftharpoons}} RCH_2CH_2* + X* \qquad \text{IV-16}$$

$$RCH_2CH_2* + S \xrightarrow{k_2} RCH{=}CH_2 + HS \qquad \text{IV-17}$$

$$X* \xrightarrow{k_3} X_{lattice} + * \qquad \text{IV-18}$$

$$2HS \xrightarrow{k_4} H_2 + 2S \qquad \text{IV-19}$$

The rate would be

$$\frac{-d[RCH_2CH_2X]}{dt} = \frac{1}{2}\frac{d[*]}{dt} = \frac{1}{2}\left(k_2[RCH_2CH_2*] + k_3[X*]\right). \qquad \text{IV-20}$$

The reversible dissociation and the mass balance of alkyl and halide give Equations IV-21

and IV-22 respectively.

$$k_1[RCH_2CH_2*][*]^2 = k_{-1}[RCH_2CH_2*][X*] \qquad \text{IV-21}$$

$$k_2[RCH_2CH_2*] = k_3[X*] \qquad \text{IV-22}$$

Substituting Equation IV-22 into both IV-20 and IV-21 gives

$$\frac{-d[RCH_2CH_2X]}{dt} = k_2[RCH_2CH_2*] \qquad \text{IV-23}$$

and

$$[RCH_2CH_2*] = \left(\frac{k_1 k_3}{k_{-1} k_2}\right)^{\frac{1}{2}} [*][RCH_2CH_2X]^{\frac{1}{2}} \qquad \text{IV-24}$$

Therefore,

$$\frac{-d[RCH_2CH_2X]}{dt} = \left(\frac{k_1 k_2 k_3}{k_{-1}}\right)^{\frac{1}{2}} [*][RCH_2CH_2X]^{\frac{1}{2}} \qquad \text{IV-25}$$

Considering the reactions of 1-chloropropane with vanadium and manganese which followed half order rate laws yet experienced hydrogen buildup on the surface, the latter interpretation of the kinetics would seem more realistic. During these reactions, some hydrogen was retained on the surface while some was immediately released into the gas phase. Hydrogen continued to appear even after dehydrochlorination was complete.

Thus, hydrogen evolution was independent of the generation of hydrocarbon products strongly suggesting independent reaction pathways. Based on the behavior of these two reactions, non-competitive adsorption of hydrogen is strongly

suggested if a rapid reversible equilibrium, indeed, did exist.

The other possibility, that there was no rapid dissociative equilibrium preceeding the rate controlling steps, must also be considered in detail since there is no definite evidence that halo-exchange should not accompany reversible dissociation. However, in the absence of a dissociative equilibrium half order kinetics are difficult to interpret. Autocatalysis or poisoning either by product or reactant has been ruled out by determination of the concentration order and studies of the effect of excess propene.

For irreversible non-dissociative haloalkane adsorption, the overall reaction to olefin and hydrogen could be represented by the sequence of reactions shown in Equations IV-26 to IV-28. Hydrogen adsorption is assumed not to occur in competition with that of haloalkane, 'S' representing a site for the former and '*' a site for the latter.

$$RCH_2CH_2X + * \xrightarrow{k_1'} RCH_2CH_2^{*}X \qquad \text{IV-26}$$

$$RCH_2CH_2^{*}X + S \xrightarrow{k_2'} RCH{=}CH_2 + X_{lattice} + HS + * \qquad \text{IV-27}$$

$$2HS \xrightarrow{k_4'} H_2 + 2S \qquad \text{IV-28}$$

The comparative sequence for irreversible dissociative adsorption is shown in Equations IV-29 to IV-32.

$$RCH_2CH_2X + 2* \xrightarrow{k_1''} RCH_2CH_2* + X* \qquad \text{IV-29}$$

$$RCH_2CH_2* + S \xrightarrow{k_2''} RCH{=}CH_2 + * + HS \qquad \text{IV-30}$$

$$X* \xrightarrow{k_3''} X_{lattice} + * \qquad \text{IV-31}$$

$$2HS \xrightarrow{k_4''} H_2 + 2S \qquad \text{IV-32}$$

For either scheme, adsorption could have occurred much faster, much slower, or at about the same rate as subsequent steps. Were it much faster, the reaction would have followed a zero order rate law in haloalkane. If much slower, haloalkane would have disappeared according to a first order rate law. However, if each step occurred at approximately the same rate, a complex expression would arise which, depending upon the reactant concentration and relative rates, would vary between zero and first order.

For example, the following rate law would result for the sequence with the non-dissociative adsorption process. The rate of haloalkane disappearance could again be ascribed to the rate of regeneration of surface sites.

$$\frac{-d[RCH_2CH_2X]}{dt} = \frac{d[*]}{dt} = k_2'[RCH_2\overset{*}{C}H_2X] \qquad \text{IV-33}$$

Assuming a steady state for the surface intermediate

$$k_2'[RCH_2\overset{*}{C}H_2X] = k_1'[*][RCH_2CH_2X]. \qquad \text{IV-34}$$

Whereas with rapid reversible adsorption, (*) could be assumed to remain constant, this is not justified for irreversible adsorption. However, the sum of the occupied and unoccupied surface sites would remain the same.

$$[*]_o = [*] + [RCH_2CH_2\overset{*}{X}] \qquad \text{IV-35}$$

Substituting Equation IV-34 into IV-35 gives

$$[*] = [*]_o/(1 + \frac{k_1'}{k_2'}[RCH_2CH_2X]). \qquad \text{IV-36}$$

Further, substituting Equation IV-36 into IV-34 and the resulting expression into IV-33 gives the rate law as

$$\frac{-d[RCH_2CH_2X]}{dt} = \frac{k_1'[*]_o[RCH_2CH_2X]}{1 + (k_1'/k_2')[RCH_2CH_2X]}. \qquad \text{IV-37}$$

Equation IV-37 reduces to zero order for $(k_1'/k_2')[RCH_2CH_2X] \gg 1$ and to first order for $(k_1'/k_2')[RCH_2CH_2X] \ll 1$. Between these extremes, the expression remains complex with the order dependent upon haloalkane pressure. The reaction would be half order only when $1 + (k_1'/k_2')[RCH_2CH_2X] = [RCH_2CH_2X]^{\frac{1}{2}}$ which would occur only when

$$[RCH_2CH_2X] = \frac{k_2' \pm \sqrt{k_2'^2 - 4k_1'k_2'}}{2k_1'}.$$

Integrating Equation IV-37 gives

$$\log_{10}\frac{[RCH_2CH_2X]_o}{[RCH_2CH_2X]} + \frac{k_1'}{2.303k_2'}([RCH_2CH_2X]_o - [RCH_2CH_2X]) = \frac{k_1't}{2.303} \qquad \text{IV-38}$$

Plotting the expression on the left against time should generate a straight line if this mechanism is truely representative of the reaction. The log term normally results from a simple first order rate law while the difference term is that which would result from a zero rate law. However, the ratio k_1/k_2 is unknown. Nevertheless, some of the properties of this expression can be revealed by assuming various ratios.

To examine this, the data used to generate the upper line in Figure IV-5 (p.154) was used. This was for a reaction of 1-chloropropane on titanium at 10^{-2} Torr and 221°C. Followed through 97% reaction, 1-chloropropane disappeared according to a half order rate law.

For $k_1 \leq k_2$, the log term predominates (first order) and the plot curves drastically concave upward. At the other extreme, for $k_1 \approx 10^5 k_2$, the difference term predominates (zero order) and the plot curves drastically concave downward. For intermediate values, the plot becomes progressively less curved until, as shown in Figure IV-26, it was essentially straight between $k_1 = 150k_2$ and $k_1 = 250k_2$. Thus, at 10^{-2} Torr, the plot of this expression appeared half order for less than a two fold change in the k_1/k_2 ratio.

For a given set of reaction conditions, this mechanism could be consistent with a half order kinetics. However, half order reactions were observed: 1) for several

FIGURE IV - 26

Data Plotted in

Figure IV-5 Plotted

According to the Rate Law

Derived for Irreversible

Adsorption

k_1/k_2

△ - 100

□ - 150

○ - 200

⬡ - 250

▽ - 300

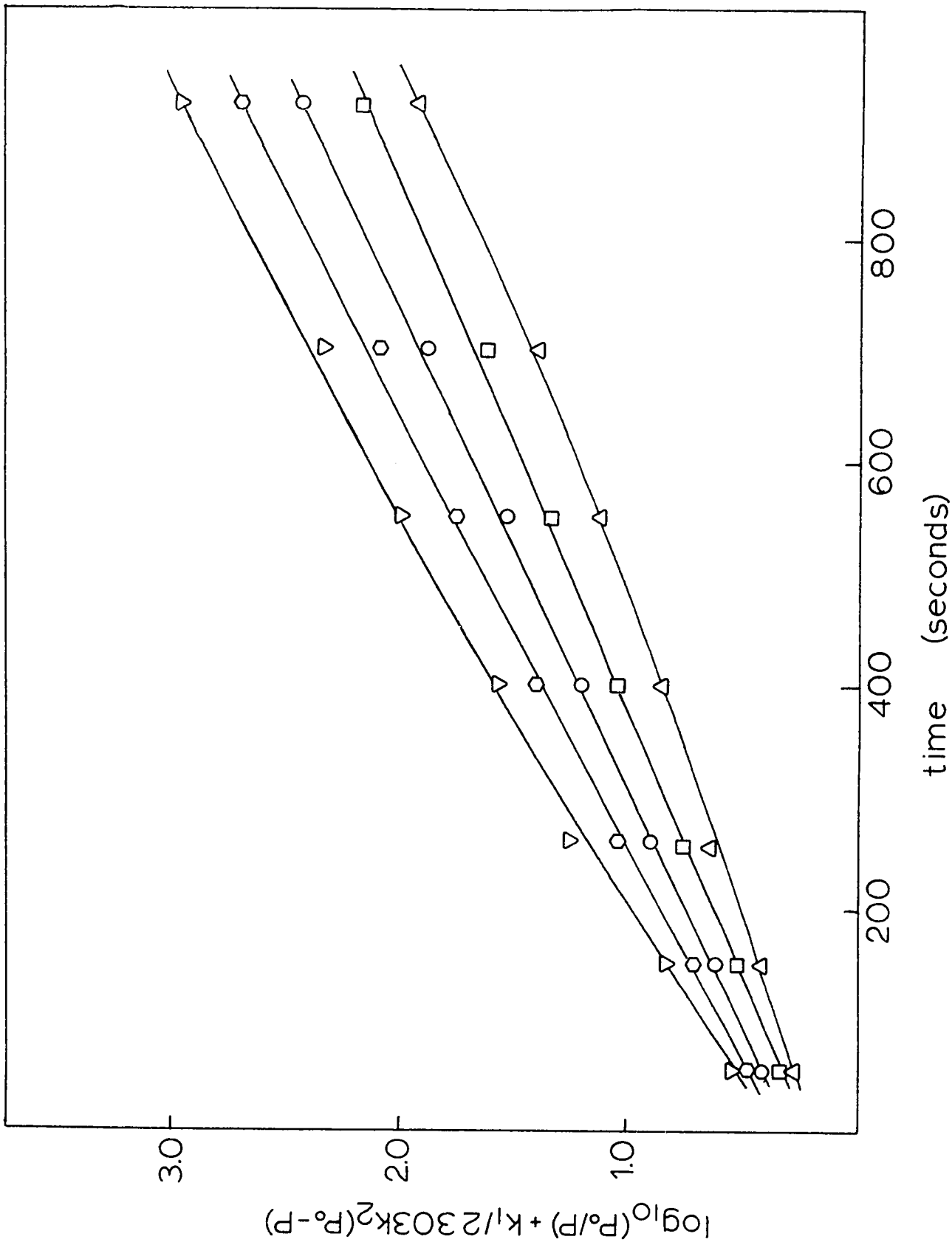
3.0
2.0
1.0
200
400
600
800
time (seconds)
log10(Po/P) + k1/2303k2(Po-P)

haloalkanes, 2) on different metals, 3) at various temperatures, and 4) at various initial reactant pressures.

It is not impossible that for various haloalkanes and on different metals the kinetics could have appeared half order; however, it would span a large variation in activation energies and necessitate fortuitous variations in k_1 and k_2 to maintain the ratio roughly constant. In fact, irreversible adsorption has already been proposed for the first order reaction of 1-fluoropropane with titanium (Harrod and Summers, 1971). For the ratio of rate constants to have remained constant with temperature would require that the activation energies for both steps be the same, again a requirement which is not entirely unreasonable.

However, for the expression to have remained unaltered by changes in the initial reactant pressure at a given temperature with a given combination of metal and haloalkane seems highly unlikely. A change in initial reactant pressure would not alter the log term; however, the difference term is directly proportional to initial reactant pressure. To maintain the two in the same relative proprotions, k_1/k_2 would have to vary inversely with initial reactant pressure.

Were the kinetics interpreted in terms of any irreversible first step followed by decomposition of the resulting surface species at about the same rate, there

would always be a dependence of reaction order on reactant pressure. In view of the large number of adventitiously coinciding factors required to have a mechanism of this type generate the observed kinetics, it seems highly unlikely that it could be a plausible explanation of the reaction sequence.

Another explanation of half order kinetics in the absence of a dissociative pre-equilibrium was presented by Halsey (1949). As described in Section I-I, this was based on the concept of heterogeneous surface structures where both the kinetics and thermodynamic properties could vary among different parts of the same surface. Evaporated metal films undoubtedly fall into this catagory.

Halsey's treatment purported to be capable of explaining half order kinetics according to a reaction scheme comprising unimolecular irreversible adsorption, reaction and desorption. A basic tenet of his derivation was that reactant and product be competitively adsorbed. However, it has been shown for the reaction of 1-chloropropane that excess propene did not reduce dehydrochlorination rate and could not, therefore, have been competitively adsorbed. Additional assumptions within the theory make it questionable on general grounds, but the above mentioned requirement of competitive adsorption make it definitely inapplicable in the present context.

In summary, non-catalytic reactions

have been shown to proceed by half order kinetics without any autocatalytic or poisoning effects. Halo-exchange studies suggest these dehydrochlorinations proceed in the absence of a rapid dissociative equilibrium. However, these experiments are not absolutely conclusive and in the absence of a dissociative equilibrium it is very difficult to interpret half order kinetics. Nevertheless, the inability to devise a thoroughly convincing mechanism is by no means evidence that reversible dissociation occurred.

IV-C-3) Catalytic Mechanisms

Catalytic behavior has been observed and thoroughly studied for the reactions of 2-chloropropane, 1-chloro-2-methylpropane, 2-chloro-2-methylpropane and 1-chloro-2,2-dimethylpropane on titanium and 1-chloro-2-methylpropane on the first row transition metals from vanadium through nickel. Detected but less thoroughly investigated were catalytic reactions of 2-chloropropane on chromium and 1-bromo-2-methylpropane on titanium.

Each of these reactions generated equimolar mixtures of olefin and hydrogen halide according to a first order rate law as determined by time order plots. However, the concentration order (for the reaction of 1-chloro-2-methylpropane on chromium) was only about 0.75. Plotting a given set of data as both first and 0.75 order (Figure IV-9) revealed that it would generally be possible to distinguish

between these two using time order plots. However, within experimental error, the concentration order could have been as high as 0.85 which would have been virtually impossible to distinguish from first order by these methods.

It has been observed during both the present studies and the work of Summers (1970) that the first order rate constant decreased with increasing initial reactant pressure during catalytic reactions. Decreasing heat of adsorption with increasing reactant pressure could account for this behavior. With surface coverage, θ, proportional to reactant pressure, heat of adsorption would decrease with increasing reactant pressure. This has been explained as either increased repulsive interaction between adsorbed molecules at higher coverage or utilization of less favorable adsorption sites as optimum sites become occupied at higher coverage (Anderson, 1971b).

In terms of the Arrhenius activation parameters, the rate constant could be expressed as

$$k = A \exp(-E_a'/RT) \qquad \text{IV-39}$$

where E_a' is the apparent activation energy. For heterogeneous reactions

$$E_a' = E_a - \Delta H_{ads} \qquad \text{IV-40}$$

where E_a is the true activation energy and ΔH_{ads} is the heat of adsorption.

For the reaction of 1-chloro-2-methylpropane on chromium, the rate constant varied with initial reactant pressure according to an expression of the type

$$k = A\text{-}BP \qquad \text{IV-41}$$

Substituting Equation IV-40 into IV-39 gives

$$k = A\exp[(-E_a + \Delta H_{ads})/RT] \qquad \text{IV-42}$$

Thus

$$\log_e k = \log_e A - E_a/RT + \Delta H_{ads}/RT \qquad \text{IV-43}$$

Since A and E_a are independent of reactant pressure, at a given temperature

$$\log_e k = C_1 \Delta H_{ads} + C_2 \qquad \text{IV-44}$$

Thus

$$\Delta H_{ads} = C_o + \log (A'\text{-}BP) \qquad \text{IV-45}$$

The coincident effects of a first order surface reaction and a decrease in heat of adsorption with an increase in reactant pressure would give an overall order less than one as has been found for the concentration order. The extent of the decrease in order would be governed by the magnitude of the change in ΔH_{ads} with surface coverage. However, with no knowledge of the surface area or surface coverage, no relationship between θ and P resulting in an

isotherm can be established.

Therefore, the most likely interpretation of the kinetics is that the order in 1-chloro-2-methylpropane was slightly less than one due to the changes in the heat of adsorption but this could not be detected in time order plots since the decrease was not large enough. However, the surface assisted decomposition of haloalkane was almost certainly a first order process.

In studies similar to those with non-catalytic reactions, no halo-exchange was detected during catalytic dehydrohalogenations of 1-halo-2-methylpropanes on titanium and nickel. Naturally, these experiments are open to the same criticisms previously described for non-catalytic reactions. For example, it is not known whether a bias for adsorption on sites formed by identical molecules occurred. This could account for a lack of exchange even in the presence of reversible dissociation. Because of the many similarities among the various catalytic reactions, it seems reasonable to generalize these results to all catalytic behavior.

In the presence of exchange, the mechanism proposed by Summers (1970) could account for the kinetics. However, in contrast to the non-catalytic case, there is no difficulty explaining first order kinetics in terms of non-dissociative adsorption. In fact, generation of olefin

and hydrogen halide according to a first order rate law has been detected extensively for homogeneous dehydrohalogenations (Maccoll, 1964).

As described previously in Section I-D, homogeneous dehydrohalogenations of haloalkanes proceed via a molecular mechanism with variations in rate between reactants attributable primarily to changes in activation energy. The pre-exponential factor remained essentially constant at about 10^{13} sec^{-1}, the value expected from simple collision theory calculations.

Comparing substituent effects and bond dissociation energies between pyrolytic dehydrohalogenations and those in solution has lead Maccoll to suggest a 'quasi-heterolytic" transition state involving considerable charge separation in the carbon-halogen bond. The evidence seems to indicate that the primary step in the reaction involves C-X bond weakening without concurrent C-H bond weakening and the absence of a significant double bond character in the transition state.

The present reactions, catalyzed by transition metals surfaces, could not have been proceeding by a free radical mechanism since known free radical inhibitors such as propene and methylpropene (Maccoll and Thomas, 1957; Jach and Hinshelwood, 1954) did not inhibit them. In the absence of dissociation, the other possibility is that the surface was facilitating the internal rearrangement postulated

to be occurring in homogeneous dehydrohalogenations. This could involve breaking down some of the symmetry restrictions which cause such high activation energies in the pyrolytic reactions (Pearson, 1970; Mango, 1967). However, since a wide variety of non-transition metals also act as catalysts (Noller, 1956,1959), the role of the metal is more complex than just providing an appropriate 'd' orbital to facilitate a symmetry allowed transition. In terms of Maccoll's quasi-heterolytic transition state, the metal surface could have been functionning as a Lewis acid, further weakening the carbon-halogen bond and making rearrangement more facile.

Catalytic reactions required more heavily halided surfaces than non-catalytic reactions, since on a given film a series of non-catalytic reactions always preceeded catalytic behavior. In addition, the weakest Lewis acid in the series, titanium, required the greatest extent of surface reaction before settling into catalytic behavior. This transition period may have marked the point where the surface became an adequately strong Lewis acid to sustain catalytic behavior. A possible formulation of the transition state is shown below.

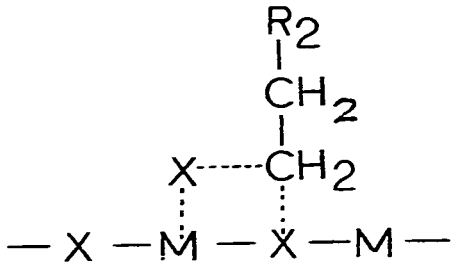

During homogeneous reactions, complete dissociation would not occur due to the high heterolytic bond dissociation energy. The extent to which the carbon-halogen bond was dissociated during catalytic rearrangement, however, cannot be estimated. In the extreme of dissociative adsorption, the kinetics would still be first order if the adsorption step was rate controlling. Nevertheless, it is postulated that reaction proceeded as it would in the gas phase with an assist from the Lewis acidic surface in weakening the carbon-halogen bond. The β-hydrogen could then combine with the halogen to complete the formation of olefin and hydrogen halide.

The principal difference between the present studies and pyrolytic dehydrohalogenations is that for the latter the frequency factors were all about 10^{13} sec^{-1} and variations in rate were dictated solely by changes in activation energy. For the former, however, increases in activation erergy were accompanied by increases in the pre-exponential such that the free energy of activation remained roughly constant.

As shown in Figure IV-27, for all the catalytic reactions studied on several metals with a variety of haloalkanes, Ea varied linearly with $\log_{10}A$. The pre-exponential factor contains a concentration term for surface sites which is probably very consistent for reactions on a given metal. In addition, among the first row transition

FIGURE IV - 27

Compensation Effects

Among Catalytic Reactions

	metal	chloroalkane	pressure (Torr) x10^2
▽-	titanium*	2-chloropropane	1
▼-	titanium*	2-chloropropane	5
△-	titanium*	2-chloropropane	25
◇-	titanium*	1-chloro-2-methylpropane	1
◎-	titanium*	1-chloro-2-methylpropane	5
■-	titanium*	2-chloro-2-methylpropane	2.8
○-	titanium*	1-chloro-2,2-dimethylpropane	1
●-	titanium*	1-chloro-2,2-dimethylpropane	2.5
⬡-	vanadium	1-chloro-2-methylpropane	1
⬢-	chromium	1-chloro-2-methylpropane	1
▲-	manganese	1-chloro-2-methylpropane	1
◆-	manganese	1-chloro-2-methylpropane	5
◎-	iron	1-chloro-2-methylpropane	1
◘-	cobalt	1-chloro-2-methylpropane	1
⚠-	nickel	1-chloro-2-methylpropane	1

* Summers (1970)

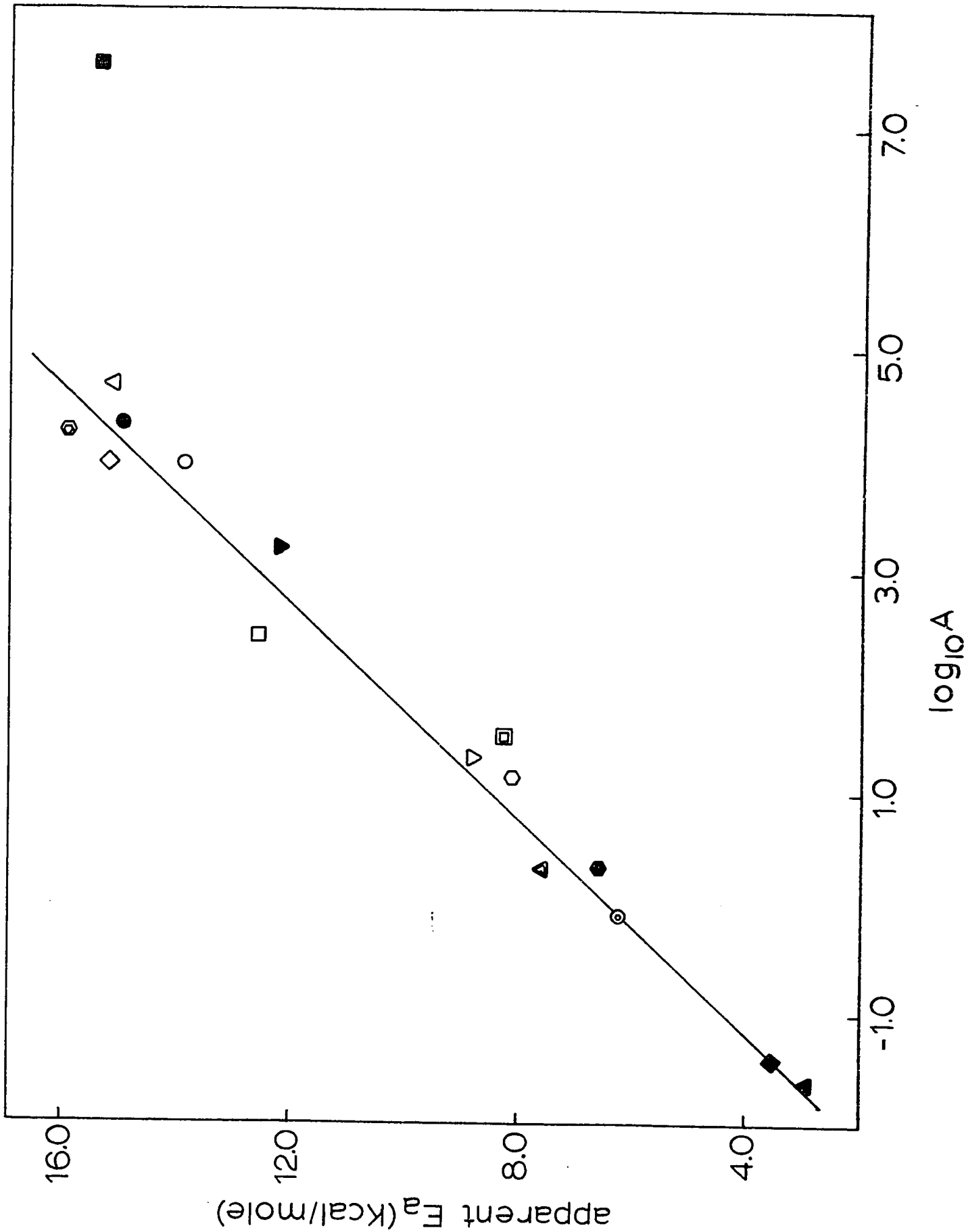
apparent E_a (Kcal/mole)
16.0
12.0
8.0
4.0
-1.0
1.0
3.0
5.0
7.0
$\log_{10} A$

metals this concentration should vary less than a factor of ten, based on known roughness factors (Anderson, 1971a). Thus, the error in log $_{10}$A due to these uncertainties would probably be less than one unit. A similar compensation effect was observed for the hydrogenation of ethylene on nickel/copper films as the alloy composition was varied (Campbell and Emmett, 1967).

As described previously, on heterogeneous surfaces, the energy and entropy of activation would vary proportionally on different patches. The same reasoning may be applied to mechanistically identical reactions on closely related surfaces such as those utilized in these studies. On a surface requiring more energy to form the transition state, the ensuing complex would be more disordered resulting in a greater increase in entropy. For surface reactions, these variations in the apparent activation energy could arise from changes in either the true activation energy for the reaction or the heat of adsorption.

IV-C-4) Factors Deciding Mechanisms

As described previously, different mechanisms likely prevailed for the non-catalytic and catalytic reactions on halided surfaces. Some haloalkanes proceeded catalytically after a non-catalytic induction period while others continued to dehydrohalogenate until the film deactivated. The principal difference between the two sets of products

was the disposition of halide, as hydrogen halide for catalytic reactions and as metal lattice halide for non-catalytic reactions.

With any reaction, when more than one set of products can arise, two factors determine the path of preference: the thermodynamic stability of the products and the reaction mechanism. With no kinetic barrier to reaction, the products will be those resulting in the greatest decrease in free energy. However, if the route to the thermodynamically most stable products requires too great a free energy of activation, then less stable products could be formed according to the kinetically more favorable mechanism.

That the thermodynamics of the catalytic reaction could have been determining the pathway can be ruled out since in the range of 10^{-2} Torr and 200°C, free energies for catalytic reaction to olefin and hydrogen halide were large negative numbers for all the chloroalkanes studied (Appendix B). In addition, the free energies followed the sequence 1-chloro-2-methylpropane < 1-chloropropane < 2-chloro-2-methylpropane < 2-chloropropane < 1-chloroethane, with the catalytic and non-catalytic reactants occurring according to no particular pattern.

For titanium and manganese, the two cases for which both classes of reaction could be studied in detail, the catalytic reaction was kinetically more favorable. Over the temperature range studied, catalytic activation energies

were lower and, although non-catalytic frequency factors were greater, catalytic reactions proceeded more rapidly and at lower temperature. This was most obvious during the transition from non-catalytic to catalytic behavior which was characterized by an increase in reaction rate.

However, since catalytic replaced non-catalytic behavior at a given temperature, this is not a simple case of kinetic displacing thermodynamic control. Instead, it seems that catalytic reaction could not proceed until the film had been halided to a certain extent. This may be ascribed to an increase in the Lewis acidity of the surface with halide deposition.

Once catalytic behavior was possible, kinetic control may have been competing with thermodynamic control. This is evidenced by the behavior of 2-chloropropane on titanium, which reversibly regained some of the properties of non-catalytic reactions at higher temperatures (Summers, 1970). Although this was not detected for any of the other catalytic reactions, it may have resulted from the inability to follow the reaction at adequately elevated temperatures.

Some haloalkanes continued to react non-catalytically even on extensively halided surfaces. Lack of catalytic behavior for chloroethane and the 1-haloalkanes has been attributed to the paucity of methyl groups available for hydrogen abstraction (Summers and Harrod, 1972). Each

haloalkane which reacted catalytically possessed at least two methyl groups as opposed to one methyl for those which did not. Within both the α -methyl and β -methyl series, catalytic frequency factors increased with the number of methyl groups. By extrapolation from the tri and dimethyl homologs, the hypothetical $\log_{10}A$ for 1-chloropropane and chloroethane should have been 0.9 and -4.9 respectively at 10^{-2} Torr. Although Summers and Harrod attributed to these small catalytic frequency factors the ability to force non-catalytic behavior, this must be reconsidered in terms of the observed compensation effect. Compensation suggests that decreased frequency factors would have been accompanied by decreased activation energies. Hence, methyl group effects are not a suitable explanation for the variations in reactivity patterns.

A further factor, seeming to determination of the reaction pathway, is the surface specificity for a given reaction (Section IV-B-4). Reactions of a haloalkane known to normally dehydrohalogenate catalytically on a surface previously reacted extensively with a non-catalytic reactant proceeded with higher activation energy than normal and generated paraffin. In addition, on a surface prepared by catalytic reactions, a non-catalytic haloalkane initially reacted very slowly according to a catalytic mechanism before assuming non-catalytic behavior and increasing in rate. This and other evidence presented in Section IV-B-4

strongly suggests that surfaces halided by reactions of a particular haloalkane were optimal catalysts for that particular reaction and less active toward others. Furthermore, the reaction pathway was at least partially determined by the surface sites.

Although both the arrangement of the surface sites and the molecular justification for their differentiation is unknown, this phenomenon seems to be a major factor in determining reaction mechanism. In essence, this concept is a extension of the more general multiplet theory of Balandin (1929, 1969). In this case, in addition to requiring geometrically specific sets of sites for catalysis the necessary sites are imagined to have been deposited previously during the reaction of identical molecules.

The concept of site specificity is useful in explaining halo-exchange experiments (Section IV-C-2) as well as variations in reaction pattern. Although more experimentation is necessary to establish the existence of surface site specificity, it explains the available data and may likely be the most significant kinetic variable for these reactions.

V) DISCUSSION OF ERRORS

To assess the effect of random experimental scatter on the determination of activation parameters, the errors inherent in various experimental measurements are compared with accuracy figures calculated from experimental points. Standard deviations for each of the reported activation energies and frequency factors are reported in Appendix A.

The maximum standard deviation reported is 0.4 Kcal/mole for the reaction of 1-chloro-2-methylpropane on iron. This is 6.4% error representing 68% confidence limits.

Temperature was controlled to $\pm$ 1°C. For an Arrhenius plot in a temperature range of 200°C, this introduced an error of $\pm$ 0.004°K^{-1} into the experimental values on the (10^3/T) scale. For the iron reaction, the values on this scale span 0.124°K^{-1} units. The capacitance manometer, which was used to measure reactant pressure, introduced a maximum uncertainty of 5×10^{-4} Torr for a total pressure of 10^{-2} Torr. Thus, the rate constant was about $\pm$2.2%. The resultant error was $\pm$ 0.0095 units for the experimental values on the $\log_{10}k$ scale. For the iron reaction these values spanned 0.168 units. The slope of the Arrhenius plot is calculated as shown below.

$$\text{slope} = (\Delta Y \pm d\Delta Y)/(\Delta X \pm d\Delta X)\ K^{-1}$$

$$\text{slope} = (0.168 \pm 0.0095)/(0.124 \pm 0.004)\ K^{-1}$$

$$\text{slope} = (1.45 \pm 0.1)\ K^{-1}$$

From this slope, the activation energy for the reaction of 1-chloro-2-methylpropane on iron is calculated as 6.2 ± 0.5 Kcal/mole. Thus, all the observed error can be accounted for by random errors in experimental measurements. Naturally the same would apply for greater confidence limits.

VI) CONTRIBUTIONS TO ORIGINAL KNOWLEDGE

1) Dehydrochlorination of monochloroalkanes has been investigated at low temperatures on atomically clean or lightly chlorided surfaces of all the first row transition metals.

2) On some of these atomically clean or lightly chlorided surfaces, self hydrogenation and retentive adsorption were also discovered and studied.

3) The high temperature reactions of 1-chloro-2-methyl propane to methylpropene and hydrogen chloride were studied on extensively chlorided surfaces of the whole first row transition metal series. Products, kinetics and Arrhenius activation parameters were determined.

4) The high temperature non-catalytic reactions of 1-chloropropane to hydrocarbons, hydrogen and surface chloride were also studied on extensively chlorided surfaces of all first row transition metals. Where possible, Arrhenius activation parameters were determined; however, most reactions were auto-inhibited by formation of a relatively impermeable surface chloride. This inhibition seems to be related to metal-chloride lattice energies.

5) The surface chloride layer formed during dehydrochlorination of a given chloroalkane was found to be specific to that particular reaction. Surfaces deposited during the given reaction were relatively ineffective at promoting dehydrochlorination of other chloroalkanes.

VI) CONTRIBUTIONS TO ORIGINAL KNOWLEDGE

1) Dehydrochlorination of monochloroalkanes has been investigated at low temperatures on atomically clean or lightly chlorided surfaces of all the first row transition metals.

2) On some of these atomically clean or lightly chlorided surfaces, self hydrogenation and retentive adsorption were also discovered and studied.

3) The high temperature reactions of 1-chloro-2-methyl propane to methylpropene and hydrogen chloride were studied on extensively chlorided surfaces of the whole first row transition metal series. Products, kinetics and Arrhenius activation parameters were determined.

4) The high temperature non-catalytic reactions of 1-chloropropane to hydrocarbons, hydrogen and surface chloride were also studied on extensively chlorided surfaces of all first row transition metals. Where possible, Arrhenius activation parameters were determined; however, most reactions were auto-inhibited by formation of a relatively impermeable surface chloride. This inhibition seems to be related to metal-chloride lattice energies.

5) The surface chloride layer formed during dehydrochlorination of a given chloroalkane was found to be specific to that particular reaction. Surfaces deposited during the given reaction were relatively ineffective at promoting dehydrochlorination of other chloroalkanes.

6) Extensive stuides of the mechanisms of both catalytic and non-catalytic dehydrochlorination reactions on halided surfaces were conducted.

VII) SUMMARY AND PERSPECTIVES

These studies were conducted as a continuation of research initiated by Harrod and Summers on titanium catalyzed dehydrohalogenations of simple haloalkanes. During the previous studies, a wide variety of modes of dehydrohalogenation were discovered, dependent upon both the haloalkane and the properties of the surface.

Two distinctive reaction patterns were discovered: those occurring at low temperatures on atomically clean films and those requiring high temperatures and extensively halided surfaces. The former led to formation of a surface halide and release of gas phase hydrocarbons. The latter followed one of two patterns, either a catalytic reaction to equimolar quantities of olefin and hydrogen halide or a non-catalytic reaction with formation of a surface halide and a mixture of olefin and paraffin.

Low temperature reactions usually proceeded rapidly and were inhibited by the formation of surface halide making detailed kinetic studies impossible. Reactions on halided surfaces were slower and exhibited no noticable inhibition by surface product. Non-catalytic reactions proceeded according to a half order rate law whereas catalytic reactions were first order. Mechanisms were proposed for these two modes of decomposition based on the available experimental information.

To further understand these reactions and the mechanistic differences between the two modes of high temperature decomposition, three avenues of investigation seemed most appropriate: 1) extension of the studies to other surfaces, 2) more thorough investigation of the kinetics and 3) examination of the surface structures responsible for effecting the various reactions. The lack of experimental information on which to base reaction mechanisms was the most serious weakness in the previous studies.

To examine unsupported assumptions concerning the mechanisms and to determine the universality of the reaction schemes the first and second areas were examined in detail in the present studies. By studying typical non-catalytic and catalytic haloalkanes on the first row transition metals it was hoped that the generality of the reaction patterns could be established. In addition, by selecting this series of closely related metals the effects of slight variations in surface characteristics could be assessed and possibly brought to bear on mechanisms. Furthermore, time order determinations were augmented with concentration order determinations, haloalkane exchange experiments and product inhibition studies.

Low temperature dehydrochlorination proceeded to varying degrees on all the metals studied. Products were similar in all cases and no trend was detected suggesting only that this is a general phenomenon without

implying anything concerning the mode of reaction. In addition, two further phenomena were detected and studied: retentive adsorption and self hydrogenation. The former, where gas molecules were irreversibly adsorbed by the surface without subsequent release of gaseous products, occurred primarily on vanadium and chromium and may indicate the formation of relatively stable metal alkyls. The latter occurred on the metals from vanadium through iron and involved the generation of paraffin both at the site of reaction and by addition of surface hydrogen to gas phase olefin.

During most of the non-catalytic reactions on halided surfaces, the surface was deactivated by formation of a metal-halide layer. The extent of deactivation was directly proportional to the metal-halide lattice energies. Half order kinetics were established directly for manganese and, by accounting for the inhibition, on vanadium. Hence, the kinetics seem consistent for all non-catalytic reactions implying a general mechanism. In light of the inhibition effect, transport across the metal metal-halide phase boundary probably controls the rate for uninhibited reactions whereas transport through the metal-halide layer was rate controlling for the others.

Non-catalytic reactions generated hydrogen and olefin with all the metals except titanium. Heating after the initial low temperature reactions also

liberated hydrogen for all metals except titanium. This is presumably due to the large solubility of hydrogen in titanium. Except for titanium, hydrogen solubility must have been too low to allow the hydrogen retention necessary to facilitate paraffin production in a primary process. For initial reactions, on the other hand, the ready availability of desorbable hydrogen facilitated hydrogenation.

Catalytic high temperature reactions followed the same pattern on each of the metals, producing equimolar mixtures of olefin and hydrogen chloride according to a first order rate law. Several factors could effect changes in activation parameters, making a straight forward interpretation impossible. A compensation effect between activation energy and $\log_{10}A$ has been observed.

As verified by both time and concentration order determinations, non-catalytic reactions proceed according to strict half order kinetics. Halo-exchange experiments suggested that no dissociative equilibrium preceeded the rate controlling step. If the latter conclusion is correct, half order kinetics could be explained only by a fortuitous combination of rate constants for individual steps.

Based on further halo-exchange experiments, first order catalytic reactions also seemed to proceed without a rapid dissociative equilibrium. Hence, rate control was probably determined by an irreversible adsorption

step. The mechanism is probably similar to that proposed for pyrolytic dehydrochlorinations, a 'quasi' heterolytic internal rearrangement. The surface could assist in formation of the transition state by further stretching the carbon-halogen bond.

Studies of surface site specificity suggest that the metal-halide layer formed during the reaction of each haloalkane was different and acted as a specific catalyst for that particular reaction. This could explain the existence of different reaction schemes and the possiblity of rapid dissociative equilibria in the absence of halo-exchange. Whether this is related to the phenomon of domain formation is not known.

By dint of these studies, there is now a much clearer understanding of the factors determining the products, kinetics and mechanisms of the reactions on halided surfaces. For non-catalytic reactions, strict half order kinetics has been firmly established, but the existence of a rapid dissociative pre-equilibrium is still undecided. Products are determined primarily by the solubility of hydrogen in the metal.

Understanding of catalytic reactions was not increased significantly by the present studies except to assure that it is a general phenomenon and that the mode of decomposition is determined solely by the haloalkane and

not by the metal.

The most significant discovery is the existence of specificity between the various halided surfaces. This has hitherto not been considered in formulating theories of reaction mechanisms and its role in surface studies has been largely ignored. However, there is definite evidence that haloalkanes deposit highly specific surfaces which effect certain reactions in preference to others. This may be the determining factor between various modes of decomposition and merits further investigation.

VIII) SUGGESTIONS FOR FURTHER WORK

The profit to be realized from extending these studies to other metals or haloalkanes seems limited. It is likely that other reaction systems would follow an already observed reaction sequence and would lend little insight into reaction mechanisms.

Extension of this work could most profitably be directed toward understanding the surface structures involved in catalyzing the various classes of reaction. More clearly defined surfaces such as individual crystal faces of metal or metal halides could be used as catalysts.

Further investigation of the possibility of a dissociative pre-equilibrium could be pursued by the following experiments.

1) Bromoalkanes could be reacted on surfaces prepared with chloroalkanes and vice versa to determine whether the present studies excluded dissociative equilibria due to surface site specificity.

2) If the above experiment indicates surface site specificity the dissociative equilibrium could be tested using radioactively labeled haloalkanes.

3) The possibility of reversible dissociative adsorption of the C-H bond could be tested by examining isotope effects on reaction rate using normal and deuterated haloalkanes.

The surface itself could be studied using techniques such as low energy electron diffraction to detect both composition and orientation. The most potentially rewarding area seems to be in elucidating the nature of the species responsible for surface activity.

Appendix A

Mathematical Analysis of Mass Spectral Data

1) Component Concentration

A spectrum of a mixture is the sum of the spectra of its components and from this spectrum a system of linear equations can be derived to determine the relative concentrations of each component. To fully analyze a mixture of N components, N equations must be developed from a like number of peaks. The relative contribution of each component to a peak is the product of its concentration, relative sensitivity, and peak height/base peak height ratio in the pure gas. The system of equations can be solved by Cramer's rule and the solution programmed onto either a Wang 360 calculator in the case of two analyzed components or a computer for more than two.

1a) Two Analyzed Components

HALIDE - 1-chloro-2-methylpropane

OLEFIN - methylpropene

The spectrum was analyzed using the base peaks for each component. These values, along with the relative sensitivities, are shown in Appendix C.

TABLE A-A-1

Calibration Data

	Fragmentation Value	
mass number	halide	olefin
41	0.776	1.00
43	1.00	0.00
relative sensitivity	1.00	1.12

From the values in Table A-A-1 the following set of simultaneous equations was established:

$$1.00 \times 0.776 \times (\text{HALIDE}) + 1.12 \times 1.00 \times (\text{OLEFIN}) = M_{41} \qquad \text{A-A-1}$$

$$1.00 \times 1.00 \times (\text{HALIDE}) + 1.12 \times 0.00 \times (\text{OLEFIN}) = M_{43}$$

Solving by Cramer's rule:

$$(\text{HALIDE}) = 1.12\ M_{43}/D$$

$$(\text{OLEFIN}) = (M_{41} - 0.776\ M_{43})/D. \qquad \text{A-A-2}$$

D is the determinant of the coefficient matrix and is constant for a given calibration. Concentration is expressed as mole fraction by dividing these values by the sum of the concentrations (SUM).

$$\text{SUM} = (\text{HALIDE}) + (\text{OLEFIN}) = (M_{41} + 0.344\ M_{43})/D \qquad \text{A-A-3}$$

Thus,

$$\text{mole fraction halide} = (\text{HALIDE})/\text{SUM} = 1.12 M_{43}/(M_{41} + 0.344 M_{43})$$

$$\text{mole fraction olefin} = (\text{OLEFIN})/\text{SUM} = (M_{41} - 0.776 M_{43})/(M_{41} + 0.344 M_{43}) \qquad \text{A-A-4}$$

A program for calculating mole fraction halide, mole fraction olefin and $\log_{10} P_o/P$ entitled 'Mole Fractions - Catalytic #3' is presented at the end of this Appendix.

1b) Three Analyzed Components

HALIDE - 1-chloropropane

OLEFIN - propene

PARFIN - propane

Three components were analyzed using the computer due to the lack of storage units in the Wang 360 calculator. The three peaks chosen were M_{42}=B, M_{41}=C and M_{29}=D. Concentrations as mole percent figures and $(10 - (\text{HALIDE})^{\frac{1}{2}})$ were determined. Derived according to the same principles as that for two components, a sample computer program entitled 'Mole Fractions - Non-catalytic' is shown below.

Mole Fractions - Non-Catalytic

```
      READ (5,10)N
      WRITE (6,20)
    1 READ (5,30)MSNO,D,C,B,A
      SUM=-.544*D-1.123*C-.754*B
      HALIDE=100*(-.045*D+1.077*C-1.832*B)/SUM
      OLEFIN=100*(.221*D-1.945*C+.606*B)/SUM
      PARFIN=100*(-.72*D-.255*C+.472*B)/SUM
      ANSWER=10.0-(HALIDE)**0.5
      WRITE (6,40)MSNO, HALIDE, OLEFIN, PARFIN, HYDRGN, ANSWER
      IF (MSNO-N) 1,1,2
    2 STOP
   10 FORMAT (I3)
   20 FORMAT (1HO,1X,54HMSNO  HALIDE  OLEFIN  PARFIN  HYDRGN
     1ANSWER)
   30 FORMAT (I3,4F5.1)
   40 FORMAT (1H,I5,4F10.2,1F10.4)
      END
```

2) Determination of Coefficients for a First Degree Polynomial and the Standard Deviation of the Slope and Intercept

The coefficients of the first degree polynomial $Y = a + bX$ were determined by the least squares regression technique using a standard program on the Wang 360 calculator (Wang, 1967). The standard deviation of the slope and intercept were computed using the same calculator according to equations A-A-5 and A-A-6 (Youden, 1951). These techniques assume that the error in the abcissa is insignificant compared with that in the ordinate.

$$\sigma_b = \sqrt{s^2/(\Sigma x^2 - n\bar{x}^2)} \qquad \text{A-A-5}$$

$$\sigma_a = \sqrt{s^2 \Sigma x^2/[n\Sigma x^2 - (\Sigma x)^2]} \qquad \text{A-A-6}$$

where: $\bar{x} = \Sigma x/n$,

n = number of points

and $(n-2)s^2 = \left[\Sigma y^2 - \frac{(\Sigma y)^2}{n} - \left(\frac{\Sigma xy - \frac{\Sigma x \Sigma y}{n}}{\Sigma x^2 - \frac{(\Sigma x)^2}{n}} \right)^2 \right]$

The programs are entitled "Calculation of σ_b" and "Calculation of σ_a" respectively and are presented at the end of this Appendix.

3) Standard Deviation of Kinetic Paramaters

First order rate constants and Arrhenius parameters were determined by plotting $\log_{10}$ on the ordinate

then adjusting the resultant slope by a factor of 2.30259 to give the actual value. Standard deviations were calculated according to Equation A-A-7

$$\sigma_{c \cdot b} = c \cdot b \left[\left(\frac{\sigma b}{b} \right)^2 + \left(\frac{\sigma c}{c} \right)^2 \right]^{\frac{1}{2}}. \qquad \text{A-A-7}$$

With c = constant, $\sigma_c = 0$

$$\sigma_{c \cdot b} = c \cdot b \left(\frac{\sigma b}{b} \right) = c \cdot \sigma_b. \qquad \text{A-A-7}$$

Thus, the standard deviation for the rate constant and activation energy are given by Equation A-A-9 and Equation A-A-10

$$\sigma_k = 2.30259 \ \sigma_b \qquad \text{A-A-9}$$

$$\sigma_{E_a} = 2.30259 \ \sigma_b \qquad \text{A-A-10}$$

where R is the gas constant with a value of 1.986 cal/deg-mole.

The activation energy thus calculated is in Kcal/mole rather than cal/mole since the abscissa is $10^3/T$ rather than 1/T. Standard deviations for $\log_{10} A$ are as found from the Arrhenius plots with no further adjustments. For half order reactions where $10(P_o^{\frac{1}{2}} - P^{\frac{1}{2}})$ is plotted against time the rate constant is 20% of the slope and likewise σ_b is 20% of the standard deviation of the slope.

MODEL 360 PROGRAM TITLE: Mole Fractions-Catalytic#3 NO.

(THIS SPACE FOR INSTRUCTIONS AND NOTES)

Purpose

To calculate the mole fraction of halide and olefin and $\log_{10}(P_o/P)$ for the system

1-chloro-2-methylpropane /methylpropene.

Operation

1) index M_{41}
2) press start
3) index M_{43}
4) press continue
5) read mole fraction halide
6) press continue
7) read mole fraction olefin
8) press continue
9) read $\log_{10}(P_o/P)$

No.	Cmd	Code	Comment
00	SR3	13	
01	stop	01	
02	SR2	12	
03	CRA	50	
04	.	75	
05	3	63	
06	4	64	
07	4	64	
08	enter	41	
09	R2	16	
10	X=	46	
11	+RA	52	
12	R3	17	
13	+RA	52	
14	SR1	11	SUM in R1
15	1	61	
16	.	75	
17	1	61	
18	2	62	
19	enter	41	
20	R2	16	
21	X=	46	
22	enter	41	
23	R1	15	
24	÷=	47	
25	stop	01	halide mole fxn
26	SR0	10	
27	CLA	54	
28	1	61	
29	+LA	56	
30	R0	14	
31	-LA	57	
32	stop	01	olefin mole fxn
33	1	61	
34	enter	41	
35	R0	14	
36	↑=	47	
37	logx	42	
38	enter	41	
39	2	62	
40	.	75	
41	3	63	
42	0	60	
43	2	62	
44	5	65	
45	9	71	
46	÷=	47	
47	stop	01	$\log_{10}P_o/P$
48			
49			
50			
51			
52			
53			
54			
55			
56			
57			
58			
59			
60			
61			
62			
63			
64			
65			
66			
67			
68			
69			
70			
71			
72			
73			
74			
75			
76			
77			
78			
79			

MODEL 360 PROGRAM TITLE: Calculation of σ_b; Y = a + bX NO.

(THIS SPACE FOR INSTRUCTIONS AND NOTES)

Purpose

To calculate the standard deviation of the line Y = a + bX.

Instructions

1) Perform immediately following least squares program without altering registers.

2) Registers contain:
#3- intercept (a),
#2- ΣXY,
#1- N,
#0- ΣY.

3) The following are obtained during the least squares program as indicated:
ΣX- after indexing last X and pressing start and before indexing last Y,
ΣY^2- after indexing last Y and pressing continue,
ΣX^2- after reading out ΣY^2 and pressing continue again.

Operation

1) insert σ_b card
2) index ΣY^2
3) press start
4) index ΣX
5) press continue
6) index ΣX^2
7) press continue
8) read σ_b

No.	Cmd	Code	Comment
00	CLA	54	
01	CRA	50	
02	+LA	56	
03	RO	14	
04	x^2	45	
05	enter	41	
06	R1	15	
07	÷=	47	
08	-LA	57	
09	stop	01	index ΣX
10	SR3	13	
11	R2	16	
12	+RA	52	
13	R3	17	
14	enter	41	
15	RO	14	
16	X=	46	
17	enter	41	
18	R1	15	
19	÷=	47	
20	-RA	53	
21	RRA	51	
22	x^2	45	
23	SRO	10	
24	CRA	50	
25	stop	01	index ΣX^2
26	SR2	12	
27	R2	16	
28	+RA	52	
29	R3	17	
30	x^2	45	
31	enter	41	
32	R1	15	
33	÷=	47	
34	-RA	53	
35	RO	14	
36	enter	41	
37	RRA	51	
38	÷=	47	
39	-LA	57	
40	CRA	50	
41	R1	15	
42	+RA	52	
43	2	62	
44	-RA	53	
45	RLA	55	
46	enter	41	
47	RRA	51	
48	÷=	47	
49	SRO	10	
50	CRA	50	
51	CLA	54	
52	R2	16	
53	+RA	52	
54	R3	17	
55	enter	41	
56	R1	15	
57	÷=	47	
58	x^2	45	
59	enter	41	
60	R1	15	
61	X=	46	
62	-RA	53	
63	RO	14	
64	enter	41	
65	RRA	51	
66	÷=	47	
67	$\sqrt{}$	44	
68	stop	01	read σ_b
69			
70			
71			
72			
73			
74			
75			
76			
77			
78			
79			

MODEL 360 PROGRAM TITLE: Calculation of σa; $Y = a + bX$ NO.

(THIS SPACE FOR INSTRUCTIONS AND NOTES)

Purpose

To calculate the standard deviation of the intercept of the line $Y = a + bX$.

Instructions

1) Perform immediately following σb program without altering registers.

2) Registers contain:

#3- ΣX

#2- ΣX^2

#1- N

#0- s^2

Operation

1) insert card for σa

2) press start

3) read σa

No.	Cmd	Code	Comment	No.	Cmd	Code	Comment
00	CRA	50		40			
01	R1	15		41			
02	enter	41		42			
03	R2	16		43			
04	X=	46		44			
05	+RA	52		45			
06	R3	17		46			
07	X^2	45		47			
08	-RA	53		48			
09	R0	14		49			
10	enter	41		50			
11	R2	16		51			
12	X=	46		52			
13	enter	41		53			
14	RRA	51		54			
15	÷=	47		55			
16	$\sqrt{}$	44		56			
17	stop	01	read σa	57			
18				58			
19				59			
20				60			
21				61			
22				62			
23				63			
24				64			
25				65			
26				66			
27				67			
28				68			
29				69			
30				70			
31				71			
32				72			
33				73			
34				74			
35				75			
36				76			
37				77			
38				78			
39				79			

Appendix B

Thermodynamics of the Dehydrochlorination of Alkyl Chlorides

Values of the free energy of reaction for the dehydrochlorination of various alkyl chlorides have been calculated, whenever possible, from experimentally measured values of the standard free energies of formation. When only theoretical values were available these were verified as thoroughly as possible by comparison with similar experimental data.

Standard free energies of formation were obtained from:

1) ΔG_f^o (olefins) - American Petroleum Institute, Selected Values of the Properties of Hydrocarbons and Other Related Compounds, Research Project #44

2) ΔG_f^o (HCl) - Rossini, F.P., D.D. Wagman, W.H. Evans, S. Levine and I. Jaffe, Selected Values of Chemical Thermodynamic Properties, National Bureau of Standards, Circular #500

3a) ΔG_f^o (alkyl halides) - Stull, D.R., E.F. Westrum and G.C. Sinke, The Chemical Thermodynamics of Organic Compounds, J. Wiley, New York, 1969

3b) ΔG_f^o (alkyl halides) - Manufacturing Chemists' Association Research Project, Selected Values of Properties of Chemical Compounds Chemical Thermodynamic Properties Center, Texas A & M University

Since experimental values for only chlorinated methanes and ethanes were available in '3b', theoretical values from Stull's book were used for propyl and butyl compounds. However, the comparability of these data was verified by checking Stull's values for the chlorinated methanes and ethanes, paraffins, and olefins against experimental values. Agreement was excellent for the hydrocarbons and, although not as good for the alkyl halides, was always within about 1 Kcal/mole between 273 and 1000°K. Thus, theoretical values for the higher molecular weight alkyl chlorides were used with confidence. The discrepancy for 1-chloroethane (one of the worst correlations) is indicated in the Tables and Figures. Comparing the two 1-chloroethane values, it seems that quantitative conclusions are propably valid whereas qualitative trends are certainly meaningful.

Floor temperatures for the dehydrochlorination reaction have been calculated from Figure A-B-1 by linear interpolation. In addition, the free energy of reaction (ΔG_r) for any temperature within this range can be interpolated with confidence since temperature is linearly related to ΔG_r^o in every instance.

TABLE A-B-1

Free Energies of Reaction at 1 Atm for

alkyl halide ⟶ olefin + HCl

alkyl halide	ΔG_T°					floor temp.°C
	300°K	400°K	500°K	600°K	700°K	
1-chloroethane (Stull)	7.79	4.46	1.46	-1.73	-4.91	273
1-chloroethane (MCA)			0.43	-2.79		243
1-chloropropane	4.26	1.02	-2.24	-5.49	-8.75	159
2-chloropropane	7.09	3.50	-0.09	-3.66	-7.22	227
1-chloro-2-methylpropane	2.92	-0.14	-3.31	-6.29	-9.36	122
2-chloro-2-methylpropane	6.34	2.56	-1.22	-4.96		195

Since all our reactions have been conducted between 1×10^{-2} and 5×10^{-2} Torr the comparison must be made at these pressures to be meaningful in the present context. Free energy varies with pressure as shown in Equation A-B-1.

$$\left(\frac{\partial \Delta G}{\partial P}\right)_T = \Delta V \qquad \text{A-B-1}$$

ΔV = change in molar volume during reaction

Assuming that between 760 and 0.01 Torr all three gases behave ideally, $\Delta V = RT/P$ and Equation A-B-1 can be integrated to Equation A-B-2 and further simplified to Equation A-B-3, from which free energies of reaction at 10^{-2} Torr can be calculated from values at 760 Torr.

FIGURE A-B-1

Free Energy of Dehydrochlorination at 1 Atmosphere

as a Function of Temperature

○ - 1-chloroethane (Stull)

△ - 1-chloroethane (MCA)

▽ - 1-chloropropane

⬡ - 2-chloropropane

◇ - 1-chloro-2-methylpropane

□ - 2-chloro-2-methylpropane

● - floor temperature for dehydrochlorination

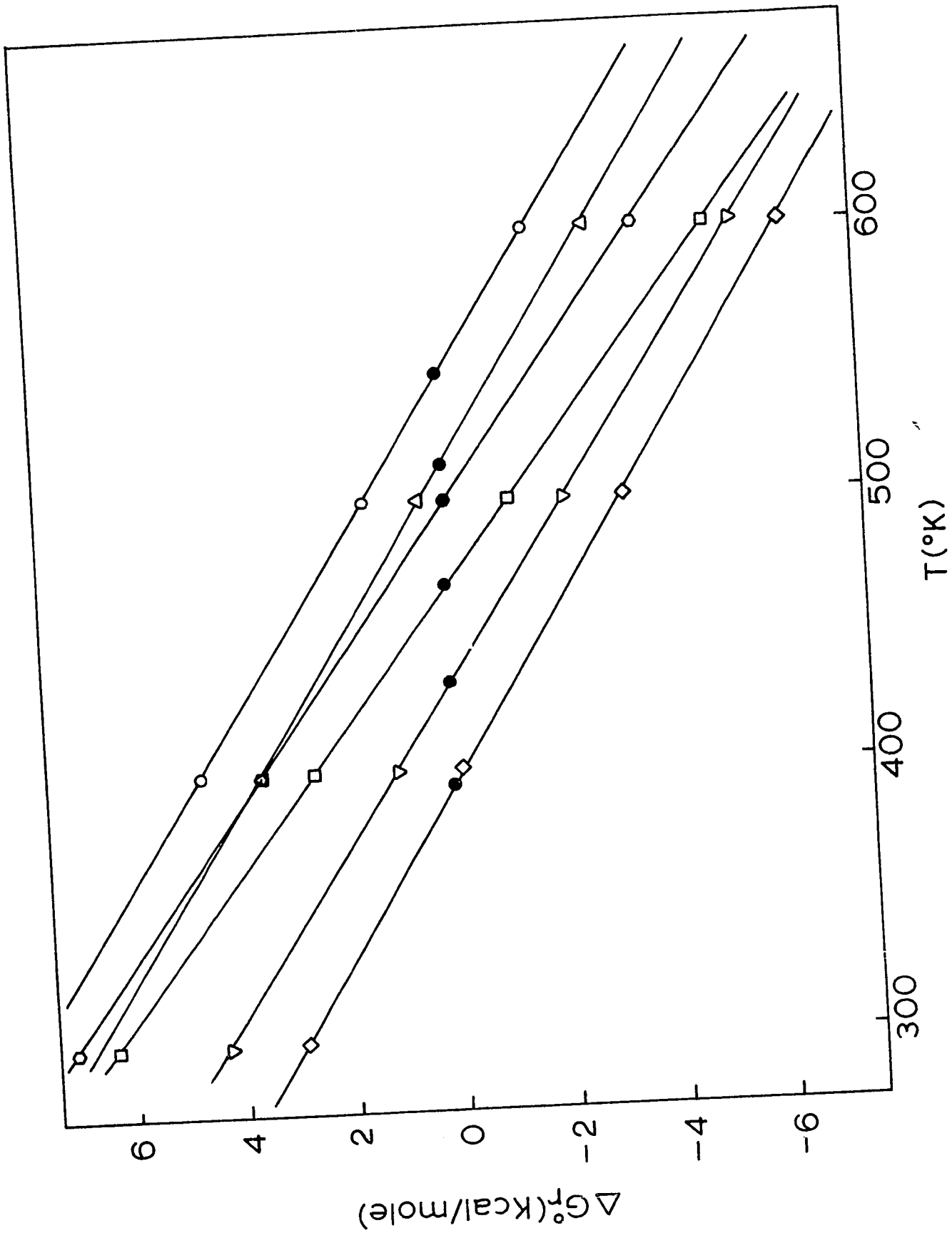
ΔGr°(Kcal/mole)
6
4
2
0
-2
-4
-6
300
400
500
600
T(°K)

$$\Delta(\Delta G_r) = (\Delta G_r^{.01} - \Delta G_r^{760}) = RT \ln \frac{0.01}{760} \qquad \text{A-B-2}$$

$$\Delta(\Delta G_r) = -0.0223\ [T(^\circ K)]\ \text{Kcal/mole} \qquad \text{A-B-3}$$

The resultant values are shown in Table A-B-2 and plotted in Figure A-B-2. Thus, in accord with LeChatelier's principle the dehydrohalogenation reaction is driven in the direction of greater volume by lowering the pressure.

TABLE A-B-2

Free Energies of Reaction at 10^{-2} Torr for

alkyl halide ⟶ olefin + HCl

alkyl halide	ΔG_r°					
	300°K	400°K	500°K	600°K	700°K	floor temp. °C
1-chloroethane (Stull)	1.09	-4.47	-9.70	-15.12	-20.53	47
1-chloroethane (MCA)			-10.73	-16.18		27
1-chloropropane	-2.44	-7.91	-13.40	-18.88	-24.37	-18
2-chloropropane	0.39	-5.43	-11.25	-17.05	-22.84	35
1-chloro-2-methylpropane	-3.76	-9.07	-14.47	-19.68	-24.98	-43
2-chloro-2-methylpropane	-0.35	-6.37	-12.38	-18.35		20

These values differ markedly from those of Summers, calculated according to a theoretical estimate (Janz, 1958). However, in spite of the difference in absolute

FIGURE IV-B-2

Free Energy of Dehydrochlorination at 10^{-2} Torr

as a Function of Temperature

○ - 1-chloroethane (Stull)

△ - 1-chloroethane (MCA)

▽ - 1-chloropropane

○ - 2-chloropropane

◇ - 1-chloro-2-methylpropane

□ - 2-chloro-2-methylpropane

● - floor temperature for dehydrochlorination

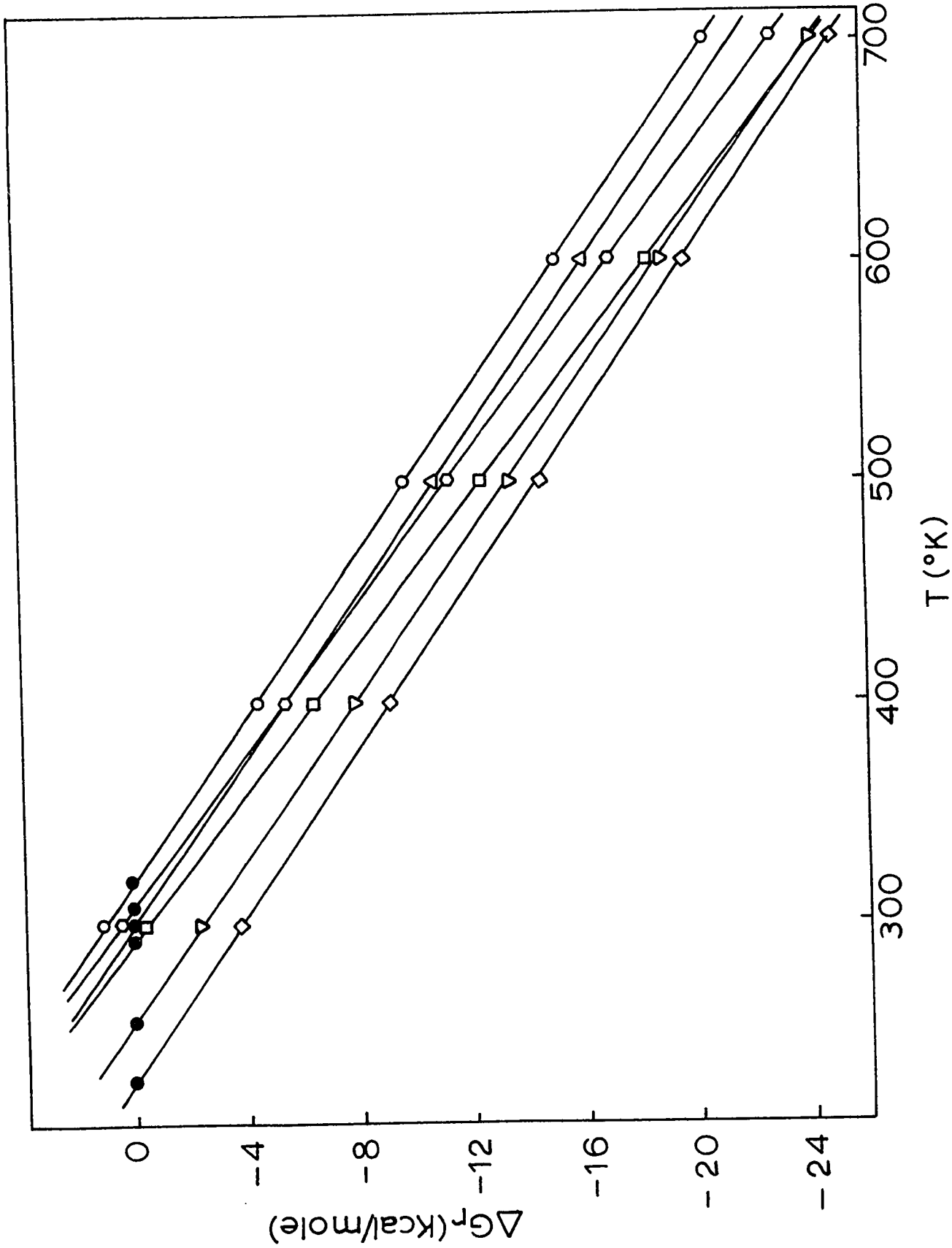
ΔGr (kcal/mole)
0
-4
-8
-12
-16
-20
-24
300
400
500
600
700
T (°K)

values, the quantitative trends in both floor temperatures and free energies of reaction are almost identical and in no way detract from the conclusions drawn regarding the thermodynamic control of reaction path (Harrod and Summers, 1971).

Appendix C

Mass Spectral Calibration Data

For convenience, fragmentation patterns and relative sensitivities of both alkyl halides and hydrocarbons are grouped according to the type of experiments during which they were present. Consequently, some appear more than once and may vary slightly due to adjustments in the residual gas analyzer. However, all patterns except hydrogen halides were found to be consistent to within a few percent even after adjusting the mass spectrometer and changing its filament.

No data is presented for the hydrogen halides since their peaks varied irreproducibly, did not overlap with the base peak of any other component, and were not included in the mathematical analysis. Mass number 28 is, likewise, not listed since it showed a consistent and irreproducible background value. Furthermore, only principle peaks are presented for most gases and minor peaks of no analytical consequence are frequently deleted. Some special features of particular reactions are delineated in the text and are not further amplified here.

Relative sensitivities were determined within each system and, although it would have been possible in some cases, no overall standard was established.

They were independent of adjustments in the mass spectrometer and seemed to depend primarily on the ability of the pumping system to remove a particular gas from the cycloid tube.

TABLE A-C-1

Calibration Spectra

Non-catalytic Exchange Experiment

Mass #	1-chloro propane	1-bromo propane	1-chloro propane-1-d_1	1-bromo propane-1-d_1	propene	propane	hydrogen
2	8.4	11.9	8.5	8.6	11.8	3.6	100
12	2.2	3.3	2.6	3.2	4.4	1.4	-
13	2.8	3.0	2.7	2.8	3.7	1.8	-
14	5.4	7.3	5.0	5.4	7.4	3.8	-
15	15.2	23.2	13.6	13.9	17.4	11.3	-
16	7.7	12.8	10.0	11.4	12.6	3.3	-
25	3.6	-	-	-	3.6	1.4	-
26	14.9	17.7	10.1	10.2	16.7	11.4	-
27	66.7	81.0	44.4	47.1	52.7	44.0	-
29	52.5	12.7	58.3	17.8	3.2	100.0	-
35	6.0				-	-	-
36	22.3				-	-	-

TABLE A-C-1 (Continued)

Mass #	1-chloro propane	1-bromo propane	1-chloro propane-1-d_1	1-bromo propane-1-d_1	propene	propane	hydrogen
37	8.6				14.1	3.9	-
38	13.4				18.9	5.7	-
39	22.6	29.6	12.5	14.4	76.2	16.2	-
40	7.6	7.9	14.4	17.4	28.1	2.9	-
41	37.1	63.3	11.1	17.4	100.0	13.0	-
42	100.0	24.2	30.6	47.5	58.7	5.2	-
43	16.4	100.0	100.0	20.5	3.9	19.9	-
44	-	16.4	17.4	100.0	-	19.8	-
45	-	-	-	6.2	-	-	-
Relative Sensitivity	1.00	0.68	1.00	0.68	0.95	1.92	1.97

TABLE A-C-2

Calibration Spectra

1-Chloropropane System

Mass #	1-chloro propane	propene	propane	hydrogen
2	8.4	11.8	3.6	100
15	15.2	17.4	11.3	-
25	3.6	3.6	1.4	-
26	14.9	16.7	11.4	-
27	66.7	52.7	44.0	-
29	52.5	3.2	100.0	-
30	1.7	-	3.3	-
35	6.9	-	-	-
36	22.3	-	-	-
37	8.6	14.1	3.9	-
38	13.4	18.9	5.7	-
39	22.6	76.2	16.2	-
40	7.6	28.1	2.9	-
41	37.1	100.0	13.0	-
42	100.0	58.7	5.2	-
43	16.4	3.9	19.9	-
44	-	-	19.8	-
Relative Sensitivity	1.00	0.95	1.92	1.97

TABLE A-C-3

Calibration Spectra - Catalytic Systems

2-Chloropropane System

Mass #	2-chloro propane	propene	propane
2	9.2	11.8	3.6
25	3.1	3.6	1.4
26	14.8	16.7	11.4
27	79.1	52.7	44.0
29	6.2	3.2	100.0
36	31.5	-	-
37	8.8	14.1	3.9
38	17.1	18.9	5.7
39	30.2	76.2	16.2
40	9.0	28.1	2.9
41	50.1	100.0	13.0
42	18.1	58.7	5.2
43	100.0	3.9	19.9
44	6.0	-	19.8
Relative Sensitivity	0.83	1.00	2.02

TABLE A-C-4

Calibration Spectra - Catalytic System

1-Chloro-2-methylpropane System

Mass #	1-chloro-2-methylpropane	methyl propene	methyl propane
2	11.7	15.5	3.7
25	3.1	-	-
26	9.3	10.2	5.9
27	45.2	27.8	37.8
29	15.1	13.9	8.3
39	27.9	53.7	18.8
40	6.8	13.1	3.2
41	77.6	100.0	47.2
42	51.1	5.4	31.1
43	100.0	-	100.0
44	-	-	4.5
49*	15.7	3.5	-
50*	7.2	10.7	-
51*	7.8	7.1	-
53*	3.6	7.1	-
55*	10.8	20.6	2.0
56*	18.1	43.5	2.0
57*	-	-	-
Relative Sensitivity	1.00	1.12	1.62

* scanned at 3 times the usual sensitivity

TABLE A-C-5

Calibration Spectra

Catalytic Exchange Experiment

Mass #	1-chloro-2-methyl propane	1-chloro-2-methyl propane-1-d_1	1-bromo-2-methyl propane	1-bromo-2-methyl propane-1-d_1	methyl propene
2	12.0	11.2	12.2	13.3	16.3
26	9.4	7.2	9.7	15.0	11.0
27	50.4	40.6	44.3	61.1	31.3
29	16.3	11.3	39.7	40.9	14.1
38	12.6	10.2	12.9	19.1	9.2
39	33.6	21.1	40.1	54.4	56.8
40	7.0	16.7	8.0	37.5	13.5
41	85.9	48.6	100.0	99.2	100.0
42	48.2	79.2	16.1	100.0	4.5
43	100.0	100.0	32.9	56.1	0
44	4.9	6.0	2.4	8.4	0
49*	16.2	6.2	2.5	4.1	3.8
53*	3.6	1.7	4.3	5.2	7.0
55*	9.8	2.6	11.7	12.1	17.7
56*	15.3	8.0	16.7	29.0	39.2
57*	3.6	12.7	102.1	29.5	0
58*	0	3.1	0	128.1	0
Relative Sensitivity	1.00	1.00	0.76	0.76	1.12

* scanned at 3 times the usual sensitivity

Appendix D

Solubility of Hydrogen in the First Row Transition Metals

The solubility of hydrogen in the first row transition metals at one atmosphere hydrogen pressure and various temperatures is listed in Table A-D-1 (Dushman, 1962).

TABLE A-D-1

Solubility of Hydrogen in the First Row Transition Metals

	Solubility (cm^3/100g metal)							
T(^oC)	Ti	V	Cr	Mn	Fe	Co	Ni	Cu
20	40740	15000						
200							1.70	
300		6500			0.16		2.35	
400	38770	3800			0.35		3.51	0.06
500	36600	1900			0.75		4.10	0.16
600	33470	1000	0.5	9.0	1.20	0.89	5.25	0.30
700	18390	640			1.85	1.22	6.50	0.44
800	14090	440	1.0	27.0	2.45	1.85	7.75	0.72
$r^{(1)}$	1.75	0.72	-	-	-	-	-	-
$rx10^{4(2)}$	-	-	0.46	1.22	0.98	4.0	4.06	0.41

(1) r-maximum number of hydrogen atoms per metal atom

(2) $rx10^4$-number of hydrogen atoms per metal atom at 800^oC.

Appendix E

Determination of the Most Thermodynamically Stable Chloride and its Crystal Structure for Each of the First Row Transition Metals

Determination of the most stable chloride was based on evaluation of the heat of reaction for the sequence of reactions

$$nMCl_{(n+1)} + M \longrightarrow (n+1)MCl_n \qquad \text{A-E-1}$$

Since the metals are all so similar, it was assumed that no significant deviation would be introduced by entropy effects and that free energies would follow enthalpy.

Heats of formation were obtained from:

Rossini, F.P., D.D. Wagman, W.H. Evans, S. Levine and I. Jaffe, Selected Values of Chemical Thermodynamic Properties, National Bureau of Standards, Circular #500

Proceeding across the row from titanium to copper, higher oxidation states became progressively less stable and the heat of formation for the trichlorides were unavailable for cobalt, nickel and copper. Thus, if a common structure holds for titanium and copper it would also hold for the metals in between.

For titanium, the monochloride was

extremely unstable (no information available) while the dichloride was more stable than the trichloride and the trichloride more stable than the tetrachloride. Thus, the dichloride would be most thermodynamically stable.

$$2TiCl_3 + Ti \longrightarrow 3TiCl_2 \quad \Delta H_r = -12 \text{ Kcal/mole} \quad \text{A-E-2}$$

$$3TiCl_4 + Ti \longrightarrow 4TiCl_3 \quad \Delta Hr = -122.1 \text{ Kcal/mole} \quad \text{A-E-3}$$

For copper, the dichloride was more stable than the monochloride.

$$CuCl_2 + Cu \longrightarrow 2CuCl_2 \quad \Delta Hr = -15.2 \text{ Kcal/mole} \quad \text{A-E-4}$$

and no information was available for the trichloride since it was extremely unstable.

As verified for vanadium, chromium and iron, the metals between titanium and copper were most stable as the dichloride.

metal	ΔHr
V	-50
Cr	-12
Fe	-49

$$\Delta Hr = (2MCl_3 + M \longrightarrow 3MCl_2) \quad \text{A-E-5}$$

The crystal structures for these dichlorides are shown in Table A-E-1.

TABLE A-E-1*

halide	crystal structure
$TiCl_2$	CdI_2
VCl_2	CdI_2
$CrCl_2$	cassiterite (Slightly distorted)
$MnCl_2$	$CdCl_2$
$FeCl_2$	$CdCl_2$
$CoCl_2$	$CdCl_2$
$NiCl_2$	$CdCl_2$

* From Wyckoff, R.W.G., Crystal Structures 2nd ed., Interscience, 1963

With the exception of chromium dichloride, these are all layer lattices of close packed anions with cations occupying half the octahedral holes. However, the anionic layers are stacked so that CdI_2 structures are hexagonal close packed and $CdCl_2$ are cubic close packed.

Appendix - F

SECTION III

Data In Support Of Figures In Experimental Results*

FIGURE III-1

time	$\log_{10} P_o/P$
191	0.292
464	0.580
905	1.040
1332	1.607
1691	1.983

FIGURE III-2

time	$\frac{(\text{propane})}{(\text{propene})}$
191	0.641
464	0.738
905	0.853
1332	0.972
1691	1.078
2230	1.186
3130	1.330
3500	1.385
4260	1.506

FIGURE III-3

time	$\log_{10} P_o/P$
1691	0.3224
2230	0.3354
3130	0.3605
3500	0.3665
4260	0.3850

FIGURE III-4

Reaction 5

time	$\log_{10} P_o/P$
0	0
759	0.1147
1240	0.1691
1936	0.2670

Reaction 6

time	$\log_{10} P_o/P$
0	0
714	0.0441
1214	0.0790
1810	0.1116

FIGURE III-5

time	$\log_{10} P_o/P$
70	0.2066
139	0.5119
550	1.249
913	2.268

*Pressure values in Torr - time values in seconds

FIGURE III-6

time	$\frac{(\text{methylpropane})}{(\text{methylpropene})}$	time	$\frac{(\text{methylpropane})}{(\text{methylpropene})}$
70	0.7196	1375	1.3776
139	0.7783	2211	1.6318
550	1.0844	3380	2.080
913	1.2053		

FIGURE III-7

time	$\log_{10}P_o/P$
913	0
1375	0.0258
2211	0.0742
3380	0.1368

FIGURE III-8

time	$\log_{10}P_o/P$
200	0.1057
550	0.2503
1180	0.3463
4100	1.340

FIGURE III-9

time	$\log_{10}P_o/P$	time	$\log_{10}P_o/P$
487	0	3572	0.6405
1055	0.1218	4152	0.6524
1633	0.2237	4987	0.7583
2359	0.3492		

FIGURE III-10

time	mole percent	time	mole percent	time	mole percent	time	mole percent
75	68.02	70	75.53	80	79.31	161	76.67
200	49.37	200	59.26	200	65.52	330	63.11
350	33.23	350	44.30	340	50.42	500	52.16
510	22.02	510	31.99	510	37.62	700	41.85
630	15.50	670	22.70	775	22.88	920	30.37
						1210	20.58
						1475	13.48

FIGURE III-11

P_o^T(Torr)	$-\frac{dP}{dt}_o \times 10^3$
0	3.123
0.0130	2.686
0.0265	2.170
0.0528	1.386

FIGURE III-12

time	$\log_{10} P_o/P$	$10(P_o^{\frac{1}{2}}-P^{\frac{1}{2}})$
75	0.1670	0.19980
200	0.3065	0.33904
350	0.4785	0.48288
510	0.6572	0.60519
630	0.8097	0.69130

FIGURE III-13

time	$\log_{10} P_o/P$	$10(P_o^{\frac{1}{2}}-P^{\frac{1}{2}})$
161	0.1149	0.1472
330	0.1999	0.2433
500	0.2827	0.3286
700	0.3783	0.4178
920	0.5156	0.5311
1210	0.6866	0.6464
1475	0.8703	0.7488

FIGURE III-14

time	P term
75	17.067
200	24.118
350	32.560
510	41.173
630	47.430

FIGURE III-15

time	P term
161	22.125
330	36.815
500	51.112
700	68.269
920	85.426
1210	109.23
1475	130.26

FIGURE III-16

time	$\log_{10} P_o/P$
382	0
930	0.0347
1495	0.0746
3400	0.2010
4460	0.2917
5321	0.3569

FIGURE III-17

time	$10(P_o^{\frac{1}{2}}-P^{\frac{1}{2}})$	$\log_{10} P_o/P$
119	0.0610	0.1024
420	0.1154	0.2055
768	0.1653	0.3125
1127	0.2125	0.4260
1480	0.2566	0.5482
1976	0.2950	0.6716
2628	0.3532	0.8996
3026	0.3830	1.0438
3412	0.4126	1.2654
4018	0.4441	1.4461

FIGURE III-18

time	$10(P_o^{\frac{1}{2}}-P^{\frac{1}{2}})$	time	$10(P_o^{\frac{1}{2}}-P^{\frac{1}{2}})$	time	$10(P_o^{\frac{1}{2}}-P^{\frac{1}{2}})$
	158°C		169°C		177°C
160	0.0185	110	0.0259	135	0.0628
460	0.0912	446	0.1146	403	0.1712
850	0.1289	792	0.2101	630	0.2593
1280	0.1876	1140	0.2989	945	0.3619
1690	0.2682	1490	0.3758	1400	0.4958
2160	0.3258	1960	0.4701	1640	0.5985
2660	0.3970	2610	0.6090	1880	0.6930
	189°C		198°C		200°C
100	0.0860	105	0.1356	80	0.1111
300	0.2338	310	0.3351	210	0.2324
530	0.3668	490	0.4843	380	0.3694
800	0.5370	680	0.6147	560	0.4926
1006	0.6286	980	0.8577	700	0.6625
1230	0.8146			930	0.8142

FIGURE III-19

$10^3/T^oK$	$4 + \log_{10}k$	$10^3/T^oK$	$4 + \log_{10}k$
2.1142	0.9204	2.2222	0.5443
2.1231	0.9095	2.2624	0.3661
2.1645	0.7933	2.3202	0.1709

FIGURE III-20

time	$\log_{10}P_o/P$	time	$\log_{10}P_o/P$	time	$\log_{10}P_o/P$
	186°C		200°C		214°C
80	0.0966	70	0.1154	95	0.1595
224	0.2130	220	0.2670	260	0.3716
370	0.3100	390	0.4353	505	0.6562
600	0.4781	680	0.6925	710	0.9003
830	0.6478	950	0.9485	900	1.1248
1060	0.8398	1330	1.2559		
1450	1.0799				
	214°C		221°C		
90	0.1538	70	0.1821		
290	0.3940	200	0.3972		
515	0.6621	310	0.5648		
695	0.8778	420	0.7364		
910	1.1397	590	0.9996		
		720	1.1916		

FIGURE III-21

$10^3/T°K$	$3 + \log_{10}k$	$10^3/T°K$	$3 + \log_{10}k$
2.024	0.4985	2.115	0.3200
2.053	0.4418	2.179	0.2240
2.053	0.4400		

FIGURE III-22

time	$\log_{10} P_o/P$
150°C	
165	0.0943
400	0.1660
687	0.261
1076	0.375
1370	0.461
1660	0.552
2034	0.665
2464	0.771
183°C	
103	0.111
343	0.213
727	0.416
1154	0.658
1494	0.860

time	$\log_{10} P_o/P$
171°C	
135	0.097
483	0.263
752	0.376
1054	0.506
1340	0.637
1796	0.798
2202	1.012
198°C	
82	0.135
253	0.260
416	0.379
627	0.544
855	0.695
1040	0.768
1326	1.033

time	$\log_{10} P_o/P$
183°C	
101	0.101
352	0.249
723	0.459
1135	0.679
1504	0.878
198°C	
96	0.107
302	0.264
583	0.444
877	0.681
1202	0.907

FIGURE III-23

$10^3/T^\circ K$	$4 + \log_{10} k$
2.364	0.867
2.268	1.004
2.193	1.097
2.193	1.104
2.123	1.210
2.123	1.223

FIGURE III-24

time	$\log_{10} P_o/P$
177°C	
170	0.084
500	0.263
850	0.401
1150	0.549
1530	0.707
1930	0.873
2400	1.066
207°C	
100	0.058
355	0.203
510	0.296
740	0.414
960	0.542
1170	0.617

time	$\log_{10} P_o/P$
192°C	
150	0.082
406	0.213
705	0.362
1010	0.515
1350	0.681
1730	0.854
2070	1.004
220°C	
100	0.047
300	0.172
500	0.290
720	0.433
900	0.553
1100	0.642
1550	0.893
1930	1.064

time	$\log_{10} P_o/P$
207°C	
140	0.067
450	0.261
850	0.493
1030	0.583
1375	0.762
1740	0.942
2170	1.159
234°C	
90	0.072
300	0.220
500	0.530
720	0.367
910	0.637
1150	0.796
1410	0.930
1700	1.121

FIGURE III-25

$10^3/T^oK$	$4 + \log_{10}k$	$10^3/T^oK$	$4 + \log_{10}k$
2.222	1.0065	2.083	1.0874
2.151	1.0453	2.028	1.1103
2.083	1.0889	1.972	1.1723

FIGURE III-26

time	$\log_{10}P_o/P$	time	$\log_{10}P_o/P$
	177^oC		178^oC
200	0.089	140	0.045
380	0.148	430	0.171
800	0.267	740	0.286
1176	0.462	1160	0.493
1610	0.637	1525	0.596
2040	0.771	2000	0.774
2480	0.935		
	196^oC		224^oC
160	0.072	120	0.079
400	0.195	410	0.249
870	0.410	920	0.544
1280	0.589	1200	0.709
1690	0.785	1510	0.873
2130	0.954	1865	1.037
2610	1.153		

FIGURE III-27

$10^3/T^{\circ}K$	$4 + \log_{10}k$
2.222	0.9410
2.217	0.9567
2.132	1.0065
2.012	1.1072

FIGURE III-28

time	$\log_{10}P_o/P$
210°C	
124	0.0945
575	0.330
966	0.555
1558	0.871
2143	1.157
2614	1.387
3031	1.620
226°C	
117	0.116
419	0.368
792	0.579
1195	0.840
1612	1.090
2018	1.403
2575	1.624

time	$\log_{10}P_o/P$
210°C	
125	0.122
590	0.395
966	0.586
1558	0.897
2143	1.190
2631	1.409
241°C	
90	0.089
401	0.366
722	0.652
1030	0.852
1540	1.224
2073	1.626

FIGURE III-29

$10^3/T^oK$	$4 + \log_{10}k$
2.070	1.0772
2.070	1.0792
2.004	1.1530
1.946	1.2450

FIGURE III-30

time	$\log_{10}P_o/P$
	202°C
250	0.044
605	0.113
1050	0.206
1420	0.272
1890	0.352
2270	0.428
2800	0.527
	234°C
120	0.059
550	0.247
830	0.375
1170	0.519
1430	0.616
1900	0.789
2480	1.048
	214°C
250	0.062
620	0.154
980	0.237
1370	0.336
1840	0.443
2260	0.547
	246°C
110	0.086
340	0.208
770	0.419
1080	0.573
1400	0.727
2080	1.041
	223°C
140	0.045
430	0.129
900	0.271
1300	0.384
1610	0.476
2000	0.594

FIGURE III-31

$10^3/T^{\circ}K$	$4 + \log_{10}k$	$10^3/T^{\circ}K$	$4 + \log_{10}k$
2.105	0.6365	1.972	0.9782
2.053	0.7110	1.927	1.0481
2.016	0.8319		

FIGURE III-32

time	$\log_{10}P_o/P$	time	$\log_{10}P_o/P$	time	$\log_{10}P_o/P$
	190°C		209°C		218°C
135	0.030	110	0.037	130	0.045
500	0.096	510	0.126	430	0.143
900	0.187	930	0.243	810	0.272
1400	0.278	1380	0.340	1250	0.404
2050	0.403	2100	0.509	1640	0.492
2500	0.481	2560	0.615	2030	0.615
		3300	0.867	2510	0.770
				3050	0.892
	230°C		239°C		
110	0.057	110	0.055		
480	0.209	440	0.202		
810	0.354	850	0.389		
1330	0.533	1240	0.546		
1900	0.705	1600	0.685		
2550	0.947	2000	0.862		

FIGURE III-33

$10^3/T^oK$	$4 + \log_{10}k$
2.160	0.6454
2.075	0.7649
2.037	0.8261
1.988	0.9165
1.953	0.9896

Appendix - F

SECTION IV

Data In Support of Figures In Experimental Results*

FIGURE IV-1

time	$10(P_o^{\frac{1}{2}}-P^{\frac{1}{2}})$	time	$10(P_o^{\frac{1}{2}}-P^{\frac{1}{2}})$
Reaction 1		Reaction 2	
97	.1345	141	.1286
185	.1820	310	.2406
453	.3408	504	.3471
762	.5042	750	.4816
1071	.6849	930	.5972
1320	.8106	1120	.6827
1624	.9713	1336	.8157
		1658	.9781
Reaction 3		Reaction 4	
130	.1694	125	.1413
326	.2826	341	.2645
570	.4386	691	.4512
846	.5702	980	.5988
1200	.7699	1254	.7765
1525	.9623		

* Pressure values in Torr - time values in seconds

FIGURE IV-2

P_o(propene) $x10^2$(Torr)	$kx10^4$ (Torr$^{\frac{1}{2}}$-sec^{-1})
0	1.100
1.30	1.138
4.45	1.126
0	1.107

FIGURE IV-3

time	$Px10^2$
1.23	
50	0.9903
150	0.8210
250	0.6821
350	0.5520
475	0.4132
6.00	
90	5.1414
310	4.4058
463	3.8040
640	3.2952
840	2.6700
1050	2.0952

time	$Px10^{-2}$
1.34	
60	1.0414
171	0.8578
320	0.6550
475	0.4805
635	0.3346
11.10	
85	10.0500
248	9.0188
446	8.1718
630	7.1861
840	5.9896
1100	4.8896
1320	3.9316

time	$Px10^{-2}$
3.70	
70	3.1376
200	2.7484
400	2.2455
640	1.7138
850	1.3076
1050	0.9442

FIGURE IV-4

$2 + \log_{10} P_o$	$5 + \log_{10} v_o$
1.0453	0.7563
0.7782	0.5907
0.5682	0.5167
0.0881	0.2916
0.1271	0.2847

FIGURE IV-5

time	$10(P_o^{\frac{1}{2}} - P^{\frac{1}{2}})$
before large dose	
55	0.1495
150	0.2335
260	0.3502
400	0.4795
550	0.6117
700	0.7255
920	0.8946

time	$10(P_o^{\frac{1}{2}} - P^{\frac{1}{2}})$
after large dose	
60	0.0105
165	0.1657
300	0.2417
460	0.3323
650	0.4407
840	0.5564
1070	0.6909
1330	0.8550

FIGURE IV-6

time	$Px10^{-2}$
1.32	
50	1.2400
87	1.2000
121	1.1700
163	1.1300
199	1.0900
236	1.0500
402	0.9000
687	0.6800
971	0.4900
1160	0.4600
5.48	
62	5.2600
92	5.1100
126	5.0000
163	4.8800
222	4.6900
278	4.5400
339	4.3500
495	3.9000
682	3.4400
906	2.9200
1140	2.4400

time	$Px10^{-2}$
1.99	
87	1.8400
114	1.8000
144	1.7400
196	1.6700
242	1.6100
490	1.2800
670	1.1000
937	0.8600
1194	0.6600
7.58	
51	7.1700
84	7.1300
132	6.8800
185	6.7200
246	6.4700
292	6.2800
354	6.0800
514	5.3100
712	4.7600
957	4.0500
1283	3.3200
1556	2.6500

time	$Px10^{-2}$
3.51	
116	3.1600
328	2.7100
615	2.1400
909	1.6800
1220	1.2600
1790	1.0800

FIGURE IV-7

$2 + \log_{10} P_o$	$5 + \log_{10} v_o$
0.1206	0.0693
0.2995	0.1976
0.5453	0.4300
0.7388	0.5349
0.8797	0.6388

FIGURE IV-8

$P_o x 10^2$	$k x 10^4$
1.32	9.429
1.99	9.332
3.51	8.432
5.48	7.660
7.58	6.595

FIGURE IV-9

time	$\log_{10} P_o/P$	$10(P_o^{.25} - P^{.25})$	time	$\log_{10} P_o/P$	$10(P_o^{.25} - P^{.25})$
	201°C			220°C	
96	0.0812	0.144	90	0.0982	0.178
270	0.1386	0.242	265	0.1968	0.346
530	0.2298	0.392	507	0.3257	0.554
767	0.3041	0.507	780	0.4615	0.755
1080	0.3937	0.641	1100	0.6334	0.990
1340	0.4817	0.765	1471	0.8156	1.213
1620	0 5702	0.885	1990	1.1070	1.587
1950	0.6621	1.001			
2297	0.7930	1.159			
2600	0.3882	1.267			

FIGURE IV-10

time	42/43 ratio	44/43 ratio	time	42/43 ratio	44/43 ratio
50	.332	.157	310	.403	.163
70	.337	.153	330	.394	.163
90	.345	.145	350	.406	.158
110	.344	.152	370	.413	.162
130	.350	.154	390	.422	.160
150	.360	.154	410	.423	.159
170	.361	.155	430	.427	.167
190	.373	.160	450	.435	.171
210	.377	.163	470	.443	.171
230	.374	.160	490	.447	.171
250	.389	.161	510	.456	.172
270	.384	.161	530	.460	.171
290	.394	.160	550	.461	.176

FIGURE IV-11

time	42/43 ratio	44/43 ratio	time	42/43 ratio	44/43 ratio
100	.470	.181	1700	1.860	.165
300	.660	.182	1900	1.971	.166
500	.854	.183	2100	2.054	.161
700	1.058	.181	2300	2.093	.143
900	1.251	.181	2500	2.163	.155
1100	1.449	.176	3000	2.234	.145
1300	1.589	.170	3500	2.261	.139
1500	1.748	.169	4000	2.260	.136

FIGURE IV-12

time	42/43 ratio	44/43 ratio	time	42/43 ratio	44/43 ratio
50	.354	.145	160	.398	.151
60	.361	.144	170	.401	.149
70	.363	.148	180	.397	.147
80	.356	.152	190	.400	.147
90	.377	.148	200	.404	.154
100	.373	.150	210	.403	.151
110	.377	.151	220	.407	.151
120	.380	.147	230	.410	.151
130	.380	.146	240	.410	.149
140	.388	.150	250	.422	.155
150	.395	.148	260	.427	.153

FIGURE IV -13

time	42/43 ratio	44/43 ratio	time	42/43 ratio	44/43 ratio
100	.494	.162	1900	1.492	.177
300	.687	.170	2100	1.521	.179
500	.832	.181	2300	1.550	.184
700	.957	.183	2500	1.576	.179
900	1.097	.188	3100	1.692	.176
1100	1.180	.175	3600	1.744	.174
1300	1.264	.181	4000	1.749	.176
1500	1.376	.179	11270	2.237	.186
1700	1.433	.180			

FIGURE IV-14

time	43/41 ratio	58/57 ratio	time	43/41 ratio	58/57 ratio
40	.733	0	943	.400	0
100	.699	0	1382	.313	0
220	.625	0	1642	.243	0
350	.585	0	3850	.097	0
550	.509	0	5000	.097	0
700	.467	0			

FIGURE IV-15

time	43/41 ratio	58/57 ratio	time	43/41 ratio	58/57 ratio
60	.754	0	1450	.542	0
170	.729	0	1620	.519	0
260	.710	0	1920	.490	0
400	.685	0	2440	.444	0
550	.659	0	2890	.391	0
720	.626	0	3460	.363	0
925	.603	0	4250	.321	0
1090	.595	0	5840	.263	0
1250	.568	0	6405	.223	0

FIGURE IV-16

time	$\log_{10}P_o/P$	time	$\log_{10}P_o/P$	time	$\log_{10}P_o/P$	time	$\log_{10}P_o/P$
	181°C		196°C		201°C		220°C
90	0.0449	120	0.0525	96	0.0812	90	0.0982
588	0.1525	390	0.1367	270	0.1386	265	0.1968
1081	0.2388	840	0.2543	530	0.2298	507	0.3257
1390	0.2927	1240	0.3545	767	0.3041	780	0.4615
1940	0.4064	1930	0.5267	1080	0.3937	1100	0.6334
2360	0.4719			1340	0.4817	1471	0.8156
				1620	0.5702	1990	1.1070
				1950	0.6621		
				2297	0.7930		
				2600	0.8882		

FIGURE IV-17

$10^3/T°K$	$4 + \log_{10}k$
2.0280	1.0828
2.1097	0.8664
2.1322	0.7899
2.2026	0.6364

FIGURE IV-18

time	$\log_{10}P_o/P$	$10(P_o^{\frac{1}{2}}-P^{\frac{1}{2}})$
90	0	0
455	0.0279	0.0331
898	0.0728	0.0844
1535	0.1346	0.1506
2165	0.1998	0.2156
3640	0.3170	0.3207
4450	0.3812	0.3726
5800	0.4873	0.4504
7452	0.7091	0.5857
9050	0.9431	0.6947
10050	1.0894	0.7496

FIGURE IV-19

time	$\log_{10}P_o/P$	$10(P_o^{\frac{1}{2}}-P^{\frac{1}{2}})$	time	$\log_{10}P_o/P$	$10(P_o^{\frac{1}{2}}-P^{\frac{1}{2}})$
110	0.0064	0.0073	3470	0.3542	0.3349
675	0.0609	0.0677	4560	0.5197	0.4503
1436	0.1384	0.1472	5100	0.6076	0.5032
2080	0.2020	0.2075	5937	0.7575	0.5819
2800	0.2832	0.2782			

FIGURE IV-20

time	$\log_{10}P_o/P$	time	$\log_{10}P_o/P$	time	$\log_{10}P_o/P$	time	$\log_{10}P_o/P$
196°C		212°C		213°C		227°C	
240	0.0469	111	0.0317	120	0.0563	120	0.0805
420	0.0795	420	0.1259	316	0.1178	350	0.2088
715	0.1021	700	0.1898	627	0.1957	695	0.4011
1050	0.1676	965	0.2546	1020	0.3271	920	0.5240
1445	0.2161	1200	0.3254	1340	0.4265	1141	0.6557
1700	0.2567						

FIGURE IV-21

$10^3/T^oK$	$4 + \log_{10}k$
1.999	0.7505
2.058	0.4804
2.061	0.4262
2.134	0.1526

FIGURE IV-22

time	$\log_{10}P_o/P$	time	$\log_{10}P_o/P$	time	$\log_{10}P_o/P$	time	$\log_{10}P_o/P$
192°C		207°C		220°C		220°C	
124	0.1896	80	0.1037	95	0.1580	97	0.0771
260	0.3235	303	0.2623	260	0.3365	300	0.1694
400	0.4790	490	0.3975	480	0.5607	497	0.2574
570	0.6680	690	0.5470	780	0.8924	710	0.3541
807	0.9322	911	0.7211	1000	1.1524	960	0.4811
1050	1.2092	1140	0.8937			1250	0.6233
						1500	0.7417

FIGURE IV-23

$10^3/T°K$	$4 + \log_{10}k$
2.0284	1.4050
2.0284	1.4086
2.0833	1.2368
2.1505	1.0405

FIGURE IV-24

time	$\log_{10} P_o/P$	time	$\log_{10} P_o/P$
	169°C		184°C
90	0.0495	100	0.0965
382	0.1167	300	0.1994
600	0.1625	620	0.3566
926	0.2300	1020	0.5536
1210	0.2899	1272	0.6837
1510	0.3480		

time	$\log_{10} P_o/P$	time	$\log_{10} P_o/P$	time	$\log_{10} P_o/P$
100	0.1477	100	0.1579	64	0.1820
250	0.2702	270	0.3162	115	0.2576
420	0.4202	440	0.4761	200	0.3816
600	0.5888	620	0.6757	300	0.5387
760	0.7455	815	0.8653	410	0.7310
920	0.8855	1020	1.0830	506	0.8994

FIGURE IV-25

$10^3/T°K$	$4 + \log_{10} k$
2.2624	0.8386
2.1882	1.0603
2.1097	1.3220
2.0921	1.3674
2.0284	1.5737

FIGURE IV - 26

time	rate expression for k_1/k_2				
	100	150	200	250	300
55	.260	.327	.394	.461	.528
150	.407	.507	.607	.708	.808
260	.631	.775	.919	1.064	1.241
100	.854	1.035	1.215	1.396	1.577
550	1.124	1.337	1.550	1.763	1.975
700	1.394	1.629	1.890	2.098	2.359
920	1.947	2.203	2.459	2.715	2.972

REFERENCES

Addy, J. and G.C. Bond (1957). Trans. Faraday Soc. 53, 377.

American Petroleum Institute. "Selected Values of the Properties of Hydrocarbons". Research Project #44.

Anderson, J.R. and B.G. Baker (1971a). In "Chemisorption and Reactions on Metallic Films", Vol. 2 (J.R. Anderson, ed.), Academic Press, New York. Chap. 7.

Anderson, J.R. and B.G. Baker (1971b). In "Chemisorption and Reactions on Metallic Films", Vol. 2 (J.R. Anderson, ed.), Academic Press, New York. Chap. 8.

Anderson, J.R. and B.H. Mc Conkey (1967). J.Catal. 9, 263.

Anderson, J.R. and B.H. Mc Conkey (1968). J. Catal. 11 54.

Balandin, A.A. (1929). Z. Physik. Chem. B2, 289. B3, 167.

Balandin, A.A. (1969). Advan. Catalysis 19, 1.

Banthorpe, D.V. (1963). "Elimination Reactions", Elsevier, New York. Chap. 7.

Barton, D.H.R. and K.E. Howlett (1949). J. Chem. Soc. 155.

Basolo, F. and R.G. Pearson (1968). "Mechanisms of Inorganic Reactions" 2nd ed., John Wiley and Sons, New York. Chap. 3.

Bayard, R.T. and D. Alpert (1950). Rev. Sci. Instr. 21, 571.

Beeck, O. (1950). Discussions Faraday Soc. 8, 118.

Beeck, O., A. Wheeler and A.E. Smith (1939a). Phys. Rev. 55, 601.

Beeck, O. and A.Wheeler (1939b). J. Chem. Phys. 7, 631.

Benson, S.W. and A.N. Bose (1962). J. Chem. Phys. 37, 2935.

Bond, G.C. (1962). "Catalysis by Metals", Academic Press, London and New York.

Bond, G.C. and P.B. Wells (1964). Advan. Catalysis 15, 91.

Brown, W.G. (1951). "Organic Reactions" Vol. VI, Wiley and Sons, New York. Chap. 10.

Campbell, J.S. and P.H. Emmett (1967). J. Catal. 7, 252.

Campbell, J.S. and Kemball C. (1961). Trans. Faraday Soc. 57 809.

Campbell, J.S. and Kemball, C. (1963). Trans. Faraday Soc. 59, 2583.

Coeckelbergs, R., A. Crucq, A. Frennet and G. Lienard (1959) J. Chim. Phys. 56, 967.

Coeckelbergs, R., A. Frennet, P.A. Gosselain and M.J. VanderVenne (1955). J.Chem. Phys. 23, 1731.

Dunn, T.M., A.R. McClure, and R.G. Pearson (1965). "Some Aspects of Crystal Field Theory", Harper and Row, New York. Chap. 4.

Dushman, S.(1962). "Scientific Foundations of Vacuum Technique", John Wiley and Sons, New York.

Halsey, G.D. and H.S. Taylor (1947). J. Chem. Phys. 15, 624

Halsey, George D. (1949). J.Chem. Phys. 17, 758.

Halsey, George D. (1963). J. Phys. Chem. 67, 2038.

Harrod, J.F. and W.R.Summers (1971). J. Am. Chem. Soc. 93, 5051.

Hauffe, K. (1965). "Oxidation of Metals", Plenum Press, New York.

Hayward, D.O. (1971). In "Chemisorption and Reactions on Metallic Films", Vol. 2 (J.R. Anderson, ed.), Academic Press, New York. Chap. 4.

Jach, J., F.J.Stubbs and C. Hinshelwood (1954). Proc. Royal Soc. A224, 283.

Janz, G.J. (1967). "Thermodynamic Properties of Organic Compounds" Revised edition, Academic Press, New York.

Jenkins, G.I. and E.K. Rideal (1955). J.Chem. Soc. 2490, 2496.

Krishman, K.S. and S.C. Jain (1952). Nature 170, 759.

Lander, J.J. (1965). Progr. Solid State Chem. 2, 26.

Maccoll, A. (1964). In "The Chemistry of Alkenes" (S. Patai, ed.), Interscience Pubs., New York. Chap. 3.

Maccoll, A. and P.J. Thomas (1955). Nature 176, 392.

Maccoll, A. and P.J. Thomas (1957). J.Chem. Soc. 5033.

Mango. R.D. and J.H. Schachtschneider (1967). J. Am. Chem. Soc. 89, 2467.

Manufacturing Chemists' Association Research Project. "Selected Values of Properties of Chemical Compounds", Chemical Thermodynamic Properties Center, Texas A & M University.Matlack, A.S. and D.S.

Matlack, A.S. and D.S. Breslow (1965). J. Polymer Sci. A-3, 2583.

May, John W. (1970). Advan. Catalysis 21, 151.

Moore, A.S. (1945). J.Sci. Instr. 22, 101.

Morrison, R.A. and K.A. Krieger (1968). J. Catal. 12, 25.

Noller, H. and Ostermeier, K. (1956). Z. Electrochem. 60, 921.

Noller, H. and K. Ostermeier (1959). Z. Electrochem. 63, 191.

Organic Synthesis, Coll. Vol. #1 (1932a). p. 36.

Orgel, L.E. (1960). "An Introduction to Transition Metal Chemistry", John Wiley and Sons., New York. Chap. 5.

Park, R.L. and J.E. Houston (1969). Surface Sci. 18, 213.

Park, R.L. and H.H. Madden (1968). Surface Sci. 11, 188.

Pearson, R.G. (1970). Chem. Eng. News 48(41), 66.

Roberts, R.W. (1963). J. Phys. Chem. 67, 2035.

Roberts, R.W. and T.A. Vanderslice (1963). "Ultrahigh Vacuum and Its Applications", Prentice Hall, Englewood Cliffs, New Jersey. Chap. 1.

Rossini, F.D., D.D. Wagman, W.H. Evans, S.Levine and I. Jaffe (1952). "Selected Values of Chemical Thermodynamic Properties" (NBS circular #500), U.S. Gov't Printing Office, Washington D.C.

Schwab, G.M. and H. Noller (1954). Z. Elektrochem. 58, 762.

Schwab, G.M. and N. Theophilides (1946). J. Phys. Chem. 50, 427.

Smithells, C.J. (1967). "Metals Reference Book" 4th ed. Vol. 2, Butterworths, London.

Stephens, S.J. (1959). J. Phys. Chem. 63, 188.

Stull, D.R., E.F. Westrum and G.C. Sinke (1969). "The Chemical Thermodynamics of Organic Compounds", J. Wiley and Sons. New York.

Summers, W.R. (1970). "Reactions of Gaseous Halocarbons on Clena Titanium Surfaces", Ph.D. Thesis, McGill University.

Summers, W.R. and J.F. Harrod (1972). in press, Can. J. Chem.

Thomas, P.J. (1961). J.Chem. Soc. 136.

Trapnell, B.M.W. (1952). Trans. Faraday Soc. 48, 160.

Wang Laboratories (1967). "Wang 300 Series Program Library" Vol. 1, p. 42, Wang Laboratories Inc., Tweksbury, Mass.

Wyckoff, R.W.G. (1963). "Crystal Structures" 2nd ed., Interscience, John Wiley and Sons, New York.

Youden, W.J. (1951). "Statistical Methods for Chemists" (NBS Washington), John Wiley and Sons, New York.

Young, D.M. and A.D. Crowell (1962). "Physical Adsorption of Gases", Butterworths, London.